New Aspects of the Double Interrupted and Vinylogous Nazarov Cyclization

by

Yury Karpov

A thesis submitted in partial fulfillment of the requirements for the degree of

Doctor of Philosophy

Department of Chemistry
University of Alberta

Abstract

Developing diverse effective synthetic tools to generate structural complexity in molecular frameworks is considered an attractive area of pursuit. Among those tools, the Nazarov reaction is an effective route towards the generation of complex polycyclic skeletons like five-membered rings, which are widely met phenomena in potential drug candidates. The Nazarov reaction plays an important role plays an important role in the synthesis of highly functionalized cyclopentanones from 1,4-dien-3-ones with the application of Lewis acids. This dissertation will discuss new aspects of the double interruption of the Nazarov cyclization initiated by organoaluminum reagents as well as the interrupted vinylogous Nazarov cyclization.

Chapter 1 describes strategies of intra- and intermolecular trapping of the Nazarov cyclization intermediate, along with recent successful examples to access cyclopentanoid products. This chapter will have a detailed recount of methods that use a variety of traps in both fashions, providing molecular complexity with a step economy.

Chapter 2 discusses a one-pot double interrupted Nazarov sequence, which leads to the formation of the substituted α-halocyclopentanones. Organoaluminum serves as reaction initiator, a source of a nucleophile to trap an oxyallyl cation, and is proposed to deliver an electrophile closer to the aluminum enolate.

Chapter 3 describes the first example of the interrupted vinylogous Nazarov reaction. The use of intramolecular trapping allows the rapid formation of complex compound. The intermolecular interrupted vinylogous Nazarov cyclization mediated by different Lewis acids provides different trapping products. The trapping studies allows a deeper understanding of the reaction mechanism.

A new approach to access butenolides from [3]dendralenes will be disclosed in Chapter 4. This unexpected result was obtained during attempts to perform the intramolecular interrupted vinylogous Nazarov cyclization. Preliminary results on reaction scope will be included in this chapter.

Chapter 5 tells the story of the Meyer–Schuster/Nazarov cascade reaction development, in which the rearrangement of propargylic alcohol is combined efficiently with the subsequent electrocyclization. Future plans for chapters 2–5 will be discussed, as well.

Preface

Part of Chapter 2 of this thesis will be published as Y. Karpov, Y. Kwon, R. McDonald, F. G. West, "Multi-Component Coupling Nazarov Cyclization via Organoaluminum-Mediated Double Interruption," *manuscript in preparation*. I was responsible for the concept formation of the reaction of aluminum enolate with halogen electrophiles, experimental work related to that part of the research, reaction optimization, data collection, manuscript composition, and characterization of compounds **51–54** (numbering from Chapter 2). Y. Kwon was responsible for the concept formation and experimental work related to the aldehydes trapping by organoaluminum enolate, reaction optimization, data collection, characterization of compounds **26–28** (numbering from Chapter 2), and equally contributed to the manuscript preparation. R. McDonald provided X-ray data for compound **54a** (numbering from Chapter 2). F. G. West was the supervisory author and was involved with the concept formation and manuscript composition.

Part of Chapter 3 of this thesis will be published as Y. Karpov, S. Grigoryan, F. G. West, "Intramolecular and Intermolecular Interrupted Vinylogous Nazarov Cyclization," *manuscript in preparation*. I was responsible for the concept formation, experimental work, data collection, and characterization of compounds **69–71**, **77–82**, **92–100**, **103** (numbering from Chapter 3); as well as the manuscript composition. S. Grigoryan assisted with the preparation of compounds **94** and **95** (numbering from Chapter 3). F. G. West was the supervisory author and was involved with the concept formation and manuscript composition.

Dedication

For my family and friends

"You can't be disturbed by anything. There's no emotion involved. You can't feel sorrow, you can't feel pity, there's nothing you feel. The job has to be done."

Mike Tyson

Acknowledgments

First, I want to express my thankfulness to my supervisor, Dr. West that he decided to allow me to join his group. I enjoyed the amount of freedom I had during my research. In five years with Dr. West, we went through many events together and all of them forged and enhanced my self-confidence, knowledge, improved my lab skills drastically, and prepared me for my future life journey.

I would like to thank Dr. Lundgren, Dr. Lowary for being my supervisory committee members and for expressing their willingness to help me in my academic career.

I would like to express my special gratitude to people who were working with me. It was a pleasant experience to have you as my group members, and especially people who are always friendly, generous, and encouraging (Marius, Natasha, Kyle, Jenny, Shao, William). I want to express special thanks to two remarkable people I have met in Edmonton – Dr. Kseniya Revunova and Dr. Anna Jordan, who were always there to provide me with endless support and help.

I would like to thank all the staff from the MS lab, NMR facility lab, IR lab, X-ray service labs, chemical stores, and machine shop for their help.

To my family: thank you for all of your support and love.

Table of Contents

List of Tables

List of Figures

List of Schemes

List of Symbols and Abbreviations

^{1}H	proton
^{13}C	carbon-13
^{19}F	fluorine-19
A	acid
Å	Angstrom
Ac	acetyl
Ac_2O	acetic anhydride
acac	acetylacetonate
app.	apparent (spectral)
APPI	atmospheric pressure photoionization (mass spectrometry)
aq	aqueous solution
Ar	aryl
BA	Brønsted acid
Bn	benzyl
Br	broad (spectral)
Bu	butyl
ºC	degrees Celsius
Calcd	calculated
cat.	indicates that the reagent was used in a catalytic amount
cm^{-1}	wave numbers
COSY	H-H correlation spectroscopy
conc.	concentrated
d	day(s); doublet (spectral)
DBU	1,8-diazabicyclo[5.4.0]undec-7-ene
DCE	1,2-dichloroethane
DCM	dichloromethane
dd	doublet of doublets (spectral)
ddd	doublet of doublets of doublets (spectral)
dddd	doublet of doublets of doublets of doublets (spectral)

DIBAL-H	diisobutylaluminum hydride
dq	doublet of quartets (spectral)
dr	diastereomeric ratio
dt	doublet of triplets (spectral)
e^-	electron
E^+	an unspecified electrophile
EDG	electron-donating group
EI	electron impact (mass spectrometry)
endo	endocyclic
equiv	equivalent(s)
er	enantiomeric ratio
ESI	electrospray inonization (mass spectrometry)
Et	ethyl
EtOAc	ethyl acetate
EWG	electron-withdrawing group
exo	exocyclic
FLP	frustrated Lewis pair
FMO	frontier molecular orbitals
FT-IR	Fourier-transform infrared spectroscopy
g	gram(s)
h	hour(s)
HMBC	heteronuclear multiple bond coherence (spectral)
HOMO	highest occupied molecular orbital
HSQC	heteronuclear single quantum coherence (spectral)
HRMS	high resolution mass spectrometry
hν	light
Hz	hertz
i-Bu	isobutyl
i-Pr	isopropyl
J	coupling constant
kcal	kilocalorie

kJ	kilojoules
L	liter(s); unspecified ligand
LA	Lewis acid
LAH	lithium aluminum hydride
LDA	lithium diisopropylamide
LiHMDS	lithium hexamethyldisilazane
LUMO	lowest unoccupied molecular orbital
M	molar
m	multiplet (spectral)
M^+	generalized Lewis acid or protic acid; molecular ion
Me	methyl
mg	milligram(s)
min	minute(s)
mL	milliliter(s)
mmol	millimole(s)
mol	mole(s)
mp	melting point
MS	molecular sieves
m/z	mass to charge ratio
NFSI	fluoro-*o*-benzenedisulfonimide
nm	nanometer(s)
NMR	nuclear magnetic resonance
NOE	nuclear Overhauser enhancement
n-Pr	normal propyl
Nu	an unspecified nucleophile
o/n	overnight
Ph	phenyl
PMP	*p*-methoxyphenyl
pp	pages
ppm	parts per million
Pr	propyl

Py	pyridine
q	quartet (spectral)
qt	quartet of triplet
quint	quintet
R	generalized alkyl group of substituent
rac	racemate
R_f	retention factor (in chromatography)
rt	room temperature
rxn	reaction
s	singlet (spectral)
sept	septet (spectral)
SET	single electron transfer
SM	starting material
S_N	nucleophilic substitution
SOMO	singly occupied molecular orbital
t	triplet (spectral)
T	temperature
TBDMS	tert-Butyldimethylsilyl
t-Bu	*tert*-butyl
TEA	triethylamine
TEMPO	(2,2,6,6-Tetramethylpiperidin-1-yl)oxyl
Tf	trifluoromethanesulfonyl
TFA	trifluoroacetic acid
THF	tetrahydrofuran
TLC	thin layer chromatography
TMS	trimethylsilyl
TOCSY	total correlation spectroscopy
Tq	triplet of quartet
Trig	trigonal
TROESY	transverse rotating-frame overhauser enhancement spectroscopy
Ts	*p*-toluenesulfonyl

tt	triplet of triplet
p-TsOH(pTSA)	*p*-toluenesulfonic acid
UV	ultra violet light
wt.	weight
Δ	applied heat
δ	chemical shift
λ	wavelength

Chapter 1

The Interrupted Nazarov Cyclization

1.1 Pericyclic Reactions

"*When we see that we may produce hundreds of compounds from simple hydrocarbons and chlorine and that from each one of them we may obtain a great number of others… we ask with some anxiety whether, in a few years' time, it will be possible to find our way in the labyrinth of organic chemistry."*

-Auguste Laurent, about organic chemistry in 1854.[1,2]

The era at the dawn of organic chemistry in the 19th century (1830–1850s) can be called a period of theoretical anarchy. Chemists were experiencing confusion regarding compounds' structures and nomenclature. A simple molecule of water was mentioned in literature as HO, H_2O, or even H_2O_2, and a variety of formulas for a molecule of the acetic acid could fill the whole page. Scientists realized that clarifications were essential for the subsequent growth of the field. During this time, Laurent started researching substitution patterns for a variety of compounds, by comparing properties of products to their starting materials. He was able to study the influence of chlorine on naphthalene, ethylene, and other hydrocarbons. Based on his research, Laurent formulated the "least structural changes" theory.[3] He proposed that molecules undergo a minimal number of transformations during chemical processes. Based on it, Laurent implemented a clarification system of organic compound structures starting from the most common hydrocarbons. This perspective was groundbreaking for chemists working on structure elucidation of reaction materials, making the theory widely applied. As the field advanced, reputation of the concept was significantly diminished, especially after the discovery of rearrangements and cyclization reactions.[4]

Fittig reported the first reaction that violated Laurent's theory in 1860. Fittig successfully prepared pinacol **2** by heating acetone in the presence of potassium. Subsequently, he performed water elimination from an obtained the pinacol product by heating it in diluted sulfuric acid isolating ketone **3**, then-named as "pinacoline" (known

today as pinacolone).[5] Following the isolation of **3**, Butlerov successfully elucidated its then-unknown structure in 1874. This feat was accomplished through the synthesis of pinacolone **3**, by methylation of trimethylacetyl chloride **4** in the presence of dimethyl zinc (Scheme 1.1).[6]

This early work caused chemists to question the then-current dogma regarding chemical reactions and reaction mechanisms. The work of Fittig and Laurent planted the seeds for the budding field of the pursuit for mechanistic answers that still holds sway in the present day.

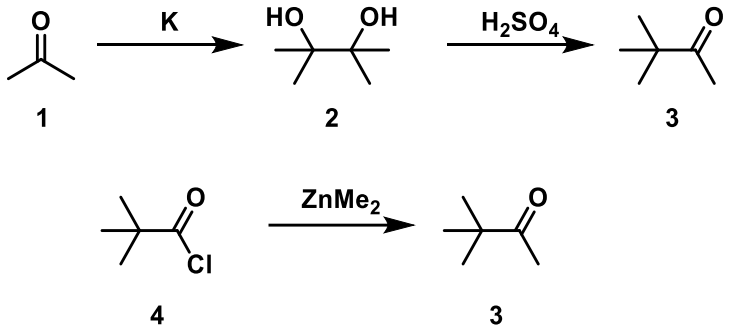

Scheme 1.1. Fittig and Butlerov studies.

Later in the 19th and 20th centuries, chemists discovered vital knowledge about molecules, their structure, and bonding. During this time covalent bonding was characterized by Gilbert Lewis, Lewis' concepts and resonance were expanded by Linus Pauling, and Sir Christopher Ingold introduced organic reaction schemes, which nowadays are known as mechanisms, to provide a better understanding of organic reactions. These and other efforts by numerous scientists resulted in the fact that organic chemistry today is among one of the most essential fields of chemistry, because of its high applicability and ability to affect everyone's lives.

Within the last 50 years, along with the other significant advancements in organic chemistry, pericyclic reactions were recognized as extremely important ones. Pericyclic reactions found their application in the synthesis of multiple drugs' precursors and essential compounds, allowing chemists to create complex molecules in a simple way. Since their discovery, pericyclic reactions have been divided into several classes:

electrocyclizations, cycloadditions, sigmatropic rearrangements, group transfers, ene reactions, cheletropic and dyotropic reactions.[7,8]

The first precedent of pericyclic reactivity ([4+2]-cycloaddition), was reported by Otto Diels and his student Kurt Alder in 1928, who successfully transformed conjugated diene **5** and dienophile **6** into product **7** (Scheme 1.2).[9] Both components contributed their π electrons to form two new σ-bonds. In 1950, for the reaction discovery, Diels and Alder were awarded the Nobel Prize.

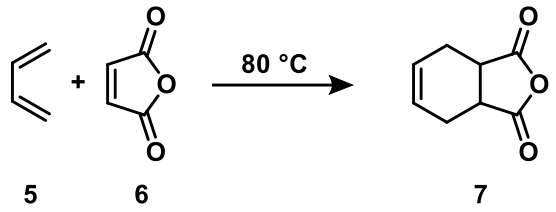

5 **6** **7**

Scheme 1.2. The Diels–Alder reaction.

The synthesis of vitamin B_{12} by Robert B. Woodward is considered to be a benchmark in organic chemistry. In the early 1960s, Woodward group initiated a 6π electrocyclization by heating compound **8** and isolated the unexpected and higher sterically congested product **9** (Scheme 1.3).[10] To explain the stereospecificity of electronic reactions under a variety of applied conditions, a theory was developed in collaboration with Roald Hoffmann, which is recognized as "*the conservation of orbital symmetry*".[11,12] During this time Kenichi Fukui was studying the frontier orbitals (the Highest Occupied Molecular Orbital (HOMO) and the Lowest Unoccupied Molecular Orbital (LUMO)). Especially, he was interested in understanding their influence on mechanisms of the reactions. He applied the Frontier Molecular Orbital Theory (FMO theory) to provide a deeper understanding of Woodward–Hoffmann rules. It is hard to overestimate an impact this work had on the understanding of pericyclic reactions and organic chemistry in general.

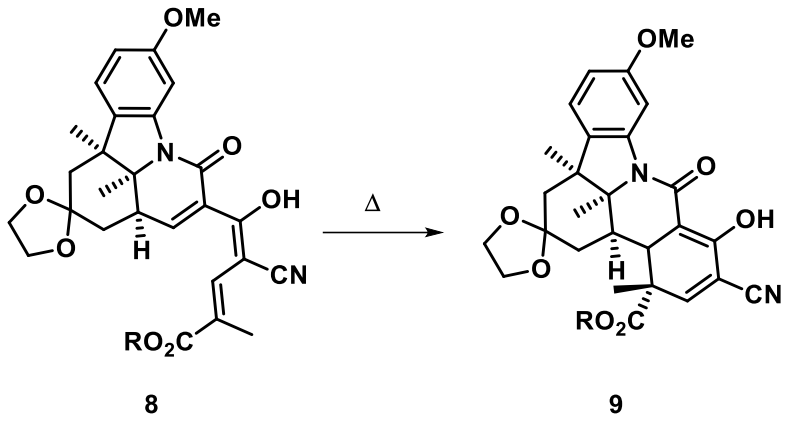

8 9

Scheme 1.3. An unexpected result occurring during Woodward's vitamin B_{12} synthesis.

Another outstanding example of the application of pericyclic reactions in nature was provided by the synthesis of the endiandric acids E and A (**12** and **13)**. Black and co-workers proposed the biosynthesis of these natural products, in the early 1980s, by assuming that in nature these families of acids are prepared by a series of pericyclic reactions. This hypothesis was justification for the racemic nature of these acids compared to most chiral natural products. In 1982 Nicolaou and co-workers developed a brilliant synthetic route towards endriandric acids A and E (8π electrocyclization, 6π electrocyclization, [4+2]-cycloaddition), accomplishing their synthesis using pericyclic reactions starting with acyclic precursor **11**, validating Black's avant-garde hypothesis (Scheme 1.4).[13]

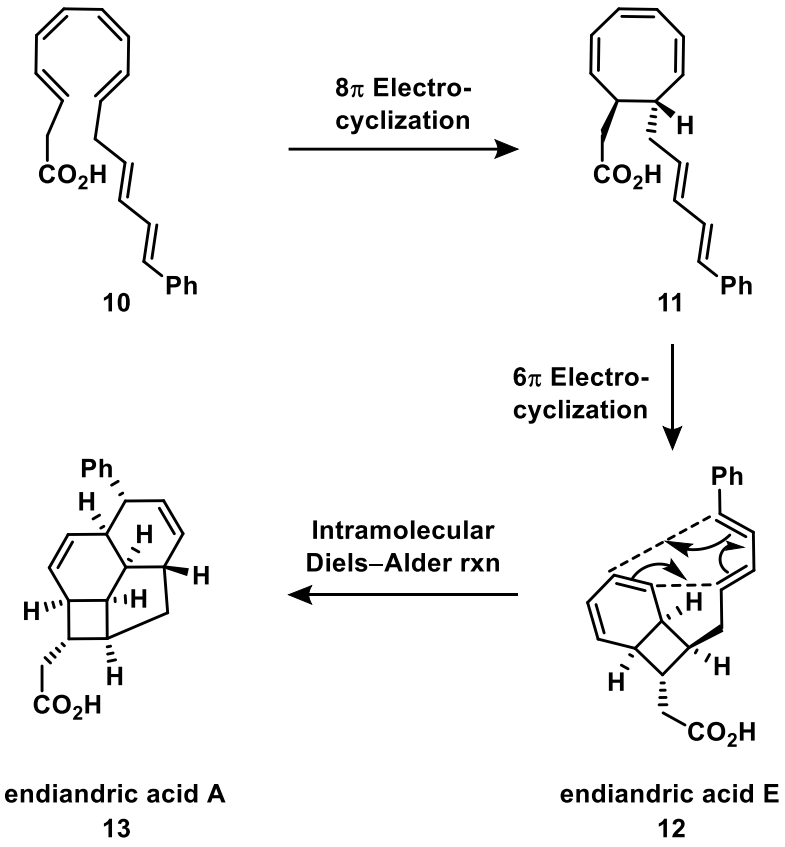

Scheme 1.4. Nicolaou's synthesis of endriandric acids E and A.

After the remarkable usefulness of pericyclic reactions for the preparation of natural products was demonstrated, the field started to grow fast, attracting more and more scientists.[14,15,16] Natural products in Scheme 1.5 were synthesized by 4π electrocyclization reactions. The 4π-electrocyclization can be split into two groups, depending on a number of atoms over which the 4 electrons are delocalized. The broad classification is 4π-electron/4-atom neutral (Scheme 1.5, a),[17] and 4π-electron/5-atom cationic species (Scheme 1.5, b),[18] which result in the formation of cyclopentanoids. Cyclopentenoids are important target structures, considering their prevalence as precursors of natural compounds and drug candidates.[19]

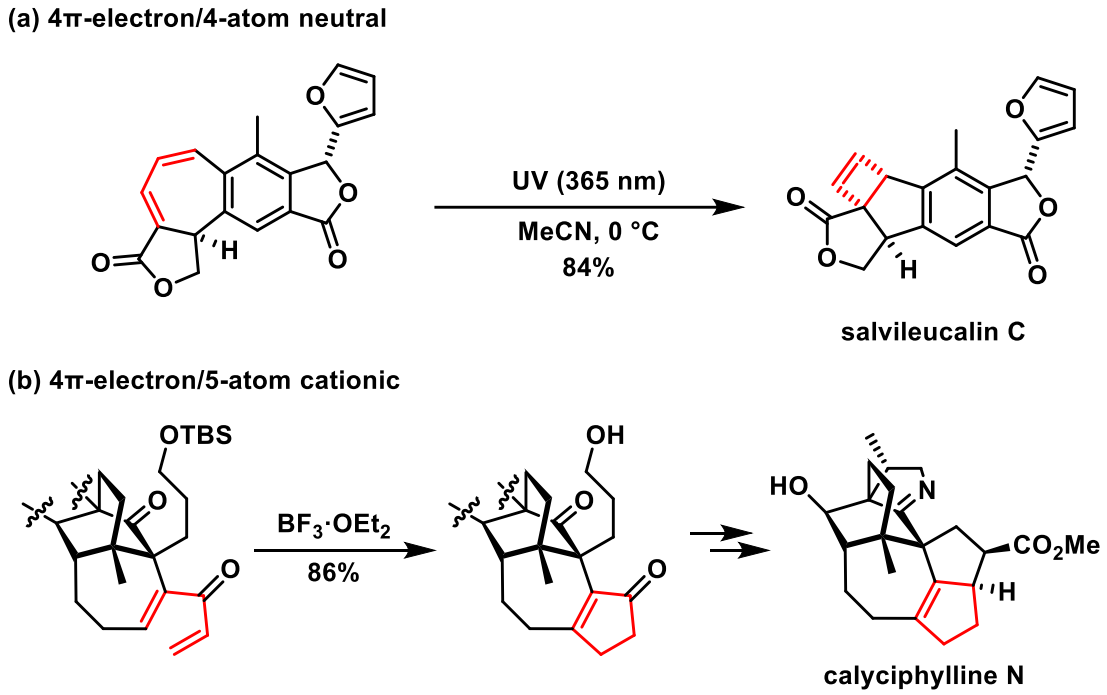

Scheme 1.5. Examples of natural products obtained via a 4π-electrocyclic reaction.

For over the past two decades, efficient and stereoselective preparation of these scaffolds has been a hot area in organic chemistry.[15] Among all well-recognized cyclopentannulation protocols two methods are stood above the rest due to diverse sets of applications, the **Nazarov cyclization**[20], and **Pauson–Khand reaction**.[21] Following sections will focus on discussion of the new aspects of the interrupted Nazarov cyclization.

1.2 The Nazarov Cyclization

The history of the Nazarov cyclization reaction began with Michael G. Kucherov. In 1881, he performed hydrolysis of acetylene **14** in the presence of mercuric salts and sulfuric acid. Kucherov was aiming to get unsaturated vinyl alcohol, which would subsequently undergo polymerization, based on his presumptions. Contrary to his expectations, Kucherov obtained a low boiling point liquid with a fruity odor, acetaldehyde **15** (Scheme 1.6). The unsaturated aliphatic alcohol formed after the reaction fell victim to El'tekov–Erlenmeyer rule and underwent keto-enol tautomerization into a

more thermodynamically stable form. The El'tekov–Erlenmeyer rule was discovered independently by El'tekov in 1877 and Erlenmeyer in 1880.[22]

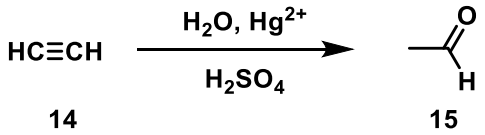

Scheme 1.6. The Kucherov reaction.

In 1941, sixty years later after the Kucherov report, Ivan N. Nazarov and his group found that dialkenylacetylene **16** can transform into allyl vinyl ketone (α,β- and β,γ-unsaturated), divinyl ketone (both sides α,β-unsaturated) and into substituted cyclopentenone **17**, when they were submitted to the Kucherov conditions (Scheme 1.7).[23] The Nazarov group with collaborators continued to study cyclization patterns, showing high efficiency of the reaction (Scheme 1.8). The discovery of such transformations was hard to overstate, because there were no general and common methods to synthesize this kind of scaffold in that era. This reaction provided a reliable method for the construction of cyclopentenone fragments.[19,24]

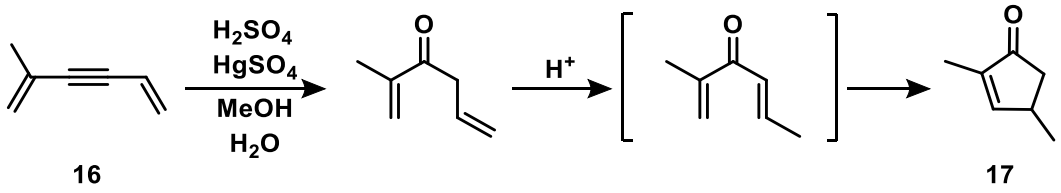

Scheme 1.7. Transformation of divinylacetylene **16**.

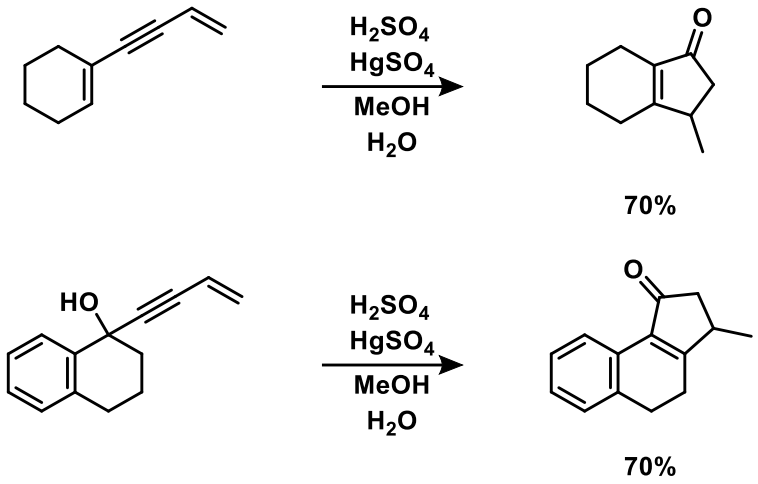

Scheme 1.8. Divinylacetylenes transformation into substituted cyclopentanones.

Although Nazarov was the first one to correctly characterize the structure of the product and study the reaction, it was not the first precedent of this reaction to be reported. Long before its discovery by Nazarov, in 1903 Vorländer and Schroedter successfully isolated unknown cyclopentenone **19**, which was obtained after ketone **18** was mixed with acetic anhydride in the presence of sulfuric acid, with subsequent alkaline hydrolysis (Scheme 1.9).[25] Vorländer and Schroedter initially misassigned the structure of compound **19**, reporting the product incorrectly. Later the Allen group corrected it in 1955 (correct structure of compound **19** is shown on Scheme 1.9).[26]

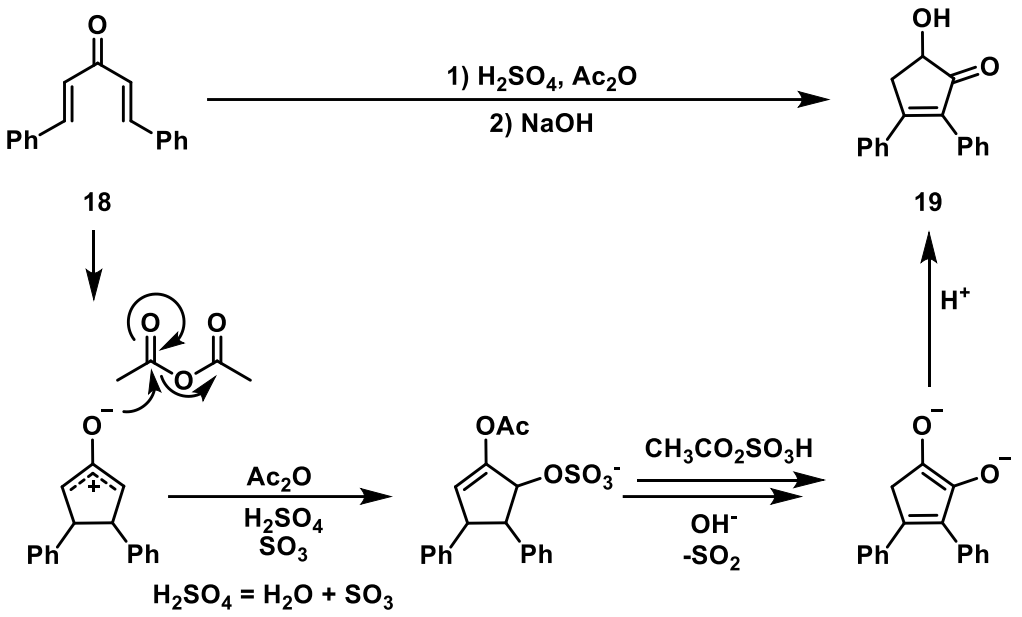

Scheme 1.9. The Vorländer and Schroedter ketol synthesis.

The discovered Nazarov reaction did not have any analogs, and its mechanism seemed to be completely unusual. In 1952 Braude and Coles proposed involvement of the pentadienyl cation into the reaction mechanism.[27] Further studies proved Braude and Coles's proposal and the generally known Nazarov reaction mechanism. It starts with the protonation of the carbonyl functional group of divinyl ketone **20** (Scheme 1.10). The 3-hydroxypentadienyl cation **A** performs a 4π electrocyclic ring-closing event in a stereospecific fashion prescribed by Woodward–Hoffmann rules. The result of the ring-closing is the formation of the 2-hydroxyallyl cation **B**, followed by deprotonation and tautomerization, which allows the formation of products **21** and **22**.[19a]

Based on Frontier Molecular Orbital Theory, the electrocyclic process involves only one molecular orbital of reactant in the ring-closing process. Conventionally, electrocyclizations happen either in a conrotatory (substituents at the termini both rotate in the same direction as the bonding takes place) or disrotatory fashion (opposite directions) to provide constructive interaction (the same sign of orbitals overlap providing bonding molecular orbital).[28] Orbital correlations clearly show that conrotatory rotation for 4π-electron/5-atom cationic species is a thermally allowed process.[29] Disrotatory rotation, in turn, is allowed photochemically. Both 4π electrocyclic reactions occur with high stereoselectivity of carbon–carbon bond formation (Scheme 1.11).

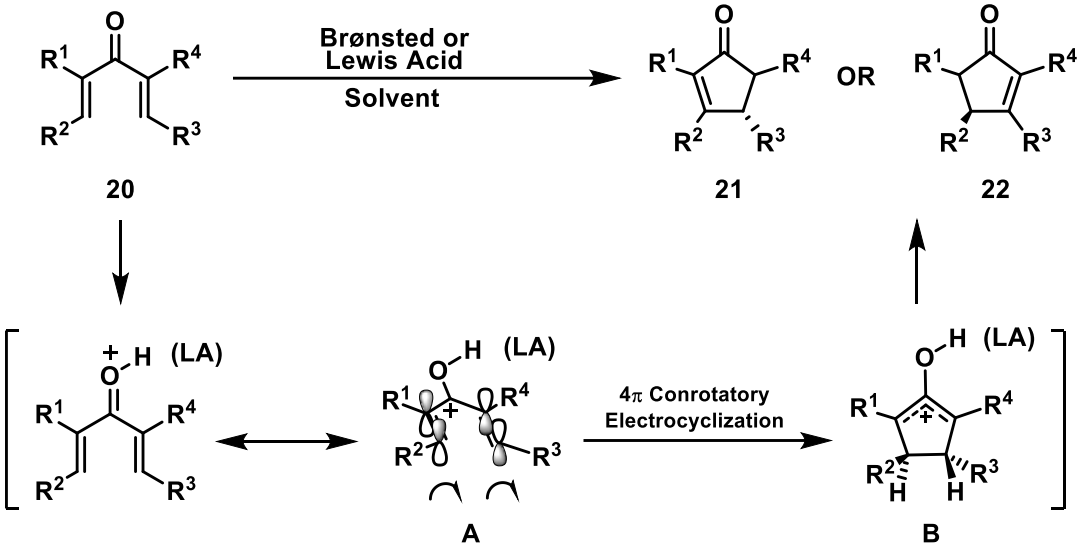

Scheme 1.10. Nazarov cyclization mechanism.

There are three main rules,[30] which were formulated based on experimental data. The bonding interactions of the thermal 4nπ electron systems can occur only during conrotatory rotation. It happens because the orbital overlap of HOMO is required to happen on the opposite faces of the system to form a bonding interaction. For (4n+2)π electron systems the required rotation is disrotatory because the overlap is happening on the same face. In the case of a photochemically initiated reaction, one electron from HOMO is pushed to the excited state (one orbital higher). This new orbital is called SOMO (Singly Occupied Molecular Orbital), resulting in a reverse terminal symmetry. Conrotatory and disrotatory systems have different types of symmetry. For conrotatory, it is a C_2 symmetry, and for disrotatory – mirror symmetry (σ).

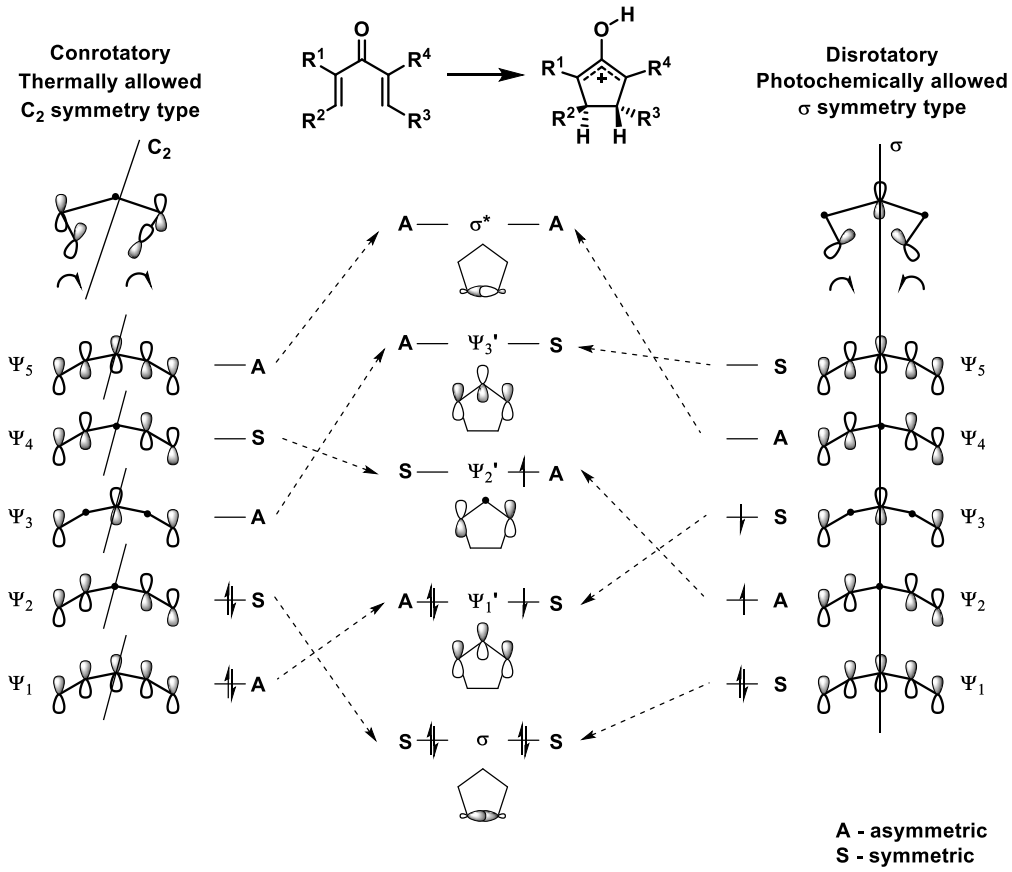

Scheme 1.11. Orbitals correlation diagram for the Nazarov cyclization.

Since the reaction discovery by Nazarov and the first experimentally elucidated mechanism by Shoppee,[31] the reaction developed into a convenient preparative method and one of the basic organic chemistry reactions, which is used in the total synthesis of natural products (Figure 1.1).[32]

The early Nazarov cyclization examples were usually performed with the application of strong Brønsted acids. Then it was found that it is possible to initiate these reactions not only by Brønsted acids but also with strong Lewis acids. This allowed scientists to apply aprotic conditions, becoming more common conditions for the Nazarov cyclization. However, in its conventional version, the Nazarov cyclization has some limitations and drawbacks, which scientists are trying to mitigate.

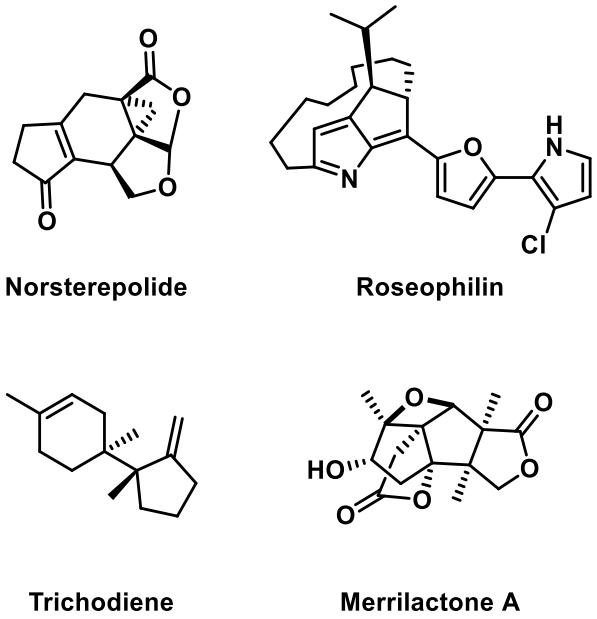

Figure 1.1. Examples of natural products synthesized using the Nazarov cyclization.

These issues are related to the reaction activation barrier and the selectivity of the proton elimination step:

a) Sensitive functional groups (alkenes, halogens and etc) may not be compatible with the strong Lewis or Brønsted acids required to activate the relatively unreactive substrates, which narrows the scope of the reaction;

b) Proton elimination during the conventional Nazarov cyclization in most cases is not completely regioselective and can lead to several isomeric products (regioisomers, diastereomers). The reason for that is the presence of multiple β-hydrogens available for the elimination, which leads to the formation of various products of the reaction, which may result in difficult compounds separation;

c) Proton elimination at one of the β-carbons often destroys one of the stereocentres that are generated during the stereospecific conrotatory electrocyclization, squandering some of the molecular complexity that results from that step;

d) Enolate protonation often leads to the formation of epimeric mixture; and as with all processes occurring via cationic intermediates, the possibility of unexpected cationic rearrangements results in additional, undesired side-products formation. An example of such complications happened in the work of Santelli, who performed a Friedel–Crafts/Nazarov reaction by mixing methylcyclopentene **23** with compound **24** in presence

of $AlCl_3$ forming enone **25**, which resulted from successive hydride and alkyl 1,2-shifts following the initial electrocyclization (Scheme 1.12).[33]

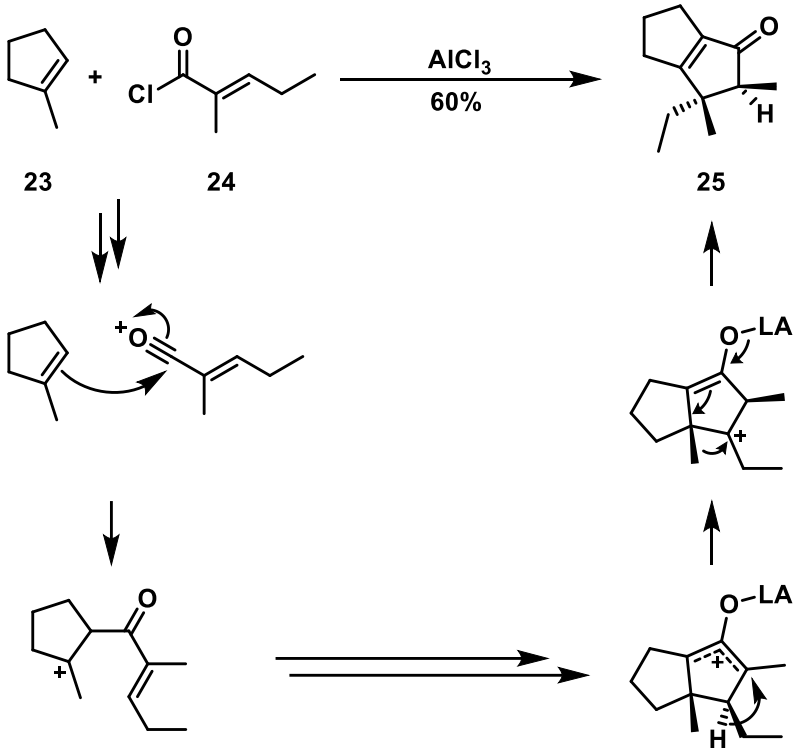

Scheme 1.12. Friedel–Crafts/Nazarov sequence complicated by Wagner–Meerwein rearrangement.

The reactivity of dienones in the Nazarov reaction primarily depends on the Lewis acids. However, starting material characteristics also influence the course of the reaction. The substitution patterns at the α- and β-positions can enhance reaction rates and yields. In the case of α-alkyl substituents, there are several possible conformations (Figure 1.2). It is documented that the W-conformation experiences an unfavorable syn-pentane interaction (R = Me), promoting an increased population of the reactive U-conformer.[19a,34]

Further deviations from conventional substrates with terminal aromatic substituents included not only alkyl α- and β-substituents but the application of electron-withdrawing (EWG) and electron-donating groups (EDG) to address existing regioselectivity issues. An additional factor that can increase the population of the U-conformation is the ability

of some Lewis acids to coordinate with both carbonyl oxygen and an α-functional group forming a chelate.[35]

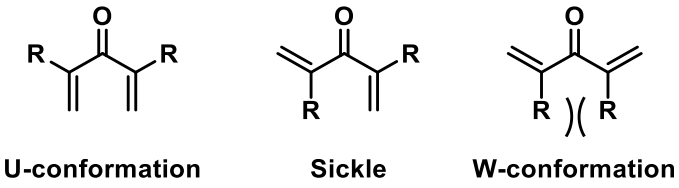

Figure 1.2. Divinyl ketone conformers.

One solution to the existing unwanted elimination regiochemistry problem was introduced by Denmark. His group reported the first regioselective methodology using substrates that have a silyl group as a substituent on one of the β-sp^2 carbons. That modification of starting material **26** allowed it to undergo the Nazarov reaction with complete regiocontrol in 95% yield (Scheme 1.13). Moreover, the efficiency of desilylative elimination completely overcomes any competing cationic rearrangement side-reactions.[36] The silyl group on β-sp^2 carbon (β to the carbonyl group), applied by Denmark, stabilizes the cyclopentenyl cation (silicon hyperconjugation), decreasing cyclization activation barrier.[37]

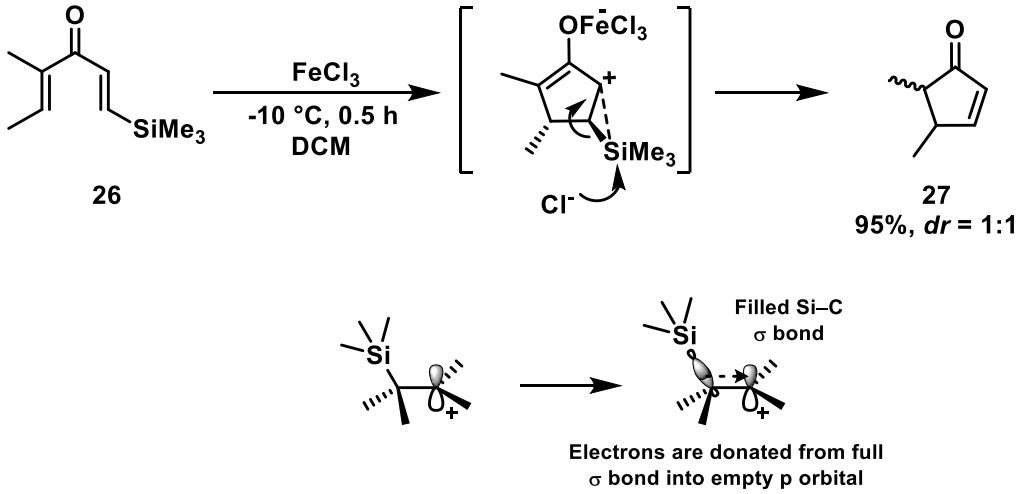

Scheme 1.13. The regioselective Nazarov cyclization.

Kocienski and co-workers discovered increased reactivity for substrates such as **28** with alkoxy substituents at C-2 of the dienone (α to the carbonyl group) and, having that knowledge, a cyclopentannulation protocol was proposed using protic acid in methanol. This synthetically important example of the Nazarov cyclization occurred in moderate yield, with the formation of single product **29** (Scheme 1.14). Noteworthy, during the reaction course C-3 oxygen formed the enol, while the cyclopentenone C=O in compound **29** is on former C-2 of the dienone, due to hydrolysis.[38,39]

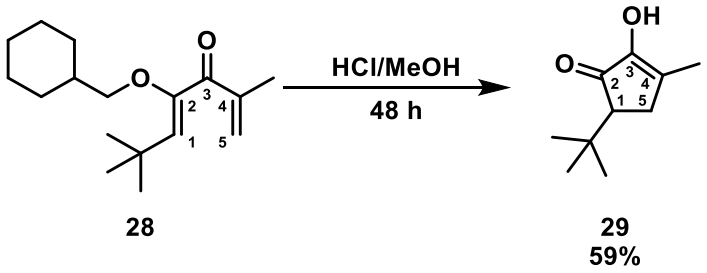

28 **29**
59%

Scheme 1.14. The polarized Nazarov cyclization/hydrolysis sequence.

In its typical manifestation, the Nazarov cyclization requires superstoichiometric quantities of strong Lewis or protic acids. However, in cases with α-functional groups, it was noticed that a rapid Nazarov reaction might be achieved with catalytic amounts of mild Lewis acid. Frontier and co-workers showed that substrates akin to **30** having both EWG and EDG as substituents showed increased reactivity and required milder conditions to initiate cyclization (Scheme 1.15). A reasonable question that can be asked is why does the presence of both an EDG and an EWG permit the reaction to occur under milder conditions? The answer can be reasoned that an EDG lowers the activation barrier for the Nazarov 4π electrocyclization. Further, an EDG also stabilizes the newly formed intermediate; the reason for this is the increased electron density on the terminal carbon of the pentadienyl cation (β-position relatively to carbonyl). On the other hand, EWG lowers the TS energy for cyclization and influences the charge distribution in the resulting oxyallyl cation, which results in the regioselective proton elimination.[40] In the absence of EWG, cyclization efficiency is reduced. More studies on an EWG influence are ongoing in the Frontier group.[41]

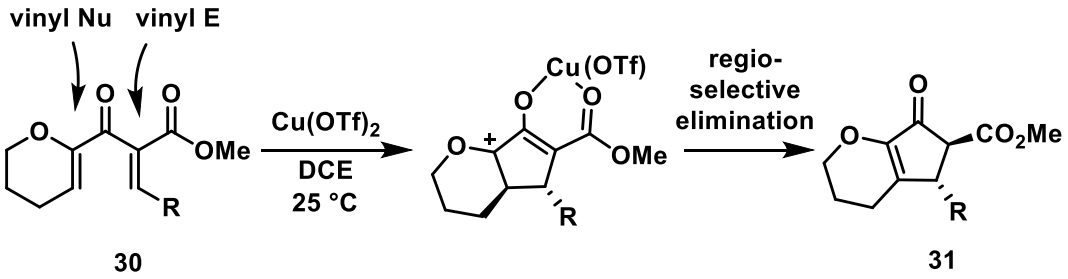

Scheme 1.15. The polarization effects on the Nazarov cyclization.

A polarized version of the Nazarov cyclization was used later by the Frontier group for the synthesis of a range of metabolites isolated by King from roots and stems of *Aglia elliptifolia*.[42] These metabolites were shown to have cytotoxic activity against human lymphocytic leukemia cell lines, as well as other tumor lines. Stereoselective total synthesis of rocaglamide (Figure 1.3) represents a fearsome task for chemists because it has five contiguous stereogenic centers. Because of such a dense substitution pattern, there are only a few reports of low yielding multi-steps syntheses.[43,44]

Frontier and co-workers succeeded in generating a pentadienyl cation with an unusual approach using allenol ether peracid oxidation, providing the desired product **33** in 13 steps. The elimination regioselectivity is controlled by polarization effects of β-substituents, p-methoxyphenyl, and a tributyltin group, which undergo protodestannylation from α-stannylketone (Scheme 1.16).[45]

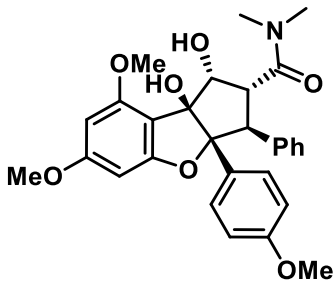

Figure 1.3. Rocaglamide.

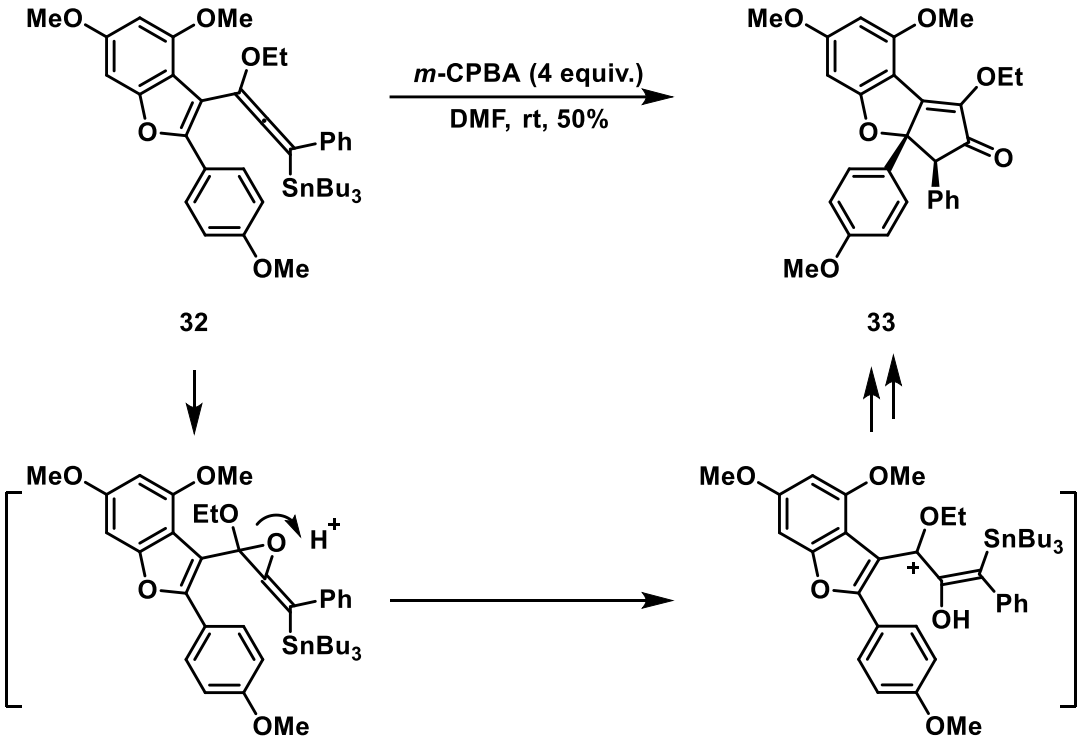

Scheme 1.16. The rocaglamide precursor synthesis.

Modifications of the Nazarov cyclization, which address previously mentioned limitations and aim to increase reaction usefulness have been a hot area for academic research for the following reasons:

a) the possibility to apply substrates different from the divinyl ketones;

b) the formation of a pentadienyl cation intermediate under different conditions that may be more compatible with sensitive functionality;

c) the interruption of the reaction course by the formation of additional bonds rather than simple elimination.

Intensive studies of the subject resulted in the generalization of all these kinds of reactions under the name of the Nazarov cyclization, as all of them have the same mechanistic template.[19,46]

1.3 The Interrupted Nazarov Cyclization

Since the discovery of the Nazarov cyclization, many researchers have put an effort into its further development. The goal was to obtain a safe, inexpensive, and operationally

simple method to build-up complexity in products,[19] providing additional functionalization and structural diversity. This group of reactions was termed collectively as the "interrupted Nazarov reaction", because of a common trend to trap reactive intermediates using electrophiles and nucleophiles in an intra- (Scheme 1.17) and intermolecular (Scheme 1.18) fashion after the event of the 4π conrotatory electrocyclization.[19,47]

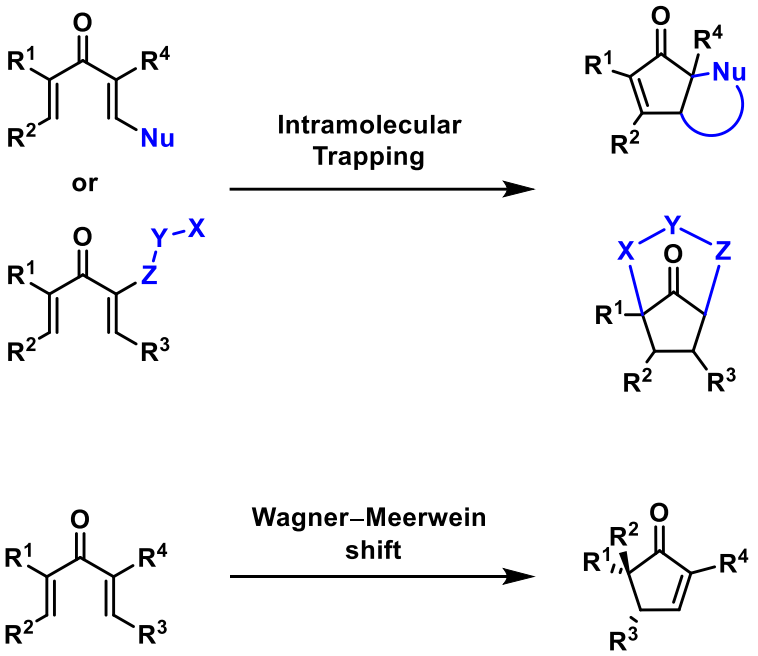

Scheme 1.17. Intramolecular variants of the interrupted Nazarov reaction.

A deeper understanding of the reaction would allow chemists not only to expand the dimension of an appropriate choice of precursors but, at the same time, to gain new reactivity and to popularize the method itself, developing numerous novel ways towards accessing functionalized cyclopentanoids. For example, studies on trapping of the oxyallyl cation will allow for the two stereocentres on the former termini carbons to be retained, as opposed to the elimination step. Bearing in mind the above, the following sections will discuss advances in intramolecular and intermolecular versions of the interrupted Nazarov reaction.

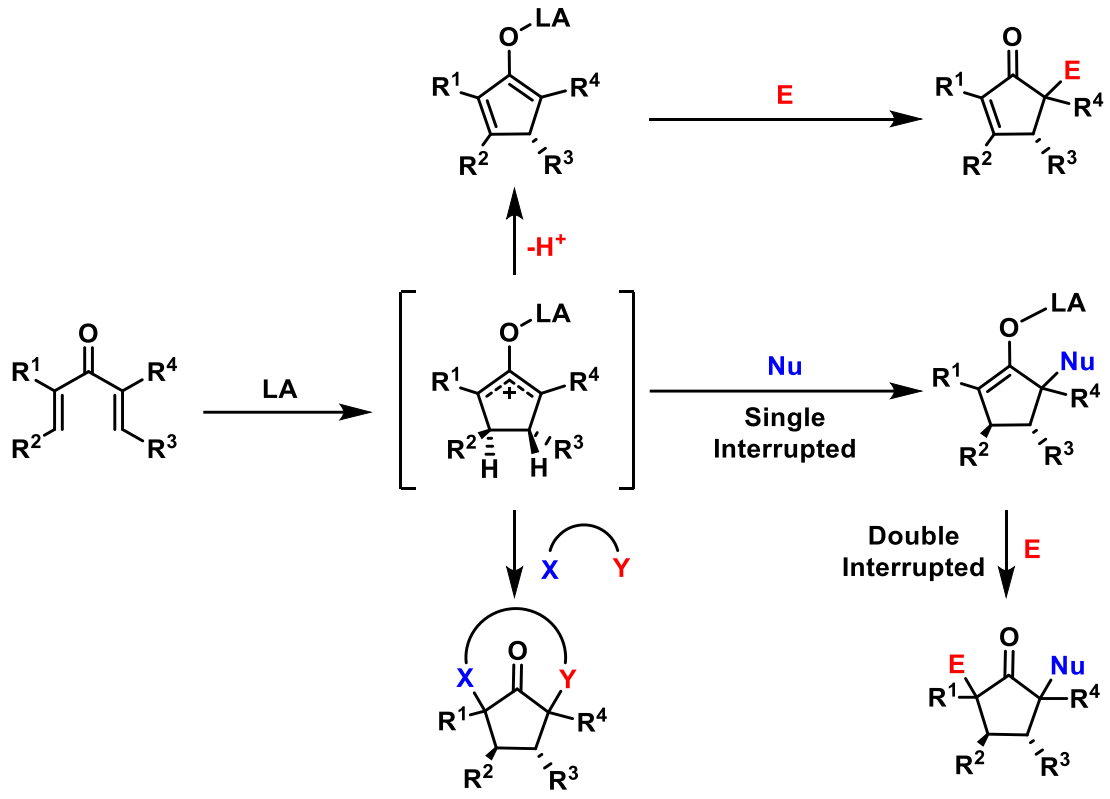

Scheme 1.18. Intermolecular variants of the interrupted Nazarov reaction.

1.3.1 The Intramolecular Interrupted Nazarov Cyclization

The first example of the intramolecular interrupted Nazarov cyclization was introduced by West and co-workers in 1998.[48] A tethered alkene in **34** was able to trap the oxyallyl cation resulting from Nazarov electrocyclization. A variety of Lewis acids were shown to initiate the desired process, but $BF_3{\cdot}OEt_2$ was shown to convert the substrate selectively into a single product, hemiketal **35**, after trapping of oxyallyl cation by olefin in a 5-*exo*-*trig* pathway. Subsequently, there is an attack of the boron enolate oxygen onto the newly formed tertiary carbocation to give a strained tricyclic enol ether. Aqueous workup of enol ether selectively hydrolyzed it solely from the top face (less-hindered), forming the desired product in excellent yield (Scheme 1.19).

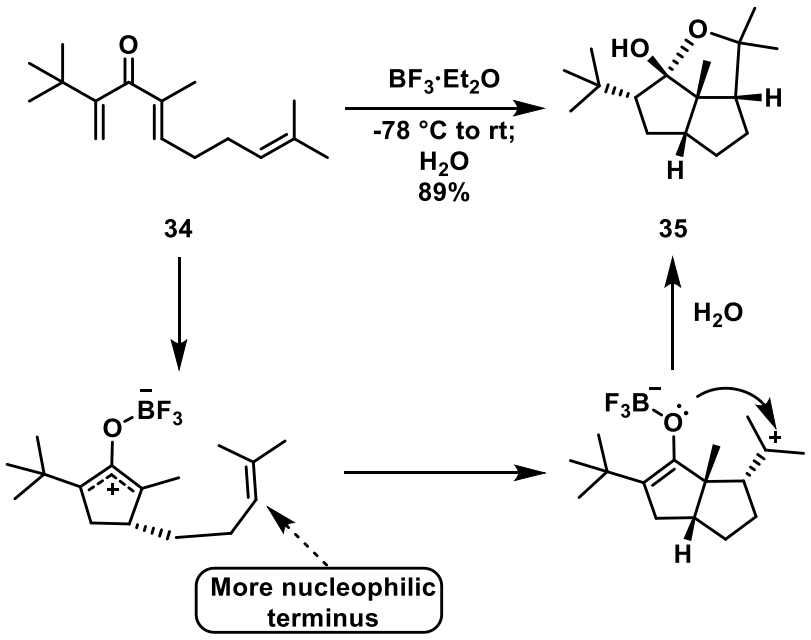

Scheme 1.19. Interrupted Nazarov reaction via oxyallyl trapping by pendent alkene.

Several attempts were made towards selective trapping of the oxyallyl cation via a *6-endo* closing fashion. A carbocation intermediate was formed efficiently from **36**, but it did not result in the selective generation of a single product. During the reaction, multiple products were formed. Conventional proton elimination led to hydrindenone regioisomers (**37a**). Product **37b** was formed by hydride shift reinforced by boron enolate, and compound **37c**, in turn, by alkylation (Scheme 1.20).[49]

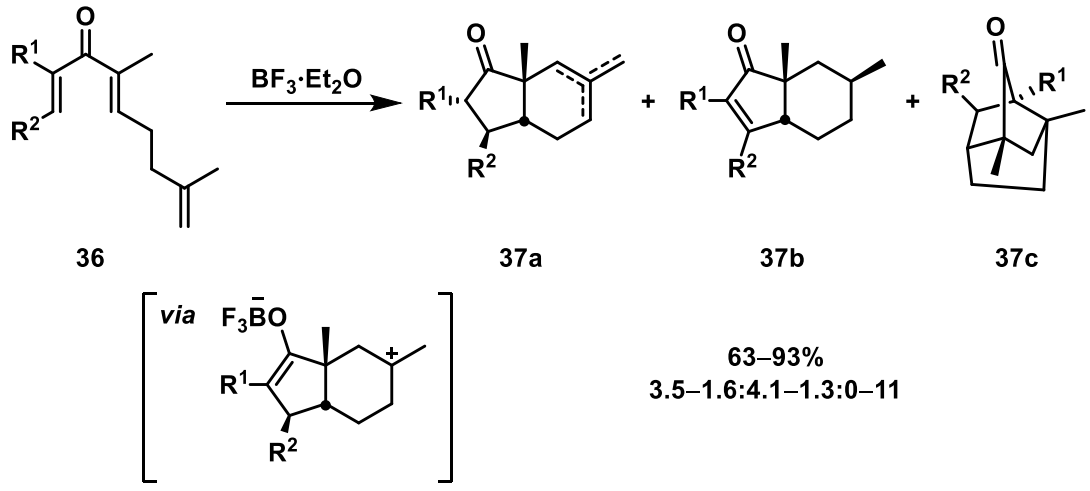

Scheme 1.20. The 6-*endo* olefin trapping.

Further studies by West and co-workers towards the taxane skeleton resulted in the discovery that an alkene, which is held close to the divinyl ketone in a rigid structure of compound **38**, also can trap the neighboring oxyallyl cation. The nucleophilic attack by the double bond results in a homoallyl/cyclopropylcarbinyl rearrangement, leading to the formation of the secondary carbocation, which undergoes subsequent hydride transfer to form highly strained cyclopropyl ketone **39** (Scheme 1.21).[50]

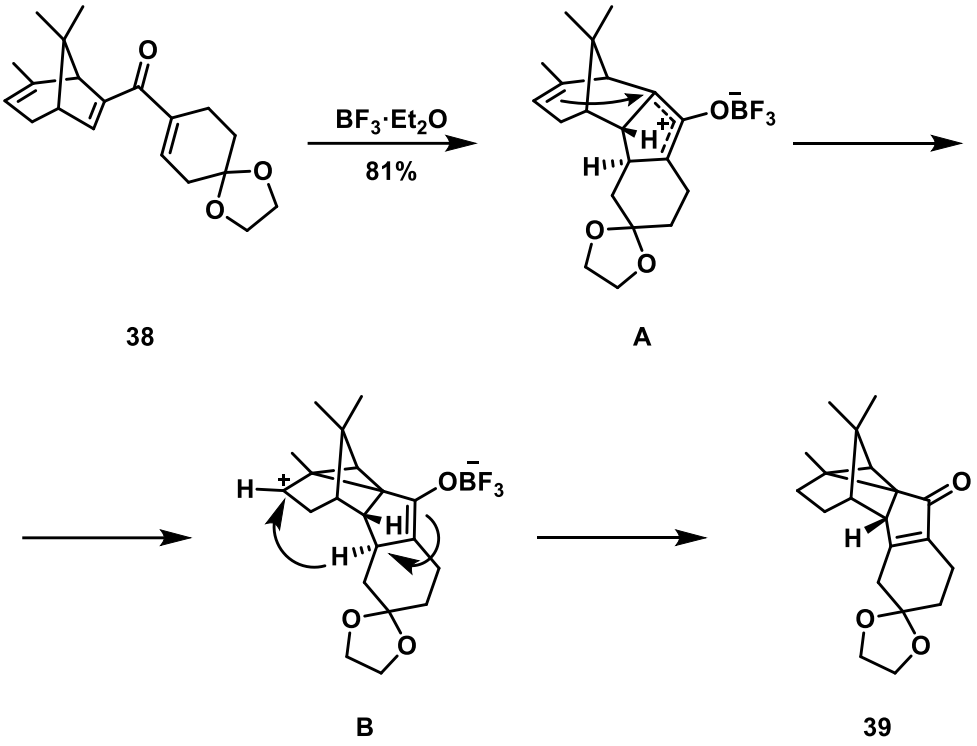

Scheme 1.21. Interrupted Nazarov reaction by olefin trapping in a rigid system.

Later, a series of trienes (**40a, b**) was synthesized by West and co-workers to study the possibility to trap oxyallyl cation at first with an intervening olefin, then with a terminal arene in a *6*-endo cascade polycyclization event. A range of protic and Lewis acids were studied. They provided different products starting from the conventional Nazarov cyclization product **41** and ending with tetracycles **43**. A stronger Lewis acid, $TiCl_4$, was shown to initiate the desired polycyclization reaction with high diastereoselectivity at the lower reaction temperature. The temperature choice limited

various undesirable side-reactions (Scheme 1.22). It is noteworthy that the West group was able to accomplish the furnishing of five new stereocenters stereoselectively in a single reaction.[51]

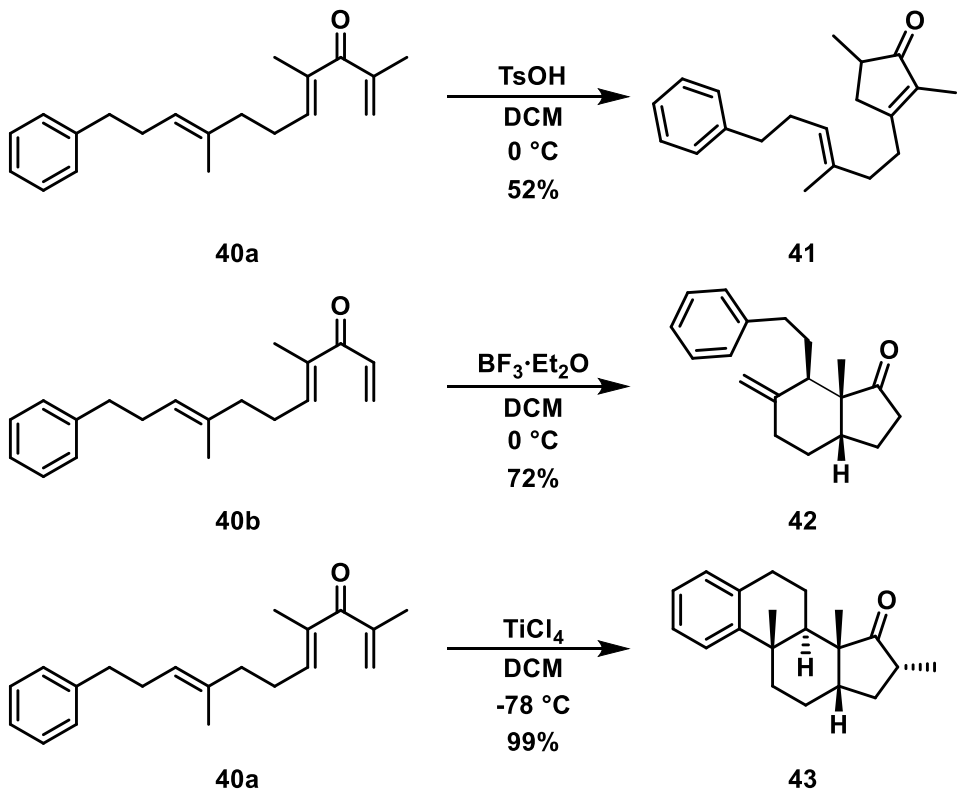

Scheme 1.22. Lewis acid-mediated cascade Nazarov polycyclization.

As the next step in the concept development, West and co-workers prepared tethered arene moieties **44** and **46**. In case of low nucleophilicity of the phenyl trap, no trapping was observed. The dienones with highly nucleophilic β-aryl substituents were shown to undergo the desired reaction with an excellent yield. The interrupted Nazarov cyclization is possible due to the efficient trapping of the oxyallylic cation by the attack from an electron-rich aromatic ring that subsequently rearomatizes (Scheme 1.23).[52] West group polycyclization examples efficiently emphasized the possibility of the interrupted Nazarov cyclization applicability for complex structures preparation.

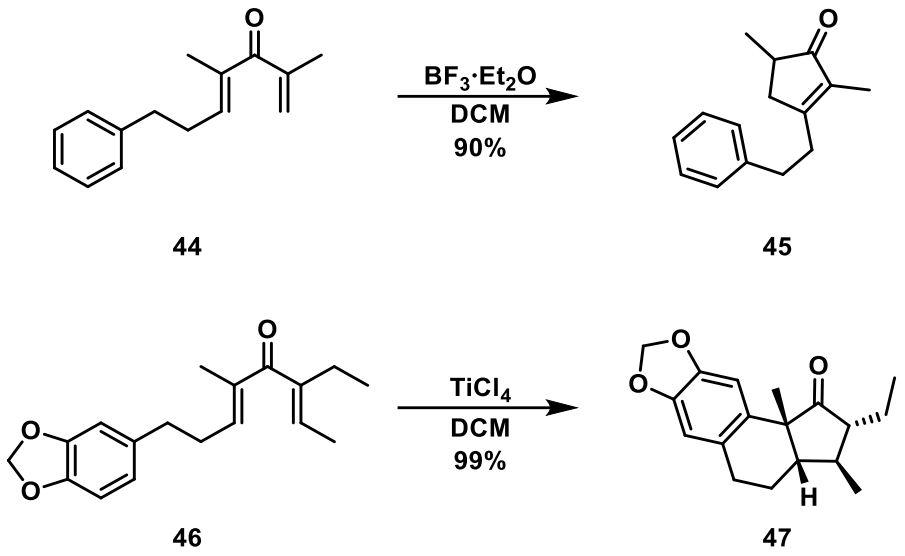

Scheme 1.23. Interrupted Nazarov cyclization via oxyallyl trapping by nucleophilic arenes.

Flynn and co-workers successfully reported the asymmetric intramolecular interrupted Nazarov cyclization example. The electron-rich arene substituent of compound **48** trapped the oxyallyl intermediate that was formed after the addition of protic acid and gave desired compound **49** in 53% yield. The formation of single product **49** was proved by means of ^{1}H NMR. As a result of a regioselective reaction, two new rings were formed with the four new contiguous stereogenic centers (Scheme 1.24).[53]

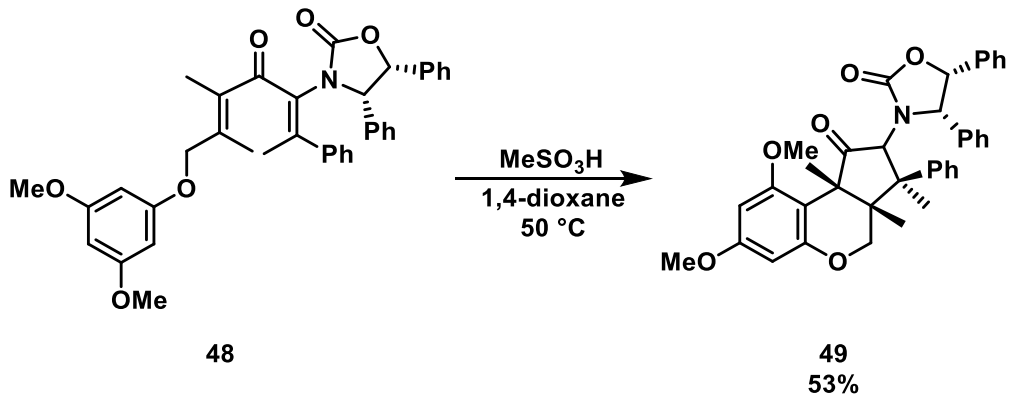

Scheme 1.24. The asymmetric interrupted Nazarov cyclization by Flynn and co-workers.

In previous studies, the oxyallyl cation has shown its capability to play the role of the electrophile. Similarly, the oxyallyl intermediate appeared to be a good dienophile for

a concerted [4+3]-cycloaddition.[54] This reaction was performed using **50a** in the presence of $FeCl_3$ at low temperatures. Cyclooctenes **51a** and **51b** with the ketone bridge were formed through exo and endo transition states. In both cases dienophile approached from the less hindered face of the intermediate. Preference for trapping mode [4+3]-cycloaddition over [3+2] was documented for compound **50b** with a longer carbon chain (Scheme 1.25).

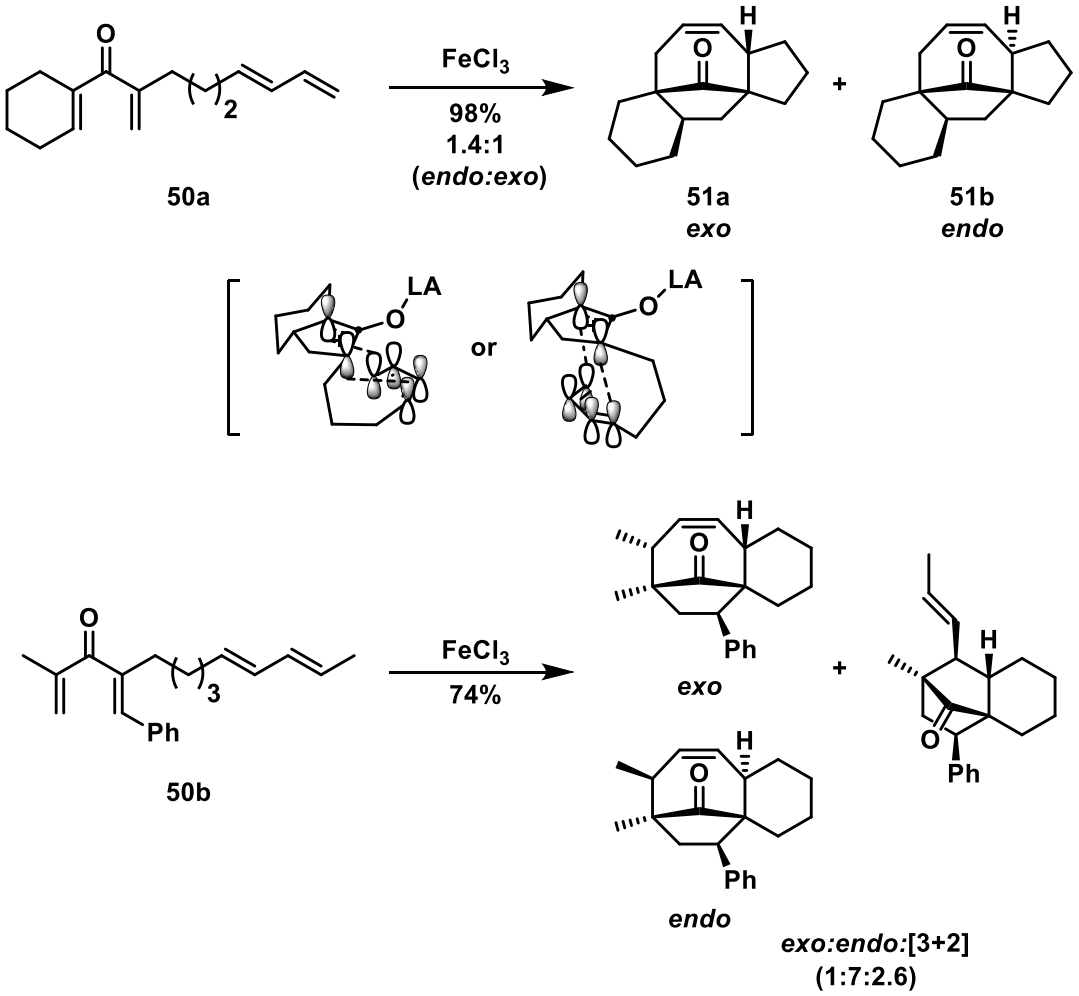

Scheme 1.25. The [4+3] intramolecular cycloaddition.

Several examples of heteroatom-based intramolecular traps have been reported. The Nair group applied oxygen traps as intramolecular nucleophiles. They formed from an atypical cross-conjugated dihydrofuran **52** the complex bicyclic lactone **53**. The

starting material was dimethyl acetylene dicarboxylate and dimethoxy carbene. The addition of $BF_3 \cdot OEt_2$ initiated conversion in excellent yield (Scheme 1.26).[55]

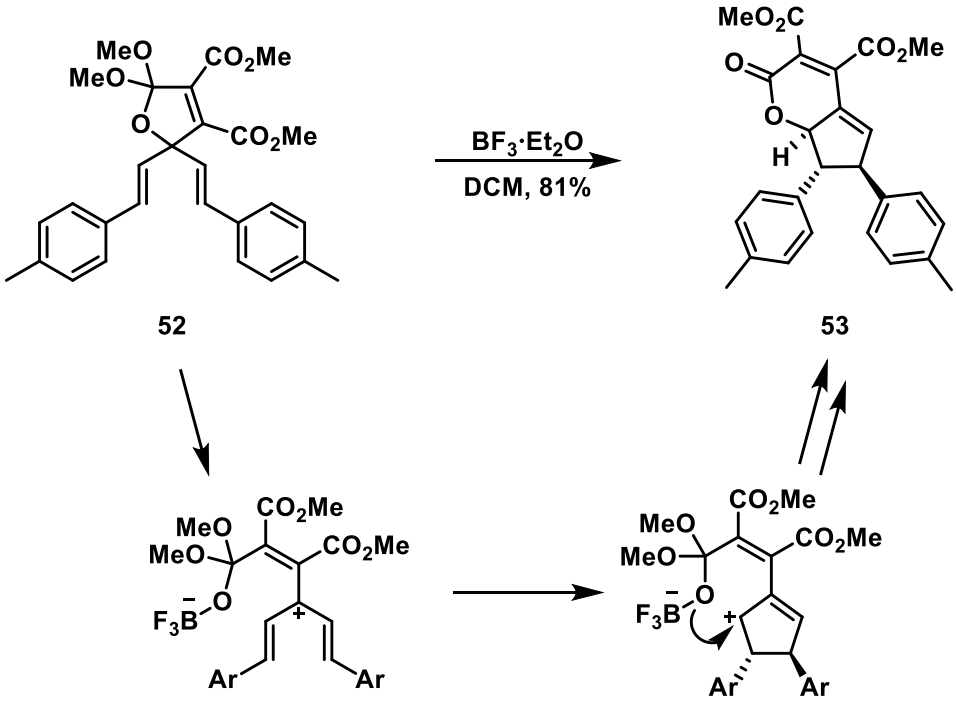

Scheme 1.26. Interrupted Nazarov cyclization via oxygen-trapping.

The treatment of dienone **54** bearing an intramolecular azide trap with $BF_3 \cdot OEt_2$ resulted in direct azide trapping of the oxyallyl intermediate. A newly formed, intriguing endoperoxide **56** was observed if the reaction vessel was subjected to aerobic conditions after cyclization, performing the second trapping event of a dipolar intermediate. Endoperoxides are known to be prone to undergo further functionalization. Dihydropyridone **57** synthesis can be accomplished if the reaction is performed in an inert atmosphere (Scheme 1.27).[56]

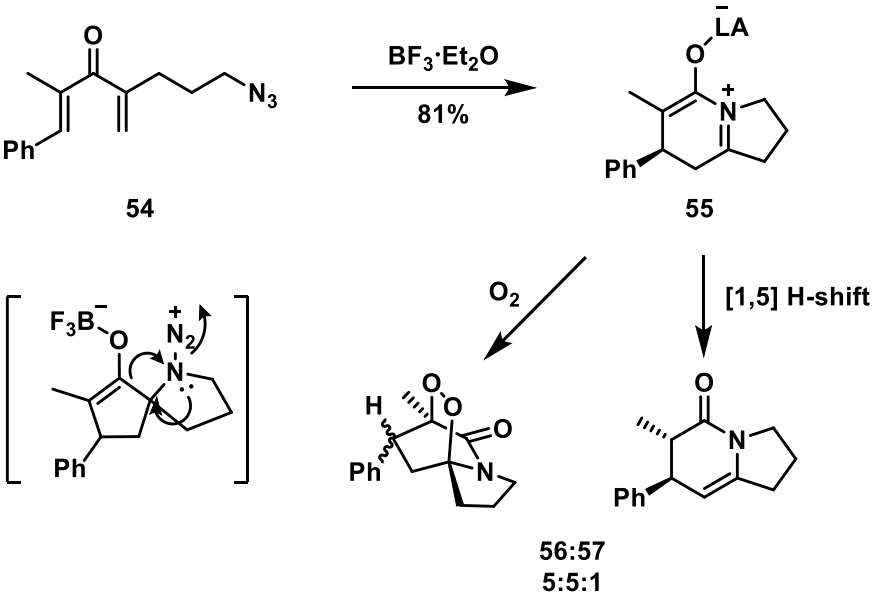

Scheme 1.27. The interrupted Nazarov cyclization via oxyallyl trapping by azide.

The intramolecular interrupted Nazarov cyclization has become an efficient method to synthesize polycyclic motifs. This efficient approach allows a complex structure synthesis in a minimum amount of steps, with efficient stereocontrol. The Nazarov intramolecular interrupted cyclization remains an active research area and provides many research opportunities.

1.3.2 The Nazarov/Wagner–Meerwein Rearrangement

The previous section discussed the intramolecular interruption of the Nazarov cyclization. The Nazarov/Wagner–Meerwein cyclization has the same concept, but the reaction normally is interrupted via a 1,2-alkyl shift.

The Wagner–Meerwein rearrangement is named after Yegor Y. Vagner, who was published in German journals as Georg Wagner.[57] At the turn of the 20th century, Wagner performed the acid-catalyzed transformation of borneol into camphene. Based on compound properties he determined that it did not have the same structure (Scheme 1.28).[58] Hans Meerwein proposed that the reaction goes through the formation of carbocation to rationalize the racemization of isobornyl chloride. He envisioned the possibility for H and C shifts to happen during rearrangements to form a carbocation with

higher stability. Meerwein's insight opened a door for further organic chemistry development.[59]

Sometimes during the Nazarov cyclization, Wagner–Meerwein shifts can take place, but in most cases, side products are undesired or formed in low yields. As one of the early examples, Denmark and co-workers were trying to get a 6π 7-membered cyclization to happen, but instead, they observed the alkenyl shift. After the Nazarov cyclization, the Wagner–Meerwein rearrangement occured trapping an oxyallyl cation that was generated in situ.[37,60] A cinnamyl group, in the presence of $FeCl_3$, underwent a 1,2-cationic shift to form cyclopentanone **59** in moderate yields (Scheme 1.29).

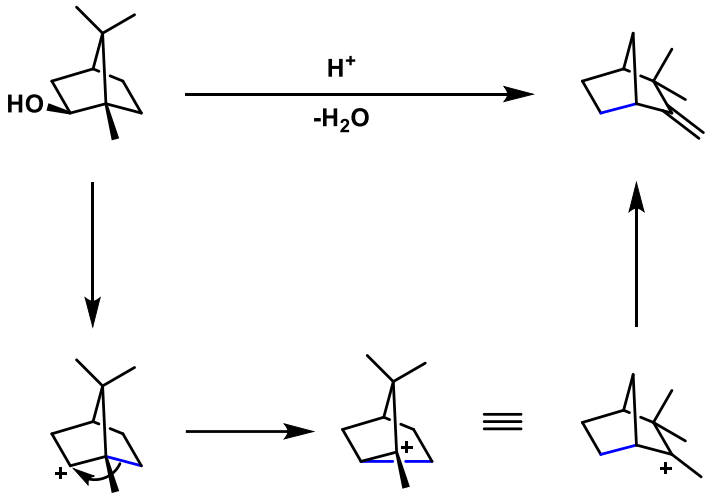

Scheme 1.28. The Wagner–Meerwein rearrangement.

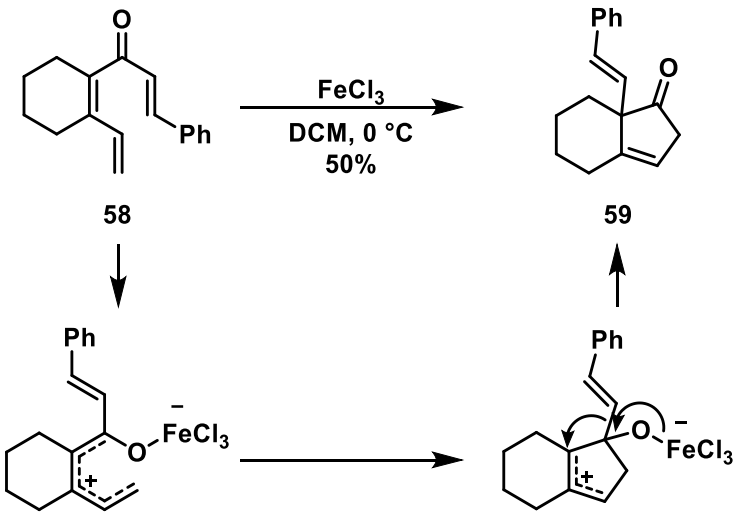

Scheme 1.29. The iron-catalyzed Nazarov cyclization interrupted by the cinnamyl group shift.

Initial attempts to form spirocyclic compound **62** were undertaken by the Kuroda group (Scheme 1.30). They treated dienone **60** with $FeCl_3$ at -30 °C and warmed it up to room temperature. The desired spirocyclic compound **62** was obtained in 56% yield. However, if the starting temperature of the reaction was higher (-10 °C), fused bicyclic product **61** was formed in a 62% yield.[61]

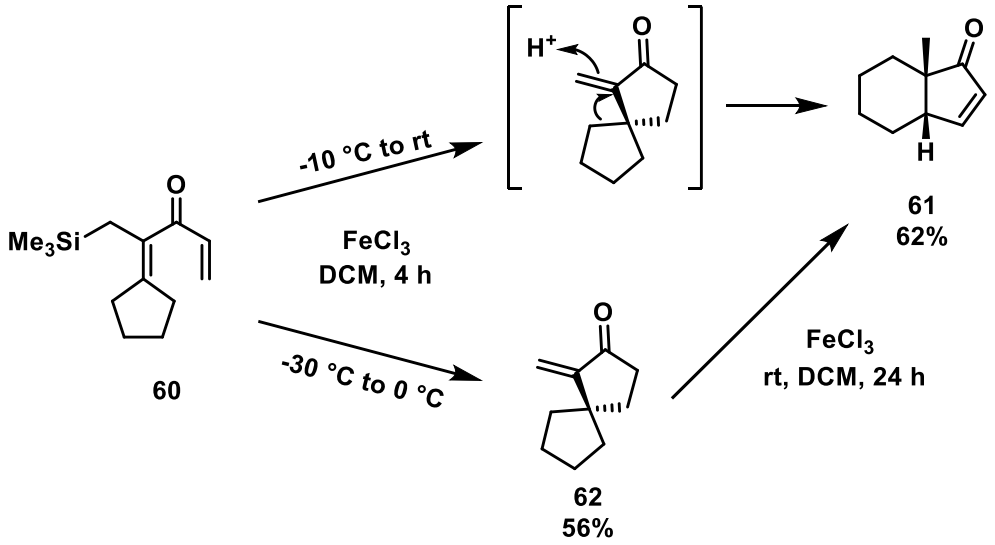

Scheme 1.30. The Kuroda group spirocyclic compound **62** preparation.

New applications of the Nazarov/Wagner–Meerwein sequence were developed in the Frontier group, as well. Formation of the expected fused bicyclic system **64** was

observed upon treatment of dienone **63** with catalytic amounts of $Cu(OTf)_2$. A stoichiometric amount of chiral Cu(II) salt resulted in the formation of spirocyclic product **65** in a high yield with up to 64% *ee*. Frontier explained the reactivity change by the basicity of oxygen, which can promote elimination in the case of catalytic amounts of Lewis acid. The increase of the Lewis acid **66** amount from catalytic to the stoichiometric amount was proposed to effect carbonyl oxygen by saturating it with the catalyst. That results in suppressing the proton elimination, allowing the Wagner–Meerwein rearrangement to take place forming the desired product **65** (Scheme 1.31).[62]

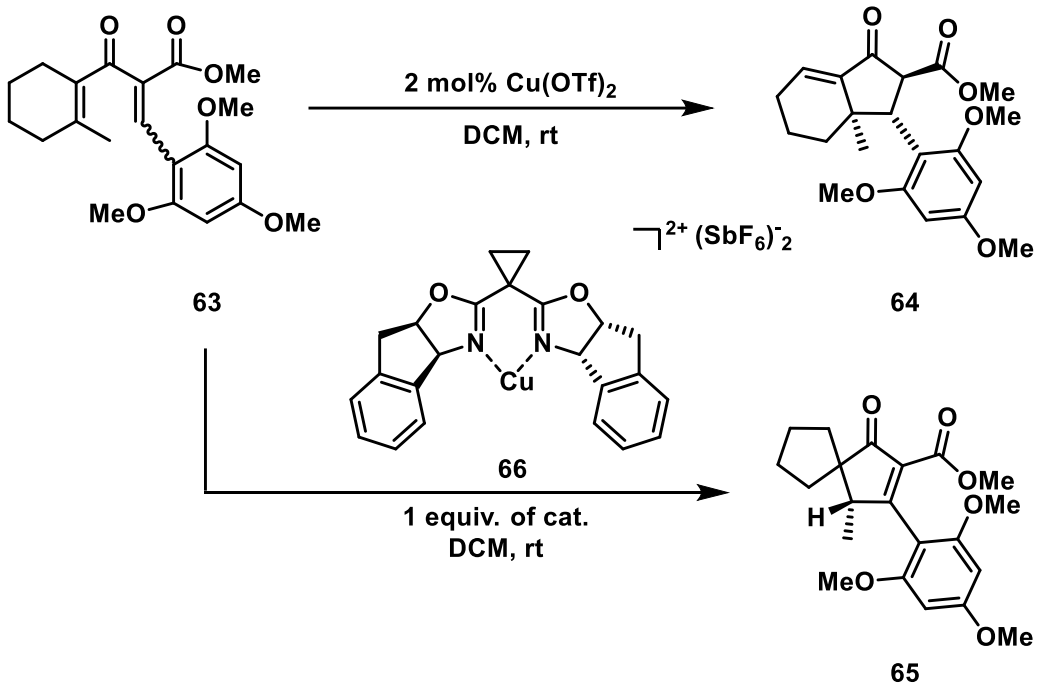

Scheme 1.31. The Cu-catalyzed Nazarov cyclization.

Regarding the mechanism of the reported Nazarov/Wagner–Meerwein reaction, several consecutive suprafacial cationic 1,2-shifts should take place (Scheme 1.32).[63] The formation of oxyallyl intermediate **67a** is followed by a 1,2-alkyl shift. Newly generated intermediate **67b** performs the second 1,2-hydride (A) or alkyl (B) migration, yielding either product **68** or **69**. Further studies of the reaction scope with alkyl β-substituted dienones showed that preference between hydride and alkyl migration highly depends on the ability of the R group to migrate (Scheme 1.33).[64] After alkyl shift (ring contraction)

next step highly depends on migratory aptitude. The migratory aptitude of alkyl chains is usually small compared to that of aromatic ones, and, in those cases, there is a higher preference for a 1,2-hydride shift (Scheme1.33, A). It is observed that cyclic starting materials in the case of bulky β-substituents both have high yields and diastereomeric ratios for 1,2-alkyl shifts (Scheme1.33, B). For the acyclic substrates, the 1,2-hydride shift is preferred (Scheme1.33, C).

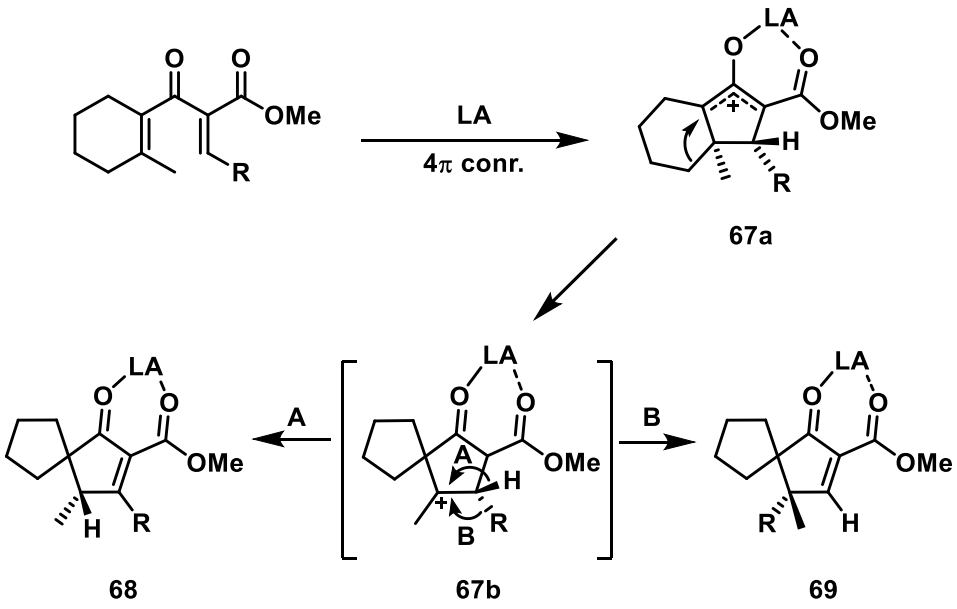

Scheme 1.32. The Nazarov/Wagner–Meerwein cyclization proposed mechanism.

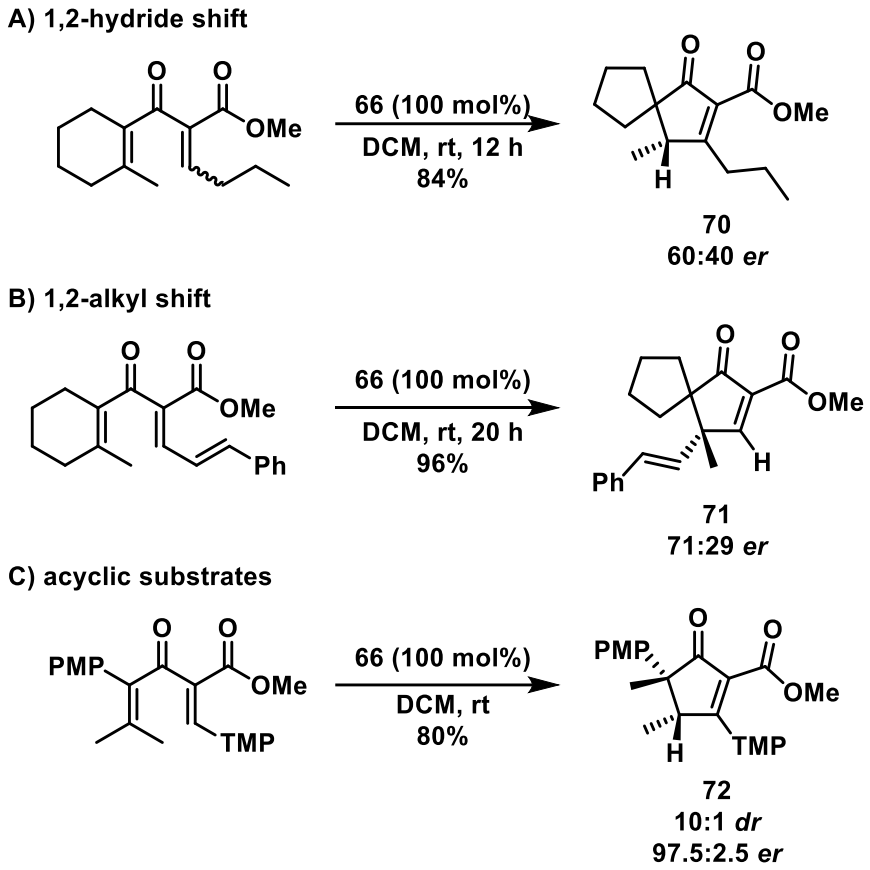

Scheme 1.33. The migratory aptitude of β-substituents in cyclic and acyclic substrates.

The previously mentioned reactivity preference between the Nazarov cyclization and Nazarov/Wagner–Meerwein cyclization caused by different Lewis acid amounts was based on oxygen basicity. Additional evidence in support of the Frontier group hypothesis was observed in experiments with stoichiometric amounts of $NaBAr^F$. The addition of a stoichiometric amount of $NaBAr^F$ to the reaction mixture resulted in a suppressed proton elimination pathway by Na^+ coordination to the carbonyl group. The counter anion BAr^{F-} noncoordinating behavior and salt's solubility is proposed to be part of the success of the additive. The additive in the presence of the catalytic amount of Cu^{II} was able to facilitate a 1,2-alkyl shift, forming compound **74** in high yield and diastereomeric ratio (Scheme 1.34).[65]

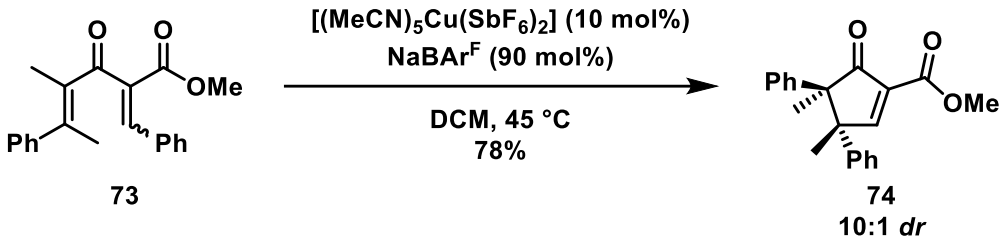

Scheme 1.34. The Nazarov/Wagner–Meerwein reaction in presence of $NaBAr^F$.

The Nazarov/Wagner–Meerwein reaction has been used towards the synthesis of diterpenoid guanacastepene A by Chiu and colleagues. The synthesis of the desired natural product has been envisaged through the application of the Nazarov cyclization. Interestingly, it was observed that preference between the conventional Nazarov reaction and the Wagner–Meerwin rearrangement was dependent highly on the Lewis acid choice.[66] Spirocyclic product **77**, was formed with BCl_3, while $BF_3{\cdot}OEt_2$ provided the product of the conventional cyclization (Scheme 1.35).

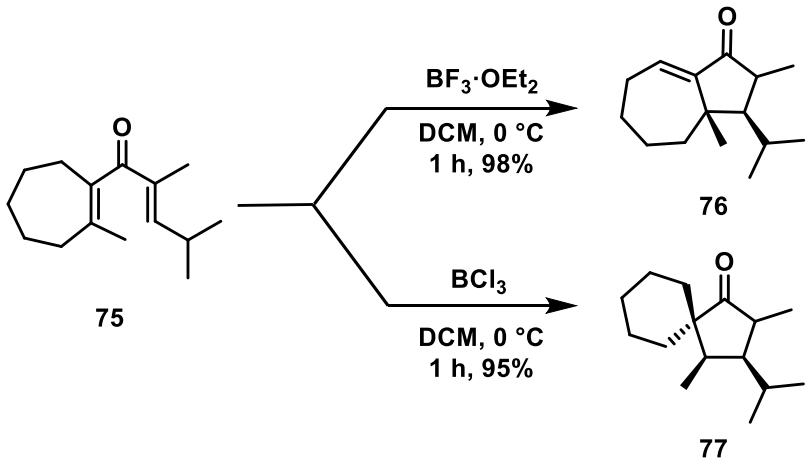

Scheme 1.35. Synthesis of the core structure of the diterpenoid guanacastepene A.

1.3.3 The Intermolecular Interrupted Nazarov Cyclization

The area of intermolecular interrupted Nazarov cyclization can be divided into three main groups: electrophilic, nucleophilic, and cycloaddition (Scheme 1.36). A nucleophilic attack usually happens only after the formation of an oxyallyl cation in a formal SN_1 fashion (formation of the carbocation is required) or in a [3+2] fashion, with the further opening of the newly formed cycle.[19,67] Electrophilic reagents have been shown as

applicable traps for interrupted Nazarov reaction. They are usually used to trap enolates, which are formed after the proton elimination from the oxyallyl cation. If no nucleophilic agent is present in the system, it is known that the predominant process is a proton elimination from an oxyallyl intermediate. This results in the formation of an enolate, which can react with Michael acceptors and halogen electrophiles.[68] The third type of Nazarov cyclization traps might be envisioned as [3+2] and [4+3]-cycloadditions of 1,3-dienes forming products **78** and **79**, complex bicyclic products with pre-setup stereogenic centers after conrotatory 4π cyclization.[69]

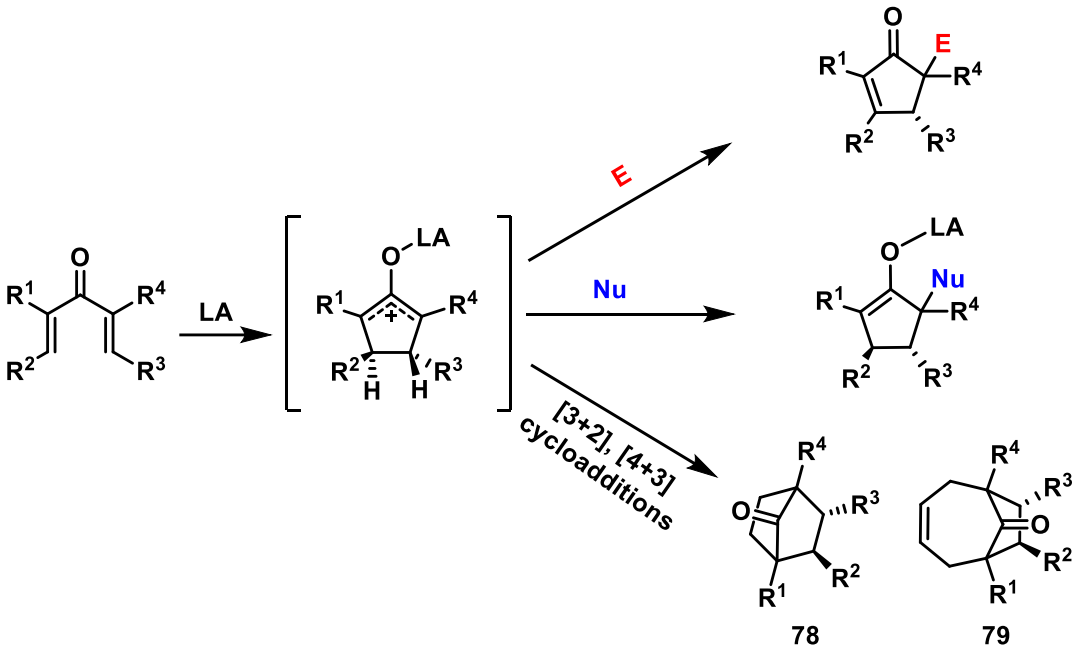

Scheme 1.36. The intermolecular interrupted Nazarov cyclization.

1.3.3.1 Nazarov Cyclization Interrupted By Cycloaddition And Nucleophiles

Interrupted Nazarov cyclization is a facile synthetic method to prepare a cyclopentanone moiety, with the formation of up to four new stereogenic centers. Two out of four stereogenic centers are usually formed during the conrotatory cyclization event. On the other hand, if the nucleophilic trapping of the oxyallyl cation takes place it results in two additional stereogenic centers formation. One during the trapping event, and one is set up during resulting enolate protonation.

The first example of the intermolecular interrupted Nazarov cyclization was a reductive Nazarov cyclization discovered by the West group. The reductive Nazarov cyclization required a hydride source that can tolerate the presence of Lewis acid in the reaction mixture to perform a stereoselective addition.[19,70] The addition usually occurs on a more highly substituted terminus of the oxyallyl cation, which is proposed to be the result of the higher charge stabilization (Scheme 1.37)[71].

The delivery of the small hydride from the more hindered side allows the bulkier substituent on the α carbon to avoid $A_{1,2}$ strain as the carbon assumes tetrahedral geometry. The protonation of the enolate occurs with lower diastereoselectivity and results in the formation of diastereomers **81** and **82**. It is noteworthy that reductive Nazarov cyclization can be performed using a catalytic amount of Lewis acid, while the vast majority of the known interrupted Nazarov cyclization examples require stoichiometric amounts.[72]

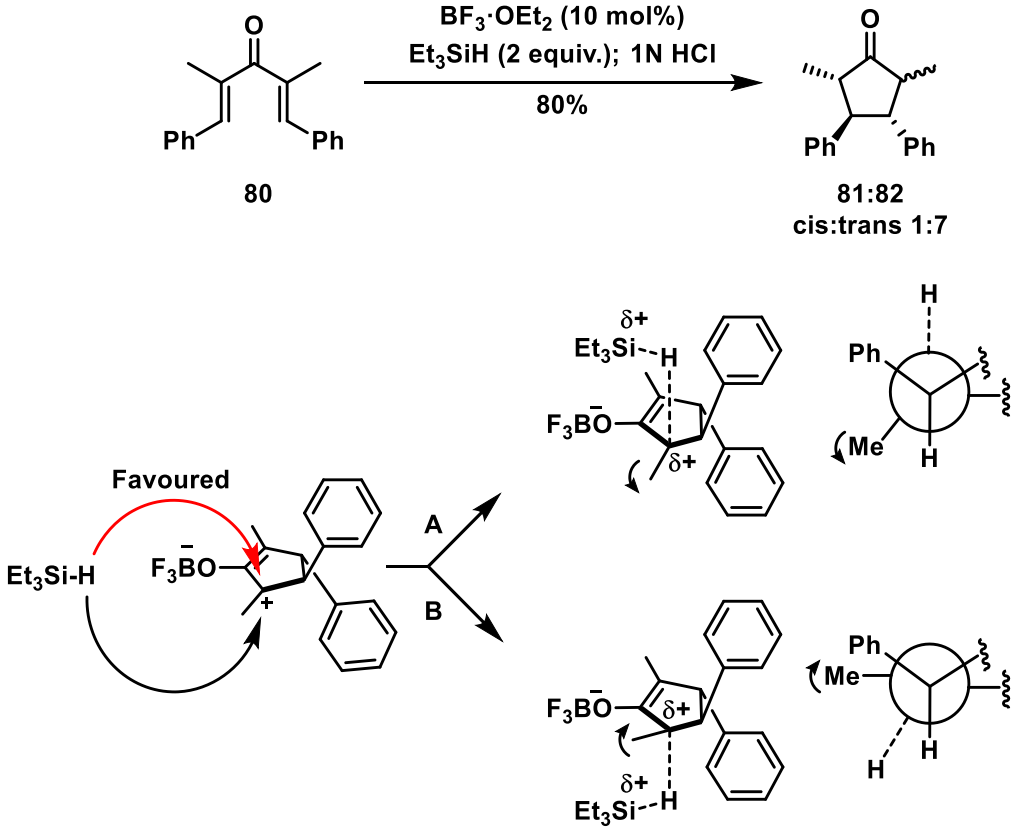

Scheme 1.37. The reductive Nazarov cyclization.

Successful interrupted Nazarov reactions employing intramolecular olefin traps inspired chemists to study the corresponding intermolecular process. Allyl silanes were a good category to study first, because of their known tolerance of Lewis acidic conditions. Later they were shown to be excellent trapping agents because of their intrinsic ability to function as nucleophiles.[73] Initial attempts to cyclize divinyl ketone in a cascade manner in the presence of allyltrimethylsilane led to a diastereomeric mixture of cyclopentanones **83**–**85**, with the combined yield of 43%, and bicycloheptanone **86**, with 49% yield. A bicyclic product was formed via a formal [3+2]-cycloaddition, with no other bicyclic by-products observed (Scheme 1.38).[74,75] West and co-workers proposed that **83** and **84** derive from desilylative elimination of a cationic intermediate resulting from allylsilane attack from the opposite face as the neighboring phenyl group, followed by unselective enolate protonation. On the other hand, **85** and **86** could be formed from the other cationic intermediate resulting from allylsilane attack *syn* to the neighboring phenyl group, where a partition is formed between desilylative elimination and C–C bond formation via enolate-carbocation capture, with the latter being favored.

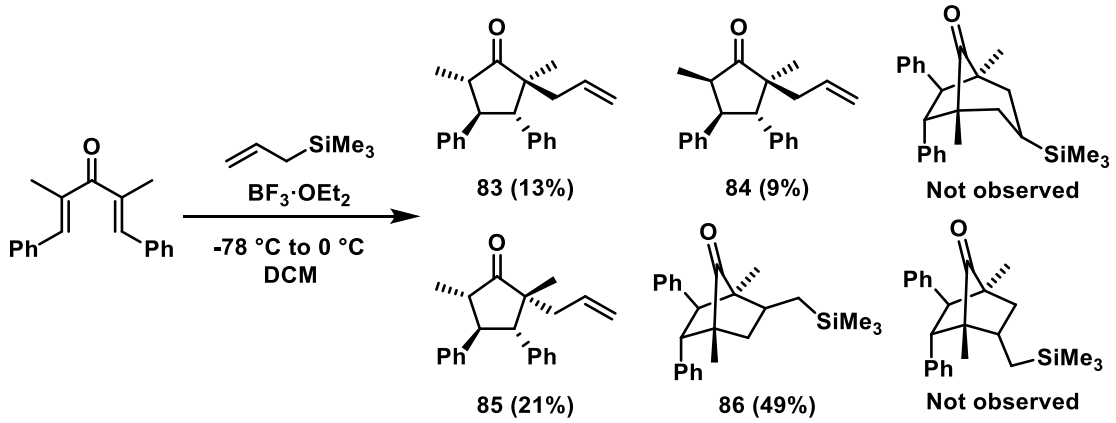

Scheme 1.38. The intermolecularly interrupted Nazarov cyclization by allyltrimethylsilane.

Further studies with the application of a triisopropylsilyl group led to the formation of products **87** in 38% and **88** in 61% yield, which can be explained by a slower desilylation during the reaction (Scheme 1.39). It is noteworthy that the change of Lewis acid from $BF_3 \cdot OEt_2$ to $SnCl_4$ results in a change of the major product. Divinyl ketones with unsymmetrical substitution formed the desired products in a regioselective fashion,

in which the least substituted terminus of the oxyallyl unit is prone to be attacked the first. The West group results are in strong correlation with the previously reported Noyori studies, in which the most stable enolate is obtained during the reaction (the attack of allylsilane occur on the least substituted end of the oxyallyl intermediate).[76] In addition to allylsilanes, the oxyallyl cation can undergo [3+2]-cycloadditions with the vinyl sulfides, forming **89** and **90** in high yields (Scheme 1.40).[77]

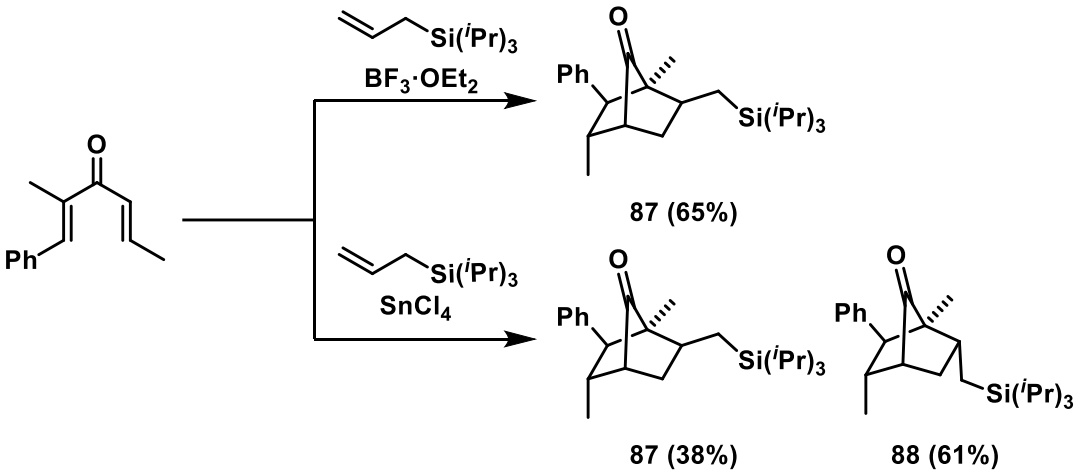

Scheme 1.39. The intermolecular interrupted Nazarov cyclization by allyltriisopropylsilane.

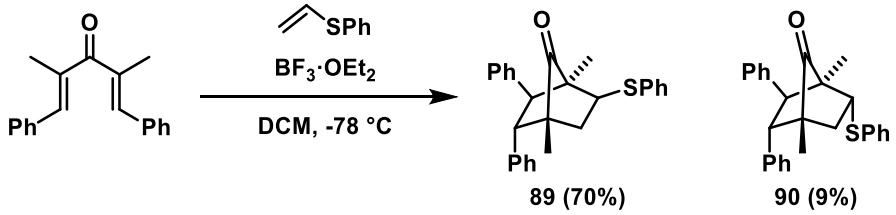

Scheme 1.40. The intermolecular interrupted Nazarov cyclization by olefins addition.

West and co-workers demonstrated that $BF_3 \cdot OEt_2$ can facilitate the cyclization of pentadienones in the presence of silyl enol ethers or silyl ketene acetals **91** (Scheme 1.41). The Nazarov/Mukaiyama addition usually results in the formation of an enolate, which after quenching forms product **92** in moderate to high yields. The reaction is stereoselective, and its scope includes aromatic and aliphatic substituents.[78]

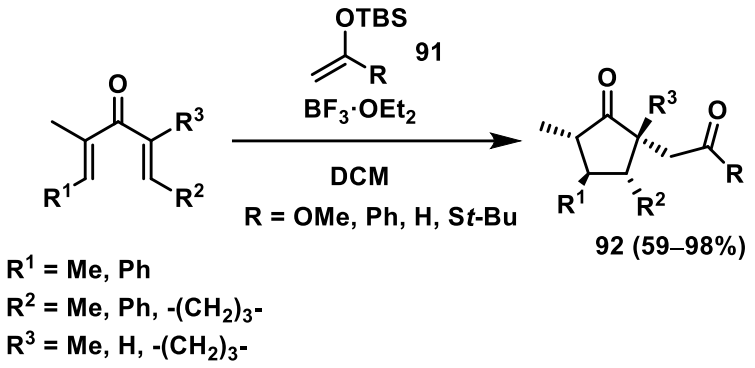

Scheme 1.41. Silyloxyalkenes application in the interrupted Nazarov cyclization.

There are only a few examples of alkynes' application as traps for the interrupted Nazarov cyclization. Mostly alkynes with aromatic substituents are used for it.[79] West and co-workers performed successful studies, showing $BF_3 \cdot OEt_2$ as the most efficient Lewis acid (Scheme 1.42). The alkyne performs the double addition with carbon and oxygen, forming intermediate bicyclodihydrofuran **93**. Compound **93** is cleaved during the quenching step, forming α-substituted cyclopentanones **94** in up to 97% yield.

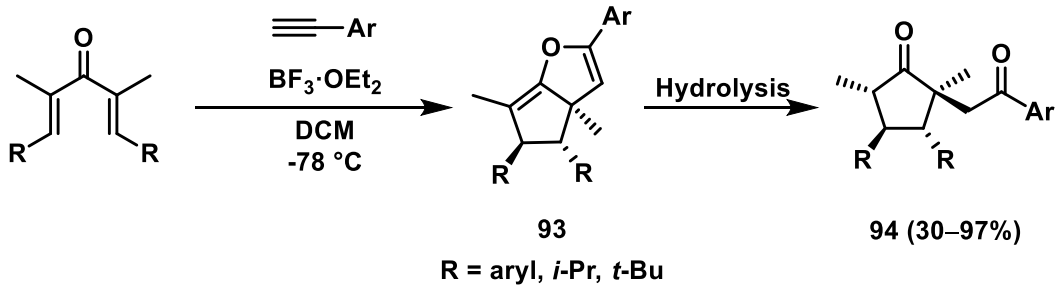

Scheme 1.42. Application of alkynes in the interrupted Nazarov cyclization.

In 2016, the Liu group discovered a possibility to trap the oxyallyl cation with an alkyne in the presence of $BF_3 \cdot OEt_2$ (Scheme 1.43).[80] Alkynyltrifluoroborate serves as an efficient promoter of the Nazarov cyclization by coordination of boron to oxygen. After a 4π conrotatory electrocyclization, coordinated to oxygen alkynyldifluoroborane serves as an efficient nucleophile by being able to deliver an alkyne to a newly formed cation from the boron center. After quenching the reaction, the desired product **95** is formed in high to excellent yields. Liu and co-workers were the first ones who successfully incorporated the Nazarov cyclization with the installation of alkyne groups as α-

substituents. Substitution patterns on pentadienones have a great impact on the course and the yield of the reaction. Only β-disubstituted divinyl ketones undergo the previously mentioned reaction; usually, no reaction was observed in the case of α-monosubstituted substrates. The delivery of the alkyne moiety takes place in a diastereoselective fashion to minimize the torsional strain.

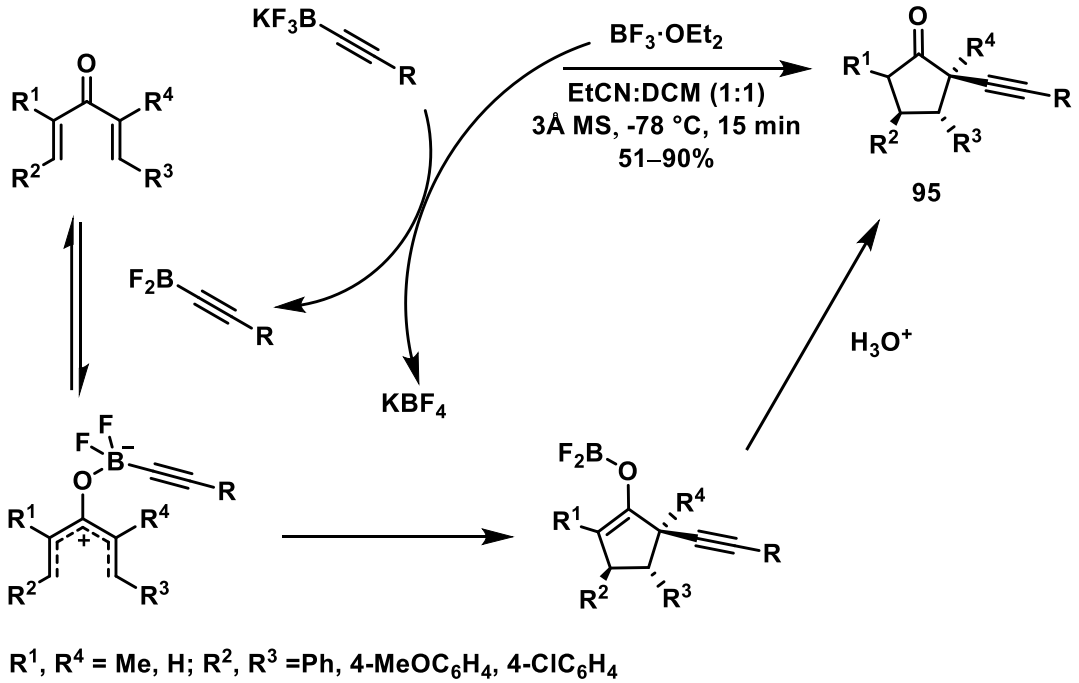

Scheme 1.43. The alkynyltrifluoroborate initiated Nazarov cyclization.

Allenes were shown to be able to act as nucleophiles by West and co-workers (Scheme 1.44).[81] Trapping with allenyl ethers took place diastereoselectively. The attack occurred from the opposite side from β-substituent to reduce torsional strain in cyclopentanone **96** forming a carbon-carbon bond with the central atom of the allene. Product **96** is formed in 37–63% yield depending on the β-substituents. The reaction scope is limited to β,β'-substituted starting materials; mono β-substituted starting materials did not provide the desired trapping products and underwent elimination of a proton instead of giving compound **97**.

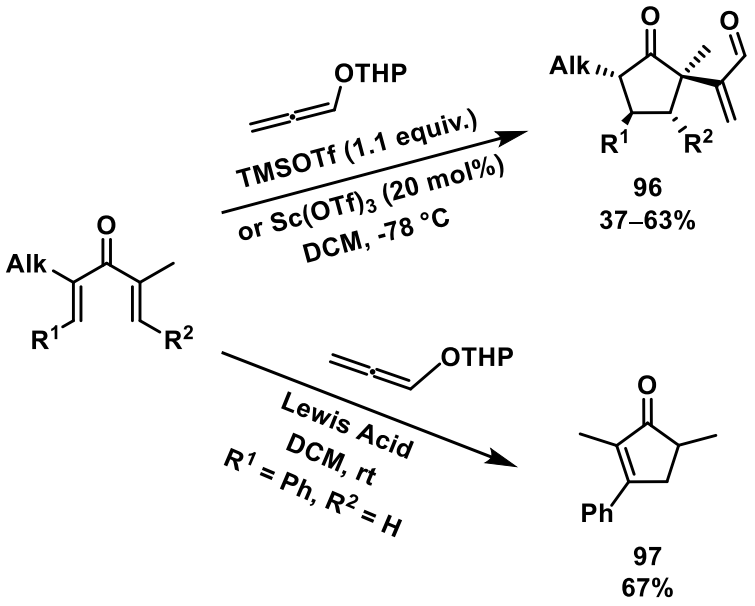

Scheme 1.44. Allenes nucleophiles in the interrupted Nazarov cyclization.

Efficient interruption of the Nazarov reaction via intermolecular [4+3]-cycloaddition was reported by the West group in 2003 (Scheme 1.45). A big range of cyclic and acyclic dienones underwent the desired process after the addition of $BF_3 \cdot OEt_2$.[82] The discovered reaction was completely stereoselective, producing cycloadduct **98** as a single diastereomer. Trapping of dienones with 1,3-dienes, followed by ozonolysis allowed to obtain triketones **100** in high to moderate yields. Triketones **100** can be applied for the synthesis of triquinacene moieties from triketones (Scheme 1.46).[83] The desired products were obtained in up to 63% yield with a 1.4:1 ratio for the isomers.

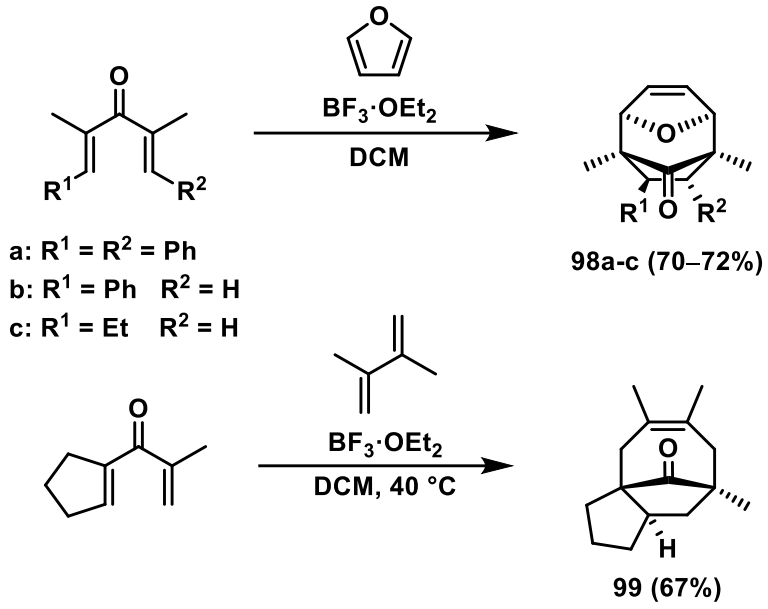

Scheme 1.45. The intermolecular [4+3]-cycloadditions during the Nazarov cyclization.

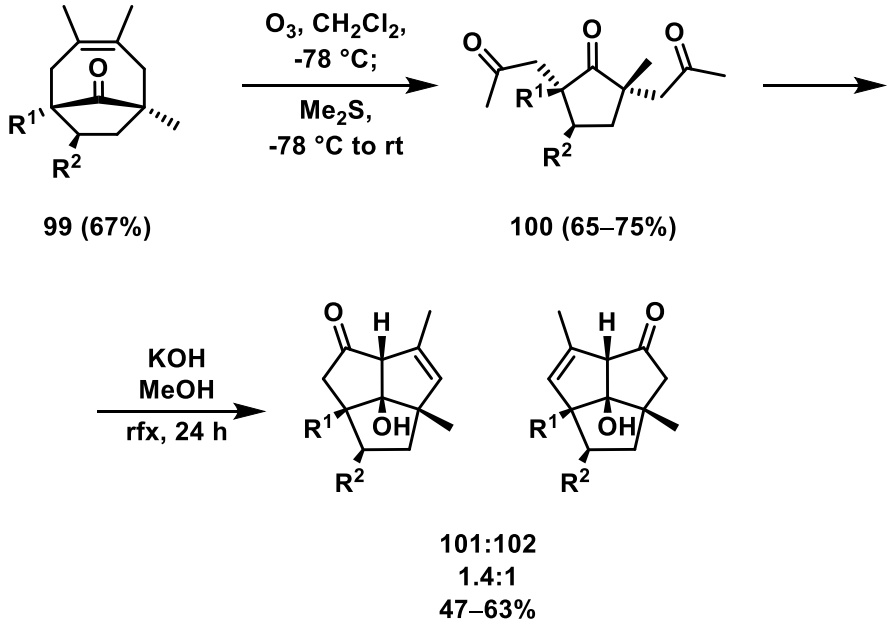

Scheme 1.46. Triquinacenes synthesis via the interrupted Nazarov cyclization.

The West group in 2008, studied the possibility of intermolecular oxyallyl trapping with aromatic nucleophiles (Scheme 1.47).[84] In all cases (electron-rich aromatic traps and heteroaromatic traps like furan, indole, thiophene, etc.) it was observed that bicyclic dienone **103** led to the arylated tricyclic product **104** in moderate to high yields and with

complete diastereoselectivity. It was demonstrated that the ring size increase from 5 to 6 members resulted in reduced reaction selectivity, giving a mixture of diastereomers **106**. In the case of the dimethoxybenzene trap, only divinyl ketone with *i*-Pr substituent resulted in the formation of product **107** through the exocyclic proton elimination from the methyl group, followed by the Michael addition of the dimethoxybenzene into the exocyclic methylene of the enone.[85]

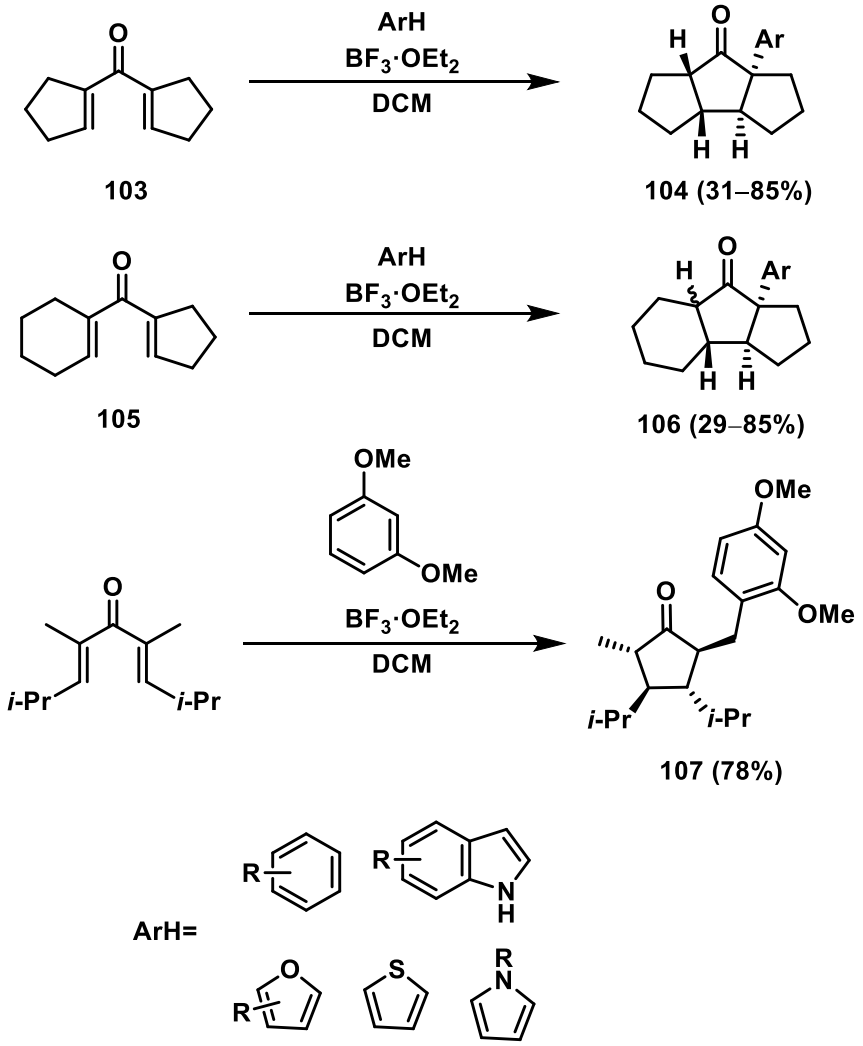

Scheme 1.47. The aromatic traps in the interrupted Nazarov cyclization.

Monoaddition of heterocycles to the least substituted end of the oxyallyl cation was achieved in the presence of TMSOTf as catalyst (Scheme 1.48).[67] Different reactivity patterns were observed for the addition of furans **110**, **111** with di- and mono-α-substituted starting materials. Trapping of disubstituted divinyl ketones cyclization

intermediates resulted in the formation of syn-addition products **108**. Anti-addition to prepare **109** happens in the case of mono-substituted starting materials. Indoles **113** and pyrroles **112** have converse trends, which is the result of a direct attack of the nucleophile on an oxyallyl intermediate instead of the formation of the [4+3] intermediate.

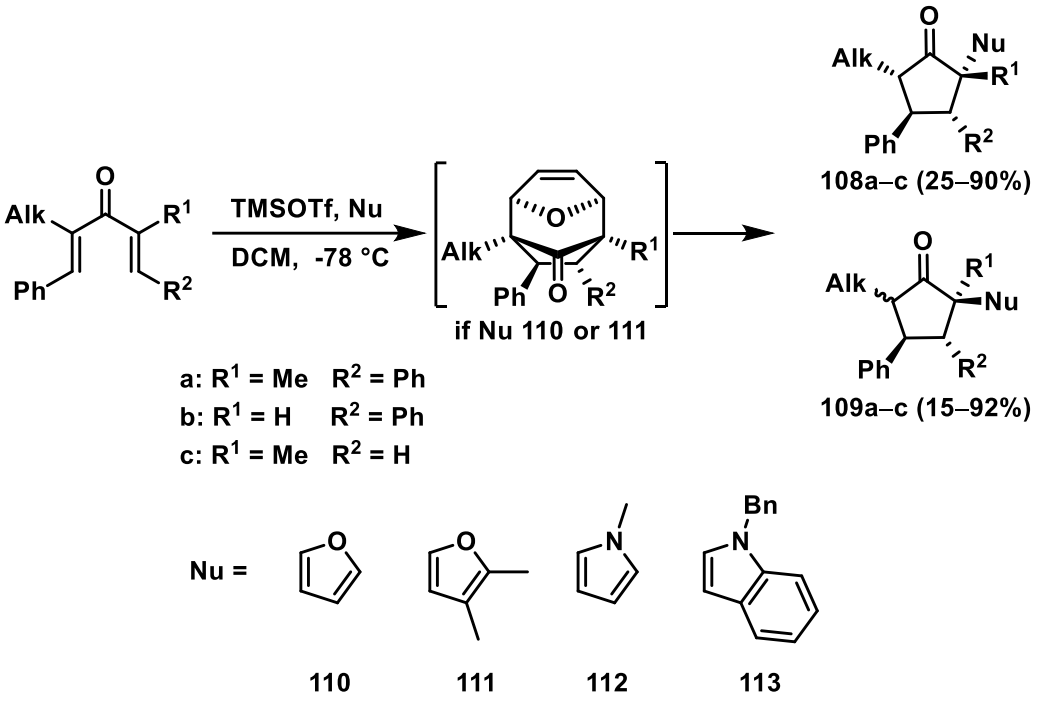

Scheme 1.48. Heteroaromatic compounds as traps in the Nazarov cyclization.

Flynn and co-workers focused on the area of stereo- and regioselective monoaddition of heterocycles (Scheme 1.49).[86,87] They applied Evans oxazolidinones as one of the α-substituents to perform the desired reaction with selectivity >99% *ee* and in excellent yields. With no trap present in the reaction, cyclopentenones **114** were obtained, whereas the presence of it led to product **115**. After isolation of the adducts, the oxazolidine substituent could be cleaved by lithium naphthalenide.

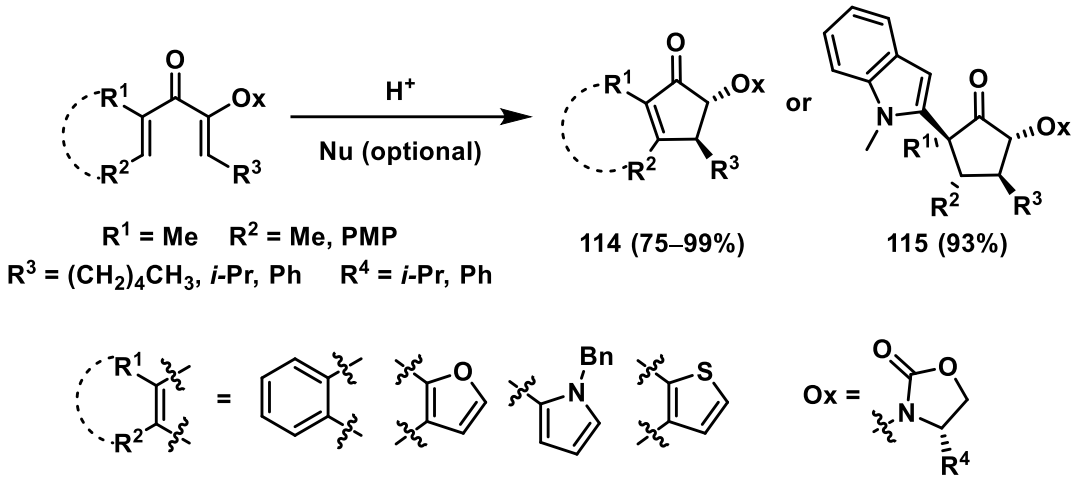

Scheme 1.49. The stereoselective Nazarov cyclization interrupted by heteroaromatic traps.

1.3.3.2 Nitrogen Nucleophiles in the Interrupted Nazarov Cyclization

The first attempts to apply nitrogen nucleophiles to trap oxyallyl cations were done by Tius and co-workers (Scheme 1.50).[88] Instead of Lewis or Brønsted acid, the Tius group applied silica gel as a reaction initiator of stereoselective interrupted Nazarov reaction of allenyl vinyl ketones generated in situ to get compound **116**. Highly effective trapping by primary and secondary amines was done under solvent-free reaction conditions; under these conditions, the nitrogen nucleophile will be close to the oxyallyl intermediate. Tius and co-workers envisioned the development of this methodology in the adoption of the mentioned conditions in the asymmetric Nazarov cyclization.[89] The enantioselectivity of the reaction has been planned to be achieved by putting camphor as one of the α-substituents, affecting the reaction's torquoselectivity. A face-specific attack of the nitrogen nucleophile resulted in the formation of product **117** in good yield (*ee* not reported).

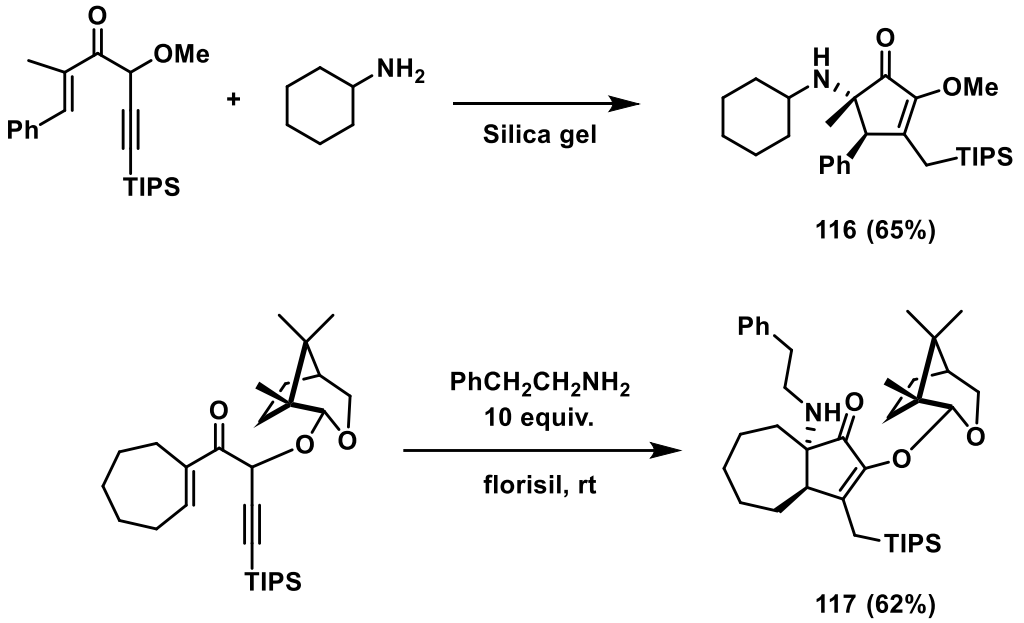

Scheme 1.50. The intermolecular interrupted Nazarov cyclization via nitrogen nucleophile addition.

Azides are applicable to trap the least substituted part of the oxyallyl cation.[90] After the formation of the C–N bond, Schmidt rearrangement takes place, providing a zwitterionic intermediate. This new intermediate undergoes a final rearrangement, with the predominant formation of a 6-membered ring product, *trans*-dihydropyridone **118** (Scheme 1.51). Compared to the intramolecular version mentioned before, no peroxy-products were observed during the intermolecular version. Two diastereomers formation is the result of the non-stereospecific protonation of the enolate on a quenching step. The application of Brønsted acid for intermolecular interrupted cyclization resulted in the synthesis of bicyclic triazene **119** in high yields.[91] The West group initially proposed that the reaction mechanism proceeds through a formal [3+3]-cycloaddition. Submission of bicyclic triazene **119** to the reaction in the presence of $BF_3 \cdot OEt_2$ did not result in the successful preparation of dihydropyridones and, at the same time, showed that the initial mechanistic proposal was incorrect. The nature of the substituents has an essential influence on the reaction pathway and regioselectivity. For example, dienone **120** with a single α-substituent instead of bicyclic triazenes gives an aziridine **121**. Dienone **103**, which bears two cyclopentenyl groups, performs Michael addition on one of the rings, giving **122** as the product.

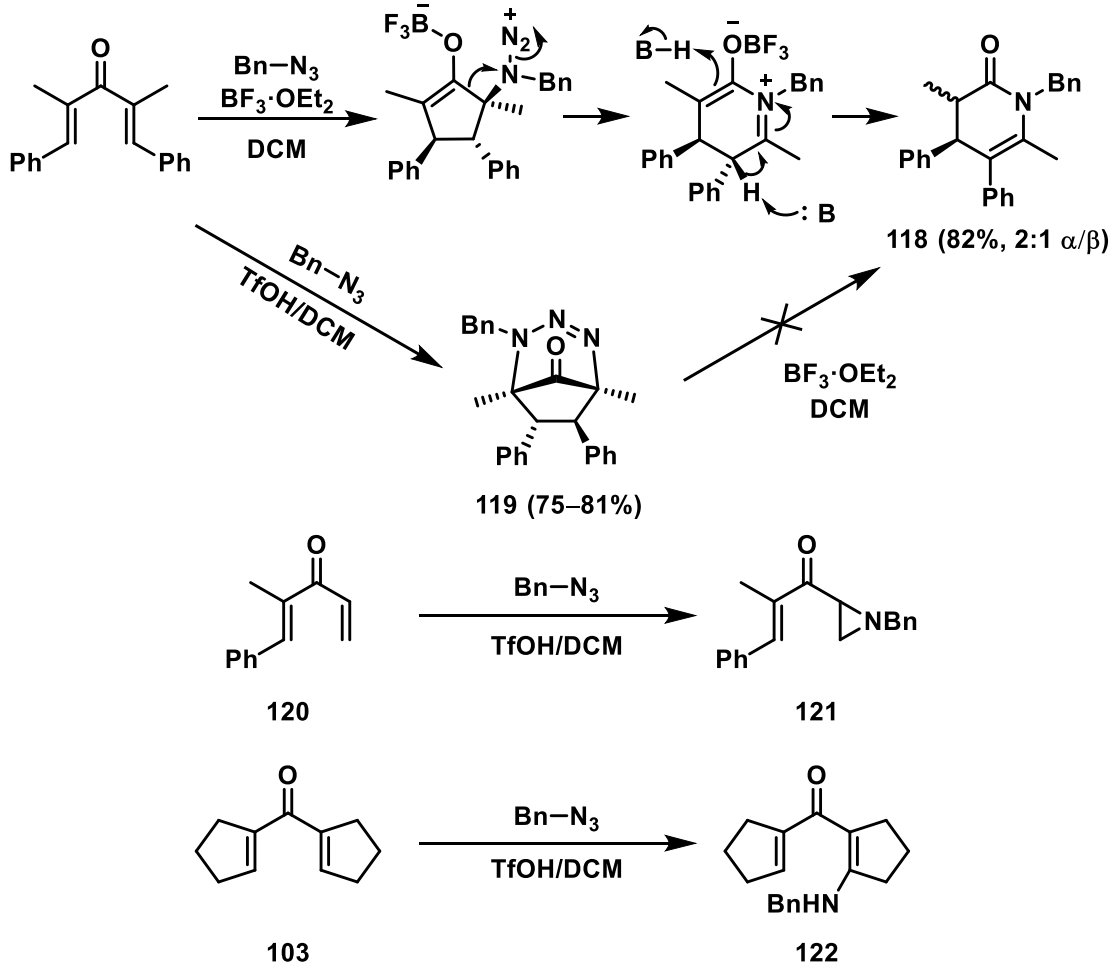

Scheme 1.51. The intermolecular interrupted Nazarov cyclization via azide trapping.

1.3.3.3 Alcohol Nucleophiles, Oxidative Sequences, And Michael Electrophiles In The Nazarov Cyclization

Burnell and co-workers submitted allenyl vinyl ketones to a variety of Lewis and Brønsted acids (Scheme 1.52). The best results among all applied acids were shown by CF_3COOH, which gave compound **124** as a single *trans*-isomer after passing through Al_2O_3. A mixture of *trans*- and *cis*-products with 1:1 ratio was obtained only when $Yb(OTf)_3$ was present in the reaction.[92]

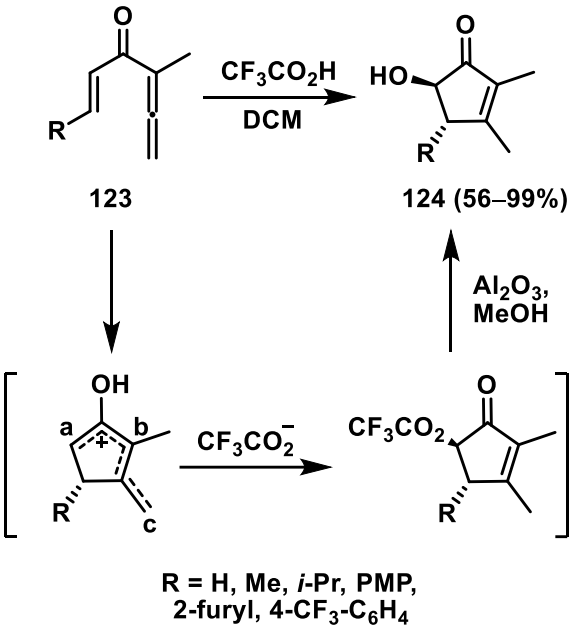

Scheme 1.52. The allenyl ketones cyclization initiated by CF_3COOH.

Shindo and co-workers reported intermolecular alcohol trapping as an entry to α-alkoxycyclopentenones via catalytic Nazarov reaction (Scheme 1.53).[93] Intermolecular alcohol migration is initiated by the addition of a catalytic amount of $Sc(OTf)_3$. After the cyclization event, the oxyallyl cation gets trapped by the nucleophilic alcohol, then the resulting enolate eliminates the β-alkoxy group, giving the desired product **125** in a 92% yield. The intermolecular nature of the reaction was proved by a crossover reaction, where the alcohol was labeled with deuterium and used as a solvent. Hydroxy group-containing product **126** and *exo*-methylene product **127** were formed as side products.

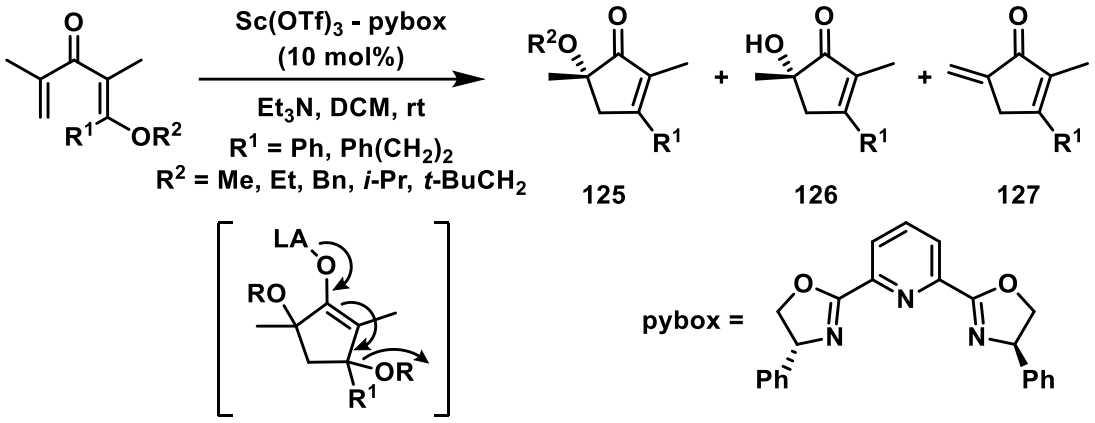

Scheme 1.53. The interrupted Nazarov reaction via alcohol addition.

West and co-workers successfully applied oxidation with $KMnO_4$ in the Nazarov cyclization/oxidative sequence (Scheme 1.54),[94] with $FeCl_3$ as a Lewis acid in the sequence. The oxyallyl intermediate reacted in one of two possible mechanistic pathways ([3+3] or [3+2] with enolate). As a result of this reaction, it is possible to obtain an open-chain hexanedione **128** bearing two stereogenic centers. The reaction can be performed only if R^1 and R^2 are aryl groups.

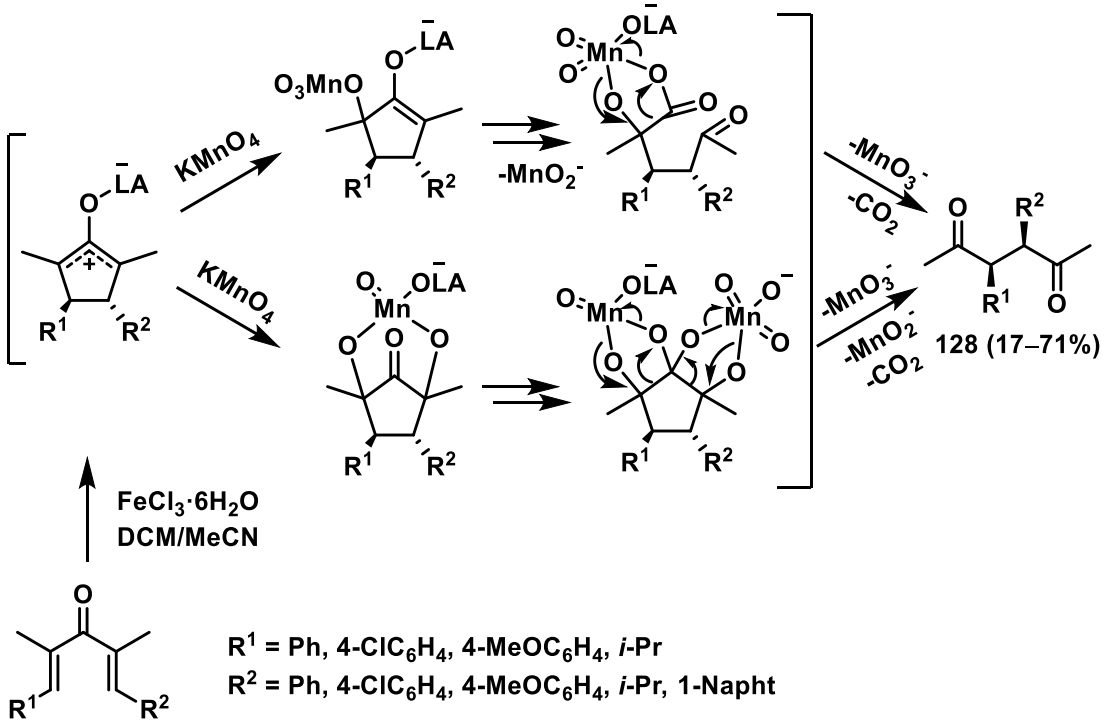

Scheme 1.54. The oxidatively interrupted Nazarov reaction.

In 2006, the Frontier group was able to introduce Michael acceptors as electrophiles in a reaction with a [IrMe(CO)dppe(DiB)](BArF$_4$) catalyst. Nitroalkenes were added to the oxyallyl cation in the presence of N-ethyl piperidine. The reaction gives **129** in excellent yield and has a high diastereomeric ratio. Two stereogenic centers in this reaction are formed during the 4π conrotatory electrocyclization, and the third one is furnished by the catalyst promoted 1,4-addition (Scheme 1.55).[95]

There are several interrupted Nazarov cyclization examples with halogen electrophiles, and double interrupted Nazarov cyclization with formaldehyde reported by the West group. For more information on these transformations, see Chapter 2.

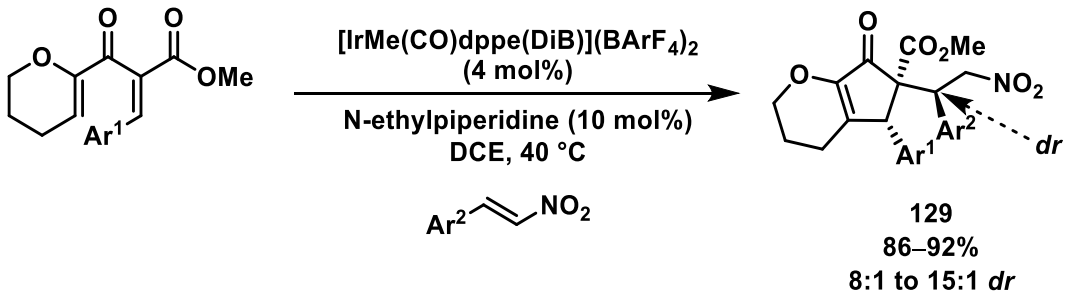

Scheme 1.55. The interrupted Nazarov reaction via Michael acceptors.

1.4 Conclusions

Over the last couple of decades, the Nazarov cyclization underwent significant development. This area of research was fruitful for many scientific groups, who successfully found valuable ways to apply this reaction to the synthesis of drug-like scaffolds and important building blocks. The Nazarov cyclization allows one to form up to four new stereogenic centers: two centers by means of 4π conrotatory electrocyclizations and the other two from trapping events. The conventional Nazarov cyclization later was modified into the interrupted Nazarov cyclization, providing chemists with additional tools to gain molecular complexity. The oxyallyl cation was shown to undergo Wagner–Meerwein rearrangement and trappings by a vast amount of nucleophiles and electrophiles. Usually, Wagner–Meerwein shift is considered to be an undesired side reaction, but chemists were able to exploit this transformation in a desired

way. At the same time, research groups got involved in interrupted Nazarov reaction studies and developed a way to control the formation of new centers in a stereoselective fashion almost on every carbon of the cyclopentanone ring during a nucleophilic attack event. For this Ph.D. project, I set out to discover and develop new methodologies utilizing variations on the Nazarov reaction as an initial step for domino processes. This included the double interruption of the Nazarov reaction and diversion of the relatively unstudied vinylogous Nazarov reaction into various "interrupted" pathways.

In Chapter 2, subsequent studies of the organoaluminum initiated double interrupted Nazarov cyclization will be discussed. Previously it was shown that dienone activation with organoaluminum reagents allowed the quasi-intramolecular delivery of one of the aluminum ligands, and the resulting aluminum enolates could react with proton, molecular oxygen, or even participate in a Simmons-Smith cyclopropanation reaction. I sought to develop a one-pot double interrupted Nazarov sequence utilizing the organoaluminum approach in tandem with positive halogen sources, furnishing densely substituted halocyclopentanones, and the results of that study are described in this chapter.

Chapter 3 will discuss the vinylogous Nazarov cyclization. The West group succeeded in cyclizing cross-conjugated trienes by activation of the remote ester by Lewis acid, reporting the first example of the vinylogous Nazarov cyclization. Further modifications of that process, intra- and intermolecular interrupted vinylogous Nazarov cyclization, will be discussed. The intramolecular trapping of the vinylogous Nazarov cyclization intermediate can allow the rapid formation of complex compounds. In the intermolecular vinylogous Nazarov cyclization, initial research of the applied nucleophilic traps and starting materials scope will be shown. Studies into fundamental reactivity and diastereoselectivity are critical for the further interrupted vinylogous Nazarov cyclization methodology development.

Chapter 4 describes an unexpected process to generate butenolides, which was discovered during attempted interrupted vinylogous Nazarov reaction. This process occurs without the need for noble metal catalysts, which are commonly employed in other butanolide syntheses. The preliminary scope of the reaction will be discussed.

Chapter 5 will compile our attempts to convert the Meyer–Schuster rearrangement and the vinylogous Nazarov reaction into a cascade reaction while retaining the same overall yield for the final product. This sequence leads to a highly efficient process, saving valuable resources and time for future research in the field of the vinylogous Nazarov cyclization. I will also discuss plans for the previously mentioned projects.

Chapter 2

Multi-Component Coupling Nazarov Cyclization via Organoaluminum-Mediated Double Interruption

2.1 Organoaluminum Reagents in Organic Synthesis

2.1.1 Organoaluminum Reagents Properties

Aluminum is among one of the most abundant metals on earth, and alkyl aluminum reagents have one of the largest organometallic tonnages in industry.[96] Since the preparation of the first organoaluminum reagents in 1859, organoaluminum chemistry started to appear occasionally in book chapters and reviews.[96] Up to the present day, trialkyl substituted organoaluminum reagents are used widely in organic and organometallic synthesis. As a result of the elevated interest in organoaluminum chemistry, it is no surprise that many attempts have been devoted to better understanding the chemistry of the organoaluminum compounds.[97] Trialkylaluminum compounds with small alkyl chains are known for their ability to form dimers in solution (Figure 2.1, Compound A). Usually, they are represented as symmetrical structures that have alkyl bridges with the central carbon connected to two aluminum atoms by a 3-centered-2-electron bond.[98]

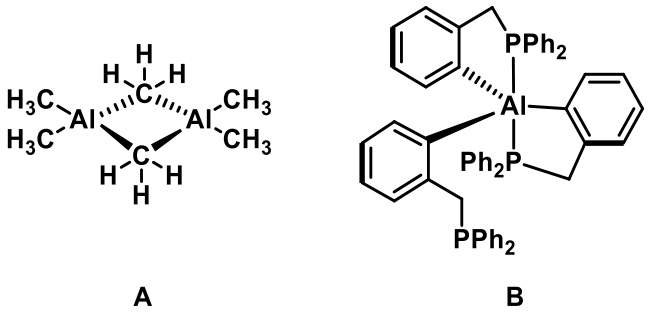

A B

Figure 2.1. Representative organoaluminum compounds.

Organoaluminum species have a trend to increase their coordination number by coordinating to donor neutral ligands or by self-aggregation, and can have tri-, tetra- and

pentacoordination. There are only a few examples of pentacoordination reported in the literature.[99] Normally, for pentacoordination to occur, two or more alkyl chains must carry appropriately placed functional groups (Figure 2.1, Compound B). The phosphorus-bearing organoaluminum compound $Al[(2\text{-}Ph_2PCH_2)C_6H_4]_3$ is an example of such pentacoordination with trigonal bipyramidal geometry.[100]

Organoaluminum reagents are well-known for their strong Lewis acidic nature, because of the empty *p*-orbital present on the sp^2 aluminum center. Heteroatoms in a variety of functional groups can coordinate favorably to the aluminum atom, simultaneously completing an electron octet on aluminum and activating heteroatom bearing electrophiles for nucleophiles to attack them (Figure 2.2).

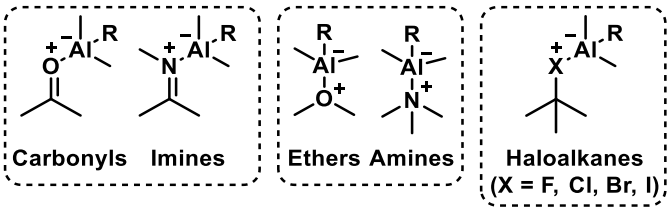

Figure 2.2. Organoaluminum activation of Lewis basic functional groups.

Organoaluminum reagents are usually moisture and oxygen-sensitive, and well-known to be highly reactive.[101] Their ability to react robustly with oxygen and act as an activator of the oxygen-containing substrates can be explained by the strong oxophilicity. The high dissociation energy of the Al–O bond (580 kJ/mol) offers evidence of its thermodynamic favorability.[101]

The first documented organoaluminum autoxidation (spontaneous oxidation of compounds in the presence of oxygen) mechanism was reported by Davies and co-workers in 1968. They calculated the amount of oxygen absorbed by trimethylaluminum in cyclohexane. Based on their observations, they hypothesized that trimethylaluminum underwent oxygen insertion, forming methylperoxyaluminum **I**, which subsequently reorganized into the more stable alkoxides **II** and **III** (Scheme 2.1).[102]

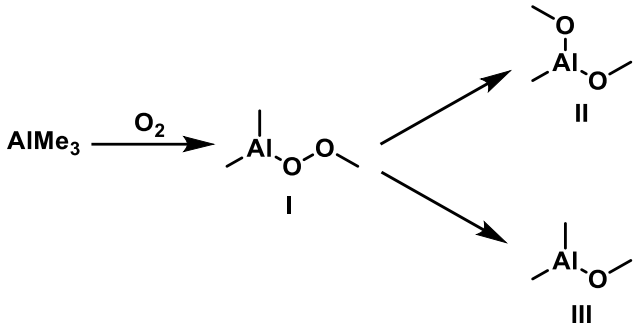

Scheme 2.1. Organoaluminum autooxidation.

Another insight into the properties of organoaluminum species was reported recently by the Henderson group. In the presence of trimethylaluminum 2,4,6-trimethylacetophenone **1** forms the aluminum enolate dimer species **2** with the central Al_2O_2 core (Scheme 2.2). The reported dimer was isolated successfully and defined by X-ray crystallography. Henderson's work served as proof for the previously proposed dimeric organoaluminum structures.[103]

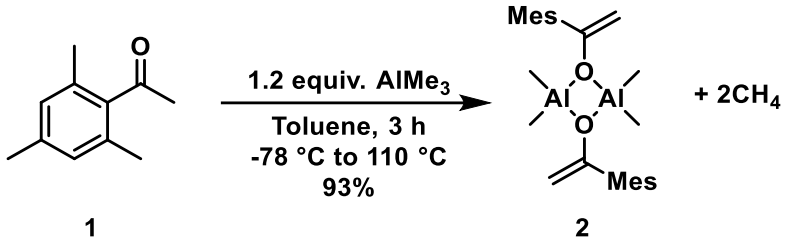

Scheme 2.2. Dimerization of organoaluminum enolates.

2.1.2 Organoaluminum Reagents as Nucleophiles

In addition to Lewis acidic properties, organoaluminum reagents can act as strong nucleophiles. Substituents (aliphatic and aromatic) on tetracoordinated aluminum can migrate to an activated electrophile in a 1,2- or 1,4-addition fashion, forming the corresponding products.[96] The first application of trialkyl organoaluminum reagents as nucleophiles was reported by Lundeen's group in 1970, where they were used as nucleophiles during the opening of epoxides (Scheme 2.3). Epoxide **3** was mixed with an excess of triethylaluminum at 80 °C. Both symmetrical and non-symmetrical substrates underwent reaction in high yields, with a preference for intramolecular migration of one

of the aluminum's ethyl groups onto the more substituted carbon of the epoxide. Since the initial report of epoxide opening utilizing organoaluminum reagents as nucleophile, research in this area has received more attention.[104]

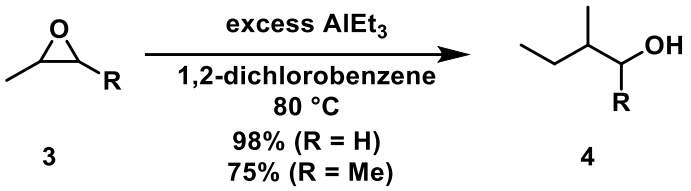

Scheme 2.3. Regioselective ring-opening of epoxides in the presence of triethylaluminum.

Later, Yu and co-workers successfully reported that trimethylaluminum can effect nucleophilic attack on a ketone carbonyl group (Scheme 2.4). Coordination was proposed to involve two molecules of trimethylaluminum, permitting a 6-center transition state (TS) for delivery of a methyl group.[105] Reaction TS was proposed relying on previous kinetic studies.[106] Subsequently, one of the methyl groups was furnished intramolecularly by 1,2-addition on to carbonyl group, converting 4-*t*-butylcyclohexanone **5** into 4-*t*-butylcyclohexanol **6**.

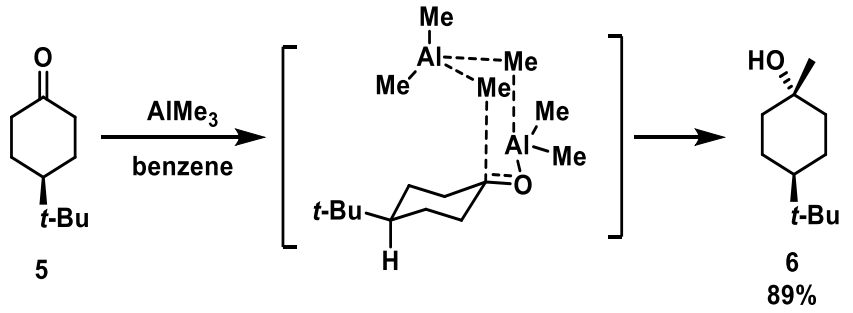

Scheme 2.4. 1,2-Addition to the carbonyl in the presence of trimethylaluminum.

Initial attempts to utilize trialkylaluminum reagents as both Lewis acids and nucleophiles resulted in their application in the Prins reaction reported separately by Snider in 1981.[107,108] Trimethylaluminum was used as the Lewis acid that coordinated to paraformaldehyde before nucleophilic addition of alkenes **7** and **10**. The subsequent migration of a methyl group from aluminum to the intermediate carbocation provided the desired products **8**, **11**, and **12** in moderate to high yields (Scheme 2.5). By-product **9** is

formed if proton elimination occur instead. The example reported in the early 1980s of trialkylaluminum utilization in the Prins reaction to perform a hydroxymethylation sequence might be considered as one of the first examples of a double interrupted reaction initiated by organoaluminum reagents.

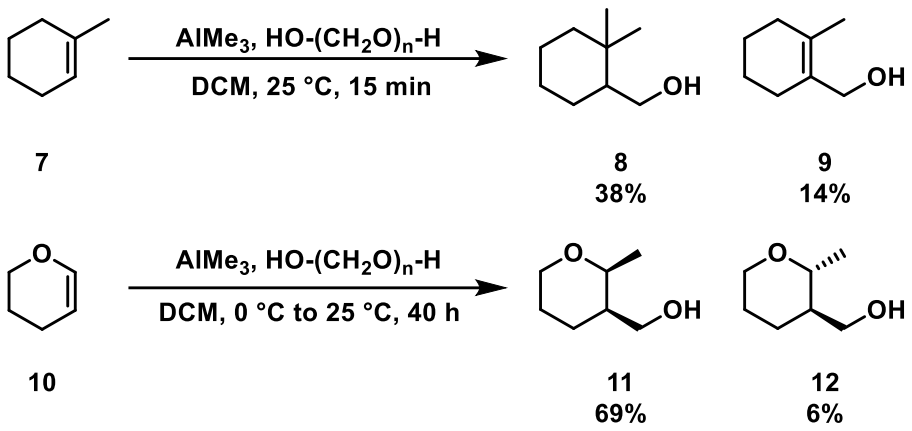

Scheme 2.5. Prins reaction initiated by organoaluminum.

2.2 The Double Interrupted Nazarov Cyclization

The conventional interrupted Nazarov reaction involves a single trapping event of the oxyallyl cation, which interrupts the reaction before elimination of the β proton in the traditional Nazarov reaction.[19a] The double interrupted Nazarov cyclization concept development started with the discovery that Nazarov cyclization can be performed in the presence of organoaluminum. A previously unexploited approach to deliver alkyl groups quickly became one of the important methods to functionalize the α-position of the cyclopentanone.[109]

The West group succeeded in preparing compounds **14–17** by delivering various functional groups (azides, nitriles, and alkyl groups) on the cyclopentanone's α-position (Scheme 2.6). The enolate quenching during aqueous workup for disubstituted starting materials is highly selective due to product development control and results in the formation of *trans*-related α- and β-substituents. The intramolecular character of the interruption made the process highly effective. Normally, one of the organoaluminum substituents is delivered to one of the oxyallyl cation termini after Lewis acid coordination to carbonyl oxygen and 4π electrocyclization.[110]

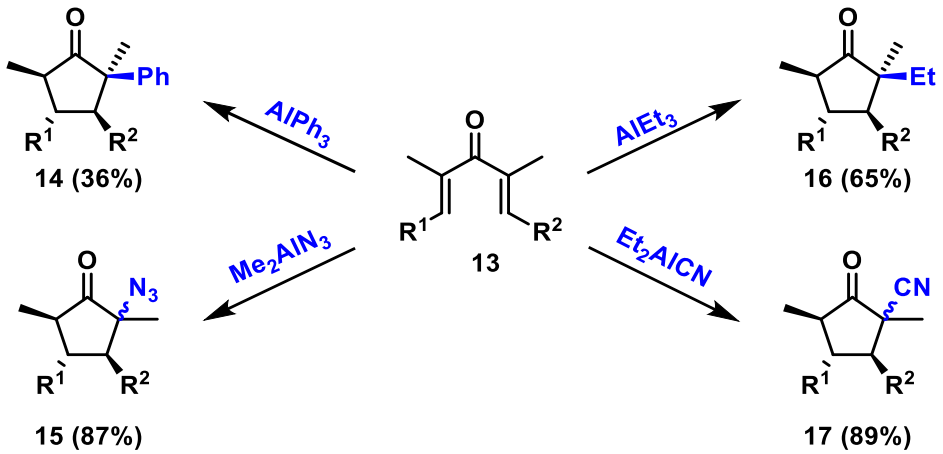

Scheme 2.6. The organoaluminum interrupted Nazarov cyclization.

The organoaluminum interrupted Nazarov cyclization offered an approach to the "double interrupted" Nazarov cyclization (Scheme 2.7). For the double interrupted Nazarov cyclization to occur both electrophile and nucleophile trapping agents must be present in the system. Often, as a result, two traps can undergo undesired side reactions with each other. However, in the organoaluminum-mediated interrupted Nazarov reaction, a strong nucleophilic moiety is formed only after transfer of one of the aluminum ligands to the oxyallyl, generating an aluminum enolate. This reduces the likelihood of undesired premature reaction involving an electrophilic trap. Nonetheless, some reactivity requirements are imposed on the electrophile: it should tolerate the presence of an organoaluminum reagent in the reaction vessel and be able to react with the aluminum enolate formed in-situ. The new methodology can be described as a reaction with three new bond-forming events, with the formation of four new stereogenic centers, where two of them are fully substituted.

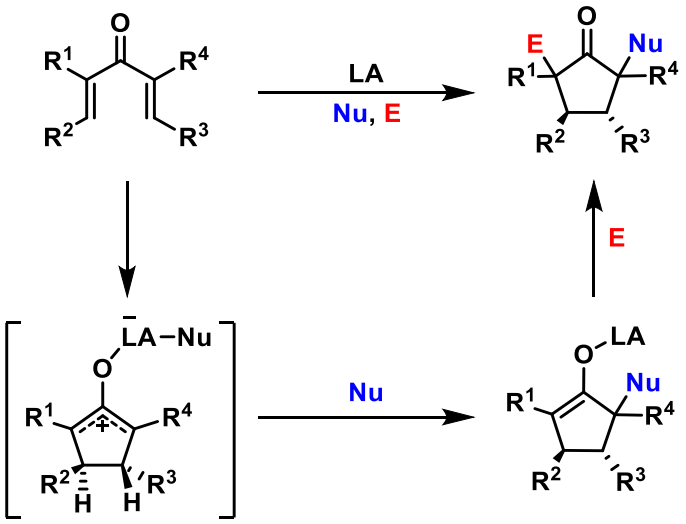

Scheme 2.7. Double interrupted Nazarov cyclization.

The one-pot synthesis of α-hydroxycyclopentanones was the first example of the double interrupted Nazarov cyclization (Scheme 2.8).[111] Nucleophilic/electrophilic trapping of the oxyallyl cation starts with the migration of an alkyl group from the organoaluminum reagent. This forms an aluminum enolate, which can trap an electrophile. In the case of α-hydroxycyclopentanone **18** synthesis, the passage of oxygen through the system results in oxidation of the aluminum enolate to form a peroxyaluminum intermediate (MeO_2AlMe–O-cyclopentenyl) followed by intramolecular oxygenation of the enolate carbon. It results in the formation of diastereomeric mixture **18** in good yields but with low selectivity 1.2:1. Oxidation also can be performed in the presence of Davis oxaziridine with lower yields but higher selectivity.[112]

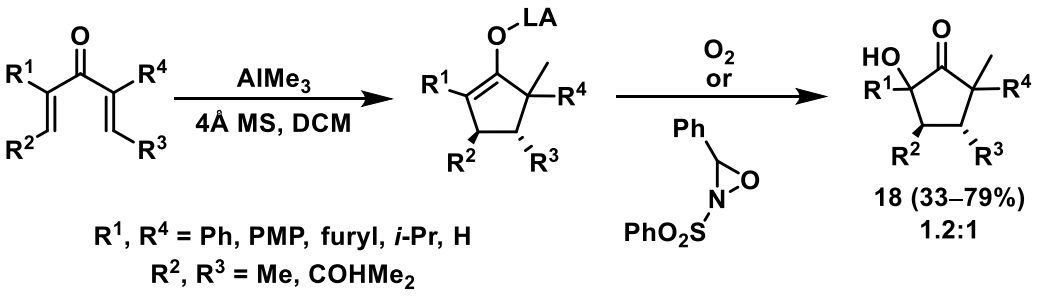

Scheme 2.8. The double interrupted/oxidative Nazarov cyclization.

The West group showed that it is possible not only to obtain α-hydroxycyclopentanones but to perform a Simmons–Smith type of interruption, as well, utilizing the double interrupted Nazarov reaction (Scheme 2.9).[113] The organoaluminum enolate reacts with the carbenoid, which originates from the diiodomethane present in the reaction system. The formed bicyclohexanols **19** were highly unstable due to ring strain and underwent facile aerobic oxidation.[114] *In situ* acetylation of the obtained alcohol **19** resolved stability issues. It was reported that EWG on aromatic β-substituents of the divinyl ketones allows the reaction to proceed with higher efficiency. Fully alkylated substrates and substrates bearing EDG were shown to be inert to the applied conditions.

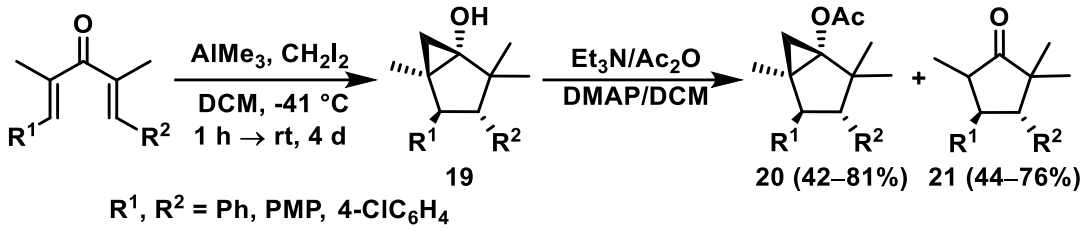

Scheme 2.9. Double interruption of the Nazarov reaction via sequential organoaluminum methyl-transfer and Simmons-Smith cyclopropanation.

Cleavage of the bridging C–C bond in compound **19** via oxidative trapping of a radical intermediate followed by triphenylphosphine reduction of resulting peroxides **23** and **24** gives **22** in high yields (Scheme 2.10).[115] The cyclohexanone products with three contiguous stereogenic centers are not normally accessible using the interrupted Nazarov cyclization.[116] The authors present an important application of the methodology by subjecting bicyclic product **19** to the excess of $FeCl_3$ and sequentially treating it with DBU, forming cyclohexenone **25** in 60% yield (Scheme 2.11).

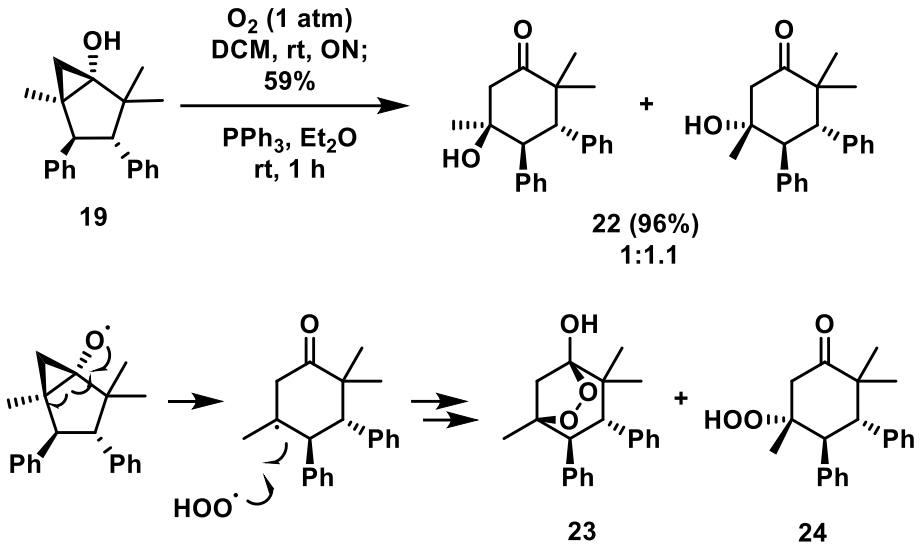

Scheme 2.10. The oxidation/reduction sequence of the bicyclohexanol.

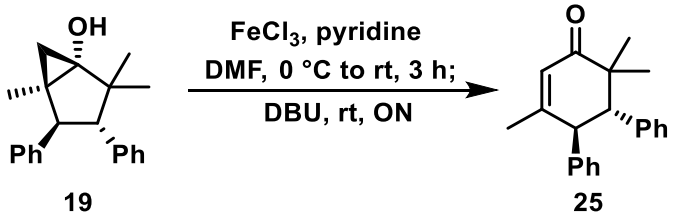

Scheme 2.11. Synthesis of a cyclohexanone from a bicyclohexanol.

Further development of the double interrupted Nazarov cyclization West and co-workers envisioned in the trapping of the enolate, which is obtained after the first nucleophilic trapping, with carbonyl-containing compounds. [108,117] Initial attempts were performed in the presence of paraformaldehyde (Scheme 2.12). Desired products **26** were afforded in great yield with high diastereoselectivity of 13:1. High yields and selectivity were observed only for tetrasubstituted diaromatic substrates, whereas tetraalkyl substrates remained unreacted. The utilization of the trialkylaluminums other than trimethylaluminum was shown to be successful.

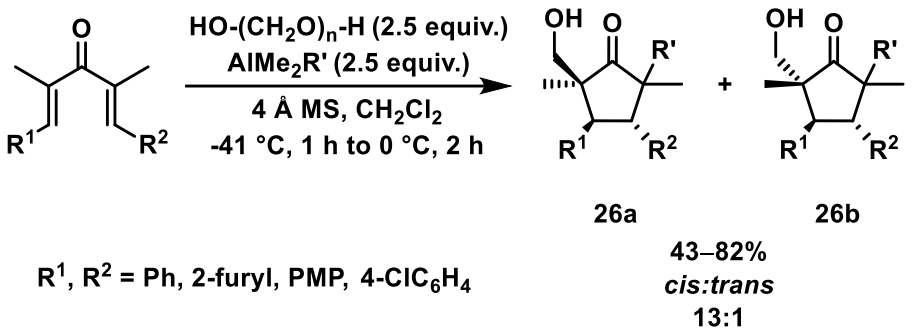

Scheme 2.12. Double interrupted Nazarov cyclization with sequential introduction of R group and CH_2OH using $AlMe_2R$ and paraformaldehyde.

A further application of this process employed initial reductive trapping of the Nazarov intermediate.[118] A multicomponent mixture of Et_2AlCl, Et_3SiH, and paraformaldehyde formed the desired products **27** and **28** in 59% overall yield (Scheme 2.13). Stereoselectivity trends are the same as for the previously reported reductive Nazarov cyclization examples. The potential application of Et_2AlCl is broad and opens possibilities to study the introduction of other nucleophiles via an intermolecular trapping pathway.[110]

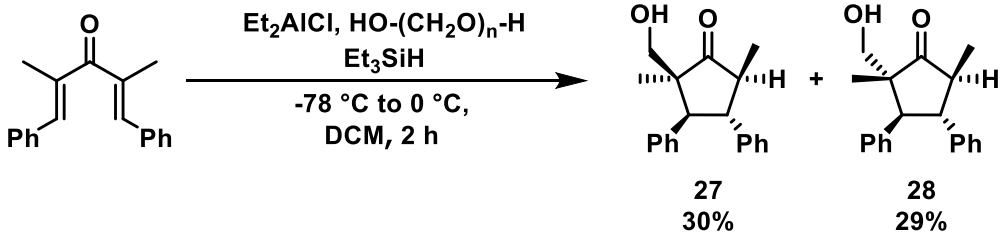

Scheme 2.13. The double interrupted reductive Nazarov cyclization.

In summary, the West group was able to demonstrate the ability to perform the double interrupted Nazarov cyclization in a variety of ways. The cyclization is shown to have the possibility to form highly substituted cyclopentanones with a maximum of four new stereogenic centers, and three new C–C bonds. The progress in the double interrupted Nazarov cyclization studies will be discussed in the results and discussion section.

2.3 The Halogen Interrupted Nazarov Cyclization

In 2005, West and co-workers performed trapping of bridged polycyclic dienone **29** during Nazarov cyclization in the presence of stoichiometric $TiCl_4$. Lewis acid in the reaction acts as an activator and as a nucleophilic halide source at the same time (Scheme 2.14).[119] This study was the first to report the possibility of trapping the oxyallyl cation with a halide derived from a Lewis acid.[120,121] Starting material **31** underwent skeletal rearrangements (1,2-alkyl shift) after the cyclization to form product **32**.

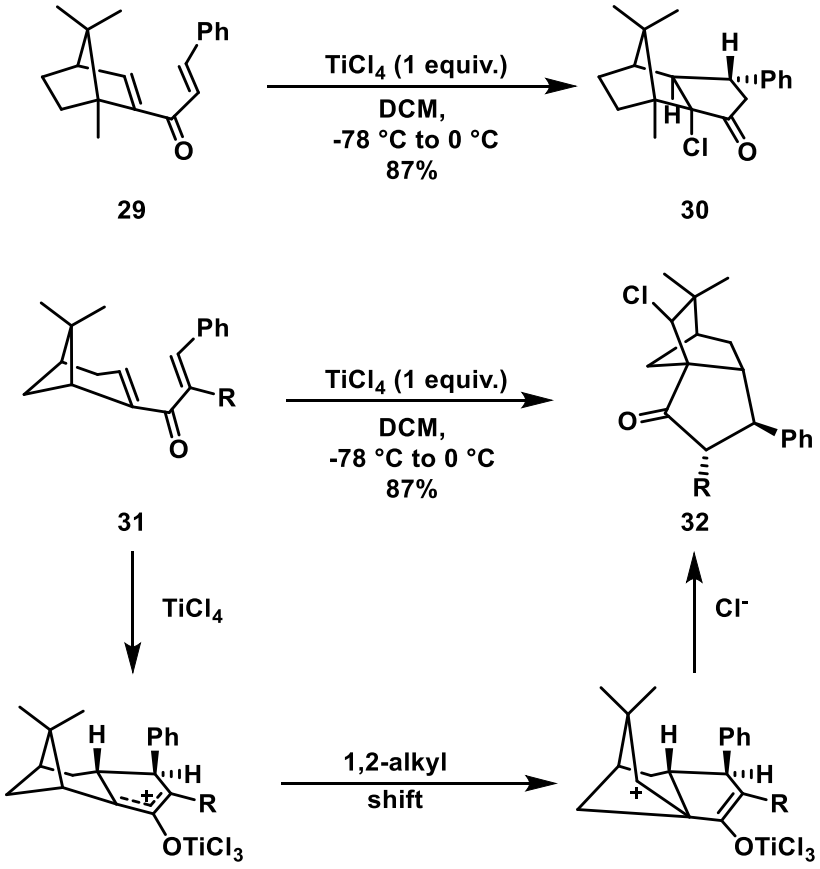

Scheme 2.14. $TiCl_4$ as a source of nuclophilic halide in the Nazarov cyclization.

Initial attempts to perform the intermolecular interrupted Nazarov cyclization with simpler substrates were done with the application of a strong Lewis acid containing halogens using trienones as starting materials (Scheme 2.15). There are three different possible sites for nucleophilic attack on allenyl vinyl ketones by nucleophilic halogens (Scheme 2.15, **a**, **b**, and **c**).[122,123] Addition of Lewis acids, such as $AuCl_3$, $InCl_3$, $TiCl_4$,

InI_3 led to the products **33**, **36**, **37**, **38**, respectively, in moderate to high yields.[124] Chlorination was successful only in the presence of $AuCl_3$ and gave 32% of product **33**. Interestingly, $TiCl_4$, which was previously reported to perform the desired reaction on more complex starting materials, did not give the desired product.[119] Nucleophilic attack at position **c** was usually observed with the application of $InCl_3$, InI_3, and TiI_4, although yields were low for all substrates. Phenyl bearing substrates with Lewis acids mentioned above gave **35** in 96% with no nucleophile addition. The product **35** can be derived from iodinated cyclopentanones, which undergo de-iodination.[119] The $TiBr_4$ initiated Nazarov cyclization provided mixtures of products with higher complexity because of multiple competing pathways that depend on the nature of the allenyl vinyl ketone. Starting materials with β-alkyl substituent gave mixtures of **34** (16–80%) and **37** (16–29%); and β-phenyl substituted substrates form **34** in excellent yield (80%) and selectivity. Nucleophilic attack at position **b** was not observed with applied Lewis acids.

Further development of the halogen interrupted Nazarov cyclization shifted into the area of electrophilic agents. Various research groups utilized the traditional elimination pathway for the oxyallyl cation intermediate to obtain a nucleophilic dienolate, which can be used for new bond-forming events. In 2007, the Ma group applied a new methodology to prepare the halogenated indanone derivatives **40** from the polarized substrate precursor **39** (Scheme 2.16). A triple cascade one-pot reaction Knoevenagel condensation/Nazarov cyclization/electrophilic halogenation process was catalyzed by a Lewis acid ($FeCl_3$ for fluorination, $AlCl_3$ for bromination and chlorination), forming desired product **40** in high stereoselectivity, with moderate to high yields.[125]

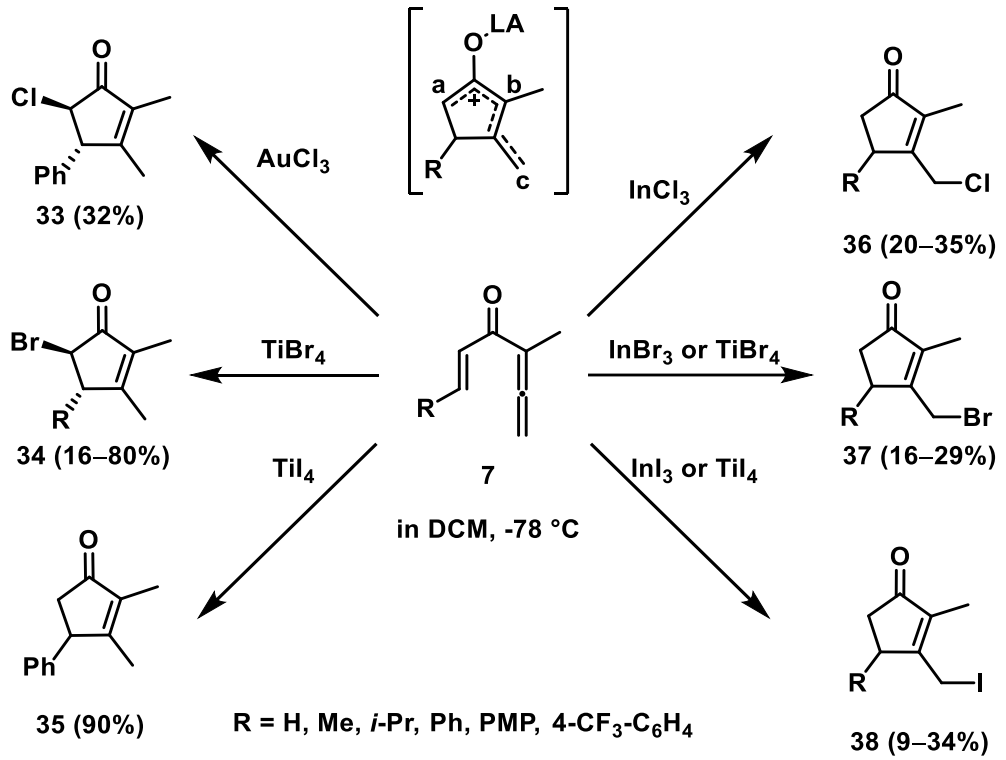

Scheme 2.15. Halogen-interrupted Nazarov reaction of allenyl vinyl ketones.

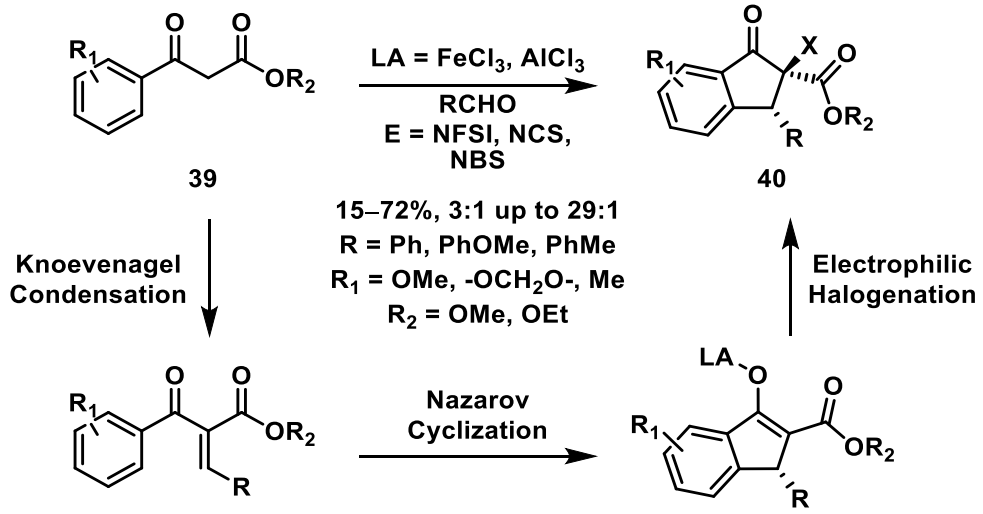

Scheme 2.16. The triple cascade reaction catalyzed by Lewis acids.

The highly efficient electrophilic bromination of the Nazarov intermediate was reported by Rueping and Ieawsuwan in 2011 (Scheme 2.17). The polarized dienone in the presence of the bulky chiral Brønsted acid cyclized into the enantioenriched mixture of diastereomers. The α-brominated products **42** and **43** (2:1 ratio) were obtained in high

yields (92%) and high enantioselectivity (89% *ee* for both diastereomers). It is the first report that demonstrates the chiral Brønsted acid application for the enantioselective Nazarov cyclization/halogenation reaction.[126]

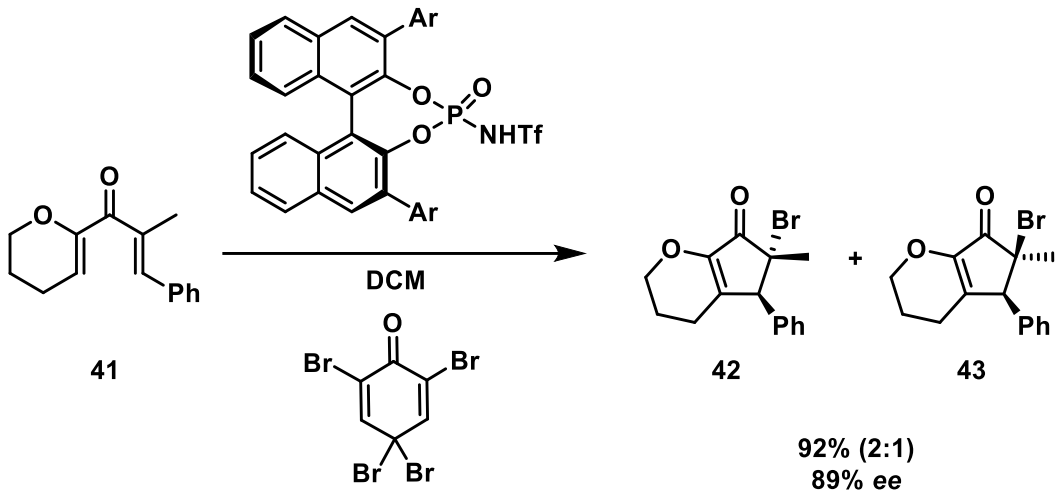

Scheme 2.17. The enantioselective Nazarov cyclization/bromination reaction.

Lu and co-workers successfully performed the enantioselective interrupted Nazarov cyclization by utilizing an enantioenriched cobalt(II) complex **47** as a Lewis acid and NFSI as electrophilic halogen source (Scheme 2.18). Enantioselective reactivity was achieved by manipulation with the thiazoline iminopyridine ligand that was used in the reaction. The newly formed cobalt enolate was trapped enantioselectively by an electrophilic fluorine source, forming fluorinated cyclopentenones **44**.[127] Heating the product of the Nazarov cyclization/halogenation sequence in the presence of sulfuric acid, in turn, resulted in decarboxylation during reflux at 100 °C, forming a mixture of cyclopentenones **45** and **46** in 69% yield with 5:1 *syn*:*anti* ratio.

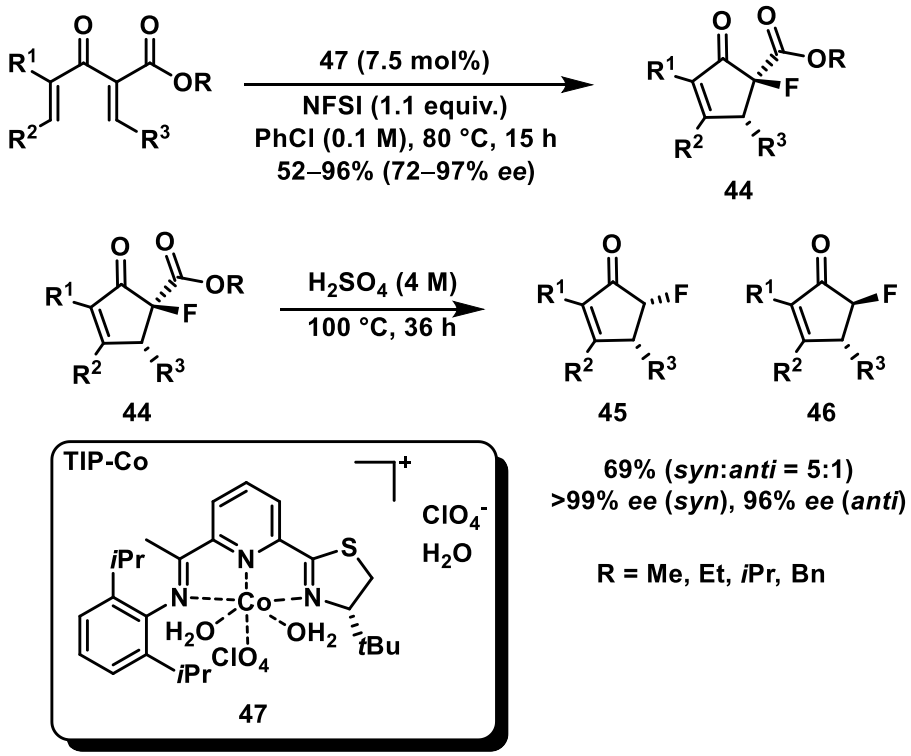

Scheme 2.18. The enantioselective Nazarov cyclization/fluorination reaction.

The first example of the double interrupted Nazarov cyclization/dihalogenation sequence was reported by the West group (Scheme 2.19).[128] The formation of the first stereogenic center is under product development control with preferred attack of the bromine from the more hindered side (*syn*-addition to the neighbouring R^2 group), constructing product **48** with *trans* relation between Me and R^2 group. The second bromination usually happens in a less stereoselective way. As halogen sources, bromine and pyridinium bromide perbromide were studied. The bulkier pyridinium bromide perbromide provided higher diastereoselectivity. Substrates bearing β-aromatic substituents gave the desired product **48** in high yields. Substrates with alkyl chains as β-substituents had decreased reaction yield and selectivity. Product **49** was observed in the case of β-monosubstituted substrate.

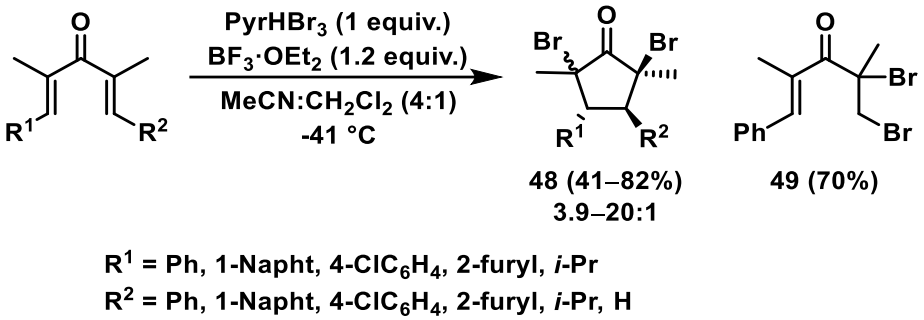

Scheme 2.19. The double interrupted dibromination Nazarov reaction.

2.4 Results and Discussion

As previously mentioned, the West group succeeded in investigating the possibility of a double interruption of the Nazarov cyclization.[111] After nucleophilic trapping of the oxyallyl cation, the remaining reactive enolate moiety was shown to undergo the second bond-forming event with aldehydes, or oxidize in the presence of oxygen, giving alcohols, or react in a Simmons–Smith type reaction.

Initially, we were curious if it was possible to trap the aluminum enolate with Michael acceptors (Scheme 2.20). Based on the previously reported literature on electrophilic enolate trapping, we selected analogous conditions and screened for compatible electrophiles. Not all electrophiles were able to tolerate the organoaluminum reagent present in the system, forming complex mixtures as the outcome of the reaction (Scheme 2.21). Michael acceptors and other carbon electrophiles that could tolerate harsh conditions (acrylonitrile, allyl bromide, and Eschenmoser's salt) remained unreacted, providing product **50**.

Scheme 2.20. The Michael acceptor addition proposal.

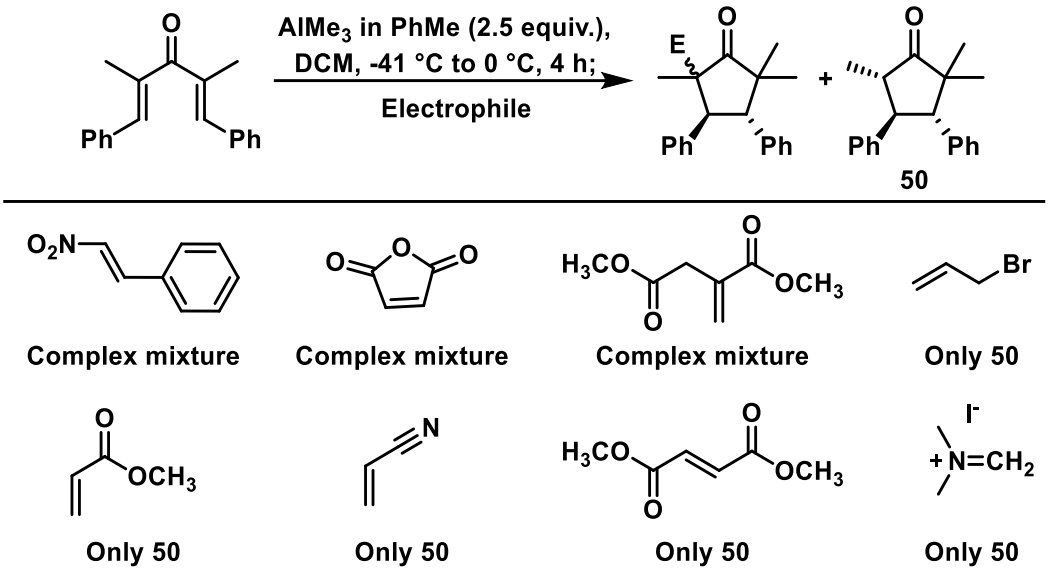

Scheme 2.21. Screening of Michael acceptors and other carbon electrophiles.

Examples of the interrupted Nazarov cyclization/halogenation reactions are scarce, although α-halocarbonyl compounds have potentially broad applications in synthesis.[110] Usually, the interrupted Nazarov cyclization/halogenation requires the use of various metal catalysts, such as copper and iron.[125,127] These methods were fruitful for the preparation of α-halocarbonyl compounds, but most of them cannot be applied practically because of the need for harsh conditions. As a result, there is still a need for developing new methods that will allow a more convenient and efficient synthesis.[19,120]

The West group had previously shown that bromine could function as both a nucleophile and electrophile with the Nazarov intermediate, albeit with a different Lewis acid mediator for the electrocyclization.[128] The products were α,α'-dibromocyclopentanones, whereas, in the present study, our objective was carbon–carbon and carbon–halogen bond formation to afford highly substituted cyclopentanones.

We encountered an intriguing example by the Burns group (Scheme 2.22),[129] where they applied *N*-halosuccinimides (NXS) as stable electrophilic halogen sources in the presence of chlorotriisopropoxytitanium(IV), for highly selective allylic alcohol bromochlorination reaction. The ability of succinimides to function as Lewis basic species allows the efficient pseudointramolecular delivery of the electrophilic halogen to the nucleophilic olefin moiety via coordination to titanium alkoxide. This compatibility with strong Lewis acids and the potential for efficient trapping via proximity effects made

NXS (NCS, NBS, NIS) attractive electrophiles for double-interrupted Nazarov trapping under the organoaluminum conditions (Figure 2.3). Broadening the hypothesis we also decided to test fluorine electrophiles (NFSI and Selectfluor).

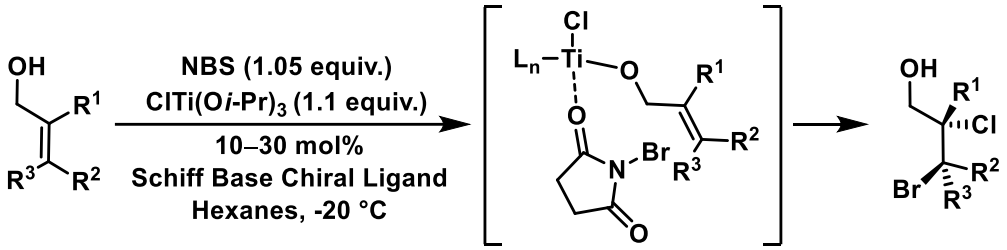

Scheme 2.22. Bromochlorination reaction.

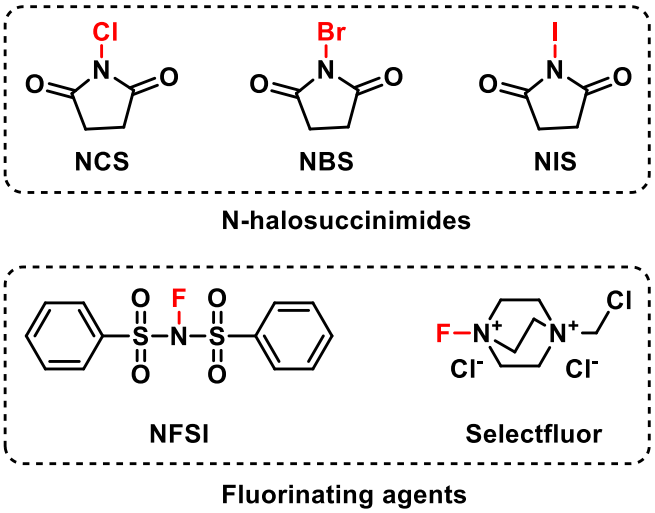

Figure 2.3. Proposed electrophiles scope.

Optimization tests (Table 2.1) were carried out using trimethylaluminum as a reaction initiator. Trapping of the aluminum enolate was then investigated using several electrophilic halogen sources. We found that NBS provides higher yields of the desired product **51b** than pyridinium bromide perbromide. Bromination using bromine resulted in a complex mixture, with a trace amount of the desired product. The highest bromination yield was obtained using 5 equivalents of NBS, 4 hours reaction time, and allowing the reaction vessel to warm up to room temperature after Lewis acid addition and one hour at -41 °C. Reaction time of less than four hours resulted in diminished yields. These

optimized conditions were applied for other halogen sources and organoaluminum reagents.

Table 2.1. The Nazarov Cyclization/Halogenation Optimization[a]

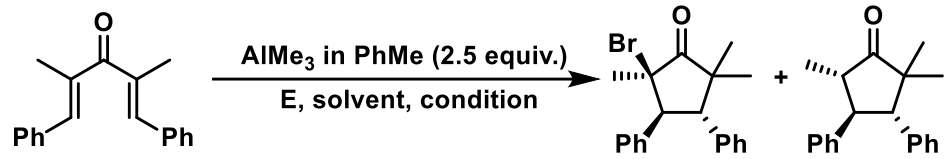

13 51b 50

Entry	Electrophile	Equiv.	Time, h	T, °C	Yield **51b** (%)[b]
1	NBS	5	24	-41 → rt	75
2	Br_2	2	24	-41 → rt	~trace
3	Pyridinium bromide perbromide	2	24	-41 → rt	28
4	NBS	2	4	-41 → rt	60
5	NBS	5	4	-41 → rt	76
6	NBS	5	4	-41	53

[a] α-Halogencyclopentanones construction representative procedure described in Section 2.6.4 [b] Yields and ratio are based on the isolated product after chromatography.

We began the substrate scope studies with the symmetrical substrate 2,5-dimethyl-3,4-diphenylpentadien-3-one (Table 2.2, entries 1–8). After the model substrate **13a** cyclization and methyl migration, an attempt was made to trap the organoaluminum enolate with halogen electrophiles. Halogen succinimides were shown to be applicable for this reaction: NCS gave an excellent yield of **51a**, 96% of the single diastereomer; NBS gave **51b**, with a 76% overall yield (Table 2.2, entries 1–2). The product was formed with excellent diastereoselectivity using NCS and NBS as electrophilic halogen sources, giving a single product with a *trans* relation between methyl and phenyl groups. The excellent diastereoselectivity might arise from possible reversibility of halogen addition to the enolate. Unfortunately, iodine electrophiles gave only product **49**, which is, presumably, due to the reverse reaction during quenching where iodine undergoes elimination (Table 2.2, entries 6–8).

Table 2.2. The Halogenation Nazarov Cyclization Scope[a]

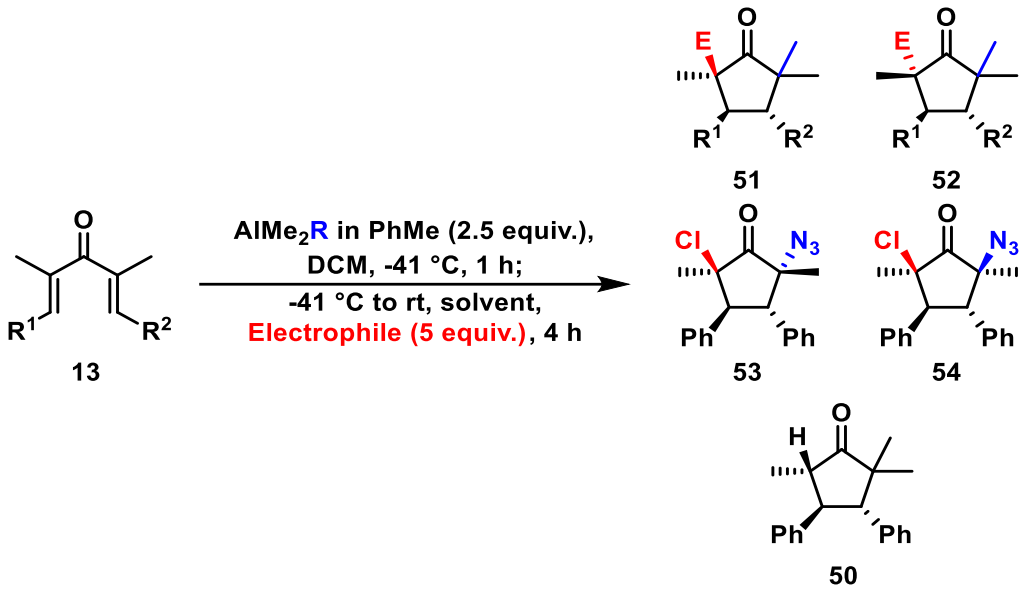

Entry	SM	R^1, R^2	Electrophile	LA	Product[b] (Yield %) [*dr*]
1	13a	Ph	NCS	$AlMe_3$	**51a/52a** (96) [24:1][c,e]
2	13a	Ph	NBS	$AlMe_3$	**51b** (76)[c]
3	13a	Ph	NFSI	$AlMe_3$	**51c/52c** (74) [4:1]
4	13a	Ph	Selectfluor	$AlMe_3$	**51c/52c** (85) [12:1]
5	13a	Ph	NCS	$AlMe_2N_3$	**53a/54a** (82) [1:1.2]
6	13a	Ph	NIS	$AlMe_3$	**50** (87)
7	13a	Ph	ClI	$AlMe_3$	**50** (90)
8	13a	Ph	I_2	$AlMe_3$	**50** (86)
9	13b	PhOMe	NBS	$AlMe_3$	**51d** (54)
10	13c	2-Napth	NCS	$AlMe_3$	**51e/52e** (81) [6:1]
11	13d	2-Furyl	NCS	$AlMe_3$	**51f/52f** (65) [49:1]
12	13e	PhCl	NCS	$AlMe_3$	**51g** (76)
13	13f	Ph, H	NCS	$AlMe_3$	**51h/52h** (88) [3:1]
14	13g	*i*Pr	NCS	$AlMe_3$	--[d]

[a] α-Halogencyclopentanones construction representative procedure described in Section 2.6.4. [b] Yields and ratio are based on the isolated product after chromatography. [c] Reaction was performed on a gram scale. [d] Decomposition of starting material was observed. [e] Second diastereomer formation observed only on a gram scale.

The first choice among electrophilic fluorinating reagents was NFSI (Table 2.2, entries 3, 4). Sulfonyl groups of NFSI, presumably, can coordinate with aluminum. NFSI gave 74% overall yield after 24 hours, with low diastereoselectivity of **51c**/**52c** in a 3.7:1 ratio. Low selectivity of fluorine trapping of the enolate might be explained that NFSI possibly creates less steric interaction compare to NCS and NBS halogenating reagents. Consequently, it is easier for NFSI to deliver fluorine from both sides of the enolate. The

trans orientation is preferred still over the *cis* because it creates less steric interactions between neighboring methyl and phenyl groups. Facial selectivity and yield for the fluorination reaction can be improved by using bulkier fluorine electrophilic source (Selectfluor). Selectfluor provides an 85% yield of products **51c/52c** in a 12:1 ratio.

The relative structure identification of the compounds **51c**/**52c** was based on the ^{1}H NMR studies (Figure 2.4). The β-stereogenic centers were set up during a conrotatory ring-closing event, and are presumed to have a *trans* relationship based on the ample precedent from the Nazarov cycliation literature. We were especially interested in the stereogenic center which is created during the enolate trapping event. First of all, the hydrogen shift in the ^{1}H NMR of the methyl group that is in the *cis/trans* position relative to the phenyl group must be under the influence of the anisotropic shielding effect. **51b** with the methyl *trans* to the neighboring phenyl, has a higher methyl chemical shift (1.50 ppm) than **51c** where the methyl is *cis* to the neighboring phenyl (1.12 ppm), an therefore anisotropically shielded. Following the discussed trends in chemical shifts, the relative configurations of other molecules were assigned.

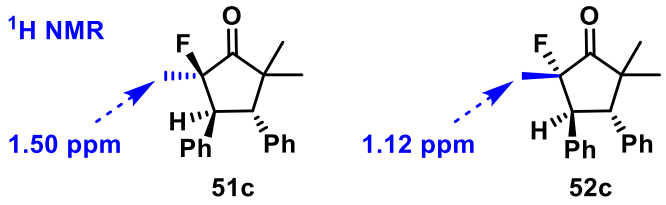

Figure 2.4. Spectroscopic evidence for structural assignments of **51c** and **52c**.

The double interrupted Nazarov reaction can be initiated by a variety of organoaluminum reagents. This was demonstrated by the reaction initiated by $AlMe_2N_3$ yielding 82% of desired **53a/54a** products, with a diastereomeric ratio of 1:1.2 on the stereogenic center formed during the delivery of the azide. The oxyallyl trapping can be relatively unselective in case of the Me_2AlN_3 due to rapid *pseudo*-intramolecular delivery of azide from aluminum. The configuration of **54a** was determined by X-ray crystallography (Figure 2.5). The X-ray crystal structure indicates that the chlorination occurred *cis* to the β-substituent, indicating product development diastereocontrol to avoid a developing eclipsing interaction of the vicinal methyl and phenyl groups. The

relative configurations of **51a–h/52a–h** were assigned based on their respective NMR comparisons to **54a**. It was done by relying on a consistent trend towards downfield ^{1}H NMR chemical shifts for α-methyl groups with a neighboring halogen atom and in a *trans* relationship to neighboring β-aryl groups.

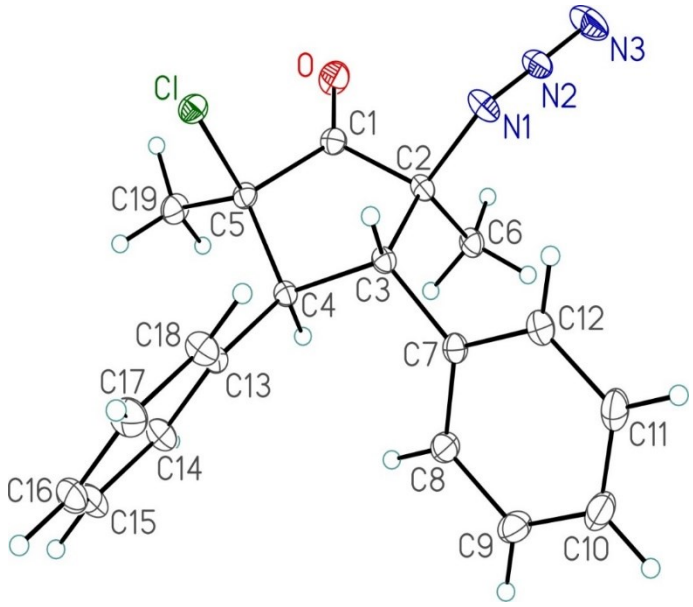

Figure 2.5. The OPTEP structure of **54a**.

Substrates with EDG in *para* position on aromatic rings (**13b** and **13c)** underwent desired reaction in slightly reduced yields compare to substrate **13a** for both chlorination and bromination (54% for bromide **51d** and 76% for chloride **51g**). In the case of expanded aromatic systems substrate **13c** reaction affords the formation of **51e/51e** in 81% yield (6:1 ratio). Heteroaromatic-containing substrate **13d** provided double-interrupted Nazarov products **51f** and **52f** in 65% yield, with a diastereomeric ratio of 49:1; substrate with no β-substituent **13f** forming **51h/52h** in 88% yield, with a diastereomeric ratio of 3:1. Substrate **13g** with alkyl groups at the remote β-termini underwent decomposition instead of the desired one-pot trapping process.

Performing the reaction under the standard reaction conditions with heteroaromatic substituents resulted in halogen trapping not only by the aluminum enolate. Mono and dihalogenation were observed on the heteroaromatic rings of the substrate (Figure 2.6). A mixture of **51f**, **52f**, **55f,** and **56f** compounds was formed, with an overall yield of ≈70%

and an approximate ratio for the isolated compounds **51f**:**56f**:**55f** equal to 23:9:1. Milder reaction conditions were used: the second step of the reaction (after the electrophile addition) was perfomed at - 41 °C for 1 h. Milder reaction conditions with a one equivalent of halogen electrophile provided a 65% overall yield, with a high diastereoselective ratio for **51f**:**52f** of 49:1 (based on isolated yields).

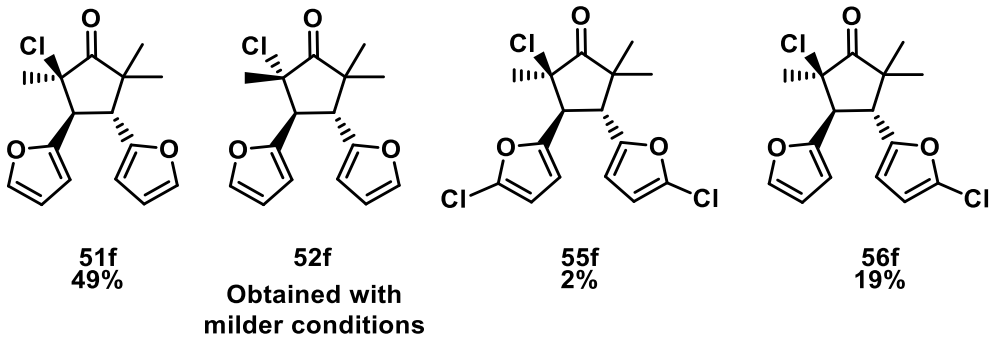

Figure 2.6. Products of the double interrupted Nazarov cyclization for heteroaromatic substrates.

To test the scalability of the reaction, it was performed on a gram scale (Scheme 2.23). A slightly diminished yield was observed in both cases: the NCS yield reduced insignificantly, dropping from 96% to 90%, although the formation of the second diastereomer was observed as an inseparable mixture, with a ratio of 24:1. The **52a** product was observed only after the reaction was performed on a gram scale. Bromination in the presence of NBS, in turn, formed only a single product **51b**, although some unreacted product **50** was still present in the system even after one day.

The advantages of the one-pot methylation/halogenation method were probed by examining the relative efficiency of a two-step sequence (Scheme 2.24). 2,2,5-Trimethyl-3,4-diphenylcyclopentanone **50** was treated with a strong base, such as LDA, and the formed enolate was trapped by MeI to test the enolate reactivity. The tetramethylated product **57** was formed in high yield, 82%. We continued our studies of enolate reactivity by changing the electrophile to NBS, and brominated products **51b/52b** formed in lower yield and with reduced diastereoselectivity (5:1).

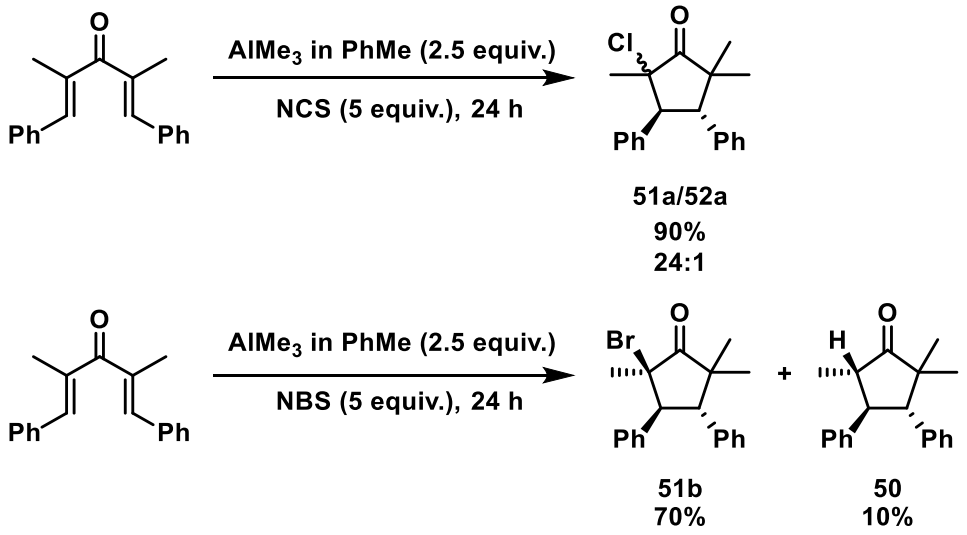

Scheme 2.23. The gram scale double interrupted Nazarov cyclization.

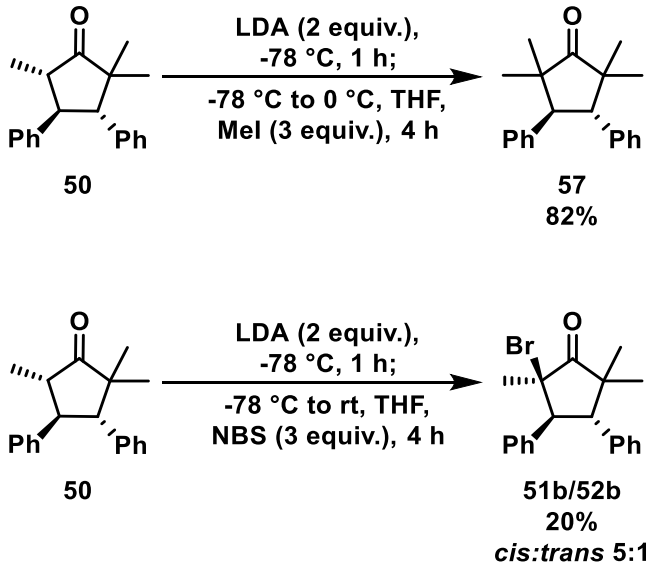

Scheme 2.24. The base mediated enolate trapping by NBS.

The next step was to test the possibility to perform the reaction under open-air conditions to be able to manipulate the reaction with no need for an inert atmosphere (Scheme 2.25). To achieve this goal the reaction was performed in the presence of DABAL-Me_3 which is a non-pyrophoric analog of $AlMe_3$ and has an excellent handling characteristics (solid, can be handled in air). The addition of the organoaluminum reagent resulted in the decomposition of the desired product.[130]

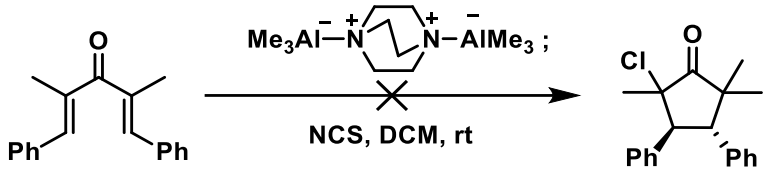

Scheme 2.25. The cyclization reaction under open-air conditions.

The exact mechanism of halogen introduction using electrophilic halogen sources is unclear. Alkylaluminum species are postulated to undergo a 1,2-transfer of one of their substituents to afford aluminum enolate intermediate **II**.[111] Therefore, we think that our aluminum enolate plays a dual role in the reaction (Scheme 2.26).[99,101] The coordination of the halogen succinimide to aluminum activates the enolate **III**, with the subsequent delivery of the halogen.[129] The formation of both (a better electrophile and a more nucleophilic enolate) in close proximity to each other could explain the high efficiency of the transformation.

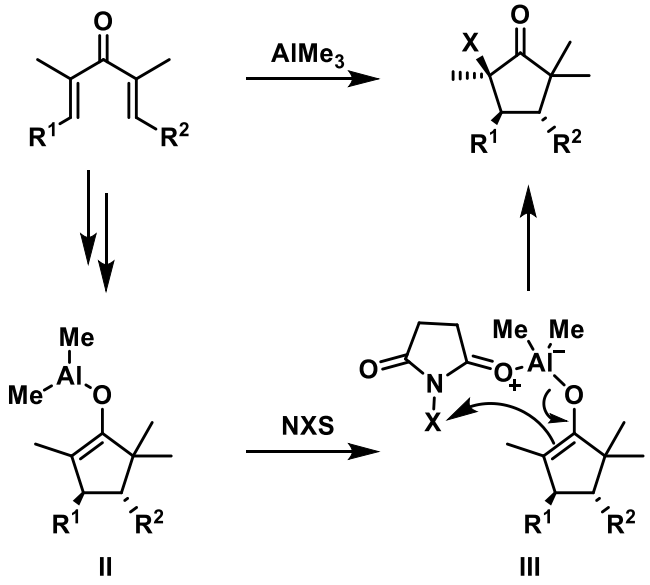

Scheme 2.26. The proposed mechanism for the double interrupted Nazarov cyclization with halogen electrophile.

2.5 Conclusion

In summary, we demonstrated a new one-pot, multi-component, convenient synthetic method to prepare α-halocyclopentanones via the double interrupted Nazarov cyclization

initiated by organoaluminum reagents. Organoaluminum serves as an initiator, a nucleophile source to trap an oxyallyl cation, and proposed to deliver an electrophile closer to the aluminum enolate. The new method leads to the desired product formation with high diastereoselectivity in most cases. During the reaction course, up to four stereogenic centers were set and two new C–C and one C–Hal bonds were formed, affording highly substituted cyclopentanones in good to excellent yields.

2.6 Experimental

2.6.1 General Information

Reactions were carried out in flame-dried glassware under a positive argon atmosphere unless otherwise stated. Transfer of anhydrous solvents and reagents was accomplished with oven-dried syringes or cannulae. The 4 Å molecular sieves were stored in an oven and flame-dried before use. THF and DCM solvents were purified using the LC Technology Solutions Inc. solvent purification system. Anhydrous MeCN was distilled over calcium hydride under a nitrogen atmosphere before use. All other solvents were purchased as ACS reagents and used without further purification. Thin-layer chromatography was performed on glass plates precoated with 0.25 mm Kieselgel 60 F254 (Merck). Flash chromatography columns were packed with 230–400 mesh silica gel (Silicycle). ^{1}H NMR and ^{13}C spectra were recorded at 400/500/700 and 100/125/175 MHz, respectively, and coupling constants (*J*) are reported in Hertz (Hz). NMR chemical shifts are reported relative to the residual $CHCl_3$ in $CDCl_3$ (7.26 ppm) internal standard. Standard notation is used to describe the multiplicity of signals observed in ^{1}H NMR spectra: broad (br), apparent (app), multiplet (m), singlet (s), doublet (d), triplet (t), etc. Infrared (IR) spectra were measured with a Mattson Galaxy Series FT-IR 3000 spectrophotometer. High-resolution mass spectrometry (HRMS) data (APPI/ESI technique) were recorded using an Agilent Technologies 6220 oaTOF instrument. HRMS data (EI technique) were recorded using a Kratos MS50 instrument.

Dienones can be prepared using the method listed below or via literature procedures: **13a**,[131] **13b**,[132] **13c**,[130] **13d**,[110] **13e**,[133] **13f**.[134] *N*CS and *N*BS were recrystallized via standard procedures before use.[135,136,137] Me_2AlN_3 was generated via standard procedure before use.[120]

2.6.2 General Procedures

2.6.2.1 General Procedure A for Preparation of Dienones 13a and 13d

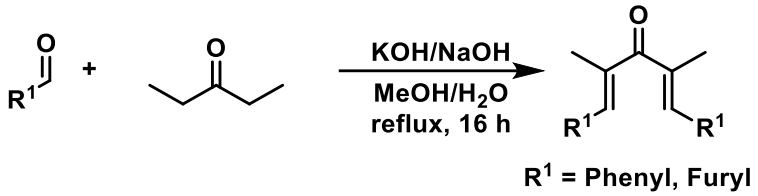

Into a 250 mL, round-bottom flask equipped with a reflux condenser and stir bar was added a mixture of solvents (40.0 mL of MeOH: 20.0 mL of H_2O). KOH (7.00 g, 125 mmol) and NaOH (2.00 g, 50.0 mmol) were added into the flask at rt. After cooling down the flask, aldehyde was added (122 mmol), followed by 3-pentanone (5.00 g, 58 mmol). The resulting solution was heated to reflux overnight. The next day, the mixture was cooled down to rt and neutralized with 1.0 M HCl to pH = 7 (the solution changes color from orange to white and some product might precipitate out of the solution). Solution was transferred into a separatory funnel, and was extracted with DCM (3 x 50 mL). Combined organic layers were rinsed with water and brine, dried over $MgSO_4$ and concentrated in vacuo. The crude mixture was triturated with MeOH, filtered under vacuum, and washed with cold MeOH to afford **13a** and **13d** as a white (28–40% yield) or orange (15–35% yield) solid, respectively.

2.6.2.2 General Procedure B for Preparation of Dienones 13b, 13c, and 13e

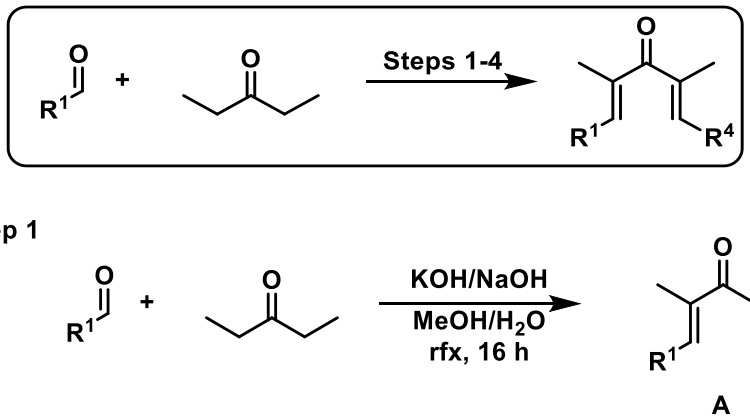

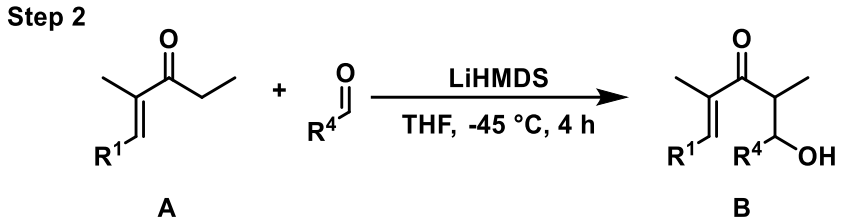

Step 1: Intermediate compound A obtained via known literature procedure.[113,138] The desired enone was formed in 40–49% yield.

Step 2: Into a 250 mL flame dried round-bottom flask with a magnetic stir bar charged with argon was added solution of LiHMDS (1.0 M in THF, 12 mL, 12 mmol, 1.5 equiv) and diluted with dry THF (1.0 mL of solvent per each 1 mmol of reagent) and cooled down to -45 °C. Intermediate **A** (1 equiv) was dissolved in dry THF (0.3 M) under an argon atmosphere in a separate flame dried flask. The solution of intermediate **A** was transferred via cannula into the solution of LiHMDS at -45 °C and stirred for 1 h at that temperature. To the formed enolate solution, a solution of aldehyde (1.2 equiv) in dry THF (1.0 M) was added dropwise. Stirring was continued for an additional 2 h. The reaction mixture was quenched with saturated NH_4Cl and transferred into a separatory funnel. Extraction was performed with EtOAc (3 x 50 mL). The combined organic layers were washed with water and brine, dried over $MgSO_4$, filtered under vacuum, and concentrated under vacuum. The crude mixture was purified by flash column chromatography (EtOAc/hexanes 1:9) to obtain intermediate **B** as a mixture of diastereomers in 60–65% yield.

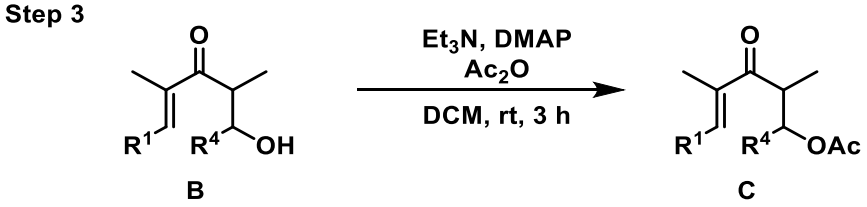

Step 3: In a flame dried round bottom flask, the mixture of alcohols **B** (1 equiv) was diluted by DCM (0.2 M), and dry Et_3N (10 equiv) was added to the flask. DMAP (0.05 equiv) and Ac_2O (1.3 equiv) were added to the solution at 0 °C and stirred for 3 h at rt. The reaction was quenched with a saturated solution of NH_4Cl. Extraction was performed with EtOAc (3 x 50 mL). The combined organic layers were washed with water and brine,

dried over $MgSO_4$, filtered under vacuum, and concentrated under vacuum. The crude reaction mixture was purified using flash column chromatography (EtOAc/hexanes 1:9) to obtain intermediate **C** in 90–93% yield.

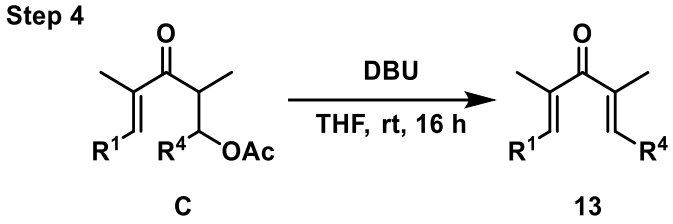

Step 4: To intermediate **C** (1 equiv) diluted in THF (1.0 M) was added DBU (1.5 equiv) and stirred at rt for 24 h. The solvent was concentrated under reduced pressure, and the crude mixture was subjected to flash column chromatography (EtOAc/hexanes 1:9) to obtain pure dienone **13**.[130–134]

2.6.2.3 Procedure C for Preparation of Dienone 13f

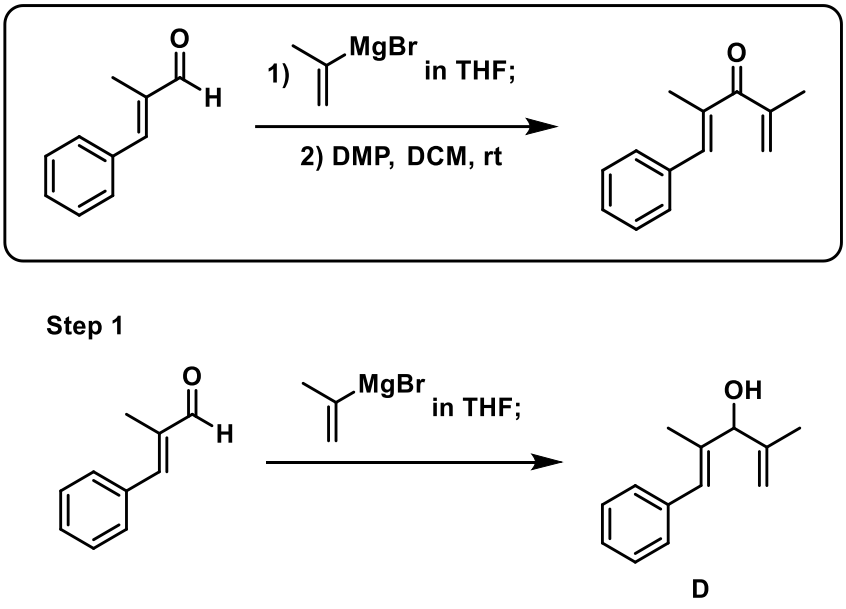

Step 1: To a solution of α-methyl-*trans*-cinnamaldehyde (1.5 g, 10 mmol) in THF (10 mL) was added a solution of isopropenylmagnesium bromide (1.2 equiv) in THF (0.5 M). The reaction mixture was stirred at rt for another 3 h. The reaction was quenched with water. Solution was extracted with DCM (3 x 50 mL). The combined organic layers were

washed with brine, dried over $MgSO_4$, filtered, and concentrated under vacuum. The crude reaction mixture was purified using flash column chromatography (EtOAc/hexanes 1:5) to obtain intermediate **D** as a colorless oil (1.5 g, 80%).

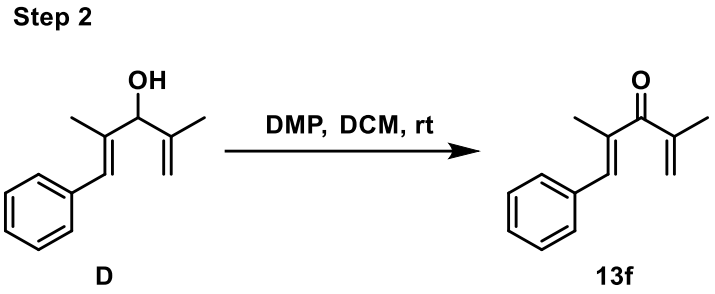

Step 2: Into a flamed dried round bottom flask was added Dess–Martin periodinane (1.2 equiv) in DCM (0.1 M). Solution of the dienol **D** in DCM (1.0 M) was added dropwise. The reaction mixture was stirred for 24 h at rt. The reaction was cooled down to 0 °C and quenched with aqueous solution of NaOH (1.0 M, 20 mL). Solution was extracted with DCM (3 x 50 mL). The combined organic layers were washed with sodium hydroxide (3 x 50 mL), water (2 x 50 mL) and brine, dried over $MgSO_4$, filtered, and concentrated under vacuum to afford pure dienone **13f** (1.3 g, 85%) as a colorless oil.

2.6.2.4 General Procedure D for Preparation of Enolate with Subsequent Trapping by Electrophiles

To a solution of **50** (260 mg, 1.00 mmol) in DCM (0.3 M) under a nitrogen atmosphere at -78 ºC was added LDA (2.0 M in THF, 1.0 mL, 2 mmol, 2 equiv) dropwise. The reaction mixture was stirred for 1 h. The electrophile (MeI (3 equiv); NBS (3 mmol, 3 equiv) in THF (0.5 M)) was added at -78 ºC, then the solution was allowed to warm to 0 ºC and stirred for 4 h. The reaction was quenched with aqueous solution of HCl (2.0 M, 3 mL) at 0 ºC and warmed to rt. After separation of the phases, the aqueous layer was extracted with DCM (3 x 10 mL). The combined organic layers were washed with brine and dried over $MgSO_4$, filtered, and concentrated under vacuum. Purification by column chromatography (silica gel) provided **57** (239 mg, 82%) or **51b**/**52b** (71 mg, 20%, 5:1) as white solids.

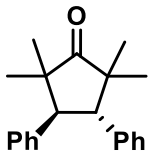

57

(3*S,4*S**)-2,2,5,5-Tetramethyl-3,4-diphenylcyclopentanone (57)**: R_f 0.60 (hexanes/EtOAc 9:1); mp 128–130 °C; IR (cast film) ν_{max} 3028, 2959, 2929, 2866, 1736, 1601, 1499 cm^{-1}; ^1H NMR (400 MHz, $CDCl_3$) δ 7.27–7.14 (m, 10H), 3.67 (s, 2H), 1.28 (s, 6H), 0.76 (s, 6H); ^{13}C NMR (125 MHz, $CDCl_3$) δ 224.8, 137.3, 129.0, 128.0, 126.6, 52.6, 49.2, 24.7, 20.5; HRMS (EI, M+) for $C_{21}H_{24}O$ calcd 292.1827, found: m/z 292.1827.

2.6.3 Representative Procedure for α-Halocyclopentanone Formation via Sequential Methyl/halogen Trapping

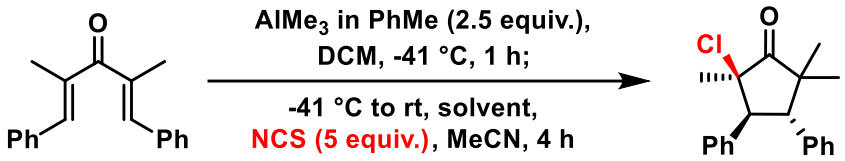

To the solution of **13a** (263 mg, 1 mmol) with activated 4 Å MS (300 mg) in DCM (0.3 M) under a nitrogen atmosphere at -41 ºC was added $AlMe_3$ (1.25 mL, 2.0 M solution in toluene, 2.5 equiv). The reaction mixture was stirred until complete consumption of the starting material was observed by TLC (1 h). The halogen electrophile (5 mmol, 5 equiv) was dissolved in a suitable solvent (0.5 M, 10 mL: NCS in MeCN, NBS in THF, NFSI in THF, Selectfluor in MeCN), added at -41 ºC, then the solution was allowed to warm to rt and stirred for 4 h. The reaction was quenched with aqueous solution of HCl (2.0 M, 3 mL) at 0 ºC and warmed to rt. After separation of the phases, the aqueous layer was extracted with DCM (3 x 10 mL). The combined organic extracts were washed with brine, and dried over $MgSO_4$, filtered, and concentrated in vacuo. Purification by column

chromatography (silica gel, DCM/hexanes 1:1) provided the desired product **51a** (300 mg, 96%).

2.6.4 Spectral Data for Compounds 51a/52a–51h/52h, and 53a/54a

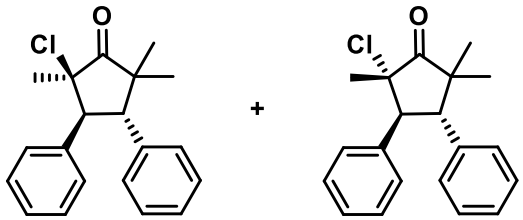

51a **52a**

The reaction was performed by the standard halocyclopentanone formation procedure with dienone **13a**. Column chromatography (DCM/hexanes 1:1) gave **51a** (300 mg, 96%) as a white solid. Formation of **52a** was detected on a gram scale reaction as an inseparable mixture with **51a**. To determine the structures and assign resonances ^{1}H NMR was used. The NMR data for the mixture was taken and major isomer **51a** peaks were subtracted out the peaks that were attributable to it. The diastereomeric ratio (24:1) was determined based on ^{1}H NMR. Formation of **52a** was not observed on 1 mmol scale.

(2*R,3*S**,4*S**)-2-Chloro-2,5,5-trimethyl-3,4-diphenylcyclopentanone (51a)**: R_f 0.38 (DCM/hexanes 1:1); mp 161–163 °C; IR (cast film) ν_{max} 3000, 2963, 1747, 737 cm^{-1}; ^{1}H NMR (500 MHz, $CDCl_3$) δ 7.29–7.15 (m, 10H), 3.96 (d, J = 13.2 Hz, 1H), 3.62 (d, J = 13.2 Hz, 1H), 1.70 (s, 3H), 1.45 (s, 3H), 0.72 (s, 3H); ^{13}C NMR (125 MHz, $CDCl_3$) δ 213.8, 136.3, 134.6, 129.8, 128.9, 128.2, 128.0, 127.5, 126.9, 72.1, 53.9, 52.4, 48.3, 26.3, 23.5, 21.3; Anal. calcd for $C_{20}H_{21}ClO$: C, 76.8; H, 6.8, found: C, 75.8; H, 6.8; HRMS (EI, M^+) for $C_{20}H_{21}{}^{35}ClO$ calcd 312.1281, found: 312.1285.

(2*S*,3*S*,4*S*)-2-Chloro-2,5,5-trimethyl-3,4-diphenylcyclopentanone (52a) (partial data): ^{1}H NMR (500 MHz, $CDCl_3$) δ 7.29–7.15 (m, 10H), 4.28 (d, J = 13.6 Hz, 1H), 3.52 (d, J = 13.6 Hz, 1H), 1.28 (s, 3H), 1.27 (s, 3H), 0.92 (s, 3H).

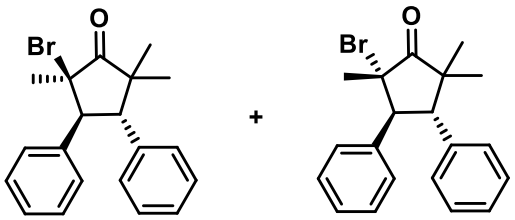

51b **52b**

The reaction was performed by the standard halocyclopentanone formation procedure with dienone **13a**. Column chromatography (DCM/hexanes 1:1) gave **51b** (271 mg, 76%) as a white solid. Formation of **52b** was not observed under the standard conditions. **52b** was obtained in the reaction with base enolate as an inseparable mixture with **51b**. The NMR data for the mixture was taken and major isomer **51b** peaks were subtracted out the peaks that were attributable to it. The diastereomeric ratio (5:1) was determined based on ^{1}H NMR.

(2*R,3*S**,4*S**)-2-Bromo-2,5,5-trimethyl-3,4-diphenylcyclopentanone (51b)**: R_f 0.38 (DCM/hexanes 1:1); mp 158–160 °C; IR (cast film) ν_{max} 3087, 2975, 1741, 740 cm^{-1}; ^{1}H NMR (500 MHz, $CDCl_3$) δ 7.25–7.12 (m, 10H), 3.96 (d, J = 13.0 Hz, 1H), 3.35 (d, J = 13.0 Hz, 1H), 1.90 (s, 3H), 1.50 (s, 3H), 0.72 (s, 3H); ^{13}C NMR (125 MHz, $CDCl_3$) δ 213.6, 136.3, 135.3, 129.6, 129.0, 128.3, 128.0, 127.5, 126.9, 69.2, 54.1, 52.9, 48.4, 26.8, 24.7, 21.2; Anal. calcd for $C_{20}H_{21}BrO$: C, 67.2; H, 5.9, found: C, 67.4; H, 5.9; HRMS (EI, M^+) for $C_{20}H_{21}{}^{79}BrO$ calcd 356.0775, found: 356.0771.

(2*S,3*S**,4*S**)-2-Bromo-2,5,5-trimethyl-3,4-diphenylcyclopentanone (52b) (partial data)**: ^{1}H NMR (500 MHz, $CDCl_3$) δ 7.29–7.15 (m, 10H), 4.52 (d, J = 13.6 Hz, 1H), 3.51 (d, J = 13.6 Hz, 1H), 1.39 (s, 3H), 1.27 (s, 3H), 1.00 (s, 3H); ^{13}C NMR (125 MHz, $CDCl_3$) δ 215.8, 135.5, 134.8, 128.9, 128.3, 128.3 127.5, 127.2, 64.4, 55.1, 52.9, 48.9, 24.1, 24.0, 21.5.

Not all sp^2 carbon resonances could be detected due to overlap with the major isomer.

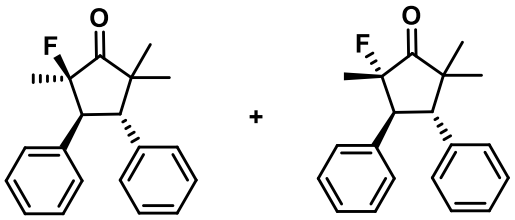

51c **52c**

The reaction was performed by the standard halocyclopentanone formation procedure with dienone **13a**. Column chromatography (DCM/hexanes 1:3) gave **51c** (231 mg, 78%) and **52c** (21 mg, 7%) as white solids.

(2*R,3*S**,4*S**)-2-Fluoro-2,5,5-trimethyl-3,4-diphenylcyclopentanone (51c)**: R_f 0.38 (DCM/hexanes 1:2); mp 71–74 °C; IR (cast film) ν_{max} 3063, 2970, 1755, 699 cm^{-1}; ^1H NMR (500 MHz, $CDCl_3$) δ 7.39–7.20 (m, 10H), 3.94 (d, J = 13.2 Hz, 1H), 3.53 (dd, J = 30.7, 13.2 Hz, 1H), 1.50 (d, J = 23.3 Hz, 3H), 1.42 (s, 3H), 0.82 (s, 3H); ^{13}C NMR (125 MHz, $CDCl_3$) δ 214.8 (d, J_{CF} = 16.3 Hz), 136.4, 134.6, 129.8, 128.9, 128.4, 128.3, 127.5, 127.0, 95.7 (d, J_{CF} = 179.8 Hz), 53.3, 52.8 (d, J_{CF} = 19.8 Hz), 48.3, 24.6, 21.0, 18.0 (d, J_{CF} = 25.9 Hz); ^{19}F NMR δ -160.0 (dq, J = 31.7, 23.2 Hz, 1F); Anal. calcd for $C_{20}H_{21}FO$: C, 81.1; H, 7.1., found: C, 80.7; H, 7.0; HRMS (EI, M^+) for $C_{20}H_{21}FO$ calcd 296.1577, found: 296.1574.

(2*S,3*S**,4*S**)-2-Fluoro-2,5,5-trimethyl-3,4-diphenylcyclopentanone (52c)**: R_f 0.31 (DCM/hexanes 1:2); mp 83–85 °C; IR (cast film) ν_{max} 3090, 2970, 1755, 700 cm^{-1}; ^1H NMR (500 MHz, $CDCl_3$) δ 7.31–7.19 (m, 10H), 4.17 (dd, J = 21.9, 13.6 Hz, 1H), 3.45 (d, J = 13.6 Hz, 1H), 1.30 (s, 3H), 1.12 (d, J = 23.3 Hz, 3H), 0.87 (s, 3H); ^{13}C NMR (125 MHz, $CDCl_3$) δ 216.7 (d, J_{CF} = 15.3 Hz), 135.8, 135.2, 128.8, 128.8, 128.4, 128,4, 127.2, 127.2, 98.7 (d, J_{CF} = 194.0 Hz), 50.4 (d, J_{CF} = 11.0 Hz), 50.3, 47.3, 24.5, 21.2, 17.8 (d, J_{CF} = 27.8 Hz); ^{19}F NMR δ -146.0 (app p, J = 22.8 Hz, 1F); Anal. calcd for $C_{20}H_{21}FO$: C, 81.1; H, 7.1, found: C, 80.2; H, 7.0; HRMS (EI, M^+) for $C_{20}H_{21}FO$ calcd 296.1577, found: 296.1573.

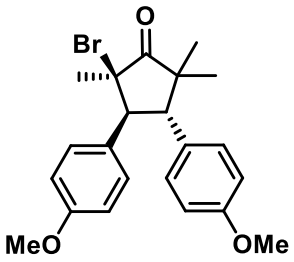

51d

The reaction was performed by the standard halocyclopentanone formation procedure with dienone **13b**. Column chromatography (DCM/hexanes 1:1) gave **51d** (225 mg, 54%) as a white solid.

(2*R,3*S**,4*S**)-2-Bromo-3,4-bis(4-methoxyphenyl)-2,5,5-trimethylcyclopentanone (51d)**: R_f 0.35 (DCM/hexanes 1:1); mp 104–106 °C; IR (cast film) ν_{max} 3036, 2965, 1771, 737 cm^{-1}; ^1H NMR (500 MHz, $CDCl_3$) δ 7.17 (d, *J* = 8.7 Hz, 2H), 7.04 (d, *J* = 8.7 Hz, 2H), 6.80 (d, *J* = 8.7 Hz, 2H), 6.76 (d, *J* = 8.7 Hz, 2H), 3.83 (d, *J* = 12.5 Hz, 1H), 3.74 (s, 3H), 3.73 (s, 3H), 3.23 (d, *J* = 12.5 Hz, 1H), 1.87 (s, 3H), 1.46 (s, 3H), 0.70 (s, 3H); ^{13}C NMR (125 MHz, $CDCl_3$) δ 213.9, 158.4, 158.3, 130.6, 130.0, 128.3, 127.4, 113.7, 113.4, 69.9, 55.1, 55.1, 53.7, 52.4, 48.4, 26.8, 24.6, 21.2; Anal. calcd for $C_{22}H_{25}BrO$: C, 63.6; H, 6.0, found: C, 62.3; H, 6.1; HRMS (EI, M^+) for $C_{22}H_{25}{}^{79}BrO$ calcd 416.0982, found: 416.0986.

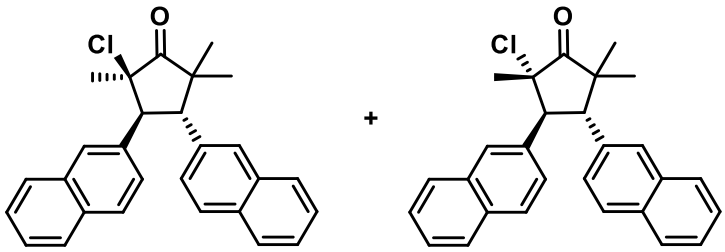

51e **52e**

The reaction was performed by the standard halocyclopentanone formation procedure with dienone **13c**. Column chromatography (DCM/hexanes 1:1) gave **51e** (289 mg, 70%) and **52e** (45 mg, 11%) as white solids.

(2*R,3*S**,4*S**)-2-Chloro-2,5,5-trimethyl-3,4-di(naphthalen-2-yl)cyclopentanone (51e)**: R_f 0.47 (DCM/hexanes 1:1); mp 195–198 °C; IR (cast film) ν_{max} 3049, 2971 1750, 779 cm^{-1}; ^1H NMR (500 MHz, $CDCl_3$) δ 8.50 (d, *J* = 8.7 Hz, 1H),

8.33 (d, *J* = 8.7 Hz, 1H), 7.82 (d, *J* = 8.0 Hz, 1H), 7.79 (d, *J* = 8.0 Hz, 1H), 7.63 (m, 4H), 7.57 (d, *J* = 8.0 Hz, 1H), 7.50 (t, *J* = 7.5 Hz, 2H), 7.27 (d, *J* = 7.5 Hz, 1H), 7.22 (t, *J* = 7.7 Hz, 1H), 7.13 (t, *J* = 7.9 Hz, 1H), 5.27 (d, *J* = 12.5 Hz, 1H), 4.92 (d, *J* = 12.5 Hz, 1H), 1.76 (s, 3H), 1.62 (s, 3H), 0.95 (s, 3H); ^{13}C NMR (125 MHz, $CDCl_3$) δ 213.9, 134.1, 133.9, 133.4, 133.2, 132.8, 130.6, 129.4, 129.1, 128.1, 127.5, 127.0, 126.3, 126.1, 125.5, 125.3, 125.3, 125.1, 125.0, 123.8, 122.7, 73.9, 49.5, 48.2, 47.2, 27.8, 24.6, 22.2; Anal. calcd for $C_{28}H_{25}ClO$: C, 78.4; H, 6.1, found: C, 76.4; H, 7.0; HRMS (EI, M^+) for $C_{28}H_{25}{}^{35}ClO$ calcd 412.1594, found: 412.1590.

(2*S,3*S**,4*S**)-2-Chloro-2,5,5-trimethyl-3,4-di(naphthalen-2-yl)cyclopentanone (52e)**: R_f 0.43 (DCM/hexanes 1:1); mp 211–213 °C; IR (cast film) ν_{max} 3050, 2980, 1750, 780 cm^{-1}; ^{1}H NMR (500 MHz, $CDCl_3$) δ 8.71 (d, *J* = 8.8 Hz, 1H), 8.34 (d, *J* = 8.8 Hz, 1H), 7.79 (m, 2H), 7.61 (m, 4H), 7.51 (q, *J* = 7.8 Hz, 2H), 7.38 (d, *J* = 7.1 Hz, 1H), 7.35 (d, *J* = 7.1 Hz, 1H), 7.18 (m, 2H), 5.49 (d, *J* = 13.3 Hz, 1H), 4.78 (d, *J* = 13.3 Hz, 1H), 1.48 (s, 3H), 1.34 (s, 3H), 1.17 (s, 3H); ^{13}C NMR (125 MHz, $CDCl_3$) δ 215.7, 134.1, 134.1, 133.5, 133.2, 131.8, 131.6, 129.2, 128.8, 128.1, 127.7, 126.1, 126.1, 125.7, 125.4, 125.3, 125.1, 125.0, 124.9, 124.7, 123.2, 71.7, 49.8, 49.7, 46.7, 25.3, 23.6, 21.9; Anal. calcd for $C_{28}H_{25}ClO$: C, 78.4; H, 6.1, found: C, 77.6; H, 5.9; HRMS (EI, M^+) for $C_{28}H_{25}{}^{35}ClO$ calcd 412.1594, found: 412.1597.

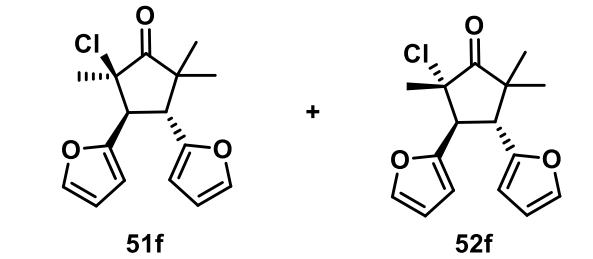

51f **52f**

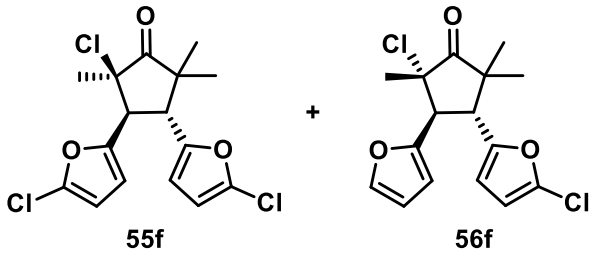

55f **56f**

The reaction, under standard halocyclopentanone formation procedure with dienone **13c**, was forming multiple compounds. Out of this mixture it was possible to isolate **51f**, **55f** and **56f**. Column chromatography (DCM/hexanes 1:2) gave **51f** (143 mg, 49%), **55f** (6 mg, 2%) and **56f** (56 mg, 19%) as yellow solids.

α-Halogencyclopentanones 51f/52f Representative Procedure (Conditions B): to a solution of **13d** (242 mg, 1 mmol) with activated 4 Å MS (300 mg) in DCM (0.3 M) under a nitrogen atmosphere at -41 ºC was added $AlMe_3$ (1.25 mL, 2.0 M solution in toluene, 2.0 equiv). The reaction mixture was stirred until complete consumption of the starting material was observed by TLC (1 h). Next, NCS (0.2 M in MeCN, 1.2 equiv) was added to the reaction mixture at -41 ºC over 5 min. The reaction was stirred for 1 h at -41 ºC. The reaction was warmed up to 0 ºC and quenched with aqueous solution of HCl (2.0 M, 3 mL). After separation of the phases, extraction was performed with DCM (3 x 10 mL). The combined organic layers were washed with brine, and dried over $MgSO_4$, filtered, and concentrated in vacuo. Purification by column chromatography (DCM/hexanes 1:2) gave **51f** (187 mg, 64%) and **52f** (3 mg, 1%) as yellow solids.

(2*R,3*S**,4*R**)-2-Chloro-3,4-di(furan-2-yl)-2,5,5-trimethylcyclopentanone (51f)**: R_f 0.31 (DCM/hexanes 1:2); mp 100–104 °C; IR (cast film) ν_{max} 3146, 2971, 1751, 742 cm^{-1}; ^1H NMR (600 MHz, $CDCl_3$) δ 7.37 (dd, *J* = 1.8, 0.8 Hz, 1H), 7.32 (dd, *J* = 1.8, 0.8 Hz, 1H), 6.31 (dd, *J* = 3.3, 0.8 Hz, 1H), 6.28 (dd, *J* = 3.3, 1.8 Hz, 1H), 6.15 (dt, *J* = 3.3, 0.8 Hz, 1H), 6.08 (dt, *J* = 3.3, 0.8 Hz, 1H), 3.78 (d, *J* = 12.7 Hz, 1H), 3.73 (d, *J* = 12.7 Hz, 1H), 1.80 (s, 3H), 1.44 (s, 3H), 0.79 (s, 3H); ^{13}C NMR (125 MHz, $CDCl_3$) δ 212.7, 152.0, 150.6, 143.0 (by HMBC), 142.9 (by HMBC), 110.3, 110.2, 108.4, 107.7, 70.9, 48.4, 48.0, 46.7, 26.3, 23.7, 21.3; Anal. calcd for $C_{16}H_{17}ClO_3$: C, 65.6; H, 5.9, found: C, 65.4; H, 5.8; HRMS (EI, M^+) for $C_{16}H_{17}{}^{35}ClO_3$ calcd 292.0866, found: 292.0868.

The peaks at 143.0 and 142.9 ppm were inferred from 2D correlations. The absence of peaks in the ^{13}C NMR experiment can be a combination of lower sensitivity, slow relaxation or broadening of signals.

(2*S,3*S**,4*R**)-2-Chloro-3,4-di(furan-2-yl)-2,5,5-trimethylcyclopentanone (52f)**: R_f 0.29 (DCM/hexanes 1:2); ^1H NMR (600 MHz, $CDCl_3$) δ 7.34 (dd, *J* = 1.9, 0.8

Hz, 1H), 7.32 (dd, *J* = 1.9, 0.8 Hz, 1H), 6.32 (dd, *J* = 3.2, 2.0 Hz, 1H), 6.27 (m, 2H), 6.06 (d, *J* = 3.2 Hz, 1H), 4.16 (d, *J* = 13.5 Hz, 1H), 3.56 (d, *J* = 13.5 Hz, 1H), 1.33 (s, 3H), 1.33 (s, 3H), 0.94 (s, 3H); ^{13}C NMR (125 MHz, $CDCl_3$) δ 214.9, 151.4, 150.0, 142.4, 142.0, 110.3, 110.2, 109.0, 107.7, 70.0, 49.5, 48.6, 46.3, 24.4, 23.0, 21.5; HRMS (EI, M^+) for $C_{16}H_{17}{}^{35}ClO_3$ calcd 292.0861, found: 292.0869.

(2*R,3*S**,4*R**)-2-Chloro-3,4-bis(5-chlorofuran-2-yl)-2,5,5-trimethylcyclopentanone (55f)**: R_f 0.21 (DCM/hexanes 1:2); mp 71–74 °C; IR (cast film) ν_{max} 3057, 2971, 1755, 741 cm^{-1}; ^{1}H NMR (600 MHz, $CDCl_3$) δ 6.17 (dd, *J* = 3.3, 0.8 Hz, 1H), 6.11 (dd, *J* = 3.3, 0.8 Hz, 1H), 6.10 (d, *J* = 3.3 Hz, 1H), 6.07 (d, *J* = 3.3 Hz, 1H), 3.67 (d, *J* = 12.6 Hz, 1H), 3.62 (d, *J* = 12.6 Hz, 1H), 1.78 (s, 3H), 1.43 (s, 3H), 0.84 (s, 3H); ^{13}C NMR (125 MHz, $CDCl_3$) δ 211.7, 151.2, 149.7, 135.9, 135.9, 110.3, 110.1, 107.0, 106.8, 70.3, 48.1, 47.8, 46.7, 26.3, 23.5, 21.4; Anal. calcd for $C_{16}H_{15}Cl_3O_3$: C, 51.3; H, 4.2, found: C, 54.9; H, 5.4; HRMS (EI, M^+) for $C_{16}H_{15}{}^{35}Cl_3O_3$ calcd 360.0087, found: 360.0084.

(2*S,3*S**,4*R**)-2-Chloro-4-(5-chlorofuran-2-yl)-3-(furan-2-yl)-2,5,5-trimethylcyclopentanone (56f)**: R_f 0.23 (DCM/hexanes 1:2); mp 85–89 °C; IR (cast film) ν_{max} 3123, 2972, 1754, 737 cm^{-1}; ^{1}H NMR (600 MHz, $CDCl_3$) δ 7.38 (dd, *J* = 1.9, 0.8 Hz, 1H), 6.33 (dd, *J* = 3.3, 1.9 Hz, 1H), 6.18 (dt, *J* = 3.3, 0.8 Hz, 1H), 6.07 (dd, *J* = 3.3, 0.7 Hz, 1H), 6.04 (d, *J* = 3.3 Hz, 1H), 3.75 (d, *J* = 12.6 Hz, 1H), 3.65 (d, *J* = 12.6 Hz, 1H), 1.78 (s, 3H), 1.44 (s, 3H), 0.85 (s, 3H); ^{13}C NMR (125 MHz, $CDCl_3$) δ 212.2, 151.7, 150.1, 135.4, 135.4, 110.3, 110.1, 108.6, 106.8, 70.7, 48.1, 47.8, 46.9, 26.3, 23.6, 21.4; Anal. calcd for $C_{16}H_{16}Cl_2O_3$: C, 58.7; H, 4.9, found: C, 58.6; H, 5.2; HRMS (EI, M^+) for $C_{16}H_{16}{}^{35}Cl_2O_3$ calcd 326.0447, found: 326.0444.

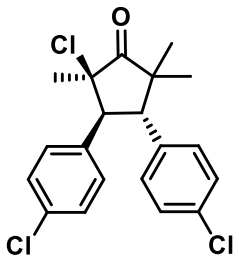

51g

The reaction was performed by the standard halocyclopentanone formation procedure with dienone **13e**. Column chromatography (DCM/hexanes 1:1) gave **51g** (316 mg, 76%) as a white solid.

(2*R,3*S**,4*S**)-2-Chloro-3,4-bis(4-chlorophenyl)-2,5,5-trimethylcyclopentanone (51g)**: R_f 0.38 (DCM/hexanes 1:1); mp 100–103 °C; IR (cast film) ν_{max} 3031, 2970, 1751, 738 cm^{-1}; ^1H NMR (500 MHz, $CDCl_3$) δ 7.27–7.18 (m, 6H), 7.06 (d, *J* = 8.4 Hz, 2H), 3.88 (d, *J* = 13.4 Hz, 1H), 3.55 (d, *J* = 13.4 Hz, 1H), 1.68 (s, 3H), 1.43 (s, 3H), 0.74 (s, 3H); ^{13}C NMR (125 MHz, $CDCl_3$) δ 212.9, 134.5, 133.7, 133.0, 132.8, 131.0, 130.2, 128.6, 128.5, 71.6, 53.6, 52.1, 48.2, 26.2, 23.4, 21.2; Anal. calcd for $C_{20}H_{19}Cl_3O$: C, 62.6; H, 5.5, found: C, 63.4; H, 5.2; HRMS (EI, M^+) for $C_{20}H_{19}{}^{35}Cl_3O$ calcd 380.0501, found: 380.0493.

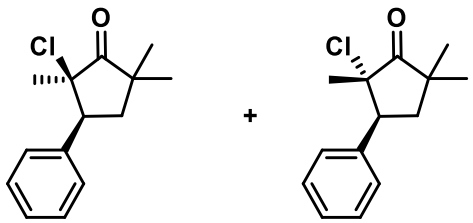

51h **52h**

The reaction was performed by the standard halocyclopentanone formation procedure with dienone **13f**. Column chromatography (DCM/hexanes 1:1) gave **51h** (156 mg, 66%) and **52h** (52 mg, 22%) as white solids.

(2*R,3*S**)-2-Chloro-2,5,5-trimethyl-3-phenylcyclopentanone (51h)**: R_f 0.67 (DCM/hexanes 1:1); mp 47–49 °C; IR (cast film) ν_{max} 3063, 2967, 1754, 700 cm^{-1}; ^1H NMR (500 MHz, $CDCl_3$) δ 7.42–7.34 (m, 5H), 3.21 (dd, *J* = 13.1, 5.7 Hz, 1H), 2.52 (app t, *J* = 12.2 Hz, 1H), 1.99 (dd, *J* = 12.4, 5.8 Hz, 1H), 1.61 (s, 3H), 1.44 (s, 3H), 1.19 (s, 3H); ^{13}C NMR (125 MHz, $CDCl_3$) δ 214.6, 136.3, 129.4, 128.1, 127.8, 72.7, 51.1, 44.1, 39.4, 27.4, 25.6, 23.0; Anal. calcd for $C_{14}H_{17}ClO$: C, 71.0; H, 7.2, found: C, 71.2; H, 7.3; HRMS (EI, M^+) for $C_{14}H_{17}{}^{35}ClO$ calcd 236.0968, found: 236.0969.

(2*S,3*S**)-2-Chloro-2,5,5-trimethyl-3-phenylcyclopentanone (52h)**: R_f 0.55 (DCM/hexanes 1:1); mp 39–41 °C; IR (cast film) ν_{max} 3063, 2967, 1754, 700 cm^{-1}; ^1H NMR (500 MHz, $CDCl_3$) δ 7.42–7.30 (m, 5H), 3.79 (dd, *J* = 12.6, 6.8 Hz, 1H), 2.18 (app t, *J* = 13.1 Hz, 1H), 2.12 (dd, *J* = 12.6, 6.8 Hz, 1H), 1.29 (s, 3H), 1.29 (s, 3H), 1.15 (s,

3H); ^{13}C NMR (125 MHz, $CDCl_3$) δ 216.6, 136.4, 128.6, 128.4, 127.7, 72.2, 51.1, 44.1, 38.8, 26.0, 25.7, 21.8; Anal. calcd for $C_{14}H_{17}ClO$: C, 71.0; H, 7.2, found: C, 71.2; H, 7.3; HRMS (EI, M^+) for $C_{14}H_{17}{}^{35}ClO$ calcd 236.0968, found: 236.0969.

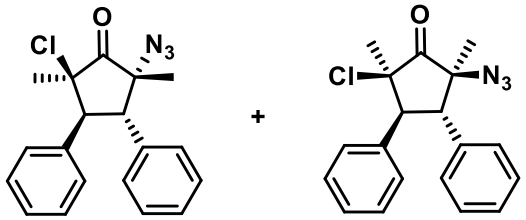

53a **54a**

The reaction was performed by the standard halocyclopentanone formation procedure with dienone **13a** with Me_2AlN_3 as Lewis acid. Column chromatography (DCM/hexanes 1:1) gave **53a** (126 mg, 37%) and **54a** (153 mg, 45%) as white solids.

(2*R,3*S**,4*S**,5*R**)-2-Azido-5-chloro-2,5-dimethyl-3,4-diphenylcyclopentanone (53a)**: R_f 0.68 (DCM/hexanes 1:1); mp 130–132 °C; IR (cast film) ν_{max} 3064, 2975, 2105, 1756, 699 cm^{-1}; ^{1}H NMR (500 MHz, $CDCl_3$) δ 7.35–7.20 (m, 10H), 3.85 (d, *J* = 12.8 Hz, 1H), 3.85 (d, *J* = 12.8 Hz, 1H), 1.81 (s, 3H), 1.71 (s, 3H); ^{13}C NMR (125 MHz, $CDCl_3$) δ 204.7, 133.7, 133.6, 129.8, 129.8, 128.2, 128.1, 127.8, 127.7, 71.3, 67.3, 53.9, 52.0, 23.5, 18.9; Anal. calcd for $C_{19}H_{18}ClN_3O$: C, 67.2; H, 5.3; N, 12.4, found: C, 67.1; H, 5.4; N, 11.6; HRMS (EI, M^+) for $C_{19}H_{18}{}^{35}ClN_3O$ calcd 339.1138, found: 339.1144.

(2*S,3*S**,4*S**,5*R**)-2-Azido-5-chloro-2,5-dimethyl-3,4-diphenylcyclopentanone (54a)**: R_f 0.48 (DCM/hexanes 1:1); mp 136–138 °C; IR (cast film) ν_{max} 3064, 2975, 2105, 1756, 699 cm^{-1}; ^{1}H NMR (500 MHz, $CDCl_3$) δ 7.30–7.18 (m, 10H), 4.14 (d, *J* = 13.0 Hz, 1H), 3.56 (d, *J* = 13.0 Hz, 1H), 1.73 (s, 3H), 1.07 (s, 3H); ^{13}C NMR (125 MHz, $CDCl_3$) δ 207.8, 134.4, 133.3, 129.7, 128.8, 128.5, 128.3, 128.0, 127.5, 69.9, 67.9, 52.3, 50.2, 23.3, 17.7; Anal. calcd for $C_{19}H_{18}ClN_3O$: C, 67.2; H, 5.3, found: C, 67.0; H, 5.3; N, 11.6; HRMS (EI, M^+) for $C_{19}H_{18}{}^{35}ClN_3O$ calcd 339.1138, found: 339.1145.

Chapter 3

The Interrupted Vinylogous Nazarov Cyclization

3.1 Dendralenes

3.1.1 Unsaturated Systems

A variety of complex unsaturated systems can be built from simple ethylene units (Scheme 3.1). New bond connections between building blocks could be made either vicinally **2** (in blue) or geminally **3** (in red). When connection type is preserved, compounds with multiple carbon–carbon conjugated double bonds can be formed. These compounds are called "**oligoenes**".

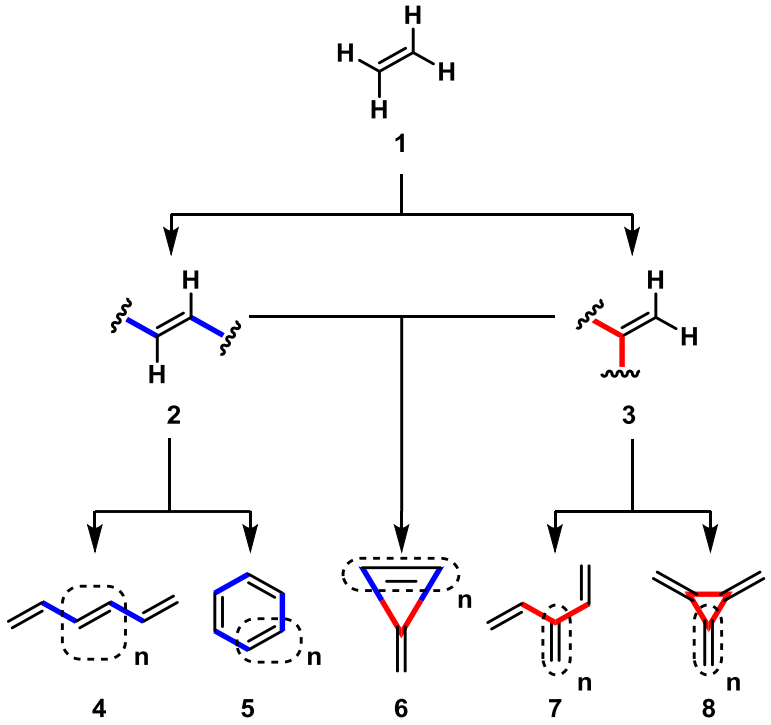

Scheme 3.1. Ethylene as a building block in polyene synthesis.

The best studied families of oligoenes are polyenes and annulenes. Several vicinal connections can form either the linear polyenes **4** or the cyclic annulenes **5**. The examples of linear polyenes (Figure 3.1) can be found in nature (terpenoids, fatty acids, and

polyketides), and they have a vast application in the polymer industry. For the linear polyenes, there are no restrictions reported, and both *E* and *Z* isomers can be used as building blocks for their systems. Cyclic annulenes **5**, in turn, have strain restrictions, and smaller than ten carbon cyclic systems can consist of only *Z* isomers.[139] Undoubtedly, aromatic annulenes, such as benzene and its derivatives, are of great importance for the chemical industry. The remaining three classes – fulvenes, dendralenes, and radialenes – have been studied less compared to the other previously mentioned two classes, mostly due to their instability and less frequent isolation. Fulvenes **6** are hybrid molecules with mixed connectivity.[140,141] For systems with only geminal connections, several structural possibilities can exist such as dendralenes **7** and cyclic radialenes **8**.[142]

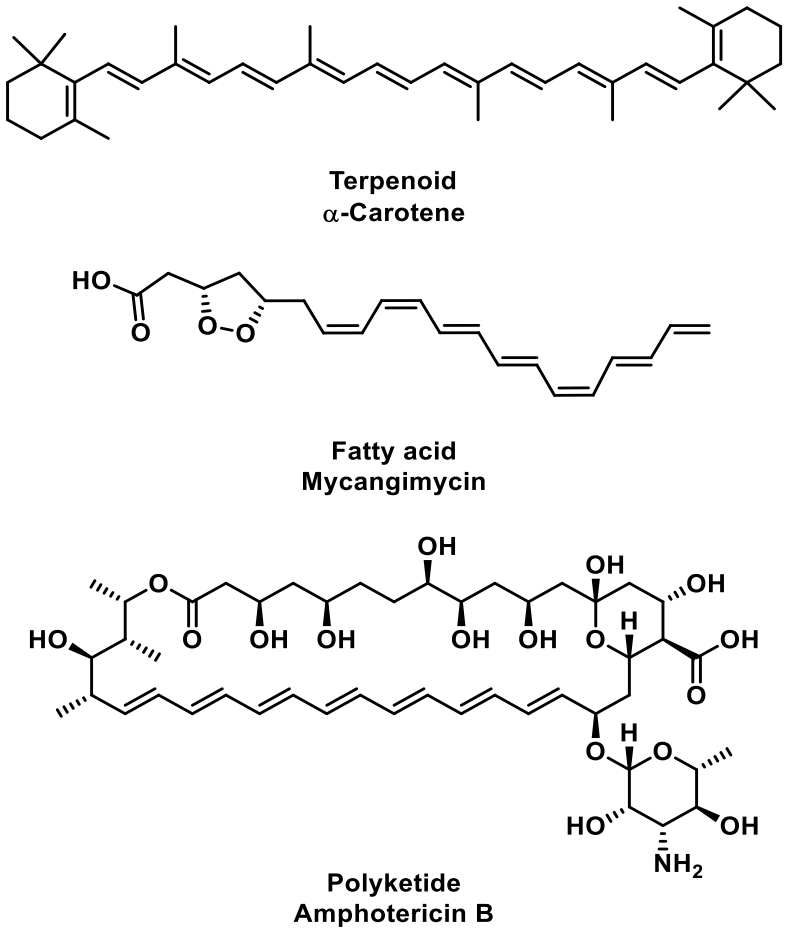

Figure 3.1. Examples of linear polyenes found in nature.

During the last decade, acyclic dendralenes and cross-conjugated π systems, in general, came to the attention of medicinal chemists. This growing interest came because of the growing number of isolated "dendralenic" natural products (Figure 3.2) such as complex dendralenic terpenoid[143] **9**, monoterpenes[144] **10**, dendralenic alcohols[145] **11**, butenolide karrikin[146] **12**, mitorubrin **13**, and others.[147] Subsequently, there was a strong impetus to develop the whole field of dendralenes.[148] This area experienced robust methodology development for the easier preparation and better understanding of their properties.

The name dendralene originates from the Greek word "dendron", which means a tree.[149] The branching of dendralenes generally happens through the replacement of the non-terminal hydrogens with vinyl groups. Longer dendralenes are obtained by increasing the number of hydrogen replacements that occur in a molecule. Various methods for the large scale synthesis and functionalization of dendralenes (up to [8]dendralenes) have been reported recently, putting this area of study at the cutting edge of the organic chemistry.[150]

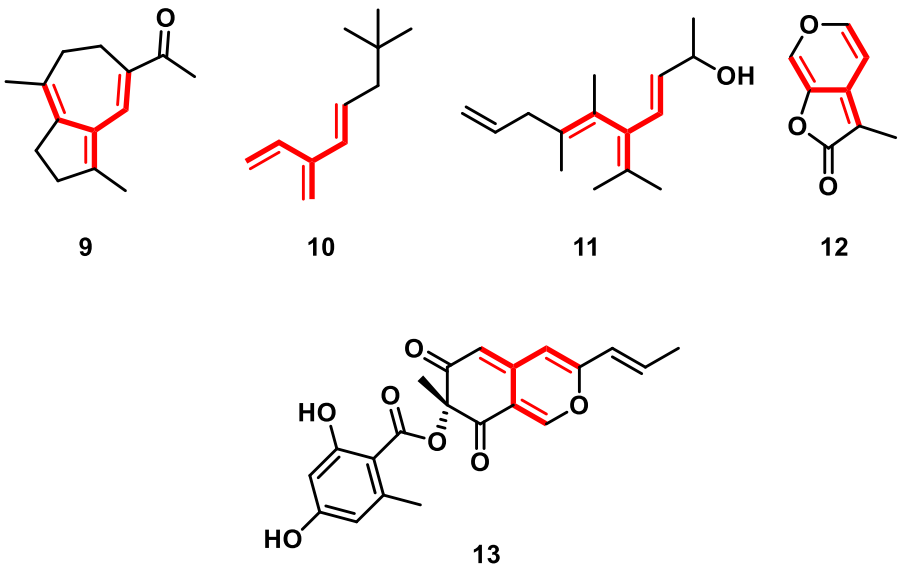

Figure 3.2. Examples of dendralenes found in nature.

The reactivity and stability of dendralenes depend on their structure: compounds with an odd number of C=C units are less stable compared to their even-numbered

analogs (Figure 3.3).[151] The reactivity difference of odd and even [n]dendralenes was shown on the example of the Diels–Alder reaction (Scheme 3.2). Normally, odd-numbered members can react as dienes and perform clean and highly selective cycloadditions; while even-numbered members undergo multiple additions, with a lack of site selectivity.[152]

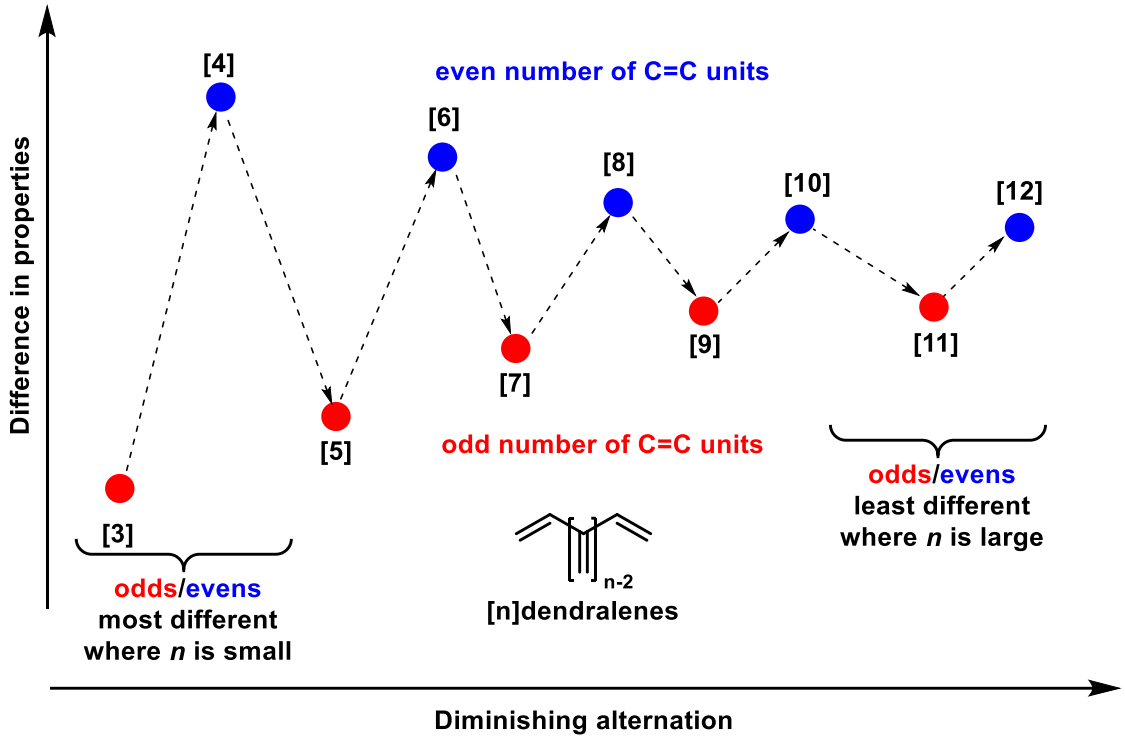

Figure 3.3. Property alterations in the dendralene family.

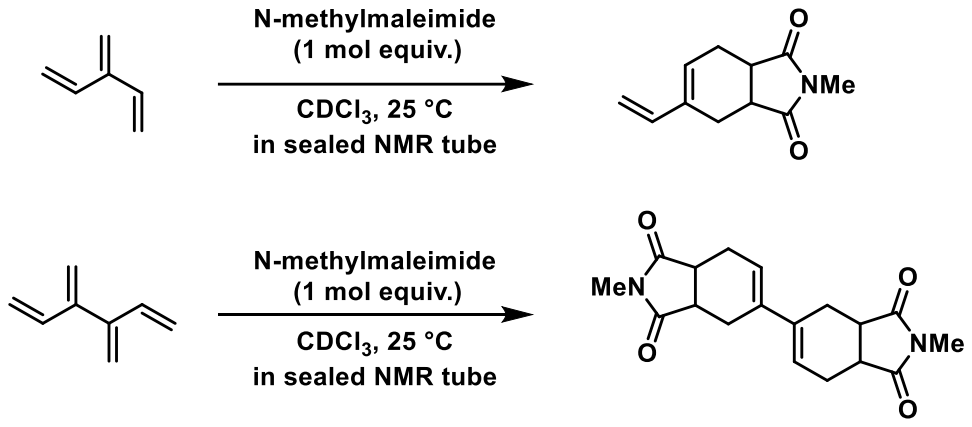

Scheme 3.2. Reactivity difference of odd- and even-membered dendralenes on the example of the Diels–Alder reaction.

Possible preferred [3]dendralene conformations were calculated using DFT calculations and later explained by Paddon-Row and Sherburn (Figure 3.4).[153] The lowest energy conformations of [3]dendralene are represented by an equivalent mixture of *s-trans* (A) and *quasi-s-cis* (B) units.[154] IR, NMR, and mass spectrometric data of dendralenes were shown to be following predictions based on compounds structure. Despite all obtained data, there is still a lack of X-ray crystallographic data for the unsubstituted [3]dendralenes.

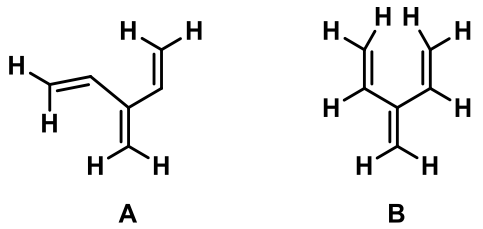

Figure 3.4. The lowest energy conformations of [3]dendralene.

In this chapter, I will focus on cross-conjugated dendralenes and their reactivity, and will not discuss cyclic and acyclic dendralenes, where one of the terminal double bonds is replaced by an alkyne or an aromatic system. For a more comprehensive review, the reader may wish to refer to reviews on various aspects of dendralenes and other cross-conjugated systems.[155]

3.1.2 Common Ways to Prepare Unsubstituted [3]Dendralenes

The early synthetic approaches towards the preparation of [n]dendralenes included classical olefin synthesis methods. Some of the most popular ones were β-halide elimination, pyrolysis, a variety of pericyclic reactions, and Hofmann elimination.[142,156] Often, application of these methods required the use of special equipment (mercury short path distillation apparatus with receiver flask), were low yielding, multistep, and required harsh conditions. The latter ones, in most cases, caused freshly prepared dendralenes to undergo undesirable side reactions. Additionally, these conditions could not be used as a generalized concept for the preparation of the whole family of [n]dendralenes. All the

initial approaches had drawbacks and left something to be desired, necessitating the development of alternative methods.

The first attempts to develop a general strategy required the preparation of precursors **15** and **17** that would include in their structure masked dendralene moieties (Scheme 3.3). For example, one of the methods used methylenecyclobutane **14** to prepare compound **15**, which will undergo electrocyclic ring-opening under heating at 335 °C to prepare [3]dendralene **18** in a quantitative yield.[157] A similar approach, which involved cheletropic extrusion of sulfolene **17**, also required a high temperature during the reaction route, releasing sulfur dioxide as the by-product.[158]

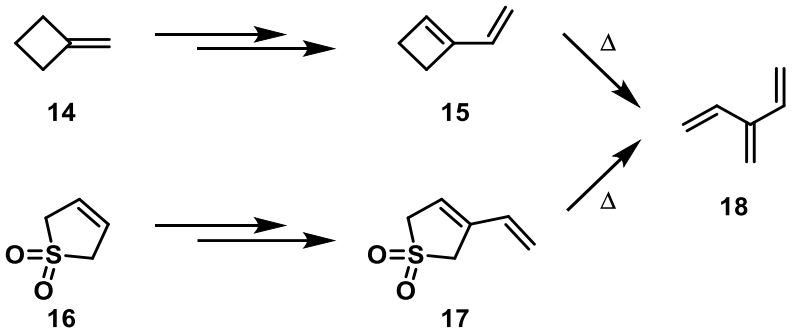

Scheme 3.3. The masked approach of [3]dendralenes preparation.

Cadogan and co-workers were among the first who gave the field a step forward. They succeeded in converting 1,3-butadiene 3-sulfolene **16** into its vinyl derivative **17** (Scheme 3.4). The Cadogan precursor **17** was prepared in 4 steps. The sulfolene **16** was transformed into epoxide **19** by the addition of performic acid. The formed epoxide was opened during the Grignard reaction. Subsequent elimination of the protected alcohol in compound **21** led to the desired compound **17**. Heating the resulting vinyl compound **17** at 550 °C gave [3]dendralene **18** in 87% yield.[159] Cadogan's precursor **17** was reported as colorless solid and was stable at room temperature under nitrogen for weeks.[160] Although the first attempts towards the development of methods for qualitative and quantitative preparation of dendralenes were not completely successful (substrates complexity, multistep synthesis, reaction chemoselectivity), they gave a stimulus to develop the whole area.

The next breakthrough in the synthesis of dendralenes was reported in 2000 by Sherburn and co-workers.[161] The group took into account the high reactivity and low stability of dendralenes, and consequently proposed to apply the "storage concept". Particularly, [n]dendralenes were masked as 3-sulfones, which were converted into the final products on a few milligram scale in high yield just before the use. At the core of the methodology was the Stille cross-coupling reaction to obtain Cadogan's dendralene precursor **17** (Scheme 3.5). Compound **23**, which was one of the reagents for Stille cross-coupling, could be gained from the iodination of Sweeney's sulfolene **22**.[162]

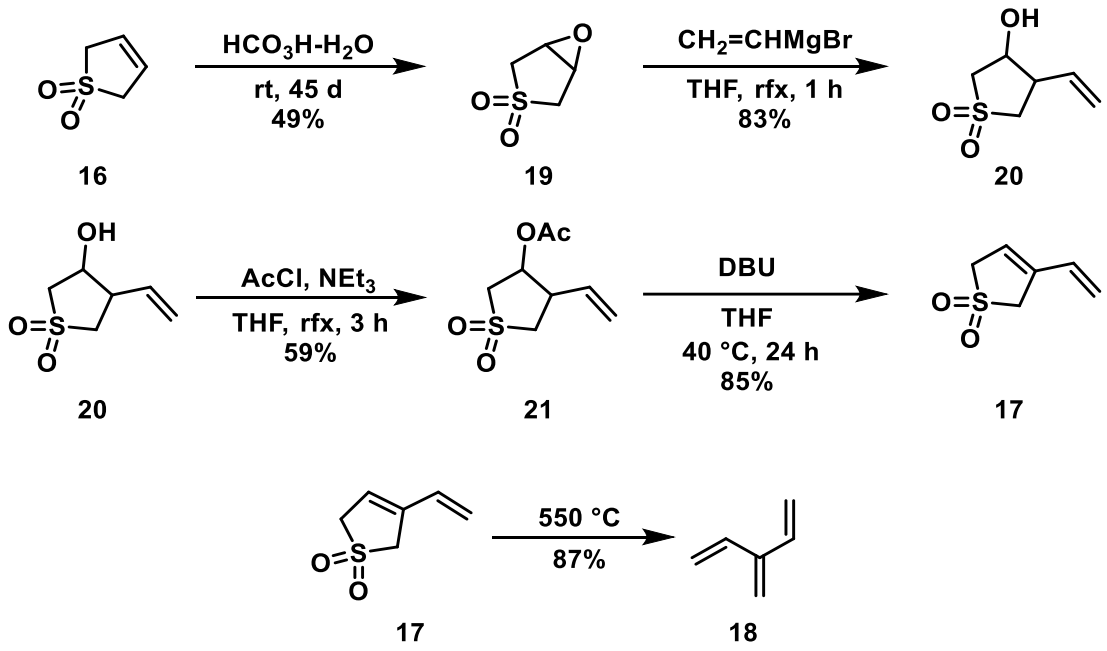

Scheme 3.4. Cadogan precursor synthesis.

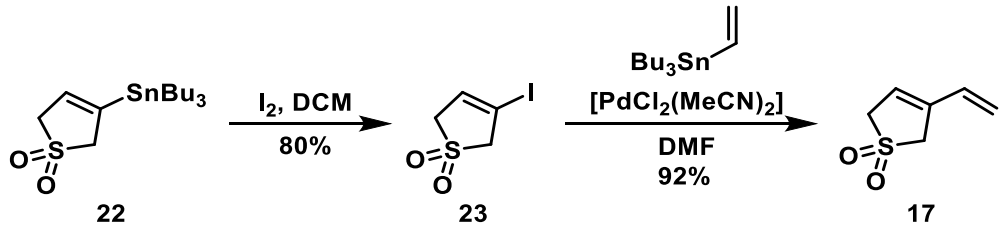

Scheme 3.5. Sherburn's pathway to prepare Cadogan's precursor.

Later, the Sherburn group was able to improve the procedure by avoiding high temperatures and the dendralene masking technique (Scheme 3.6). The synthesis

exploited the Kumada and Negishi type cross-couplings and the readily available coupling partner – the Grignard reagent **24**.[163] The newly developed strategy gave access to synthetically larger amounts (up to 5 g per run) and allowed a deeper understanding of the physical and chemical properties of dendralenes. Although Sherburn's group succeeded in developing of an extremely short synthetic route, the drawback of this methodology was the impossibility of the isolation of the product from THF due to the high proximity in boiling points of the product and the solvent.

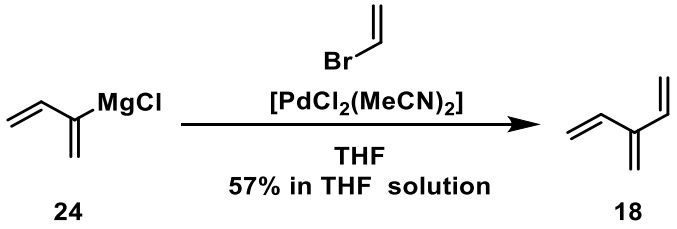

Scheme 3.6. Sherburn's Kumada type cross-coupling approach.

In 2010, Sherburn and co-workers reported new operationally simple procedure for the preparation of [3]dendralene **18** (Scheme 3.7).[164] Dendralene **18** was obtained by bromine elimination from compound **26** in the presence of DBU in DMSO solution, with no heating and under vacuum. Right after the triene formation in a reaction mixture, it was distilled and collected in to a cold trap. The facile preparation of compound **26** by the bromination of compound **25** in the presence of NBS, with no need for special laboratory equipment, made this method for the preparation of unsubstituted [3]dendralenes to be among the most attractive approaches.

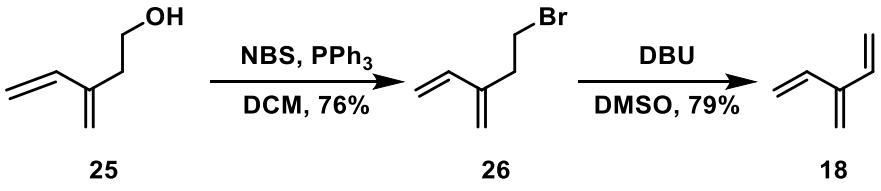

Scheme 3.7. The solvent-free method to prepare unsubstited [3]dendralene **18**.

3.1.3 The Common Ways to Prepare Substituted [3]Dendralenes

Since the discovery of synthetic methods to prepare unsubstituted dendralenes, scientists have invested substantial effort into methods for preparation of modified dendralenes. Most of these attempts, unsurprisingly, were focused on the modification of the simplest known [3]dendralenes. There are several possible positions to modify in the [3]dendralenes (Figure 3.5). Most of the methods to construct these motifs can be split into two main sections: generating a C=C bond or a C–C bond assembly in the process of making a substituted dendralene. Only C=C bond formation methods will be discussed in Chapter 3.

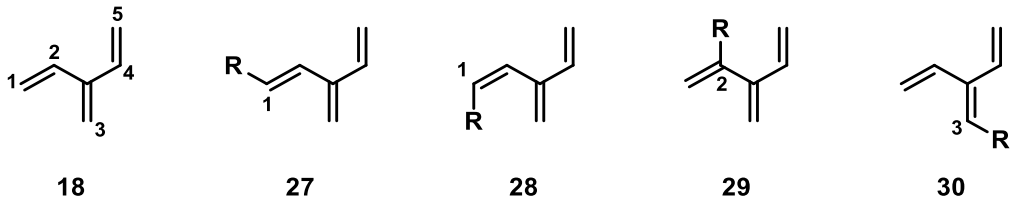

Figure 3.5. Monosubstituted analogs of [3]dendralenes.

The alkene bond assembly approaches are the most common ways for the preparation of the substituted dendralenes (Figure 3.6). All alkene bond methods can be divided into two parts: internal alkene retrosynthetic preparation, which requires divinyl ketone as an electrophile or a halogen-metal pentadienyl nucleophile (Figure 3.6, pathway a); and terminal alkene construction pathway, which uses alkene diones as starting materials (Figure 3.6, pathway b).

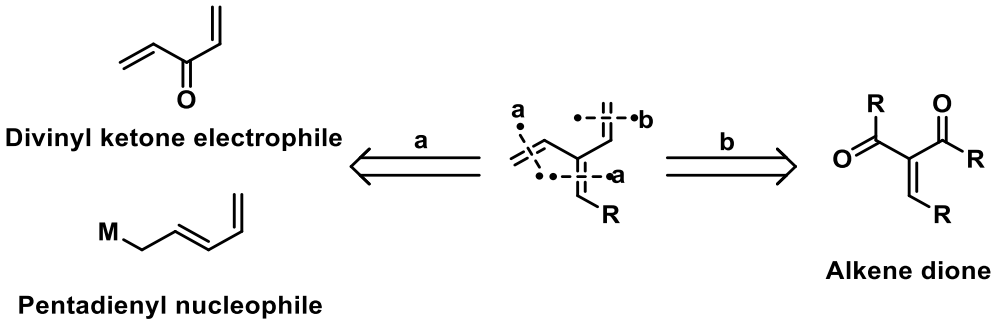

Figure 3.6. The preparation of the substituted [3]dendralenes by alkene bond assembly.

In 1951, Paul and Tchelitcheff reported the first procedure to prepare functionalized [3]dendralenes (Scheme 3.8). They treated trivinylmethane **31** with amyl sodium under a carbon dioxide atmosphere. The intermediate carbanion **A** was able to trap carbon dioxide, which resulted in the formation of product **32** after quenching.[165]

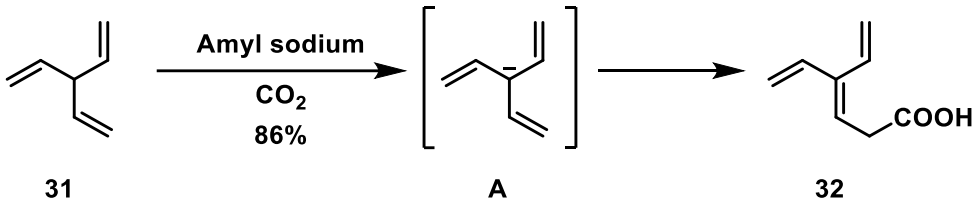

Scheme 3.8. The first synthesis of functionalized [3]dendralene.

Later, in 1963, the Selim group reported a procedure to form the cross-conjugated dienone **34** (Scheme 3.9).[166] They reduced diketone **33** to the corresponding diol using potassium borohydride. The next step of the sequence was acid-mediated dehydration of the obtained reduced intermediate to obtain the desired dienone.

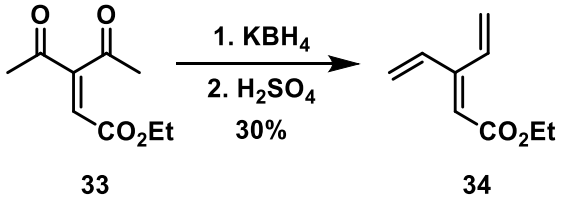

Scheme 3.9. The double carbonyl approach for the preparation of [3]dendralene.

The first example of branched dendralene synthesis is the work by Miginiac and co-workers in 1964 (Scheme 3.10), who converted compound **35** into alcohol **36** in the presence of Zn and benzaldehyde. The resulting alcohol **36** was converted in to the corresponding bromide using PBr_3, followed by hydrogen bromide elimination in the presence of a strong base. The sequence resulted in the formation of 3-phenyl-[3]dendralene **37** in a 59% yield.[167]

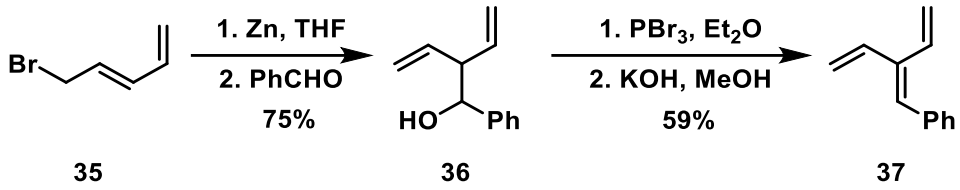

Scheme 3.10. The first synthesis of branched [3]dendralene by Maginiac and co-workers.

A delicate approach to obtain functionalized [3]dendralenes was proposed by the West group, who performed olefination of the readily available dienones **38** (Scheme 3.11).[168] Lithiation of ethoxyacetylene via *n*BuLi was followed by 1,2-addition into cross-conjugated dienone **38**, leading to the formation of propargylic alcohol **39**. This intermediate in the presence of $VO(acac)_2$ upon heating in toluene undergoes the Meyer–Schuster rearrangement to form functionalized [3]dendralene **40**.[169]

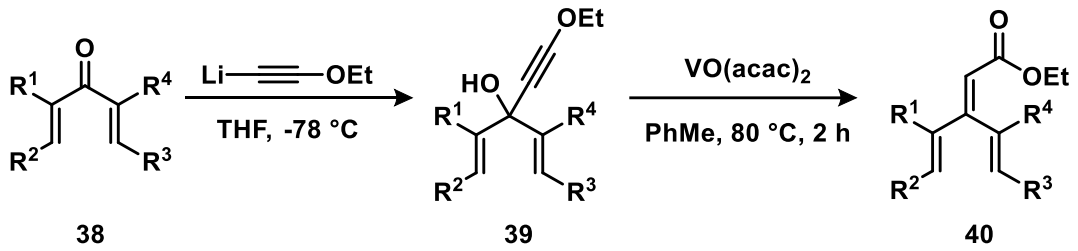

Scheme 3.11. The West group approach to form functionalized [3]dendralenes.

The reaction was shown to work on a variety of propargylic alcohols: β-substituted and unsubstituted divinyl ketones, substrates bearing both cyclic and acyclic alkyl substituents, aryl substituents, and symmetrical and nonsymmetrical starting materials (Figure 3.7). The limitation of the methodology is the preparation of heteroaryl containing substrates as they are prone to decomposition. In the case of nonsymmetrical substrates, decreased stereocontrol over alkene structure was reported which led to the formation of the mixture of *E/Z* isomers with approximately 1:1 ratio.[170]

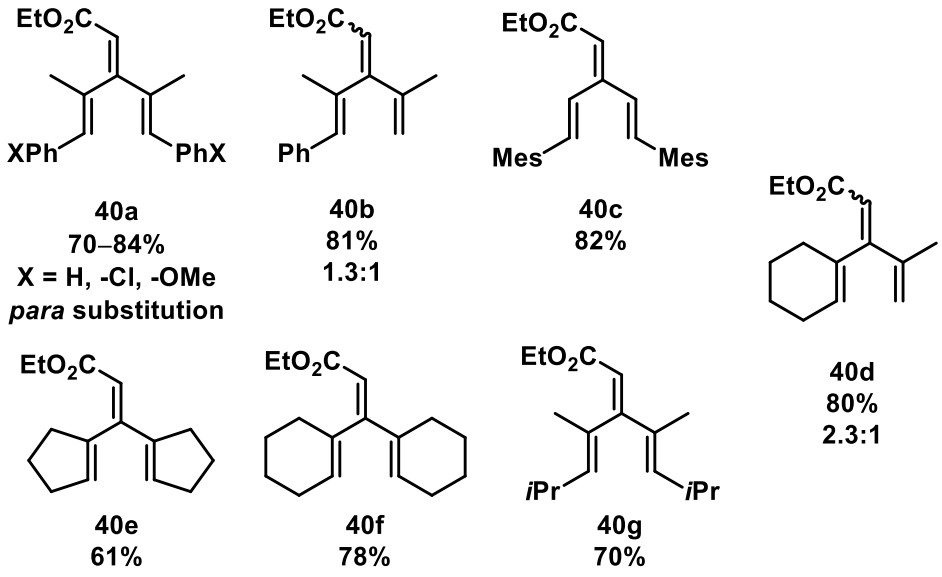

Figure 3.7. The scope of the West group approach.

3.2 Known Transformations of the Dendralenes

3.2.1 The Diels–Alder Reaction

The most studied reactivity of dendralenes to date is the Diels–Alder reaction. It has been shown that dendralenes can participate in up to two cycloadditions during one reaction. Therefore, dendralene Diels-Alder reactions can form the basis of a domino process to form multicyclic compounds rapidly, with high atom and step economy.[171]

The unusual ability of the dendralenes to undergo several Diels–Alder reactions is called "diene-transmissive Diels–Alder" (DTDA). During DTDA, dendralenes, in the role of the diene partner, undergo addition of a dienophile, leading to the formation of a new semicyclic diene **41** (Scheme 3.12). After the first Diels–Alder reaction, a new endocyclic C=C bond is established which is conjugated with the exocyclic double bond, thus "transmitting" a diene to a new location. Subsequently, this newly obtained diene can undergo another Diels-Alder cyclization event resulting in the formation of product **42**. DTDA offers the opportunity to furnish up to eight new stereogenic centers and four new C–C bonds by utilizing different dienophiles.

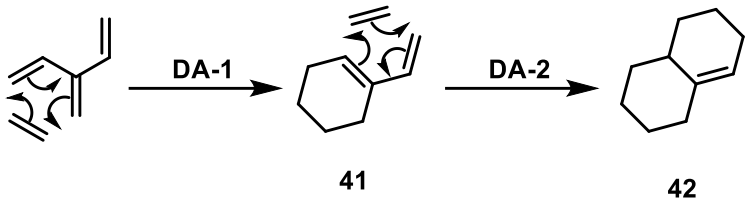

Scheme 3.12. Diene-transmissive Diels–Alder reaction.

This highly efficient cyclization process that can bring three or more molecules together has drawn scientists' attention since the 1950s.[164] The first group who took the advantage of this strategy was the Tsuge group (Scheme 3.13), and they named the process DTDA. They illustrated the importance of the unique reactivity of dendralenes to form polycyclic frameworks for organic synthesis by publishing a sequence of twelve papers related to this topic.[172] Most of the studies related were employing [3]dendralenes as dienes. For a deeper understanding of the mono Diels–Alder addition, DTDA, hetero-Diels–Alder reactivity of the [n]dendralenes refer to the cited literature and reviews.[142]

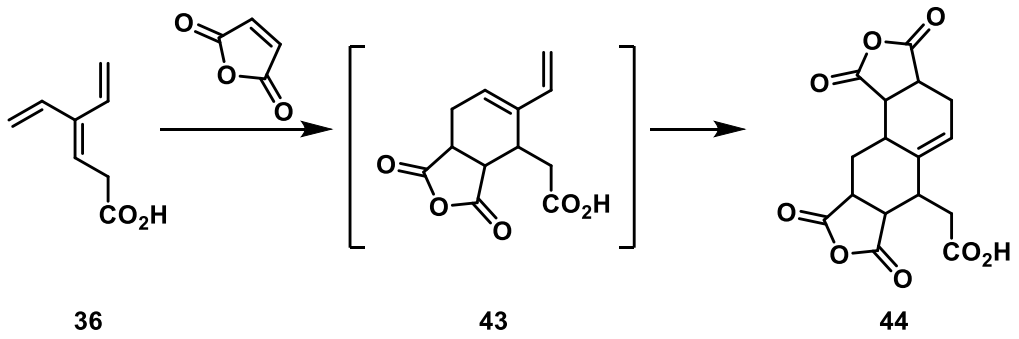

Scheme 3.13. The first example of DTDA reported by the Tsuge group.

3.2.2 Transformations of [3]Dendralenes

The other reactivity of [n]dendralenes apart from participation in DTDA reactions has barely been studied and there are only a few reports for each kind. Publications that discuss the participation of only a single alkene unit out of several of [n]dendralenes are even rarer because of the selectivity problems.

Kostikov and co-workers were the first ones who were able to perform a carbene addition to the smallest member of the dendralene family (Scheme 3.14).[173] They did addition of the dichlorocarbene to compound **18** in the presence of a strong base leading

to the formation of the single carbene addition products **45** and **46** as a mixture. Due to stability issues of **45** and **46**, they converted compounds into their saturated analogs via palladium catalyzed hydrogenation of double bonds. The 4:1 ratio of products **47** and **48** is a result of preferential addition of carbene to the central alkene rather than to the terminal one.

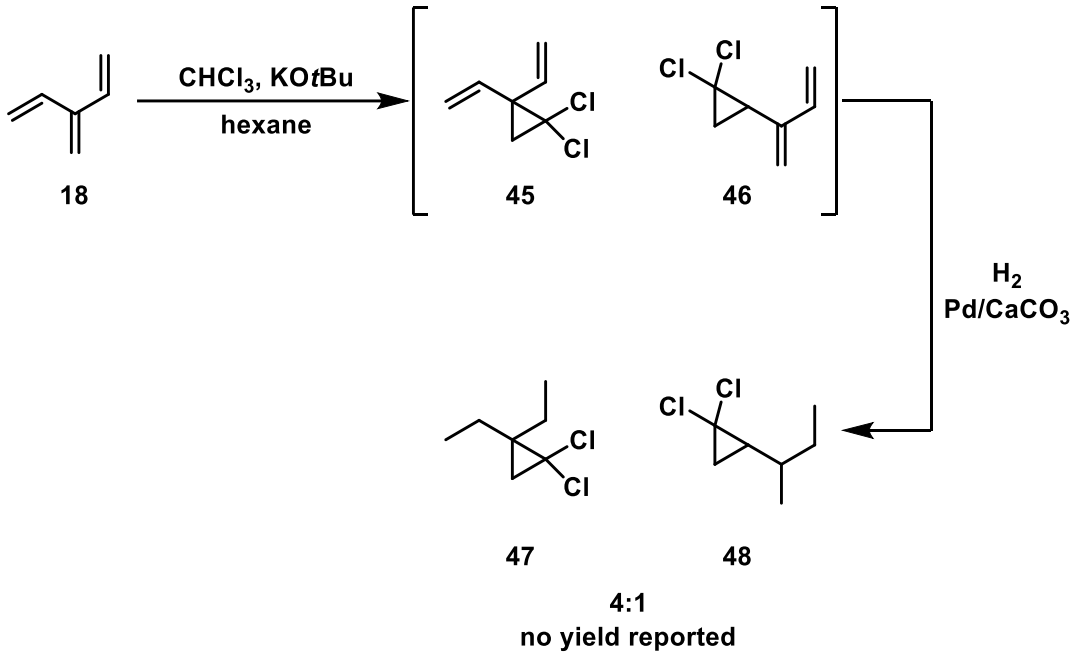

Scheme 3.14. The carbene addition to [3]dendralenes studied by Kostikov and co-workers.

Several reports on ionic additions to highly substituted dendralenes were reported (Scheme 3.15).[174] The Ter-Gabrielyan group showed the successful addition of water[175] and CsF[176] to perfluoro-[3]dendralene **49**, which is readily accessible via the trimerization of perfluoroisobutylene. The addition of water to compound **49** furnished the 1,4-addition product **50** in high yield; the CsF addition, in turn, resulted in the formation of cyclobutane ring **51** with two exocyclic alkene bonds.

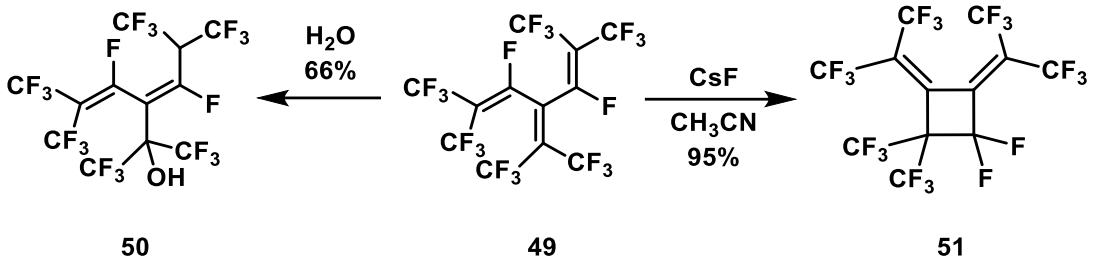

Scheme 3.15. Ionic reactions of the [3]dendralenes.

Another understudied reactivity of dendralenes is related to their performance under photochemical conditions (Scheme 3.16). To date, there are only two papers published related to this reactivity.[177] The [3]dendralene with geminal dimethyl substitution and two α-phenyl groups under irradiation undergoes the Nazarov-type cyclization, forming product **56**. Biradical **53**, through resonance, is trapped by the neighboring phenyl group in an intramolecular fashion. The recovery of aromaticity is achieved by the subsequent 1,3-hydrogen shift furnishing product **56** in excellent yield.

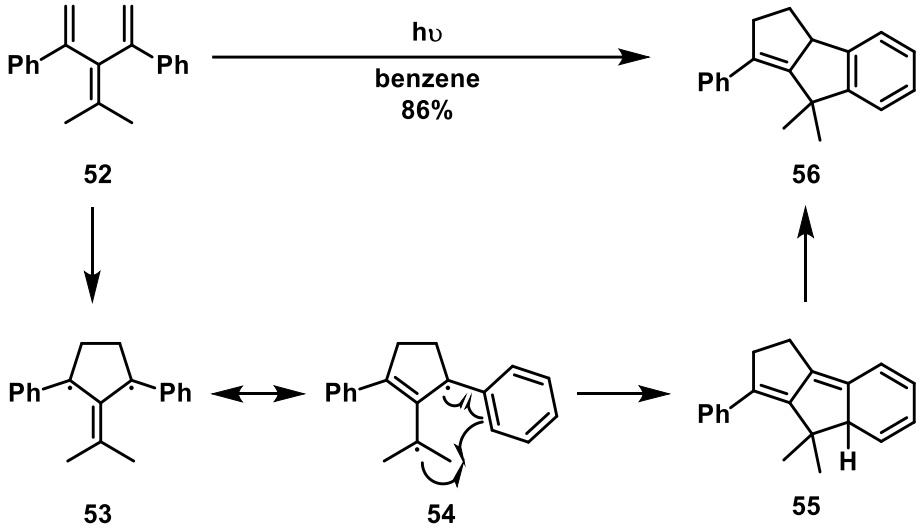

Scheme 3.16. Photochemical vinylogous Nazarov cyclization of [3]dendralenes.

3.2.3 The Earlier Progress Reports on the Vinylogous Nazarov Cyclization

The first group to develop a new type of reactivity of substituted [3]dendralenes, was the West group.[19,168,178] They envisioned that imposing an extra C=C bond into a dienone-

type system, transposing the carbonyl group further away from the 5 carbons of the incipient pentadienyl carbocation could be prone to undergo cyclization. New type of reactivity was termed as **vinylogous Nazarov cyclization** (Scheme 3.17). The cyclization of substrates is possible only if the ester moiety can promote activation of the 4π electrocyclization process remotely. The vinylogous Nazarov cyclization was initiated by the addition of $TiCl_4$ to [3]dendralene or catalytically by heating it to 80 °C in the presence of $Sc(OTf)_3$ (3 mol%) in DCE.

The method's generality was tested on a variety of substrates. The formation of the single exocyclic regioisomer **57** in the presence of $TiCl_4$ was reported to happen for all the starting materials except one. If compound **40** had α-dimethyl-β-diphenyl substitution it provided endocyclic alkene regioisomer **58** as well. The vinylogous Nazarov cyclization was tested on different types of carbonyl compounds such as amides, aldehydes, and ketones, as well. All substrates successfully underwent the desired cyclization efficiently forming compound **57**. Substoichiometric amounts of $Sc(OTf)_3$ afforded a mixture of two regioisomers **57** and **58** in excellent yield.

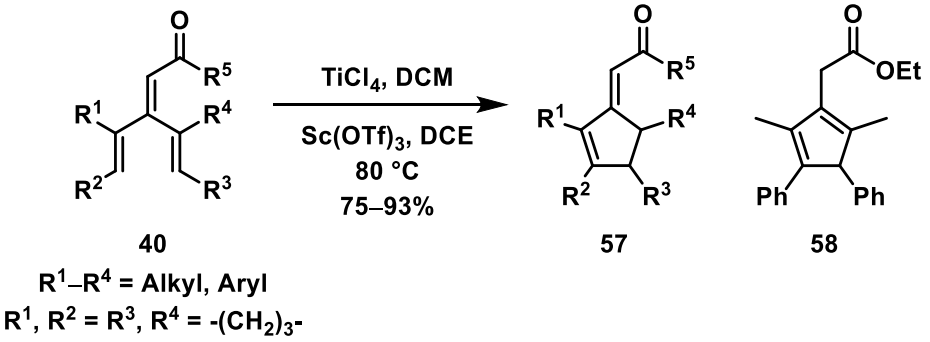

Scheme 3.17. The vinylogous Nazarov cyclization.

As the closest analogy to the vinylogous Nazarov cyclization can be considered the example of cyclization of aryl vinyl/divinyl donor–acceptor cyclopropanes (DAC) reported by Sudhakar and co-workers in 2017.[179] The Sudhakar group was able to achieve the Nazarov cyclization by opening a divinylcyclopropane ring (Scheme 3.18). The reaction was initiated by $BF_3 \cdot OEt_2$, and the cyclopentenyl cation resulting from electrocyclization was trapped by various nucleophiles. Also, it was shown to participate in a [4+2]-cycloaddition with aldehydes, leading to the bicyclic products **61** with a high

yield and diastereoselectivity. However, the reaction was shown to be limited in the scope of the divinylcyclopropane starting materials.

Inspired by the successful examples of [3]dendralene vinylogous Nazarov cyclization and by the Sudhakar group examples, we decided to explore the capability of various nucleophiles to participate in the **interrupted vinylogous Nazarov cyclization**. Details on our efforts to find intra- and intermolecular traps that can interrupt the vinylogous Nazarov cyclization process after the electrocyclization event will be discussed in Section 3.3. This new approach also led to the isolation of unexpected dimethylfuranones, the details of which will be disclosed in Chapter 4.

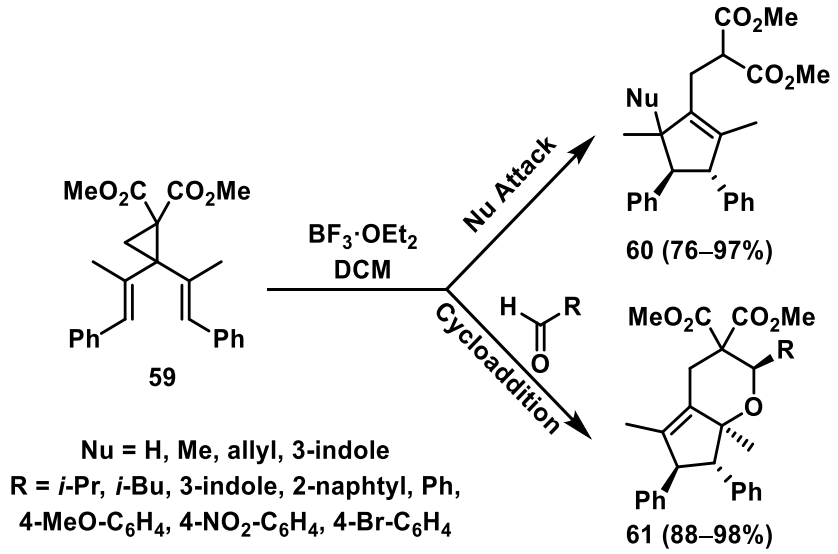

Scheme 3.18. The intermolecularly interrupted Nazarov cyclization and tandem [4+2]-cycloaddition reactions of DAC.

3.3 Results and Discussion

3.3.1 Meyer–Schuster Rearrangement of Divinyl Propargylic Alcohols

The studies on the vinylogous Nazarov cyclization started with the aim to gain a deeper understanding of the vinylogous Nazarov cyclization and to prepare new dendralene substrates. The first step in starting material preparation is alkynyllithium addition to the dienone. This step went smoothly for all the substrates. Normally, the yield of the first step was highly dependant on the dryness of the conditions (Scheme 3.19). We applied reported methodology as well for substrate with no α-methyl substituents (simple

preparation of substrate).[180] Latter substrate underwent Meyer–Schuster rearrangement on silica gel giving **40c** in 51% yield.

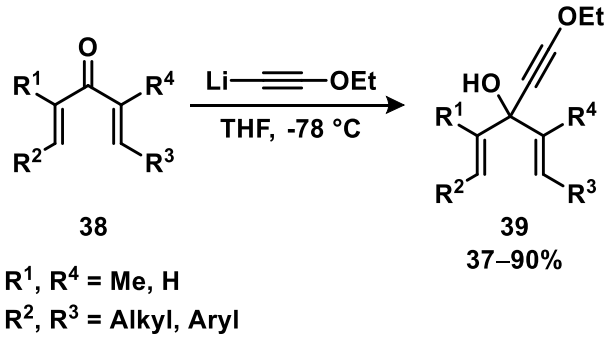

Scheme 3.19. Preparation of the propargylic alcohols.

In the procedure first developed by a prior group member, Dr. Rieder, the next step in dendralene formation entails $VO(acac)_2$ catalyzed Meyer-Schuster rearrangement. After several optimization tests, it was found that exposure of the reaction mixture to the air leads to the formation of previously unprecedented side products **62** and **63** up to overall 50% yield (Scheme 3.20). Under oxygen-free conditions (nitrogen or argon atmosphere) side products **62** and **63** were formed in reduced quantities with an overall 20–30% yield. Product **63** was previously observed during Meyer–Schuster rearrangement of propargylic alcohol **39** in presence of TsOH.[168]

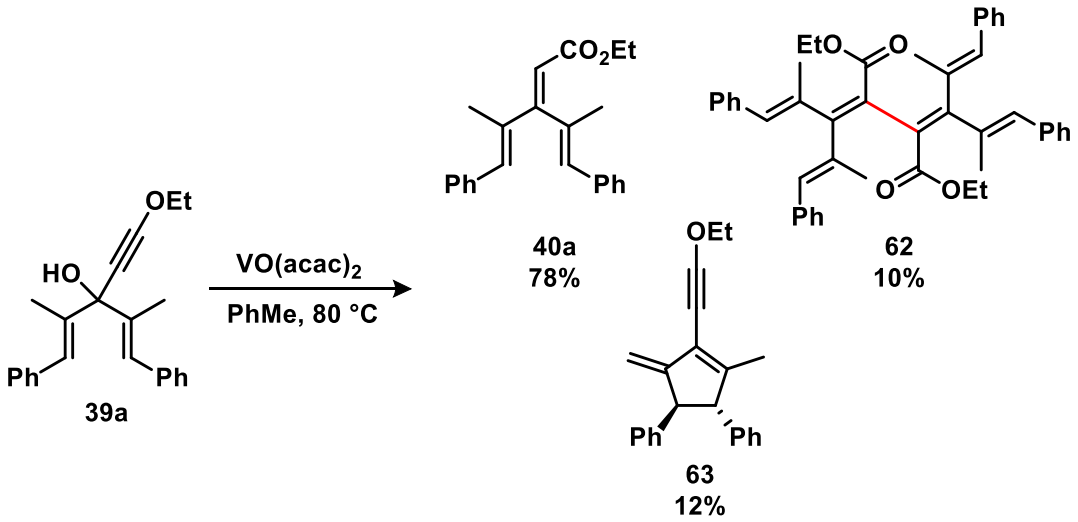

Scheme 3.20. Meyer–Schuster rearrangement products.

The identity of side product **62** was deduced from the basis of detailed analysis of chromatographic and spectroscopic data. The benzylic alkenyl and methyl protons were nearly identical, with minor deviation in chemical shifts; the key difference from the substituted functionalized [3]dendralene **40a** was the absence of the alkenyl proton adjacent to the ester group. (Figure 3.8). This key feature in combination with ^{13}C and IR data, which indicated the presence of a carbonyl group and the same number of peaks as **40a**, prompted us to propose a symmetrical structure. This proposal was in strong agreement with ESI-MS data, where the molecular formula of $C_{46}H_{46}O_4$ and molecular ion mass of 662 *m/z* perfectly correlated with the double molecular weight of **40a** (332 *m/z*) minus two – 2[M-H]. Additionally, the APT analysis showed the absence of CH signal at 115.8 ppm and the presence of a quaternary carbon at 158.5 ppm instead. The R_f value of compound **62** was lower with respect to the expected R_f value of the Meyer–Schuster rearrangement product **40a**.

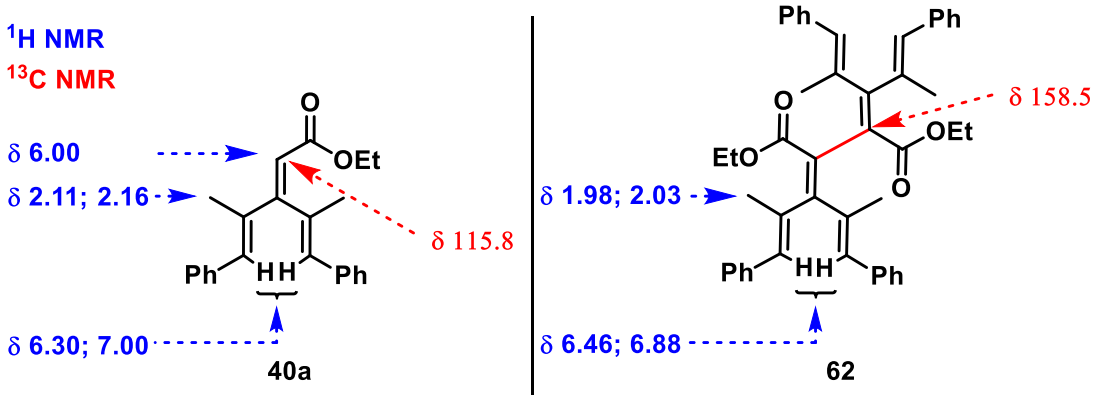

Figure 3.8. The ^{1}H NMR and ^{13}C NMR diagnostic correlations for **40a** and **62**.

The Meyer–Schuster rearrangement of **39** was reported to form product **40** in a high yield for most of the dienone substrates that were studied. The mechanism of the vanadium (IV) promoted Meyer–Schuster rearrangement was proposed to be similar as for allylic alcohols (Scheme 3.21).[181] The initial ligand exchange between catalyst and alcohol **39a** leads to the formation of complex **A** which via 1,3-transposition of the alcohol resonates with vanadate enolate **B**, collapse of which serves as the driving force to form highly conjugated ester **40a**. The formation of the unexpected dimer **62** may be

the result of a competing radical process taking place as an alternative to the rearrangement in the presence of vanadium (IV) catalyst and oxygen.

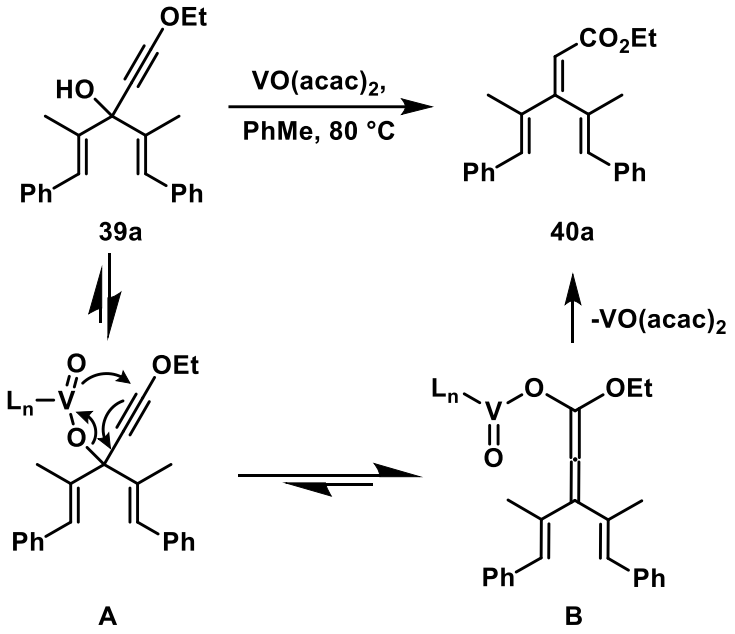

Scheme 3.21. The $VO(acac)_2$ catalyzed Meyer–Schuster rearrangement.

3.3.2 The Vinylogous Nazarov Cyclization

Initially, further development of this methodology we envisioned in the control of regioselectivity of the vinylogous Nazarov cyclization. The goals were to screen the scope of the Lewis acids other than $TiCl_4$, gain a deeper understanding of the vinylogous Nazarov cyclization mechanism, and see if we could obtain different isomers selectively one over the other (exocyclic and endocyclic alkene regioisomers).

During our recent extensive Lewis acid studies, regioisomer **64** was isolated (Figure 3.9). It was established as the regioisomer of **58** with a different position of the endocyclic double bonds. The isolated compound **64** does not contain strongly deshielded non-aromatic protons that serve as an indication of cyclization. Doublets at 3.36 and 3.53 ppm has an HMBC correlation with the carbonyl group, which suggests that it should be the methylene protons of the tether (alpha to the ester group) with each doublet integrating as a single proton. Using HSQC analysis, these two protons were shown to be at the same C atom (32.8 ppm). A quartet at 3.67 ppm in ^1H NMR spectrum is coupled to one of the methyl groups of the cyclopentadiene ring (1.09 ppm). The second methyl group appears

as a deshielded singlet at 1.82 ppm. No benzylic protons were detected in the ^{1}H NMR spectrum. Based on all the above-mentioned data, the structure of product **64** was proposed. The obtained ratios of regioisomers were updated following the newly established composition taking into account the third isolated isomer (Table 3.1).

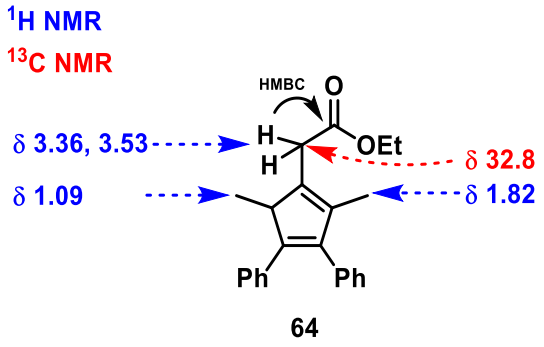

Figure 3.9. Structure of the regioisomer **64**.

Table 3.1. The Vinylogous Nazarov Cyclization Lewis Acids Scope[a]

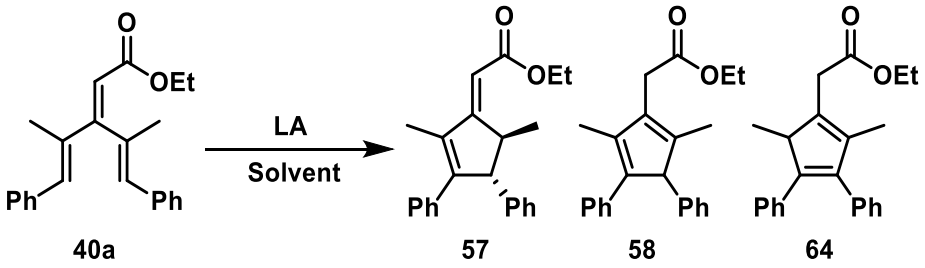

Entry	LA	Equiv.	T, °C	Time, h	Yield (%)[b] **57**/**58**/**64**	Yield (%)[c]
1	$TiCl_4$ pure	1.1	-78	2	1+38+0	39
2	$TiCl_4$ (1 M)	1.2	-78	3	68+13+8	89
3	$TiCl_4$ (1 M)	10 mol%	-78 → rt	24	31+0+0	31
4	$Sc(OTf)_3$	10 mol%	60	24	29+42+21	92
5	$BF_3{\cdot}OEt_2$	1.2	-78 → rt	4	24+41+13	78
6	$FeCl_3$	1.2	-78 → rt	24	10+24+17	51
7	$Cu(OTf)_2$	10 mol%	60	24	19+27+10	56
8	$In(OTf)_3$	10 mol%	60	24	11+4+7	22

[a] The vinylogous Nazarov cyclization representative procedure described in Section 3.5.2.3 [b] Yields are based on the isolated product after flash chromatography. [c] Combined yield of cyclization products.

Several Lewis acids were examined to assess their ability to promote the desired reaction with a higher regioselectivity. The previously reported Lewis acids ($TiCl_4$ and $Sc(OTf)_3$) provided high yields – 89% and 92% respectively. Application of $BF_3{\cdot}OEt_2$

resulted in the formation of products **57**, **58**, **64** in a 78% combined yield, with no strong preference for any of the regioisomers. It is worth noting, all the Lewis acids used in entries 2, 4, 5 required different temperatures to perform the vinylogous Nazarov cyclization. $TiCl_4$ could promote cyclization at -78 °C, while BF_3 OEt_2 could do the same job only at room temperature and $Sc(OTf)_3$ required heating up to 60 °C but only a catalytic amount can be used (10 mol%). Reactions catalyzed by $Sc(OTf)_3$ suffered from poor selectivity giving all three regioisomers. Application of $TiCl_4$ as 1 M solution in DCM has strong preference to form product **57** in a high yield. A catalytic amount of $TiCl_4$ (Table 3.1, entry 3) was not enough to convert all the substrate **40a** to the desired product, leading to only 31% of product **57** and all the remaining starting material recovered. The results of the application of the catalytic amount of $TiCl_4$ looked promising in terms of selectivity leading to the formation of a single regioisomer **57**. The addition of pure $TiCl_4$ (Table 3.1, entry 1) resulted in the formation of product **58** as a major regioisomer, with the decomposition of the significant amount of starting material. The other Lewis acids (1.2 equiv. of $FeCl_3$, and catalytic amounts of $Cu(OTf)_2$, and $In(OTf)_3$) were able to initiate the desired vinylogous Nazarov cyclization, although, with no preference for any of the regioisomers and in diminished yields (Table 3.1, entries 6–8) 51%, 56%, and 22%, respectively.

Since no selectivity was observed in the proton elimination step, we decided to try a different substrate activation pathway. Based on the recent studies by the West group, a new alternative was proposed for the activation of the vinylogous Nazarov cyclization. (Scheme 3.22).[182] West and co-workers reported the possibility to deviate from the normal protonation/LA coordination to the carbonyl in the Nazarov cyclization. The desired reaction was initiated by the application of DDQ to perform single-electron oxidation of alkylidene 1,4-pentadien-3-yl ether **65**. The substrate was shown to undergo cyclization with the formation of a single product **66** in a high yield.

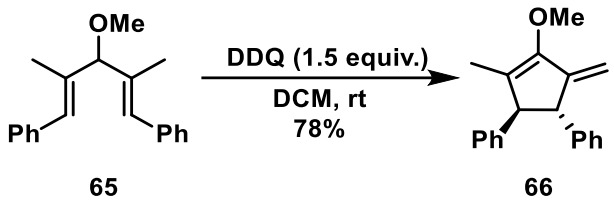

65 66

Scheme 3.22. The DDQ initiated Nazarov cyclization.

Compound **67** was chosen due to its similarity with compound **65** and its ease of preparation compared to other [3]dendralenes. The starting material was prepared from [3]dendralenoate **40a** and required two additional steps: reduction of the ester group and protection of the formed hydroxyl. (Scheme 3.23). The reduction of **40a** with DIBAL-H gave corresponding alcohol, which upon treatment with MeI in DMF at room temperature led to the formation of the protected alcohol **67**.

The initial proposal was that after DDQ assisted oxidative vinylogous Nazarov cyclization of [3]dendralene, the subsequent second cyclization event could occur, forming **68a** or/and **68b**. The addition of DDQ to compound **67** at -78 °C did not initiate the desired reaction resulting in recovery of the starting material. Warming up the reaction mixture to 0 °C resulted in the decomposition of the starting material **67**. The enol ether, which is presumably formed during the reaction, does not bear α-substituents, and presumably can undergo polymerization.[183]

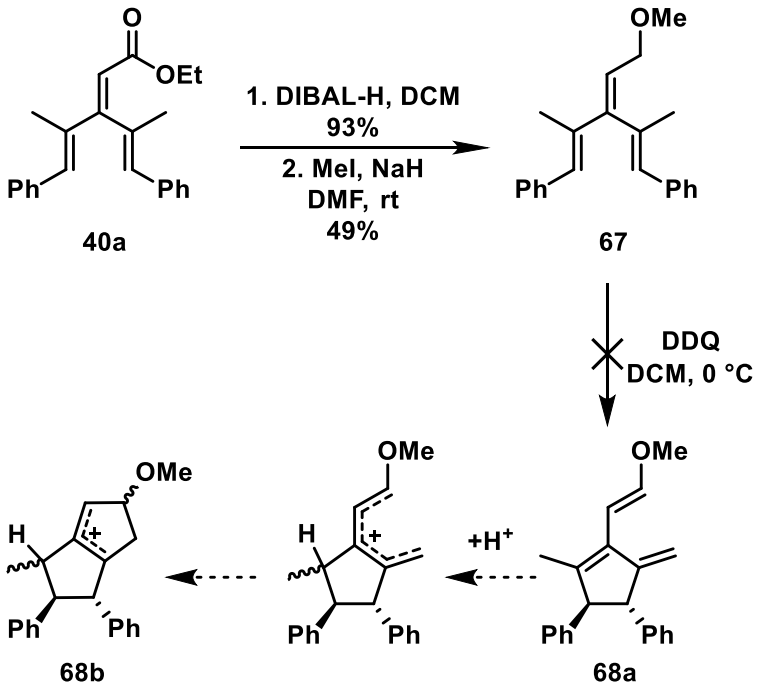

Scheme 3.23. Preparation of compound **67** and its proposed DDQ assisted oxidative cyclization.

3.3.3 The Interrupted Vinylogous Nazarov Cyclization

The vinylogous Nazarov cyclization can be considered to be special compared to the conventional Nazarov cyclization because of the formation of a unique zwitterionic reactive intermediate. Nucleophilic trapping of electrocyclization intermediates from cross-conjugated trienoates has not been examined previously. We sought to explore the possibility of new trapping processes, both inter- and intramolecular, that could be used to interrupt the vinylogous Nazarov reaction (Scheme 3.24).

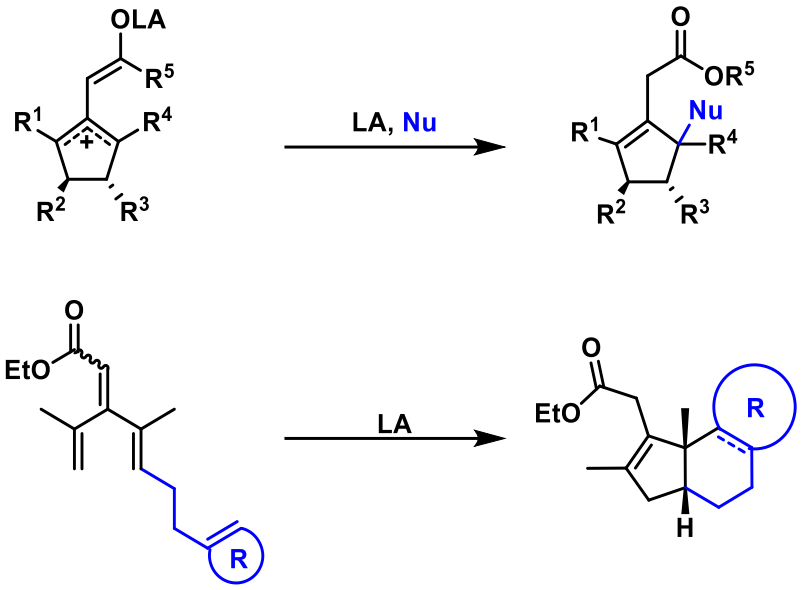

Scheme 3.24. The proposed inter- and intramolecular interrupted vinylogous Nazarov cyclization.

3.3.3.1 The Domino Intermolecular Interrupted Vinylogous Nazarov Cyclization

Initially, we attempted to perform intermolecular interrupted vinylogous Nazarov cyclization in the presence of such Lewis acids, which in conventional Nazarov cyclization are known to activate interrupted Nazarov cyclization in presence of nucleophiles or act as nucleophiles themselves. The reaction was expected to proceed as a domino process by trapping the newly formed allyl cation before the intermolecular proton elimination would occur. Compound **40a** was used as a model substrate as its transformations were most well studied, and compared to other [3]dendralenes, it was easier to prepare.

Our investigation started with the Lewis acids such as BBr_3 and $AlMe_3$. Interestingly, BBr_3 was able to initiate the vinylogous Nazarov cyclization at -78 °C, which after the sequence of transformations led to the mixture of the previously reported regioisomers **57**, **58**, and **64** (33%, 17%, 23% respectively) with a combined yield of 73% in 1 h. No trapping products of the allyl cation with bromide were observed.

Subsequently, trimethylaluminum was tested; it is known to be a Lewis acid and the nucleophile source at the same time (Scheme 3.25).[111] The organoaluminum mediated interrupted Nazarov cyclization starts at -41 °C. For the vinylogous Nazarov cyclization warming up the reaction vessel to the room temperature resulted in the formation of the

three new products **69**, **70**, and **71** in an 83% combined yield (11% of compound **69** isolated as 1:1 mixture with starting material). Product **70** had an additional methyl group delivered to the ester position by a 1,2-alkyl addition, a well-known reactivity pattern for organoaluminum mediated processes.[104] Unfortunately, during the progress of the reaction, 23% of the starting material did not undergo the desired interrupted Nazarov cyclization, and only double 1,2-alkyl migration happened, thus forming alcohol **71**. The reaction was proposed to have a mechanism analogous to the one previously reported by the West group for the organoaluminum mediated interrupted Nazarov cyclization.[111]

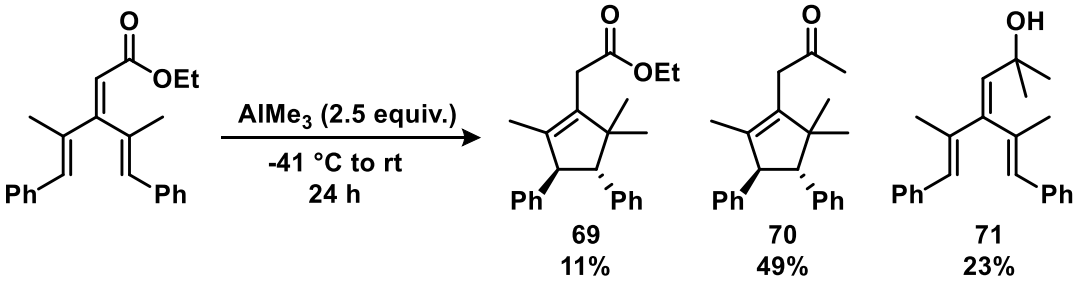

Scheme 3.25. The organoaluminum mediated interrupted vinylogous Nazarov cyclization.

Inspired by the initial results for the organoaluminum initiated cyclization process, we decided to study other nucleophilic traps that are known to capture the oxyallyl cation in the conventional interrupted intermolecular Nazarov cyclization. We aimed at performing the reaction in domino manner (all reagents are present in reaction vessel from the start) rather than one-pot fashion (reagents are added stepwise after intermediate formation).[113a] We assumed that the zwitterionic intermediate could undergo side reaction, such as quenching itself via intermolecular proton transfer or/and subsequent isomerization. The conditions were selected based on our previous cyclization studies of applicable Lewis acids (Section 3.3.2).[168,170] The advantage of the methodology is that all the reagents can be premixed before the reaction at -78 °C and subsequently warmed up to the required temperature, depending on the Lewis acid used.

The studies started with the application of nucleophilic traps. No electrophilic traps and double interruptions were examined. In the beginning, electron-rich π nucleophiles such as 2-(trimethylsilyloxy)propene, allyltrimethylsilane, and allyltributylstannane were the first choice.[73–75,77] These traps were premixed with the starting material **40a** and the

Lewis acid was added afterward. Interestingly, no vinylogous Nazarov reaction, with or without trapping, was observed in previously reported temperature regimes and conditions for $Sc(OTf)_3$. Heating the reaction vessel to 100 °C with 1.2 equivalents of $Sc(OTf)_3$ in toluene resulted in the formation of product **72** in a 45% yield, with no trapping observed in the presence of allyltributylstannane (Scheme 3.26). Product **72** was previously observed for Meyer–Schuster studies by the West group in presence of $AuCl_3$.[168]

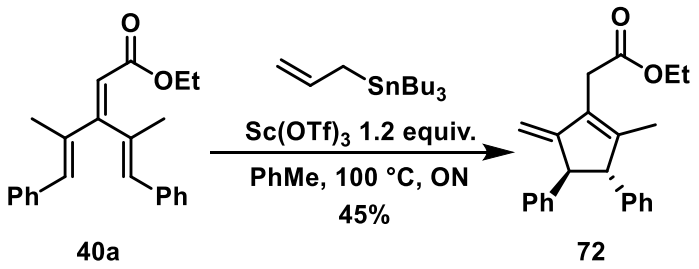

40a 72

Scheme 3.26. The initial attempts of the interrupted vinylogous Nazarov cyclization.

Subsequently, furan and Et_3SiH were applied as traps for the cascade intermolecular interrupted Nazarov cyclization. Both of them were shown to be potent nucleophiles for the interrupted Nazarov cyclization.[67,70,82,84] There was a possibility in the case of furan that it could undergo [4+3]-cycloaddition as well, as it does with oxyallyl cations. Surprisingly for us, the products obtained with $TiCl_4$ were different from the ones formed with the $BF_3{\cdot}OEt_2$ (Scheme 3.27). In the presence of $BF_3{\cdot}OEt_2$, the two expected diastereomers **73** and **74** were formed. The treatment of the starting material **40a** with $TiCl_4$ in the presence of the trap resulted in the formation of the unexpected products **75** and **76**, via Michael addition of the nucleophile to the exocyclic alkene (i.e., reaction of the nucleophilic trap with the elimination product, rather than interception of the zwitterionic cyclization intermediate).

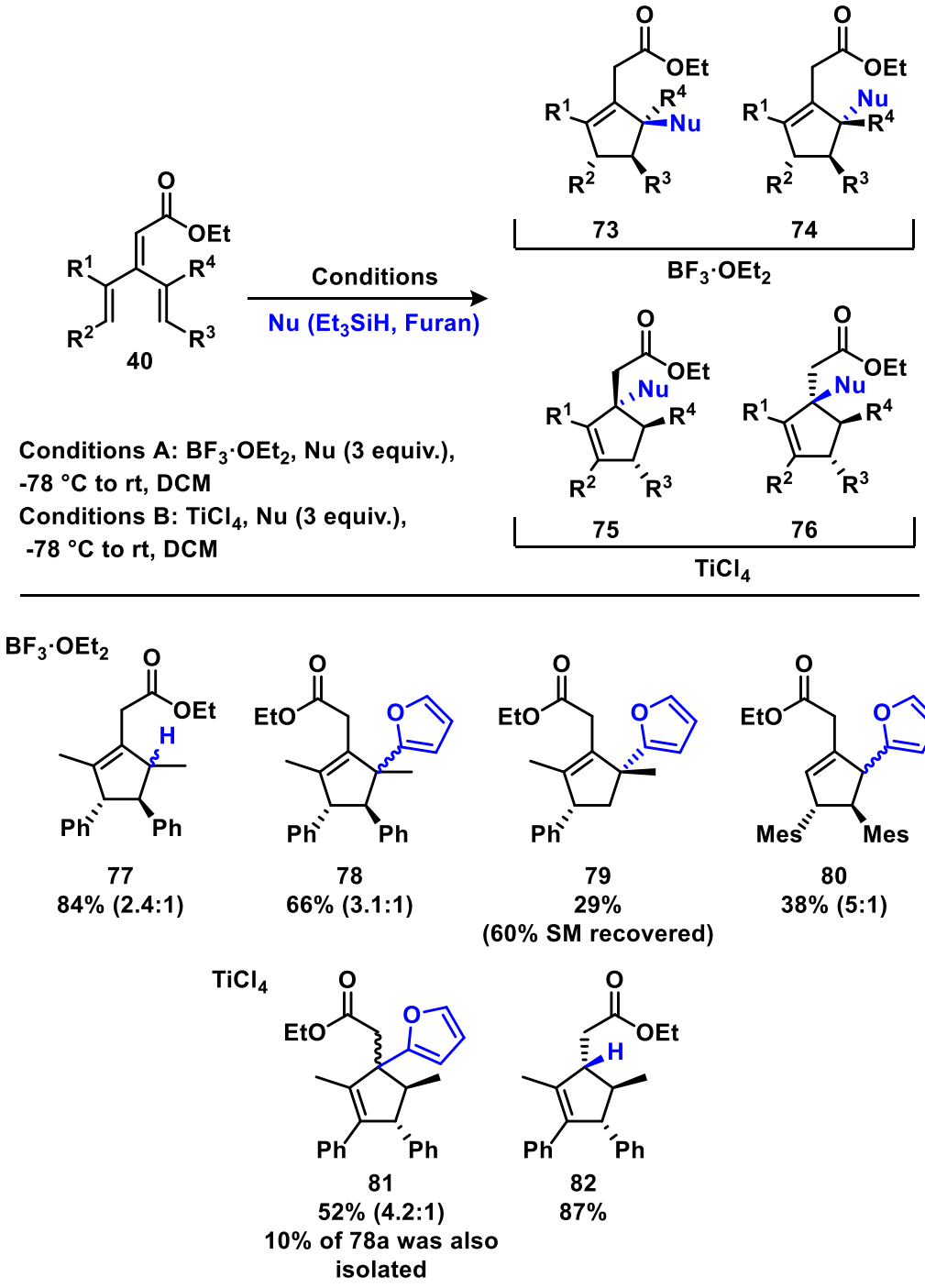

Scheme 3.27. The scope of the domino intermolecular interrupted vinylogous Nazarov cyclization.

The scope studies started with the application of both traps in the presence of $BF_3 \cdot OEt_2$ with substrate **40a**. Both furan and Et_3SiH formed the desired products in high yields: **77** in 84% with a 2.4:1 ratio, and **78** in 66% yield, with a 3.1:1 diastereomeric ratio. Only diastereomers with the endocyclic alkene were observed. The substrate with

the single phenyl group underwent the desired transformation slower, forming only 29% of the product **79** as an inseparable mixture with the starting material after 4 h at room temperature (60% of starting material was still present).

Attempts to cyclize the [3]dendralenoate **40c** with no α-methyl groups in the presence of the furan resulted in the formation of the product **80** in a 38% yield (5:1 ratio). One of the possible reasons for this cyclization to occur is that the ethyl ester tether can have interactions with the δ-hydrogen atom on the terminal alkene. This unfavorable interactions results in the decreased population of *s-cis/s-trans* conformation (**40c**) over *s-trans*/*s-trans* conformation (**40c'**) in the mixture (Figure 3.10), which is promoting the vinylogous Nazarov cyclization.[110,111]

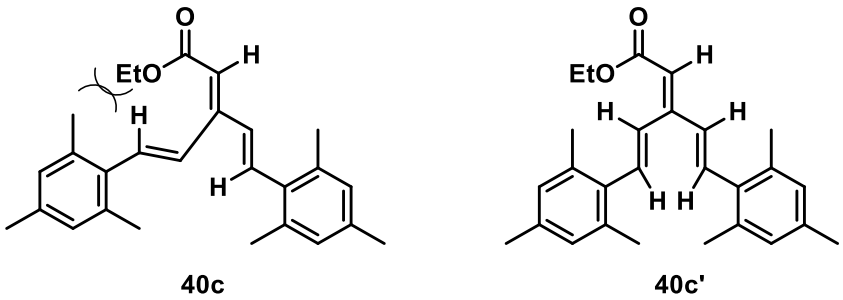

Figure 3.10. Possible conformations of the bis(mesityl) α,α'-unsubstituted trienoate.

The structures of compounds **77a** and **77b** were analyzed as an inseparable mixture. The analysis started with the assignment of methylene protons next to the C=O. Subsequent HMBC studies showed that there is a neighboring endocyclic alkene bond in a cyclopentene ring. To do a relative structure determination, we needed to analyze the anisotropic effect on the methyl group by the neighboring phenyl group (Figure 3.11). The required doublet experienced an anisotropic shielding effect in the minor diastereomer and appeared at significantly lower ppm (0.63) compared to the one in the major diastereomer (1.09 ppm).

The mixture of compounds **78** was analyzed as an inseparable mixture. The structures **78a** and **78b** were assigned in an analogous way as for products **77a** and **77b**. The methyl singlet that experienced an anisotropic shielding effect appeared at 1.18 ppm, which is significantly lower in ppm compared to the one appearing in the major diastereomer (1.53 ppm). Data analysis showed that the vinylogous Nazarov cyclization

trapping products were formed under product development control in the presence of $BF_3 \cdot OEt_2$, in analogy to the conventional Nazarov reaction. In these cases, approach of the nucleophilic trap from the sterically more demanding face of the carbocation is favored due to avoidance of an undesirable steric clash between the methyl group on the carbon being attacked and the neighboring phenyl group.

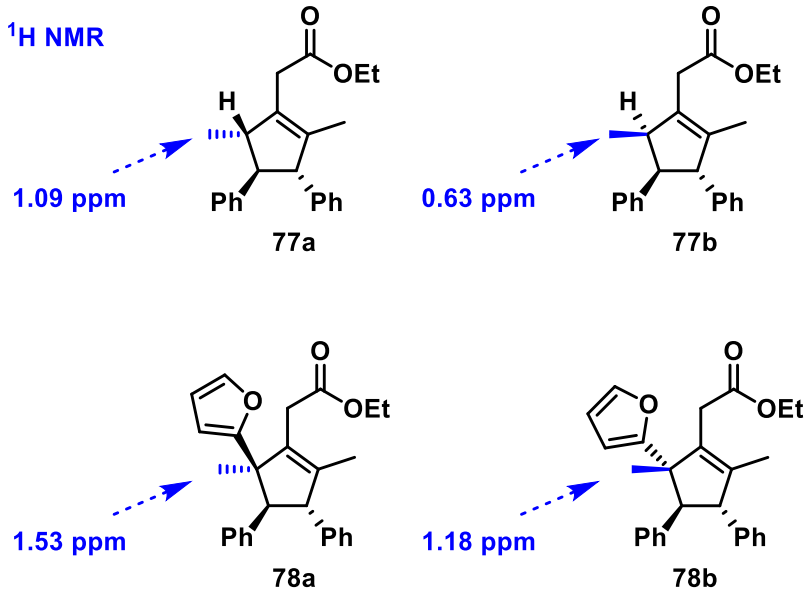

Figure 3.11. Diagnostic methyl chemical shifts in ^{1}H NMR data for **77** and **78**.

In all the examples studied for the $TiCl_4$ initiated domino interrupted processes, the addition of the nucleophile occurred in the Michael addition fashion, forming products **81** in a 52% yield with a 4.2:1 ratio (10% of compound **78a** was isolated as well), **82** in an 87% yield (Scheme 3.27). It seems that the trapping event have happened after the product **57** was formed. Once this electron-deficient alkene is available, conjugate addition of the nucleophile is possible.

To support our proposal, a reaction with the single regiostereomer **57** was performed to reduce the exocyclic alkene (Scheme 3.28). The exocyclic alkene regiostereomer was resubmitted to $TiCl_4$ in the presence of the reducing reagent Et_3SiH. After the reaction workup, a single diastereomer **82** was formed, and the second diastereomer was not observed. The other conclusion, which one can make, is that attack from a more hindered face (**83**) to form product **82** is a result of product development

control to move away the bulky carbon chain from the neighboring methyl group. The structure assignments of the regioisomers mixture of **81** was based on obtained data for compound **82** and previously reported data on stereochemistry for compound **57**.[170]

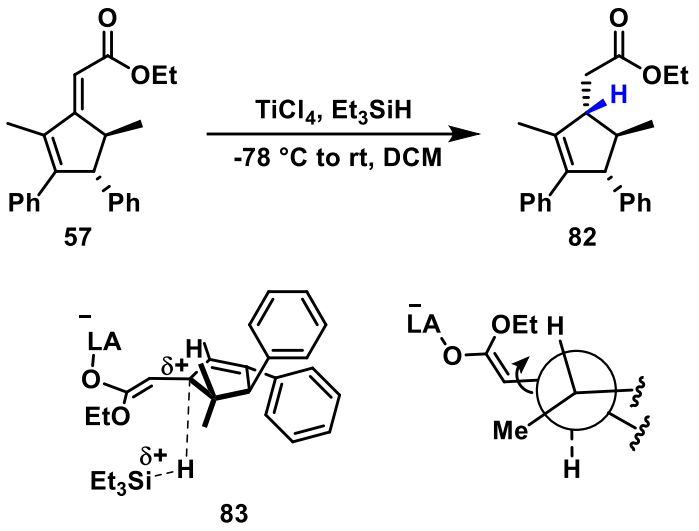

Scheme 3.28. The product development control studies for compound **82** formation.

The assignment of the relative stereochemistry for material **79** was based on NMR analysis of the geminal methylene protons on the cyclopentene ring (Figure 3.12). Utilizing HSQC analysis, it was found that, both of these hydrogens appear to be situated on the same carbon at 48.4 ppm, and significantly differ in chemical shifts. One of them shows up relatively upfield at 1.78 ppm, while the other one is shifted more downfield with 2.75 ppm chemical shift. A chemical shift difference of a full 1.0 ppm indicates drastically different magnetic environments for these two protons, consistent with anisotropic shielding of one of them by both neighboring aryl groups.

Based on obtained NMR data, we assigned the relative stereochemistry of the major product **80a**. First, the position of all methyl groups was determined by means of nOe. *Ortho*-methyl group of mesityl at C-4 (2.55 ppm) has nOe correlations with *ortho*-methyl groups of mesityl at C-3. It also has correlations with C-H neighboring the furan ring (4.51 ppm) and with C-H next to the mesityl ring (4.79 ppm) at C-3 (Figure 3.13). *Ortho*-methyl group of mesityl at C-3 (2.62 ppm), in turn, have correlations with protons, which appear at 5.96 and 4.34 ppm. The proton that appears at 5.96 ppm does not belong to any

aromatic system on the cyclopentene ring. This proton has HMBC correlations with a neighboring carbon at 51.7 ppm, which bears mesityl at C-3, and with sp^2 quaternary carbon at 156.2 ppm. The latter one, in turn, has HMBC correlations with the methylene protons next to the C=O.

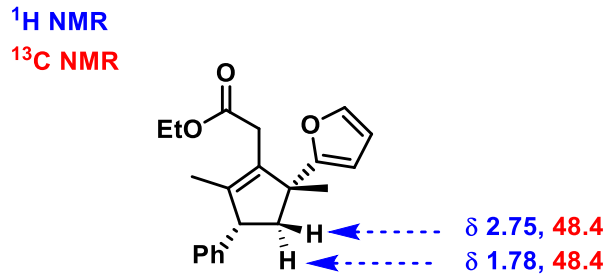

Figure 3.12. The assignment of relative stereochemistry of product **79**.

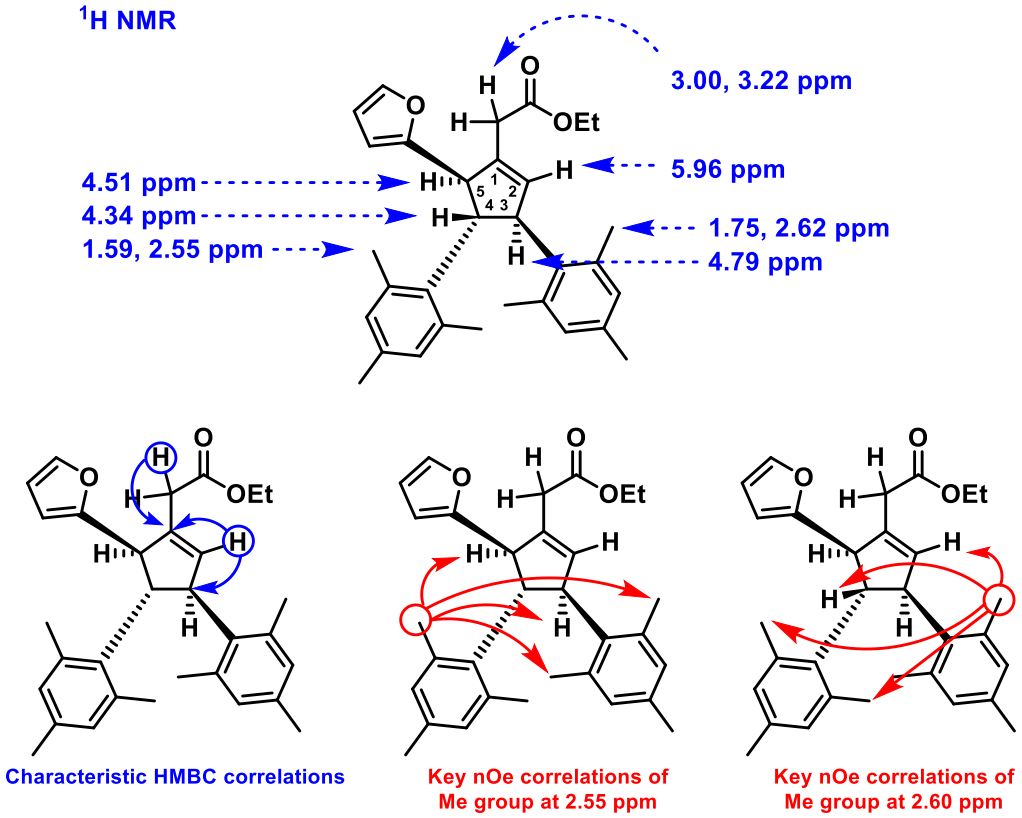

Figure 3.13. NOE and HMBC correlations supporting an all-trans relative configuration for **80a**.

Cross-conjugated trienoates **40** were shown to act as cyclized cationic intermediates, which can be trapped after their cyclization in a domino manner by furan

or Et_3SiH. Trapping of the allyl cation preserve stereochemistry formed during the 4π conrotatory ring-closing event. Trapping of zwitterion with nucleophiles in the presence of $BF_3 \cdot OEt_2$ was less selective compared to $TiCl_4$. Both Lewis acids provided different trapping products, which is an efficient tool for gaining structural complexity. The trapping studies allowed us to gain a deeper understanding of the vinylogous Nazarov cyclization mechanism, especially, about its proton elimination pathways. This knowledge can be applied for studies in the area of the trapping of the zwitterionic intermediate with electrophiles. We also applied the obtained data to the area of intramolecular vinylogous Nazarov cyclization.

3.3.3.2 The Intramolecular Interrupted Vinylogous Nazarov Cyclization

In analogy to the previously reported work by West and co-workers (Scheme 3.29), we decided to explore the capability of pendent electron-rich aryl groups to trap the zwitterionic electrophile resulting from vinylogous Nazarov cyclization.[51,52] For this purpose, a series of trienoates with different aromatic traps were prepared following the previously reported literature in 7–9 steps.

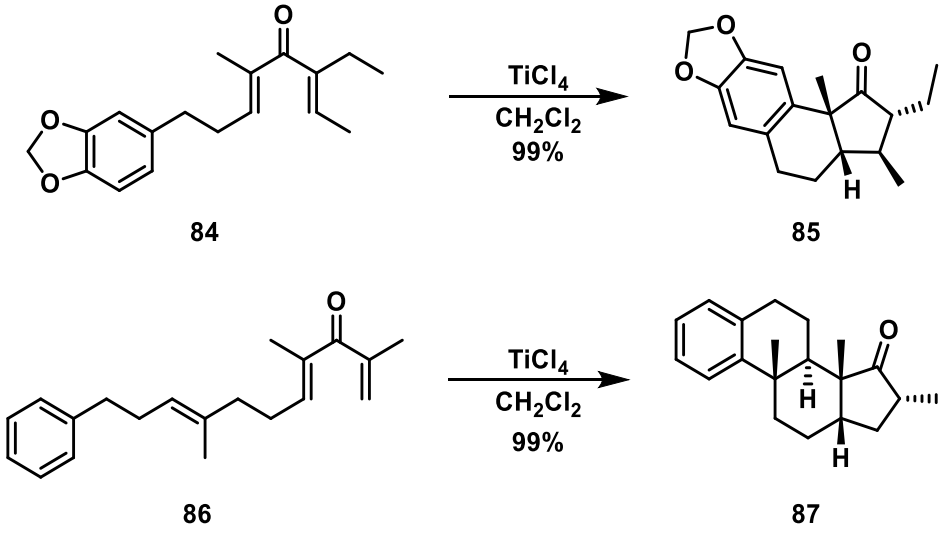

Scheme 3.29. Previous examples of the intramolecular interrupted Nazarov cyclization.

The representative procedure to prepare dienones with the intramolecular traps is shown on the example of substrate **91** (Scheme 3.30). The oxidations in the substrate

preparation sequence were done by the use of DMP reagent, which did not require additional purification steps after basic workup. The Horner–Wadsworth–Emmons (HWE) reaction furnished both, *E* and *Z* isomers and proceeded in high to excellent yields, with a high preference for the *E* isomer. After separation, only the *E* isomer was used for subsequent reactions. The overall yield of the sequence after seven steps was 43%; all reactions for the preparation of the starting material were done on a gram scale.

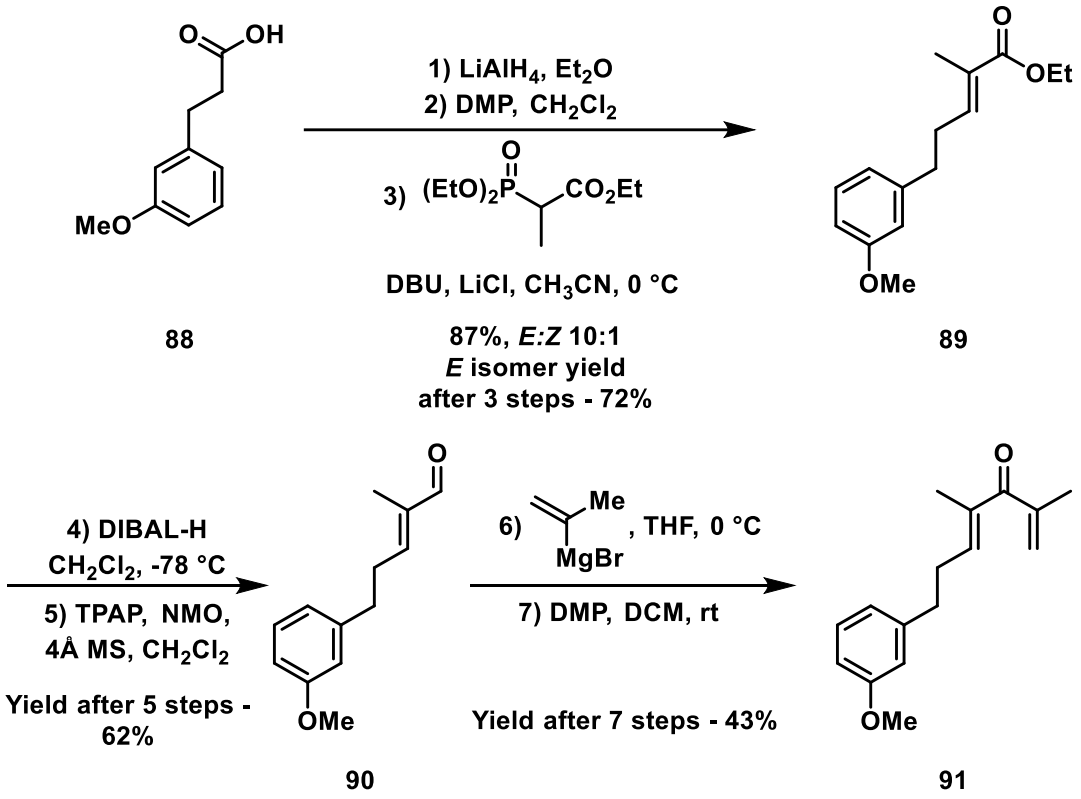

Scheme 3.30. The reaction sequence to prepare starting material **91**.

Each of the dienones required two additional steps to furnish the desired trienoates **93**, **95**, **97**, **99** (Scheme 3.31). Ethoxyacetylene addition to the dienone had an excellent yield in all cases. However, the Meyer–Schuster rearrangements were shown to have diminished yields when applied to these more structurally elaborate substrates. No significant preference to form the *E* isomer over the *Z* isomer was observed (1.2–1.5:1 ratio).

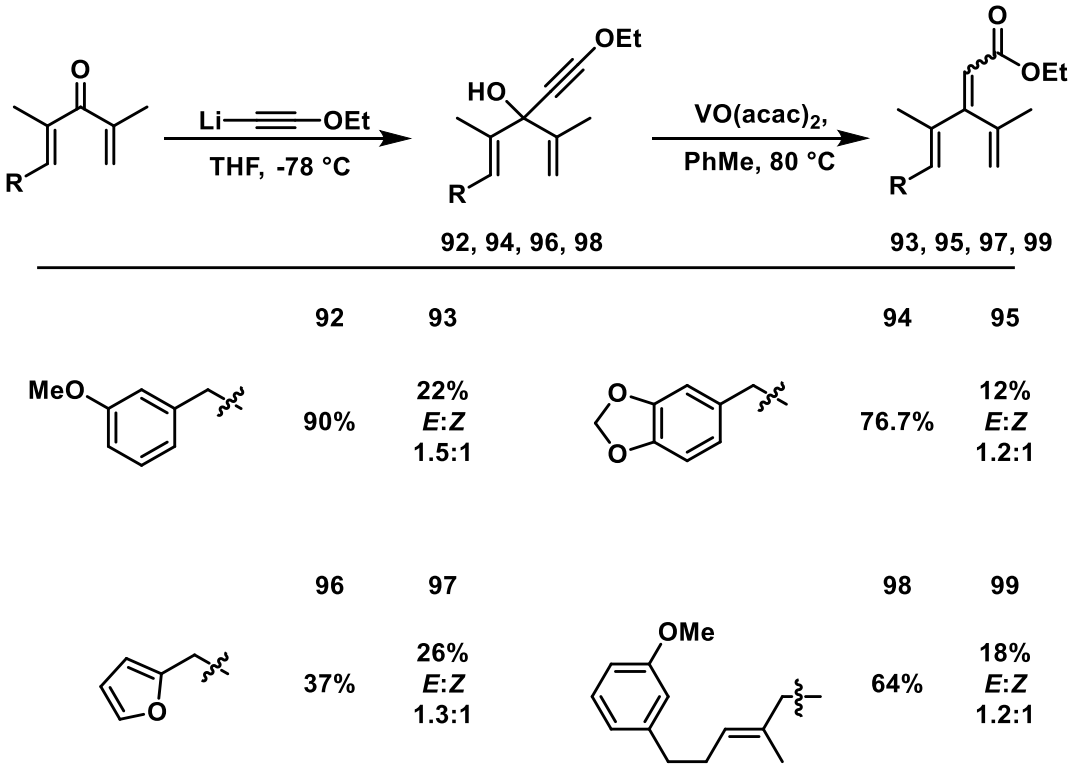

Scheme 3.31. The scope of starting materials for the proposed intramolecular interrupted Nazarov cyclization.

A mixture of *E* and *Z* isomers of **93** was modified further to obtain the substrate with a different carbonyl functional group to study its influence on cyclization (Scheme 3.32). An ester **93** was added to the mixture of isopropylmagnesium bromide with N,O-dimethylhydroxylamine hydrochloride in THF. The desired Weinreb amide **100** was obtained in a 46% yield after 3 h.

The *E*/*Z* isomers mixtures of **93**, **95**, **99**, and **100** were successfully separated and characterized. The chemical shifts and structure assignments will be discussed on the example of products **93a** and **93b**; the other products' assignments were accomplished in the same manner and had analogous correlations (Figure 3.14).

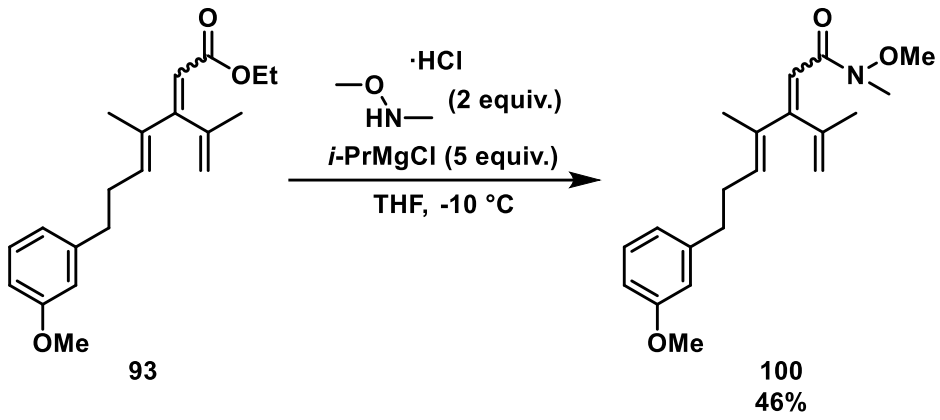

Scheme 3.32. Conversion of ester **93** to Weinreb amide **100**.

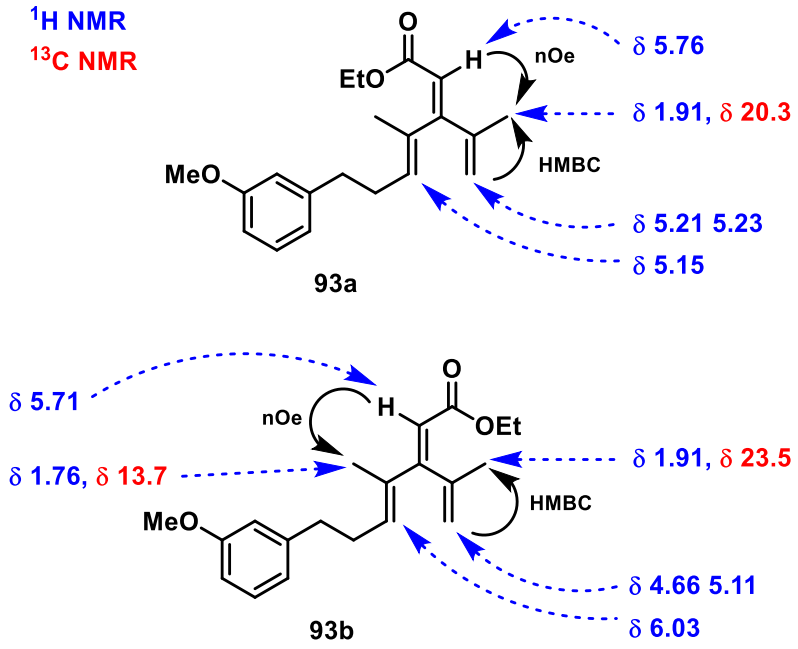

Figure 3.14. ^{1}H NMR diagnostic correlations for the products **93a** and **93b**.

The characterization of compounds **93a** and **93b** started with the identification of the positions of methyl groups. The methyl group at δ 1.91 has HMBC correlations with geminal protons at δ 5.21 and δ 5.23 (same correlations were observed for *Z* isomer). Geminal protons were identified using HSQC correlations. Alkene protons neighboring C=O in compounds **93a** and **93b**, to our delight, each displayed diagnostic nOe correlations to one allylic methyl group, clearly indicating which alkene was *cis* to that

proton. The lack of significant selectivity in alkene geometry indicates that the two transition states are roughly equivalent in energy.

The Lewis acid choice and initial conditions for the desired cyclization were dictated by previously reported literature precedents for the conventional intramolecular interrupted Nazarov cyclization and by the results obtained in the intermolecular trapping experiments described above (section 3.3.3.1).[52] Later, the reaction temperature was changed from -78 °C to ambient, since after 1 h at -78 °C, there was no conversion according to ^{1}H NMR analysis of an aliquot of the reaction mixture. The scope of the intramolecular interrupted vinylogous Nazarov cyclization is presented in Scheme 3.33. Initial attempts with compound **97** bearing a heteroaromatic trap resulted in the decomposition of the starting material under the given conditions. Use of a methylenedioxy-substituted phenyl trap resulted in the formation of a complex mixture instead of the desired product **102**, which may be a result of the inadequate nucleophilicity of the aryl trap.

Subsequently, after the first obtained results, we decided to switch our attention to the monosubstituted arenes bearing a single electron-donating substituent. Switching to the substrate **93**, which contained a *meta*-methoxy aromatic group, resulted in a clean and rapid transformation, with the formation of desired product **103** in an 80% yield. Product **103** could be formed in a high yield from both *E* and *Z* isomers of **93** separately. It is noteworthy, due to the similarity in R_f values of the starting material and product, that it was necessary to use ^{1}H NMR analysis to monitor the reaction progress. Complete starting material consumption was observed after 4 h at room temperature.

Inspired by the outcome for substrate **93**, we decided to test polyene **99** for cascade polycyclization. Unfortunately, only a complex mixture was obtained upon treatment of **99** with $TiCl_4$, with no sign of desired tetracyclic product **105**. In this case, the requirement for initial cyclization via an intervening trisubstituted olefin may derail the process. Furthermore, the possibility for various truncated products in this multistep process increases the probability of a complex outcome. No substrates with gem-dimethyl group was tested in order to study the Thorpe–Ingold effect.

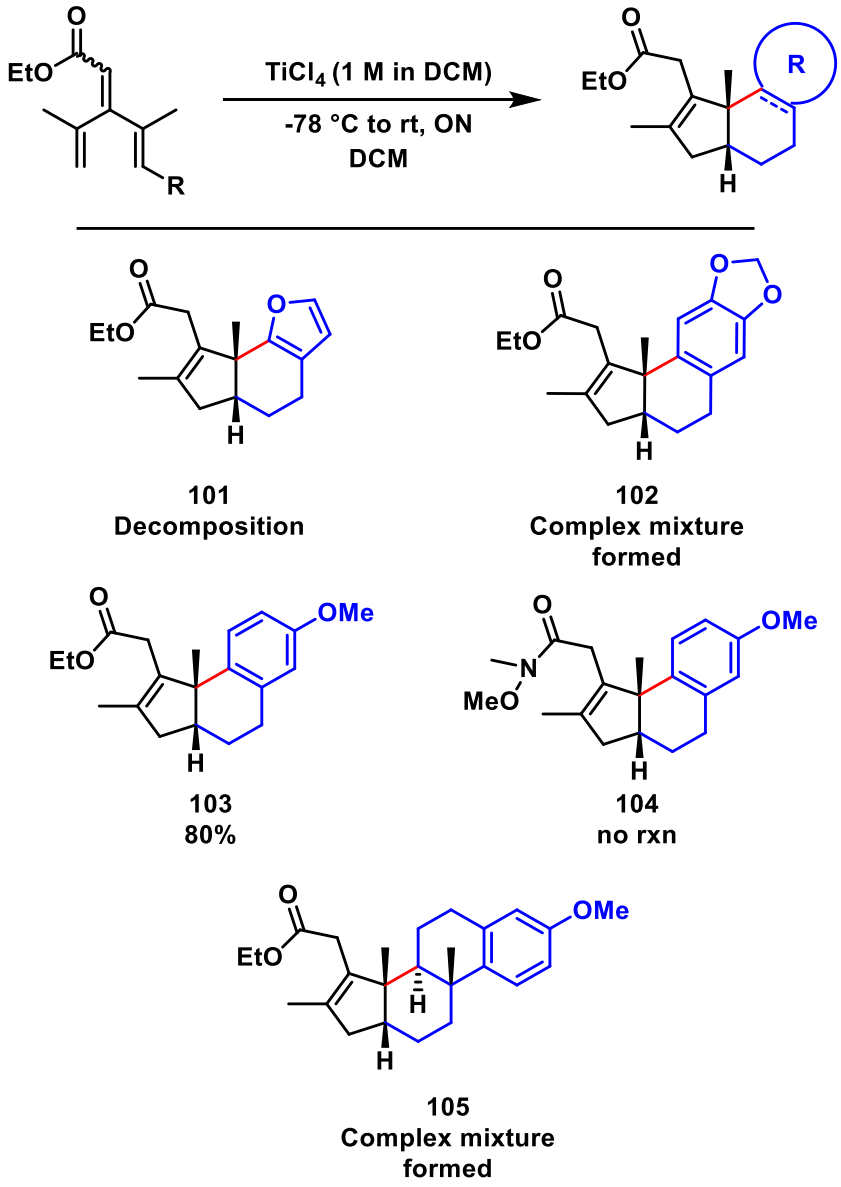

Scheme 3.33. The intramolecular interrupted vinylogous Nazarov cyclization.

Substrate **100**, in which the Lewis basic activation site was an amide rather than an ester, required higher temperatures for conversion. The use of $TiCl_4$ and warming the reaction mixture from -78 °C to room temperature did not result in the cyclization of the amide leaving the starting material intact. During this time it was decided to apply $TiCl_4$ as a Lewis acid, which was known to work at higher temperature regime for the vinylogous Nazarov cyclization (higher temperature regimes for $TiCl_4$ were not tested). Attempts to cyclize substrate **100** continued with the addition of catalytic amount of

$Sc(OTf)_3$ and heating to 80 °C in DCE (Scheme 3.34). Interestingly, the obtained product **106** was different to the one which was expected. Conversion of an α,β,γ,δ -unsaturated amide into a butanolide as in **100→106** appears to be without precedent. The ability of [3]dendralenes and related conjugated systems to form butenolides, the reaction mechanism, the structure elucidation, and the studied scope will be discussed in Chapter 4.

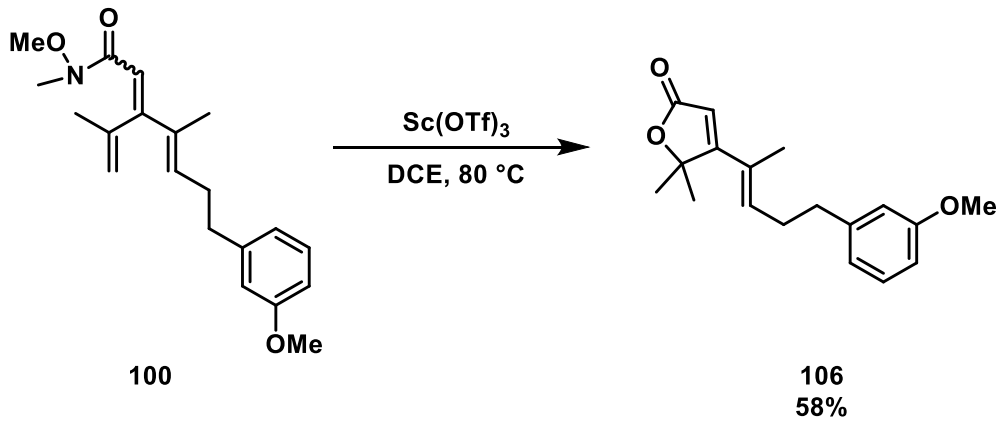

100 **106** **58%**

Scheme 3.34. The butenolide **106** formation.

Structure elucidation of product **103** was achieved via ^{1}H and ^{13}C NMR data analysis (Figure 3.15). The total count of protons came up to 26. Three methyl groups (two on the aliphatic hydrindan system and one on the aromatic ring) showed up as singlets. According to HMBC and HSQC analysis, the methyl at 1.37 ppm was found to be attached to the quaternary sp^3 carbon, while another methyl at 1.68 ppm showed HMBC correlations with the alkene sp^2 carbon at 133.9 ppm. The methyl group at 1.37 ppm has strong HMBC correlations with the aromatic carbons, neighboring quaternary and tertiary carbons (52.4 ppm and 44.0 ppm respectively), and endocyclic alkene carbon at 128.0 ppm that is attached to the ester tether. The methyl group at 1.37 ppm has nOe correlations with the angular methine proton, at 2.30–2.25 ppm. These data suggest that methyl at 1.37 ppm and hydrogen at 2.30–2.25 ppm are in a *cis* relationship. The data show that the close through-bond proximity of the aromatic ring to the angular methyl is highly suggestive of attack on the zwitterion at that position. This proposal is supported by the fact that number of aromatic protons decreased by 1. There is a pair of aliphatic,

diastereotopic methylene protons next to the ester instead of a single alkene proton. These methylene protons has HMBC correlations with neighboring carbon of endocyclic alkene moiety. Further evidence from HRMS and IR spectral data confirmed the presence of the expected ester, alkene, and arene functionality, as well as a molecular weight consistent with the expected trapping product.

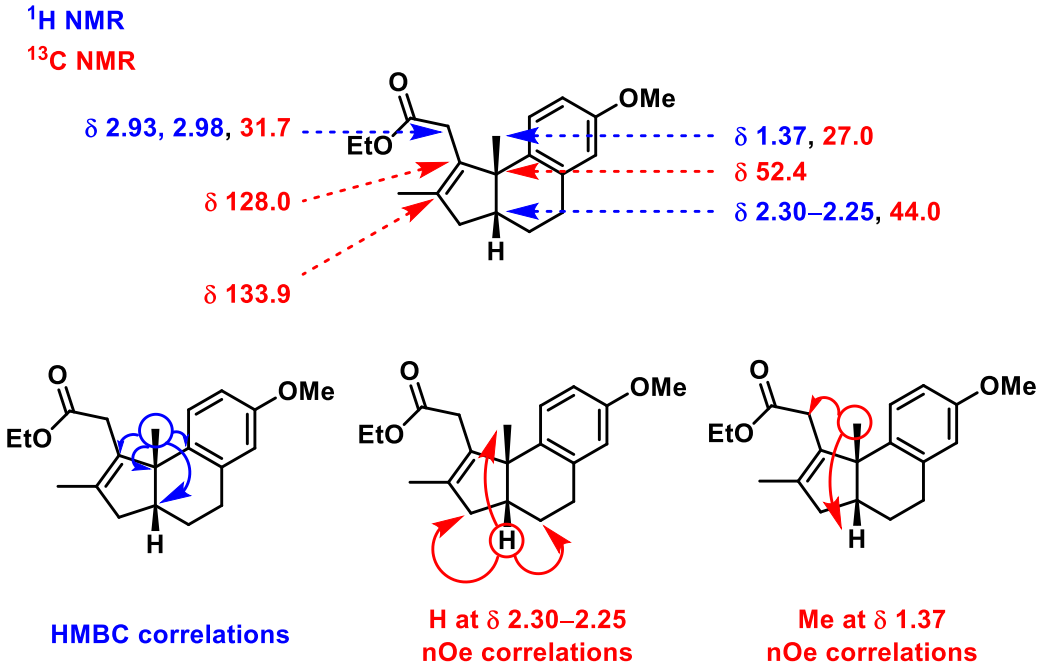

Figure 3.15. The structure elucidation of product **103**.

The X-ray crystal structure of intramolecular arene trapping product **107** was reported previously by our group (Figure 3.16).[52] Compound **103** has a similar ^{1}H NMR spectrum for the ring system as reported for **107**, which was formed via the interrupted Nazarov cyclization. The crystal structure shows the positions of the methyl groups and neighboring angular methine proton. A crystal structure of an analogous compound provides additional support to the previously discussed ^{1}H NMR assignments of the relative stereochemistry of the compound **103**.

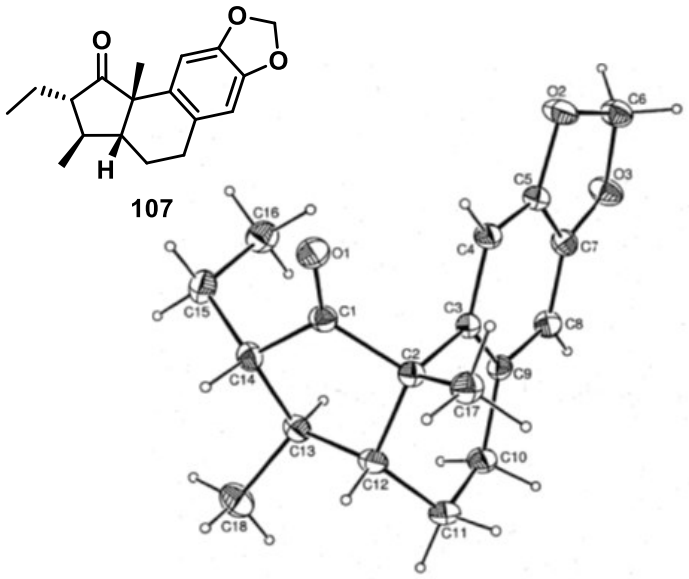

Figure 3.16. The crystal structure of previously reported interrupted Nazarov polycyclization product **107**.

Along with the attempts to put a trap on the terminal alkene of [3]dendralene, we were curious to deliver a potential trap via the carbonyl moiety. The interest was driven by the idea to have a quick and convenient pathway to form complex polycyclic structures. The proposal was that bringing in close proximity an electron rich olefin and a zwitterionic intermediate will result in the formation of polycyclic systems **109a** or/and **109b** via [3+2] cycloaddition (Scheme 3.35).

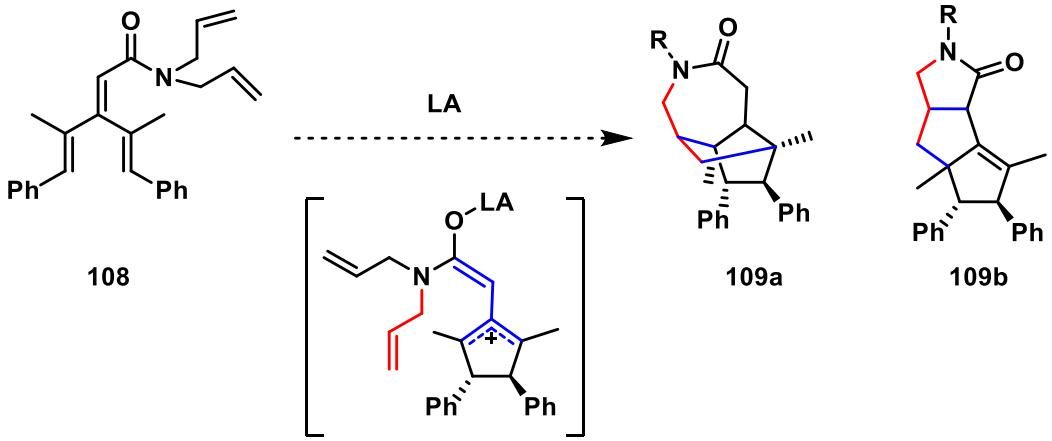

Scheme 3.35. The proposed vinylogous Nazarov/[3+2]-cycloaddition.

The substrate for the desired transformation was prepared in a single step from the ester precursor **40a**, in analogy to the previously described procedure for the Weinreb amide **100** preparation (Scheme 3.36). The formation of substrate **108** bearing two potential trapping moieties in the form of a diallylamide was accomplished with an 85% yield.

Subsequently, substrate **108** was treated with $TiCl_4$ to perform the interrupted vinylogous Nazarov cyclization (Scheme 3.37). Cyclization of **108** in the presence of $TiCl_4$ resulted in the formation of product **110** that is analogous to the compounds **64** previously discussed in Section 3.3.2. The formation of the regioisomer **110** shows that the desired vinylogous Nazarov cyclization took place, but desired [3+2]-cycloaddition event did not occur.

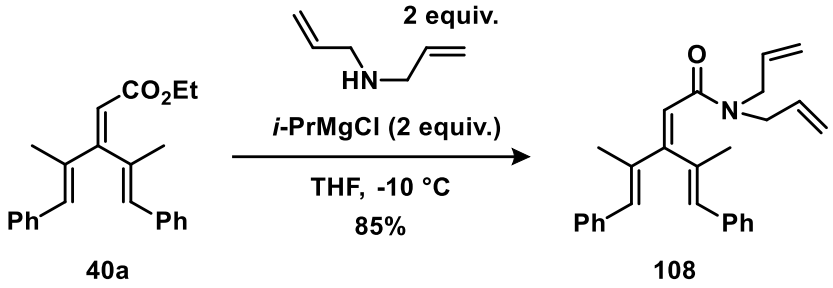

Scheme 3.36. The preparation of the substrate **108**.

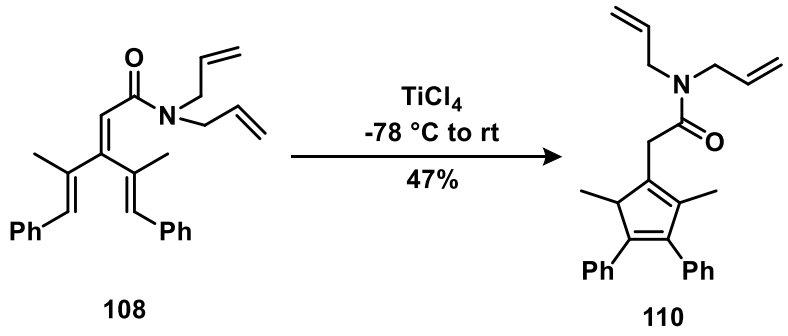

Scheme 3.37. The vinylogous Nazarov cyclization of the substrate **108**.

We were able to show that the intramolecular vinylogous Nazarov cyclization reaction with the nucleophilic trap on β-position in one case could lead to the stereoselective formation of the polycyclic system. The possibility of forming an

endocyclic alkene and two new stereogenic centers in a single step in a stereoselective fashion is intriguing. To learn if it is possible to deliver a potential trap via the carbonyl moiety further studies are required.

3.3.4 The Interrupted Vinylogous Nazarov Cyclization Mechanism

The initial steps of activation and cyclization in the vinylogous Nazarov cyclization should be similar to the conventional Nazarov cyclization (Scheme 3.38). In the beginning, Lewis acid coordinates to the carbonyl of the remote ester moiety of compound **40**. The resulting complex can be viewed as a pentadienyl cation with an enolate bound to the central carbon atom. Subsequent 4π electrocyclic ring-closure results in the formation of allyl cation. The elimination step is crucial since it determines the outcome of the trapping event for $BF_3 \cdot OEt_2$ and $TiCl_4$ initiated processes.

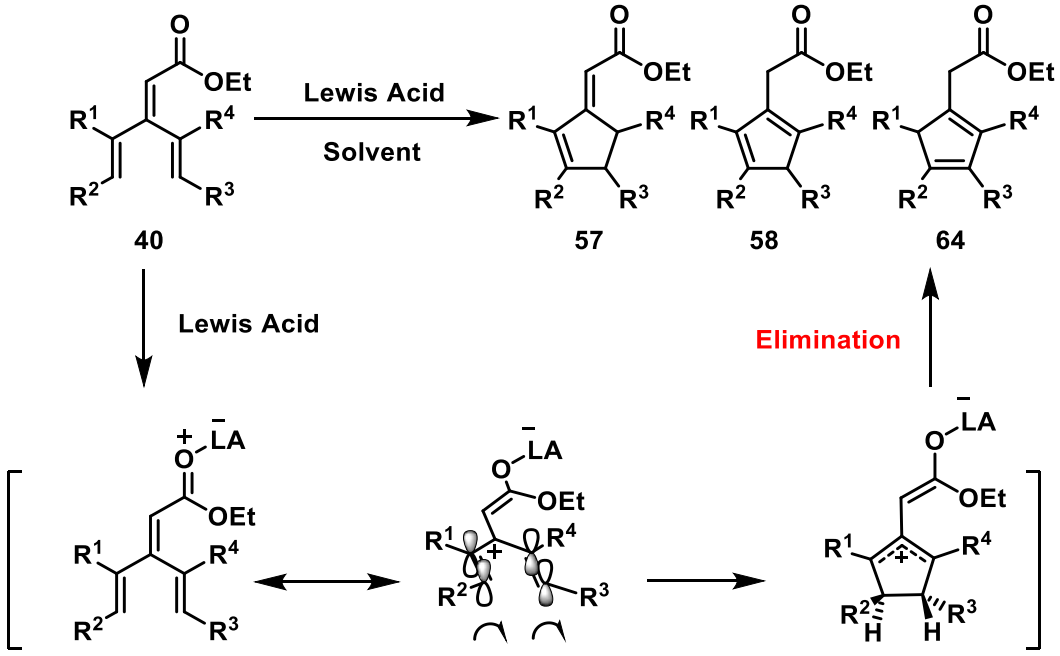

Scheme 3.38. The mechanism of the vinylogous Nazarov cyclization.

Based on the fact that in the presence of $TiCl_4$ the product of the reaction is trapped, it was assumed that titanium enolate is strong enough to perform intermolecular deprotonation furnishing two endocyclic double bonds while being regenerated afterward (Scheme 3.39). Subsequent protonation of the conjugated endocyclic double bond results

in the formation of the reported major isomer **57**. The ability of the catalytic amount of $TiCl_4$ (10 mol%) to involve 31% of the starting material in the desired process is indicative that the Lewis acid turns over and mediates another reaction.

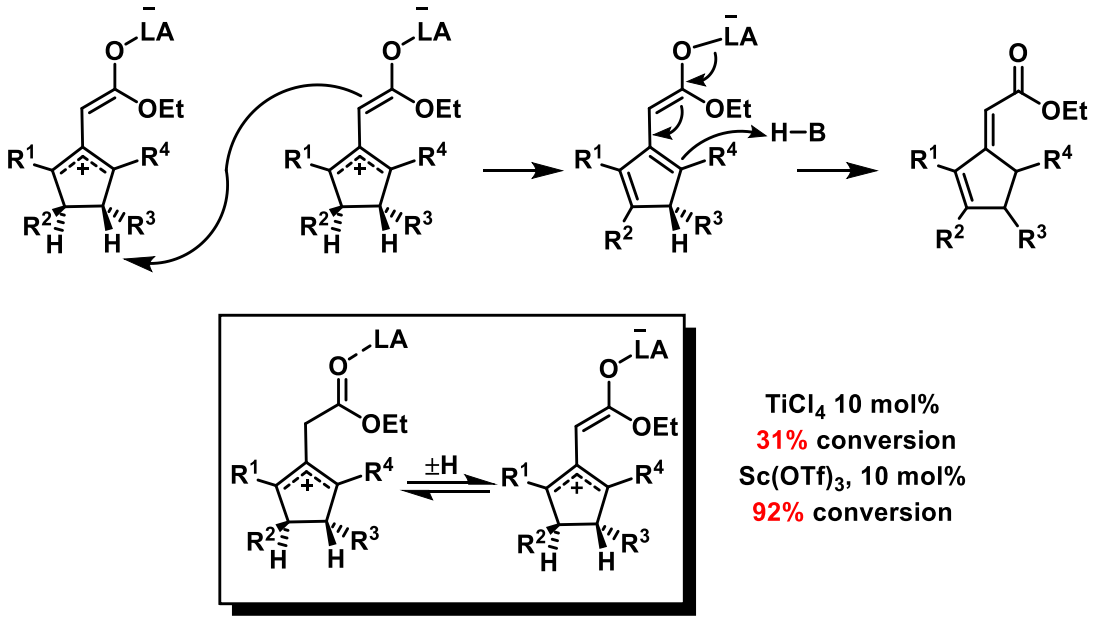

Scheme 3.39. Proposed proton elimination mechanism to obtain exocyclic alkene regioisomer.

The elimination step for titanium enolate must occur significantly faster compared to the other Lewis acids. Even if the reaction is carried out in a domino manner with three equivalents of the furan with $TiCl_4$, it still has preference for elimination of the zwitterion rather than nucleophilic trapping, followed by conjugate addition of furan into the resulting enoate (**81**:**78a** ratio is 5.2:1). The only example of intramolecular trapping for the vinylogous Nazarov cyclization initiated by $TiCl_4$ occurred in the case of a tethered *m*-methoxyphenyl group, where trapping possibly happened faster than elimination.

The same elimination pathway should occur for the other Lewis acids during the quenching step and should result in the formation of the mixture of regioisomers (both exocyclic and endocyclic). Higher selectivity for conventional trapping products shows that the elimination in the presence of $BF_3 \cdot OEt_2$ and $Sc(OTf)_3$ is slower if it happens at all. The formation of the two isomers **58** and **64** can be explained by simple [1,5] H-shift, which is known to happen rapidly in 5-methylcyclopentadiene already at room temperature (Scheme 3.40).[184] The temperatures to initiate the vinylogous Nazarov

cyclization in the presence of Lewis acids other than $TiCl_4$ are the same or higher than for the 5-methylcyclopentadiene rearrangement to occur.

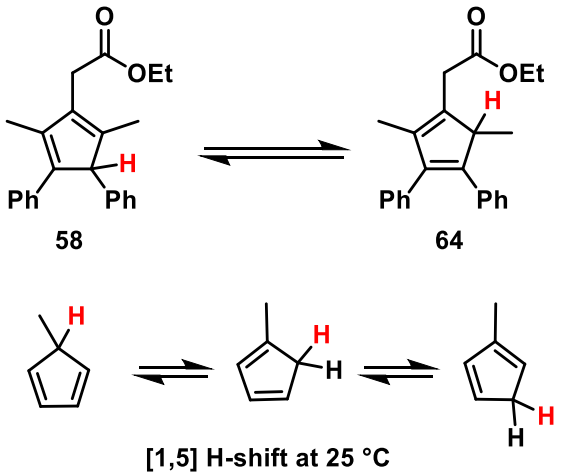

Scheme 3.40. Isomerization of the products **58** and **64**.

3.4 Conclusions

In summary, we have shown that it is possible to perform interrupted vinylogous Nazarov cyclization. To the best of our knowledge, this is the first report of the intra- and intermolecular interrupted cyclization of the [3]dendralenes. They were shown to form cyclized cationic intermediates, trapping of which is leading to highly substituted cyclopentene rings with three contiguous stereogenic centers. The trapping modality can be changed by application of different Lewis acids. Single example of stereoselective formation of the polycyclic system during intramolecular vinylogous Nazarov cyclization was reported.

3.5 Experimental

3.5.1 General Information

Reactions were carried out in flame-dried glassware under a positive argon atmosphere unless otherwise stated. Transfer of anhydrous solvents and reagents was accomplished with oven-dried syringes or cannulae. The 4 Å molecular sieves were stored in an oven and flame-dried before use. THF and DCM solvents were purified using the LC Technology Solutions Inc. solvent purification system. Anhydrous MeCN was distilled over calcium hydride under a nitrogen atmosphere before use. All other solvents were purchased as ACS reagents and used without further purification. Thin-layer chromatography was performed on glass plates precoated with 0.25 mm Kieselgel 60 F254 (Merck). Flash chromatography columns were packed with 230–400 mesh silica gel (Silicycle). ^{1}H NMR and ^{13}C spectra were recorded at 400/500/700 and 100/125/175 MHz, respectively, and coupling constants (*J*) are reported in Hertz (Hz). NMR chemical shifts are reported relative to the residual $CHCl_3$ in $CDCl_3$ (7.26 ppm) internal standard. Standard notation is used to describe the multiplicity of signals observed in ^{1}H NMR spectra: broad (br), apparent (app), multiplet (m), singlet (s), doublet (d), triplet (t), etc. Infrared (IR) spectra were measured with a Mattson Galaxy Series FT-IR 3000 spectrophotometer. High-resolution mass spectrometry (HRMS) data (APPI/ESI technique) were recorded using an Agilent Technologies 6220 oaTOF instrument. HRMS data (EI technique) were recorded using a Kratos MS50 instrument.

[3]Dendralenes and **dienones** can be prepared using the method listed below or via literature procedures: **38**,[130–134] **40**,[168] **86**,[51] **91.**[52]

3.5.2 General Procedures

3.5.2.1 General Procedure A for the Preparation of Functionalized [3]Dendralenes

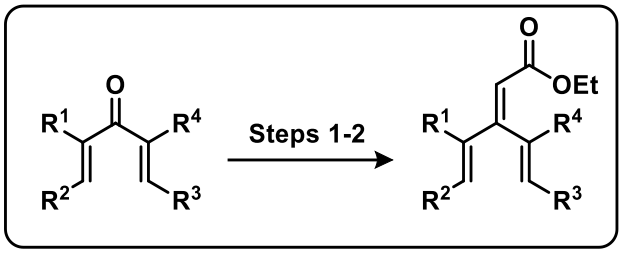

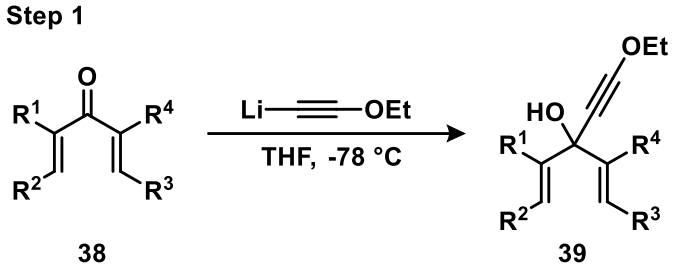

Step 1: Into a 250 mL flame dried round-bottom flask with a magnetic stir bar charged with argon was added dry THF (10 mL), ethoxyacetylene (0.6 mL, 50% wt. solution, 3 equiv), and 1.0 g of crushed 4Å molecular sieves. The solution was cooled down to -78 °C and stirred for 10 min. Subsequently, *n*BuLi (3.0 mL, 1.0 M in THF, 3 mmol, 3 equiv) in hexanes was added. After 1 h, the reaction vessel was warmed up to 0 °C and stirred at this temperature for 3 h (the mixture turned into a brown solution at this point). After cooling it down back to -78 °C, the required pentadienone **38** (1.0 mmol, 1 equiv) was added as a solution in THF (1–2 M) by transfer with cannula. After 2 h, the reaction was warmed up to 0 °C and quenched by water (10 mL). The mixture was transferred into separatory funnel and the layers were separated. Extraction of the aqueous layer was performed with Et_2O (3 x 50 mL). The combined organic layers were washed with water (2 x 50 mL) and brine (50 mL), dried over $MgSO_4$, and concentrated under vacuum. The crude mixture was purified by flash column chromatography (EtOAc/hexanes 1:4) to obtain **39** (70–86%)

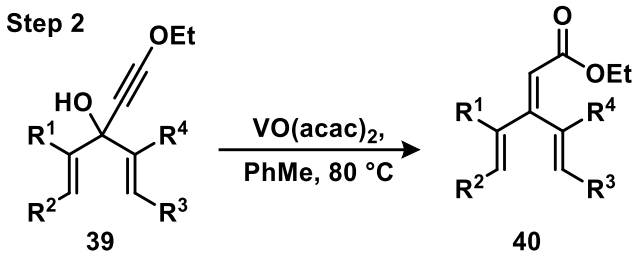

39 40

Step 2: A catalytic amount of vanadium oxyacetylacetonate (10 mol%) was added to a solution of propargylic alcohol **39** (1 mmol) in dry toluene (10 mL) under an argon atmosphere. The reaction was heated up to 80 °C and stirred at this temperature for 2 h, then was cooled to rt and filtered through a silica plug with Et_2O. The solution was concentrated under reduced pressure and purified using flash column chromatography. The desired compound **40** was obtained in 47–70% yield.

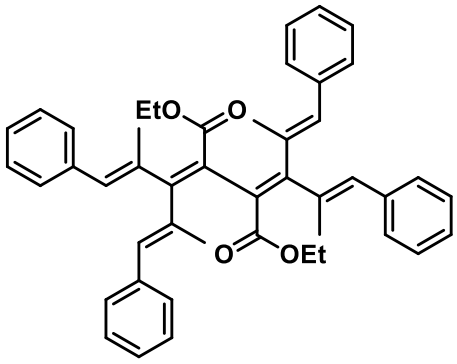

61

The product **61** was obtained following the general procedure **A**. Column chromatography (EtOAc/hexanes 1:9) gave **61** (10–20%) as a yellow liquid.

Diethyl 2,3-bis((1*E*,4*E*)-2,4-dimethyl-1,5-diphenylpenta-1,4-dien-3-ylidene)succinate (61): R_f 0.19 (EtOAc/hexanes 1:9); IR (cast film) ν_{max} 3083, 3055, 3024, 2979, 2960, 2921, 1743, 1711 cm^{-1}; ^1H NMR (400 MHz, $CDCl_3$) δ 7.40–7.31 (m, 8H), 7.36–7.28 (m, 4H), 7.26–7.19 (m, 8H), 6.88 (s, 2H), 6.46 (s, 2H), 3.93 (q, J = 7.1 Hz, 4H), 2.03 (s, 6H), 1.98 (s, 6H), 1.00 (t, J = 7.1 Hz, 6H); ^{13}C NMR (100 MHz, $CDCl_3$) δ 169.7, 158.5, 139.2, 137.6, 137.3, 135.9, 133.8, 129.6, 129.3, 129.0, 128.32, 128.26, 128.2, 127.1, 126.7, 60.7, 29.8, 17.7, 17.1; HRMS (ESI) *m/z* calcd for $C_{46}H_{47}O_4$ ($[M+H]^+$) 663.3469, found 663.3461.

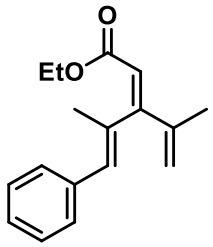

(*Z*)-40b

The product **(*Z*)-40b** was obtained following the general procedure **A**. Column chromatography (EtOAc/hexanes 1:9) gave **(*Z*)-40b** (107 mg, 42%) as a colorless liquid. *Previously reported as an inseparable mixture of E and Z isomers.*[170]

(2*Z*,4*E*)-Ethyl 4-methyl-5-phenyl-3-(prop-1-en-2-yl)penta-2,4-dienoate ((*Z*)-40b): colorless liquid; R_f 0.56 (EtOAc/hexanes 1:9); IR (cast film) ν_{max} 3059, 3025, 2981, 1720, 1598, 1493 cm^{-1}; ^1H NMR (400 MHz, $CDCl_3$) δ 7.39–7.34 (m, 4H), 7.30–7.22 (m, 1H), 6.20 (s, 1H), 5.88 (s, 1H), 5.46 (s, 1H), 5.37 (s, 1H), 4.18 (q, *J* = 7.1 Hz, 2H), 2.08 (s, 3H), 2.01 (s, 3H), 1.27 (t, *J* = 7.1 Hz, 3H); ^{13}C NMR (100 MHz, $CDCl_3$) δ 166.6, 159.8, 141.6, 137.7, 136.1, 128.9, 128.2, 127.6, 126.5, 121.7, 115.6, 60.1, 20.4, 18.9, 14.3; HRMS (EI) *m/z* calcd for $C_{17}H_{20}O_2$ (M+) 256.1468, found 256.1463.

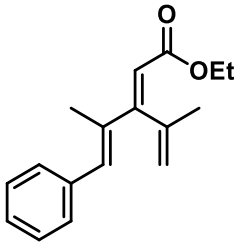

(*E*)-40b

The product **(*E*)-40b** was obtained following the general procedure **A**. Column chromatography (EtOAc/hexanes 1:9) gave **(*E*)-40b** (90 mg, 35%) as a colorless liquid. *Previously reported as an inseparable mixture of E and Z isomers.*[170]

(2*E*,4*E*)-Ethyl 4-methyl-5-phenyl-3-(prop-1-en-2-yl)penta-2,4-dienoate ((*E*)-40b): white solid; mp = 26–27 °C; R_f 0.48 (EtOAc/hexanes 1:9); IR (cast film) ν_{max} 3081, 2957, 2928, 1722, 1591, 1446 cm^{-1}; ^1H NMR (400 MHz, $CDCl_3$) δ 7.43–7.24 (m, 5H), 7.00 (s, 1H), 5.91 (s, 1H), 5.21 (dq, *J* = 1.5, 0.9 Hz, 1H), 4.80 (dq, *J* = 0.9, 0.9 Hz, 1H), 4.18 (q, *J* = 7.2 Hz, 2H), 2.05 (s, 3H), 2.03 (dd, *J* = 1.5, 0.9 Hz, 3H), 1.30 (t, *J* = 7.2 Hz,

3H); ^{13}C NMR (126 MHz, $CDCl_3$) δ 166.6, 160.7, 143.1, 137.6, 135.0, 134.9, 129.4, 128.2, 127.3, 115.0, 114.7, 60.0, 23.6, 15.3, 14.2; HRMS (EI) *m/z* calcd for $C_{17}H_{20}O_2$ (M+) 256.1463, found 256.1467.

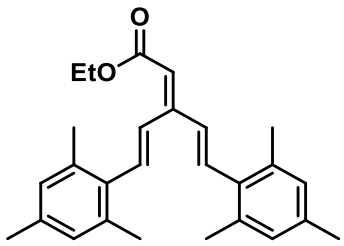

40c

The product **40c** was obtained following the step 1 of the general procedure **A**. After step 1 the obtained propargylic alcohol underwent Meyer–Schuster rearrangement on silica gel. Column chromatography (EtOAc/hexanes 1:9) gave **40c** (198 mg, 51%) as a yellow solid.

(*E*)-Ethyl 5-mesityl-3-((*E*)-2,4,6-trimethylstyryl)penta-2,4-dienoate (40c): yellow solid; mp = 60–62 °C; R_f 0.36 (EtOAc/hexanes 1:9); IR (cast film) ν_{max} 2974, 2950, 2916, 1705, 1610, 1579 cm^{-1}; ^{1}H NMR (400 MHz, $CDCl_3$) δ 7.72 (d, *J* = 16.8 Hz, 1H); 7.09 (d, *J* = 16.3 Hz, 1H), 7.08 (d, *J* = 16.8 Hz, 1H), 6.92 (s, 2H), 6.90 (s, 2H), 6.58 (d, *J* = 16.3 Hz, 1H), 6.01 (s, 1H), 4.22 (q, *J* = 7.1 Hz, 2H), 2.38 (s, 6H), 2.36 (s, 6H), 2.30 (s, 3H), 2.29 (s, 3H), 1.32 (t, *J* = 7.1 Hz, 3H); ^{13}C NMR (100 MHz, $CDCl_3$) δ 166.5 151.8, 137.0, 137.0, 136.4, 136.1, 134.9, 133.5, 133.4, 133.2, 132.6, 130.0, 129.0, 128.8, 115.0, 60.0, 21.3, 21.1, 21.0, 21.0, 14.4; HRMS (EI) *m/z* calcd for $C_{27}H_{32}O_2$ (M+) 388.2402, found 388.2405.

3.5.2.2 Procedure B for for the Preparation of Methyl Ether [3]Dendralene 67

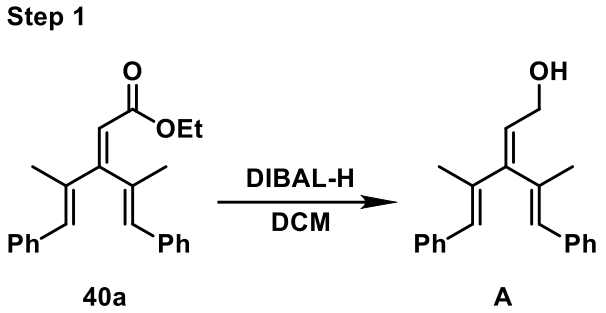

Into a 250 mL flame dried round-bottom flask with a magnetic stir bar under an argon atmosphere was added dry DCM (20 mL) and starting material **40a** (1.0 mmol, 1 equiv). The solution was cooled down to -78 °C and stirred for 10 min. Subsequently, DIBAL-H (2.0 mL, 1.0 M in THF, 2 equiv) was added. After 1 h, the reaction vessel was warmed up to rt and stirred at this temperature for 1 h. After 2 h, the reaction was quenched by sodium-potassium tartrate at 0 °C and stirred for 3–4 h. The layers were separated, and extraction of the aqueous layer was performed with DCM (3 x 50 mL). The combined organic layers were washed with brine, dried over $MgSO_4$, and concentrated under vacuum. The crude mixture was purified by flash column chromatography (EtOAc/hexanes 1:4) to obtain **A** (270 mg, 93%).

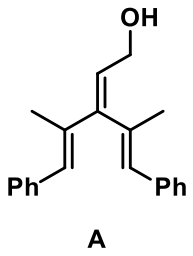

The product **A** was obtained following the procedure **B**. Column chromatography (EtOAc/hexanes 1:4) gave **A** (270 mg, 93%) as a colorless liquid. Analogous compound was previously reported.[170]

(*E*)-4-Methyl-5-phenyl-3-((*E*)-1-phenylprop-1-en-2-yl)penta-2,4-dien-1-ol: colorless liquid; R_f 0.22 (EtOAc/hexanes 1:4); IR (cast film) ν_{max} 3413 (br), 3084, 3059, 2958, 2926, 1702, 1665, 1599, 1451 cm^{-1}; ^1H NMR (400 MHz, $CDCl_3$) δ 7.39–7.30 (m,

5H), 7.28–7.21 (m, 5H), 6.64 (br s, 1H), 6.33 (q, J = 1.6 Hz, 1H), 5.85 (t, J = 6.7 Hz, 1H), 4.36 (d, J = 6.7 Hz, 2H), 3.80–3.71 (m, 1H), 2.06 (d, J = 1.3 Hz, 3H), 2.03 (d, J = 1.6 Hz, 3H); ^{13}C NMR (176 MHz, $CDCl_3$) δ 150.4, 138.2, 137.4, 135.7, 135.6, 130.2, 129.9, 129.2, 128.9, 128.2, 128.0, 126.7, 126.5, 124.9, 61.0, 19.2, 15.6; HRMS (EI) *m/z* calcd for $C_{21}H_{22}O_2$ (M+) 290,1671, found 290,1671.

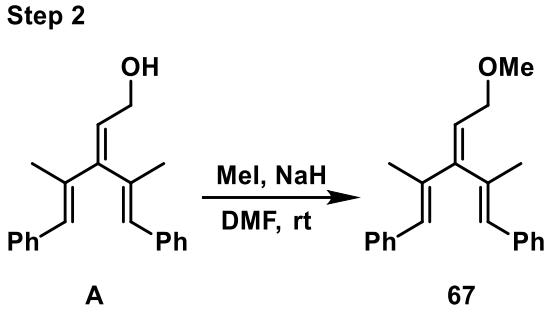

A **67**

Into a 250 mL flame dried round-bottom flask with a magnetic stir bar under an argon atmosphere was added DMF (20.0 mL) and starting material **A** (493 mg, 1.70 mmol, 1 equiv). The solution was cooled down to 0 °C and stirred for 10 min. Subsequently, NaH as 60% dispersion in mineral oil (170 mg, 4.25 mmol, 2.50 equiv) was added. After 10 min, methyl iodide (0.20 mL, 2.89 mmol, 1.50 equiv) was added into the reaction vessel, the reaction mixture was warmed up to rt and stirred at this temperature for 1 h. After 2 h, the reaction was quenched with water (10.0 mL) at 0 °C and stirred for 30 min. The layers were separated, and extraction of the aqueous layer was performed with Et_2O (3 x 50 mL). The combined organic layers were washed with water (50 mL) and brine, dried over $MgSO_4$, filtered and concentrated under vacuum. The crude mixture was purified by flash column chromatography (EtOAc/hexanes 1:9) to obtain **67** (253 mg, 49%).

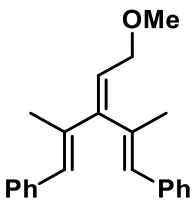

67

The product **67** was obtained following the procedure **C**. Column chromatography (EtOAc/hexanes 1:9) gave **67** (253 mg, 49%) as a colorless liquid.

((1*E*,4*E*)-3-(2-methoxyethylidene)-2,4-dimethylpenta-1,4-diene-1,5-diyl) dibenzene (67): colorless liquid; R_f 0.46 (EtOAc/hexanes 1:9); IR (cast film) ν_{max} 3062, 3029, 2979, 2928, 1723, 1494, 1451 cm^{-1}; ^1H NMR (400 MHz, $CDCl_3$) δ 7.43–7.33 (m, 6H), 7.32–7.22 (m, 4H), 6.67 (s, 1H), 6.36 (q, *J* = 1.5 Hz, 1H), 5.84 (t, *J* = 6.4 Hz, 1H), 4.17 (d, *J* = 6.4 Hz, 2H), 3.40 (s, 3H), 2.09 (d, *J* = 1.3 Hz, 3H), 2.07 (d, *J* = 1.5 Hz, 3H); ^{13}C NMR (126 MHz, $CDCl_3$) δ 150.8, 138.3, 137.6, 135.8, 135.7, 130.3, 129.7, 129.3, 128.9, 128.3, 128.1, 126.7, 126.5, 123.0, 70.7, 58.2, 19.0, 15.6; HRMS (EI) *m/z* calcd for $C_{22}H_{24}O_2$ (M+) 304.1827, found 304.1826.

3.5.2.3 Representative Procedure C for Vinylogous Nazarov Cyclization of Functionalized [3]Dendralenes Initiated by $TiCl_4$

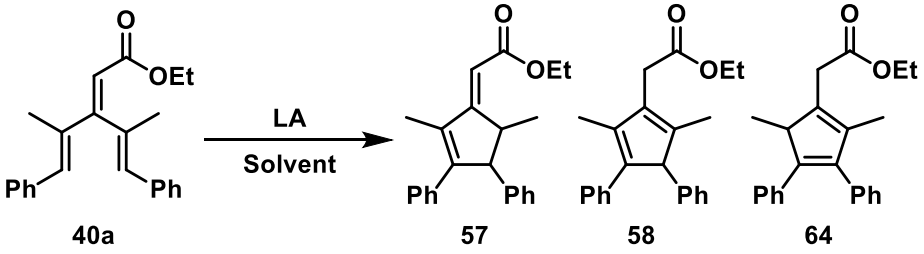

Into a 25 mL flame dried round-bottom flask with a magnetic stir bar under an argon atmosphere was added dry DCM (3 mL) and starting material **40a** (50 mg, 0.15 mmol, 1 equiv). The solution was cooled down to -78 °C and stirred for 10 min. Subsequently, $TiCl_4$ (0.18 mL, 1.0 M in DCM, 1.2 equiv) was added. After 1 h, the reaction vessel was warmed up to rt and stirred at this temperature for 1 h (4 h for intramolecular interrupted vinylogous Nazarov cyclization). After 2 hours the reaction was quenched with $NaHCO_3$ (3 mL, 1.0 M). The layers were separated, and extraction of the aqueous layer was performed with DCM (3 x 5 mL). The combined organic layers were washed with brine, dried over $MgSO_4$, filtered and concentrated under vacuum. The crude mixture was purified by flash column chromatography (EtOAc/hexanes 1:9) to obtain compounds **57**, **58,** and **64** in 68%, 13% and 8% respectively.

3.5.2.4 Representative Procedure D for Vinylogous Nazarov Cyclizaion of Functionalized [3]Dendralenes Initiated by $BF_3 \cdot OEt_2$

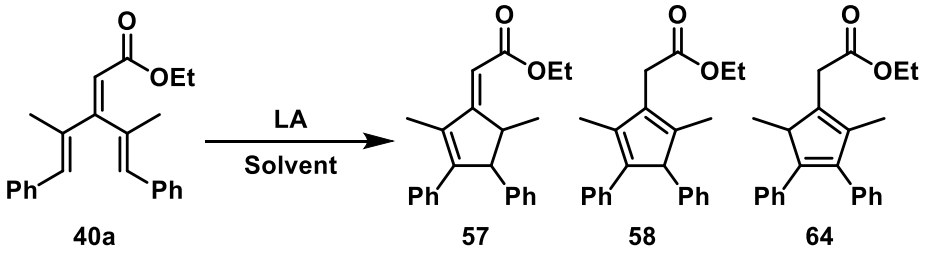

Into a 25 mL flame dried round-bottom flask with a magnetic stir bar under argon atmosphere was added dry DCM (3 mL), starting material **40a** (50 mg, 0.15 mmol, 1 equiv). The solution was cooled down to -78 °C and stirred for 10 min. Subsequently, $BF_3 \cdot OEt_2$ (0.06 mL, 1.2 equiv) was added. After 10 min, the reaction vessel was warmed up to rt and stirred at this temperature for 3 h. After 3 hours the reaction was quenched with $NaHCO_3$ (3 mL, 1.0 M). The layers were separated, and extraction of the aqueous layer was performed with DCM (3 x 5 mL). The combined organic layers were washed with brine, dried over $MgSO_4$, filtered and concentrated under vacuum. The crude mixture was purified by flash column chromatography (EtOAc/hexanes 1:9) to obtain obtain compounds **57**, **58,** and **64** in 24%, 41% and 13% respectively.

3.5.2.5 Representative Procedure E for Vinylogous Nazarov Cyclizaion of Functionalized [3]Dendralenes Initiated by $Sc(OTf)_3$

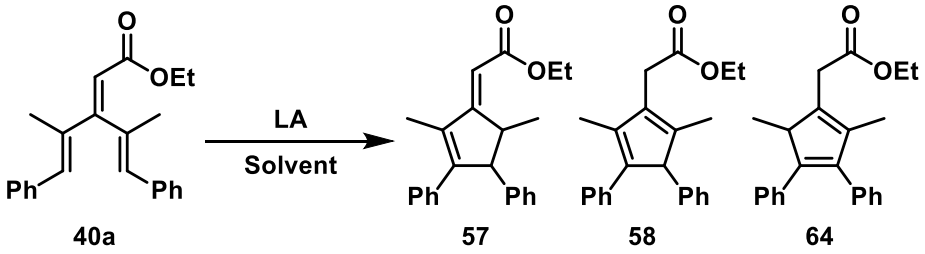

Into a 25 mL flame dried round-bottom flask equipped with condenser and a magnetic stir bar under argon atmosphere was added $Sc(OTf)_3$ (8.2 mg, 10 mol%). Starting material **40a** (50 mg, 0.15 mmol, 1 equiv) was dissolved in DCE predried by

molecular sieves. Then, the solution with starting material **40a** was transferred with cannula into the flask with $Sc(OTf)_3$. The reaction vessel was heated up to 55 °C and stirred at this temperature for 24 h. After cooling down the reaction mixture, the solution was filtered through a silica plug and flushed with DCM. The crude mixture was purified by flash column chromatography (EtOAc/hexane 1:9) to obtain obtain compounds **57**, **58,** and **64** in 29%, 42% and 21% respectively.

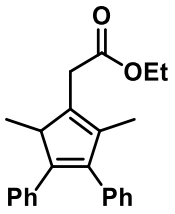

64

The product **64** was obtained following the representative procedure **E**. Column chromatography (EtOAc/hexanes 1:9) gave **64** as a colorless liquid. Compounds **57** and **58** were previously reported and obtained data were in agreement.

Ethyl 2-(2,5-dimethyl-3,4-diphenylcyclopenta-1,3-dien-1-yl)acetate (64): colorless liquid; R_f 0.36 (EtOAc/hexanes 1:9); IR (cast film) ν_{max} 3061, 3030, 2980, 2926, 1731, 1447 cm^{-1}; ^1H NMR (400 MHz, $CDCl_3$) δ 7.39–6.90 (m, 10H), 4.20 (q, *J* = 7.2 Hz, 2H), 3.67 (q, *J* = 7.7 Hz, 1H), 3.53 (d, *J* = 15.5 Hz, 1H), 3.36 (d, *J* = 15.6 Hz, 1H), 1.82 (s, 3H), 1.31 (t, *J* = 7.2 Hz, 3H), 1.09 (d, *J* = 7.7 Hz, 3H); ^{13}C NMR (175 MHz, $CDCl_3$) δ 171.6, 146.2, 142.2, 138.2, 137.2, 137.1, 135.7, 129.6, 128.7, 128.2, 127.9, 126.7, 125.9, 60.7, 49.0, 32.8, 14.9, 14.3, 12.2; HRMS (EI) *m/z* calcd for $C_{23}H_{24}O_2$ (M+) 332.1776, found 332.1776.

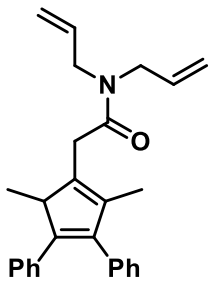

110

The reaction was performed by the representative procedure **C** with compound **108**. Column chromatography (EtOAc/hexanes 1:3), gave **110** (27 mg, 47%) as a colorless oil.

N,N-Diallyl-2-(2,5-dimethyl-3,4-diphenylcyclopenta-1,3-dien-1-yl)acetamide (110): colorless oil; R_f 0.58 (EtOAc/hexanes 1:3); IR (cast film) ν_{max} 3081, 3057, 3025, 2976, 2929, 1640, 1492, 1443 cm^{-1}; ^1H NMR (700 MHz, $CDCl_3$) δ 7.33–6.96 (m, 10H), 5.84–5.73 (m, 2H), 5. 25–5.11 (m, 4H), 4.09–3.87 (m, 4H), 3.68 (q, J = 7.6 Hz, 1H), 3.63 (d, J = 15.5 Hz, 1H), 3.34 (d, J = 15.5 Hz, 1H), 1.74 (s, 3H), 1.09 (d, J = 7.6 Hz, 3H); ^{13}C NMR (176 MHz, $CDCl_3$) δ 171.1, 146.4, 142.0, 138.6, 137.3, 136.9, 135.7, 133.3, 132.9, 129.6, 128.7, 128.2, 127.8, 126.7, 125.8, 117.4, 116.6, 49.2, 48.9, 48.2, 32.4, 15.5, 12.2; HRMS (EI) *m/z* calcd for $C_{27}H_{29}O_3N$ (M+) 383.2249, found 383.2251.

3.5.3 Intermolecular Interrupted Vinylogous Nazarov Cyclization Combined Data

3.5.3.1 General Procedure F to Perform Cascade Intermolecular Interrupted Vinylogous Nazarov Cyclization

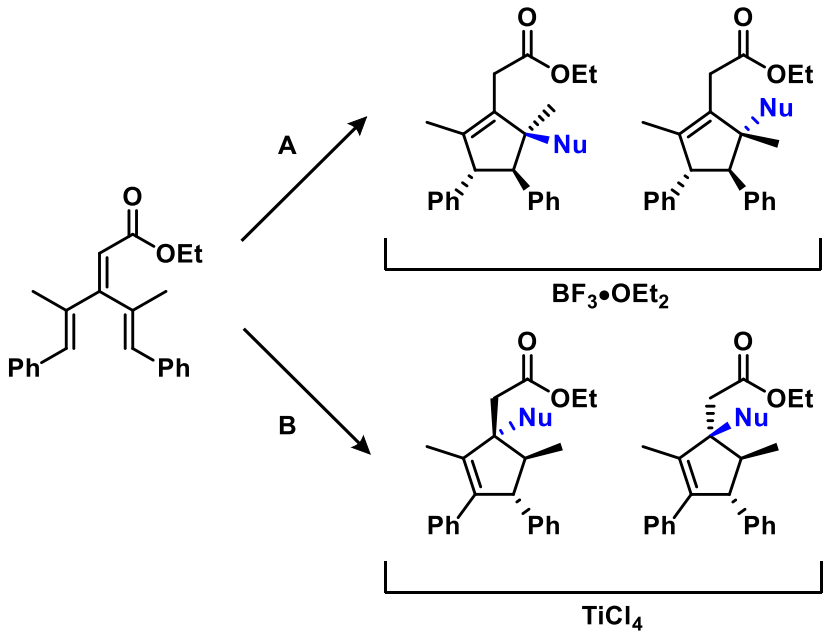

Method A: Into a 25 mL flame dried round-bottom flask with a magnetic stir bar under argon atmosphere was added dry DCM (3 mL), starting material **40** (0.15 mmol, 1 equiv),

and trapping agent (3 equiv). The solution was cooled down to -78 °C and stirred for 10 min. Subsequently, $BF_3 \cdot OEt_2$ (0.06 mL, 1.2 equiv) was added. After 10 min, the reaction vessel was warmed up to rt and stirred at this temperature for 24 h. After 24 hours the reaction was quenched by water (5 mL). The layers were separated, and extraction of the aqueous layer was performed with DCM (3 x 5 mL). The combined organic layers were washed with brine (15 mL), dried over $MgSO_4$, and concentrated under vacuum. The crude mixture was purified by flash column chromatography (EtOAc/hexanes 1:9) to obtain **77–80**.

Method B: Into a 25 mL flame dried round-bottom flask with a magnetic stir bar under argon atmosphere was added dry DCM (3 mL), starting material **40** (0.15 mmol, 1 equiv), and trapping agent (3 equiv). The solution was cooled down to -78 °C and stirred for 10 min. Subsequently, $TiCl_4$ (0.18 mL, 1.0 M in DCM, 1.2 equiv) was added. After 1 h, the reaction vessel was warmed up to rt and stirred at this temperature for 2 h. After 2 hours the reaction was quenched by water. The layers were separated and extraction of the aqueous layer was performed with DCM (3 x 5 mL). The combined organic layers were washed with brine (15 mL), dried over $MgSO_4$, and concentrated under vacuum. The crude mixture was purified by flash column chromatography (EtOAc/hexanes 1:9) to obtain **81–83**.

3.5.3.2 Procedure G to Perform Organoaluminum Initiated Interrupted Vinylogous Nazarov Cyclization

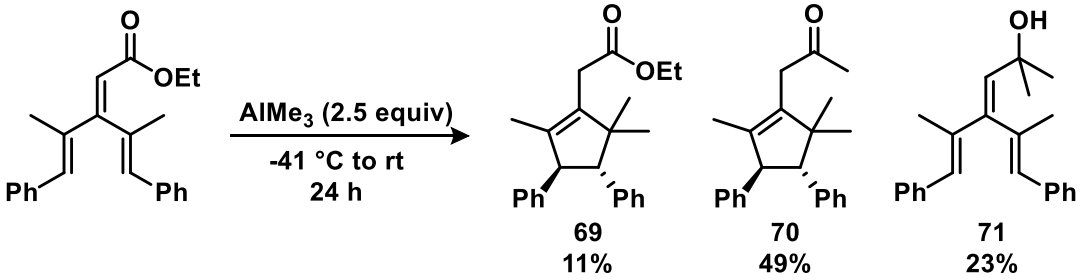

Into a 25 mL flame dried round-bottom flask with a magnetic stir bar under argon atmosphere was added dry DCM (3 mL), starting material **40a** (50 mg, 0.15 mmol, 1

equiv). The solution was cooled down to -41 °C and stirred for 10 min. Subsequently, $AlMe_3$ (0.38 mL, 1.0 M in toluene, 2.5 equiv) was added. After 10 min, the reaction vessel was warmed up to room temperature, and stirred at this temperature for 24 h, after which, the reaction was quenched by water. The layers were separated and extraction of the aqueous layer was performed with DCM (3 x 5 mL). The combined organic layers were washed with brine (15 mL), dried over $MgSO_4$, and concentrated under vacuum. The crude mixture was purified by flash column chromatography (EtOAc/hexanes 1:9) to obtain **69** (6 mg, 11% of product as an inseparable mixture with 12% of the starting material **40a**), **70** (24 mg, 49%) and **71** (11 mg, 23%) in 83% overall yield.

3.5.3.3 Spectral Data for Compounds 69–71, 77–82

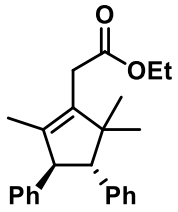

69

The product **69** was obtained following the procedure **G**. To determine the structures and assign resonances ^1H NMR was used. The NMR data for the mixture was taken and starting material **40a** peaks were subtracted to identify the resonances belonging to **69**.

Ethyl 2-((3*S,4*S**)-2,5,5-trimethyl-3,4-diphenylcyclopent-1-en-1-yl)acetate (69) (partial data):** colorless oil; R_f 0.55 (EtOAc/hexanes 1:9); IR (cast film) ν_{max} 3082, 3060, 3027, 2957, 2924, 1733, 1462, 1451 cm^{-1}; ^1H NMR (600 MHz, $CDCl_3$) δ 7.26–7.09 (m, 10H), 4.19 (q, *J* = 7.1 Hz, 2H), 4.11 (d, *J* = 10.0 Hz, 1H), 3.19 (d, *J* = 15.5 Hz, 1H), 3.08 (d, *J* = 15.5 Hz, 1H), 3.04 (d, *J* = 10.0 Hz, 1H), 1.53 (s, 3H), 1.31 (t, *J* = 7.1 Hz, 3H), 1.13 (s, 3H), 0.65 (s, 3H); ^{13}C NMR (126 MHz, $CDCl_3$) δ 172.0, 137.0, 136.3, 129.4, 128.4, 128.2, 127.8, 126.3, 126.1, 66.4, 60.6, 57.8, 31.8, 29.7, 26.4, 22.8, 14.3, 13.3; HRMS (EI) *m/z* calcd for $C_{24}H_{28}O_2$ (M+) 348.2089, found 348.2094.

Not all sp^2 carbon resonances could be detected due to overlap with the starting material.

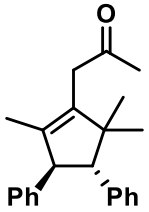

70

The product **70** was obtained following the procedure **G** with compound **40a**.

1-((3*S,4*S**)-2,5,5-trimethyl-3,4-diphenylcyclopent-1-en-1-yl)propan-2-one (70):** colorless oil; R_f 0.34 (EtOAc/hexanes 1:9); IR (cast film) ν_{max} 3084, 3060, 3026, 2958, 1710, 1494, 1451 cm^{-1}; ^1H NMR (500 MHz, $CDCl_3$) δ 7.29–7.11 (m, 10H), 4.14 (d, *J* = 10.1 Hz, 1H), 3.27 (d, *J* = 15.9 Hz, 1H), 3.17 (d, *J* = 15.9 Hz, 1H), 3.07 (d, *J* = 10.2 Hz, 1H), 2.25 (s, 3H), 1.52 (s, 3H), 1.09 (s, 3H), 0.63 (s, 3H); ^{13}C NMR (126 MHz, $CDCl_3$) δ 207.0, 143.3, 139.3, 137.7, 136.2, 129.3, 128.4, 128.3, 127.8, 126.4, 126.2, 66.4, 57.7, 49.5, 41.9, 29.2, 26.4, 22.8, 13.6; HRMS (EI) *m/z* calcd for $C_{23}H_{26}O$ (M+) 318.1984, found 318.1982.

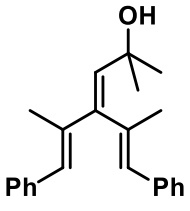

71

The product **71** was obtained following the procedure **G** with compound **40a**.

(*E*)-2,5-dimethyl-6-phenyl-4-((*E*)-1-phenylprop-1-en-2-yl)hexa-3,5-dien-2-ol (71): colorless oil; R_f 0.24 (EtOAc/hexanes 1:9); IR (cast film) ν_{max} 3433, 3061, 3028, 2976, 2931, 1718, 1601, 1494, 1451, 1378 cm^{-1}; ^1H NMR (500 MHz, $CDCl_3$) δ 7.19–7.42 (m, 10H), 6.63 (s, 1H), 6.48 (s, 1H), 5.77 (s, 1H), 2.75 (s, 1H), 2.13 (s, 3H), 2.04 (s, 3H), 1.46 (s, 6H); ^{13}C NMR (126 MHz, $CDCl_3$) δ 145.1, 138.5, 138.5, 137.0, 136.5, 133.8, 129.9, 129.3, 128.8, 128.7, 128.4, 128.1, 126.9, 126.4, 72.2, 31.6, 20.1, 16.0; HRMS (EI) *m/z* calcd for $C_{23}H_{26}O$ (M+) 318.1983, found 318.1987.

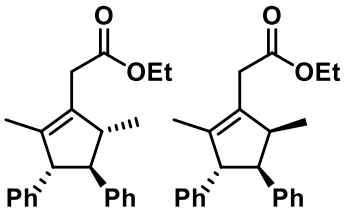

77a **77b**

2.4:1

The product **77**, an inseparable mixture of **77a** and **77b**, was obtained following the general procedure **F**, method A. Column chromatography (EtOAc/hexanes 1:9) gave mixture of products **77a** and **77b** (42 mg, 84%, 2.4:1). To determine the structures and assign resonances ^{1}H NMR was used. The NMR data for the mixture was taken and major diastereomer **77a** peaks were subtracted to identify the resonances belonging to **77b**. To do a relative structure determination, we analyzed the anisotropic effect of the phenyl group on the neighboring methyl group.

Ethyl 2-((3*R,4*R**,5*R**)-2,5-dimethyl-3,4-diphenylcyclopent-1-en-1-yl)acetate (77a):** colorless oil; R_f 0.21 (EtOAc/hexanes 1:9); IR (cast film) ν_{max} 3083, 3060, 3026, 2959, 2922, 2869, 1734, 1600, 1492, 1452 cm^{-1}; ^{1}H NMR (700 MHz, $CDCl_3$) δ 7.25–7.21 (m, 3H), 7.19–7.14 (m, 3H), 7.13–7.11 (m, 2H), 7.03–7.01 (m, 2H), 4.17 (q, *J* = 7.0 Hz, 2H), 3.73 (d, *J* = 7.5 Hz, 1H), 3.25 (d, *J* = 15.7 Hz, 1H), 3.17 (d, *J* = 15.4 Hz, 1H), 2.92 (app p, *J* = 7.3 Hz, 1H), 2.66 (t, *J* = 7.5 Hz, 1H), 1.51 (s, 3H), 1.29 (t, *J* = 7.1 Hz, 3H), 1.09 (d, *J* = 7.3 Hz, 3H); ^{13}C NMR (176 MHz, $CDCl_3$) δ 171.4, 144.5, 136.2, 133.2, 128.6, 128.3, 128.1, 128.0, 127.7, 126.2, 126.1, 64.3, 63.1, 60.6, 49.8, 32.8, 18.6, 14.3, 13.0; HRMS (EI) *m/z* calcd for $C_{23}H_{26}O_2$ (M+) 334.1933, found 334.1928.

Ethyl 2-((3*R,4*R**,5*S**)-2,5-dimethyl-3,4-diphenylcyclopent-1-en-1-yl)acetate (77b) (partial data):** colorless oil; R_f 0.21 (EtOAc/hexanes 1:9); ^{1}H NMR (700 MHz, $CDCl_3$) δ 7.25–7.21 (m, 3H), 7.19–7.14 (m, 3H), 7.13–7.11 (m, 2H), 7.03–7.01 (m, 2H), 4.17 (q, *J* = 7.0 Hz, 2H), 4.17–4.11 (m, 1H) 4.00 (d, *J* = 7.0 Hz, 1H), 3.46 (app p, *J* = 7.1 Hz, 1H), 3.26 (d, *J* = 15.9 Hz, 1H), 3.08 (d, *J* = 15.4 Hz, 1H), 1.55 (s, 3H), 1.30 (t, *J* = 7.1 Hz, 3H), 0.63 (d, *J* = 7.2 Hz, 3H); ^{13}C NMR (176 MHz, $CDCl_3$) δ 171.6, 143.7, 142.1, 137.4, 133.9, 129.4, 128.9, 128.4, 127.9, 126.0, 60.6, 59.7, 57.3, 45.4, 33.1, 14.6, 14.3, 13.0.

Not all sp^2 carbon resonances could be detected due to overlap with the major diastereomer. Sp^3 carbons were distinguishable on this ration of isomers. Additionally 2D NMR was applied do support assignments.

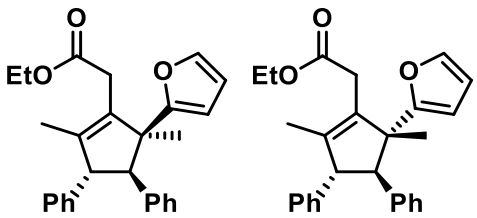

78a **78b**

3.1:1

The product **78**, an inseparable mixture of **78a** and **78b**, was obtained following the general procedure **F**, method A. Column chromatography (EtOAc/hexanes 1:9) gave mixture of products **78a** and **78b** (40 mg, 66%, 3.1:1). To determine the structures and assign resonances ^{1}H NMR was used. The NMR data for the mixture was taken and major diastereomer **78a** peaks were subtracted to identify the resonances belonging to **78b**. It was also possible to isolate compound **78a** as pure substrate. To do a relative structure determination, we analyzed the anisotropic effect of the phenyl group on the neighboring methyl group.

Ethyl 2-((3*R,4*R**,5*S**)-5-(furan-2-yl)-2,5-dimethyl-3,4-diphenylcyclopent-1-en-1-yl)acetate (78a):** colorless oil; R_f 0.41 (EtOAc/hexanes 1:9); IR (cast film) ν_{max} 3027, 2934, 2904, 1735, 1496, 1452, 1367 cm^{-1}; ^{1}H NMR (500 MHz, $CDCl_3$) δ 7.25–7.03 (m, 9H); 6.84– 6.79 (m, 2H), 6.17 (dd, *J* = 3.2, 1.8 Hz, 1H), 5.81 (d, *J* = 3.2 Hz, 1H), 4.25 (d, *J* = 10.1 Hz, 1H), 4.09 (app q, *J* = 7.1 Hz, 2H), 3.24 (d, *J* = 15.3 Hz, 1H), 3.19 (d, *J* = 10.1 Hz, 1H), 2.96 (d, *J* = 15.4 Hz, 1H), 1.69 (s, 3H), 1.53 (s, 3H), 1.26 (t, *J* = 7.1 Hz, 3H); ^{13}C NMR (126 MHz, $CDCl_3$) δ 171.5, 156.9, 143.1, 141.1, 140.3, 138.7, 133.0, 128.7, 128.4, 128.3, 127.5, 126.3, 126.3, 110.1, 107.0, 68.0, 60.6, 59.1, 55.7, 32.4, 22.4, 14.2, 13.6; HRMS (EI) *m/z* calcd for $C_{27}H_{28}O_3$ (M+) 400.2039, found 400.2038.

Ethyl 2-((3*R,4*R**,5*R**)-5-(furan-2-yl)-2,5-dimethyl-3,4-diphenylcyclopent-1-en-1-yl)acetate (78b) (partial data):** colorless oil; R_f 0.41 (EtOAc/hexanes 1:9); IR (cast film) ν_{max} 3084, 3027, 2977, 2933, 2907, 1735, 1494, 1451 cm^{-1}; ^{1}H NMR (500 MHz,

$CDCl_3$) δ 7.23–7.01 (m, 11H), 6.77–6.72 (m, 2H), 4.29–4.20 (m, 3H), 3.44 (d, *J* = 15.8 Hz, 1H), 3.13 (d, *J* = 10.2 Hz, 1H), 2.90 (d, *J* = 15.7 Hz, 1H), 1.75 (s, 3H), 1.38 (t, *J* = 7.1 Hz, 3H), 1.18 (s, 3H); ^{13}C NMR (126 MHz, $CDCl_3$) δ 171.7, 155.4, 143.1, 140.1, 138.5, 133.9, 128.7, 128.4, 128.3, 127.5, 126.3, 126.3, 107.5, 67.8, 60.8, 59.1, 55.7, 32.4, 21.2, 14.3, 13.9.

Not all sp^2 carbon resonances could be detected due to overlap with the major diastereomer.

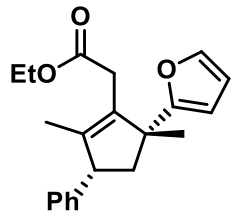

79

The product **79**, an inseparable mixture of **79** and **40b**, was obtained following the general procedure **F**, method A with compound **40b**. Column chromatography (EtOAc/hexanes 1:9), gave **79** (44 mg, 29% of **79** with 60% of **40b** ratio 1:2). To determine the structures and assign resonances ^{1}H NMR was used. The NMR data for the mixture was taken and major diastereomer **79** peaks were subtracted to identify the resonances belonging to **40b**.

Ethyl 2-((3*R,5*R**)-5-(furan-2-yl)-2,5-dimethyl-3-phenylcyclopent-1-en-1-yl)acetate (79):** colorless oil; R_f 0.48 (EtOAc/hexanes 1:9); IR (cast film) ν_{max} 2977, 2934, 1733, 1591, 1503 cm^{-1}; ^{1}H NMR (500 MHz, $CDCl_3$) δ 7.45–7.15 (m, 6H), 6.25 (dd, *J* = 3.2, 1.8 Hz, 1H), 6.00 (d, *J* = 3.2 Hz, 1H), 4.06 (q, *J* = 7.2 Hz, 2H), 3.93 (app t, *J* = 8.1 Hz, 1H), 3.10 (d, *J* = 15.7 Hz, 1H), 2.92 (d, *J* = 15.8 Hz, 1H), 2.75 (dd, *J* = 13.3, 8.4 Hz, 1H), 1.78 (dd, *J* = 13.3, 7.5 Hz, 1H), 1.53 (s, 3H), 1.46 (s, 3H), 1.23 (t, *J* = 7.1 Hz, 3H); ^{13}C NMR (176 MHz, $CDCl_3$) δ 171.6, 161.1, 160.7, 145.4, 141.2, 139.6, 134.5, 128.5, 110.3, 104.4, 60.9, 54.1, 49.1, 48.4, 32.2, 25.1, 14.3, 13.6. HRMS (EI) *m/z* calcd for $C_{21}H_{24}O_3$ (M+) 324.1726, found 324.1729.

Not all sp^2 carbon resonances could be detected due to overlap with the starting material.

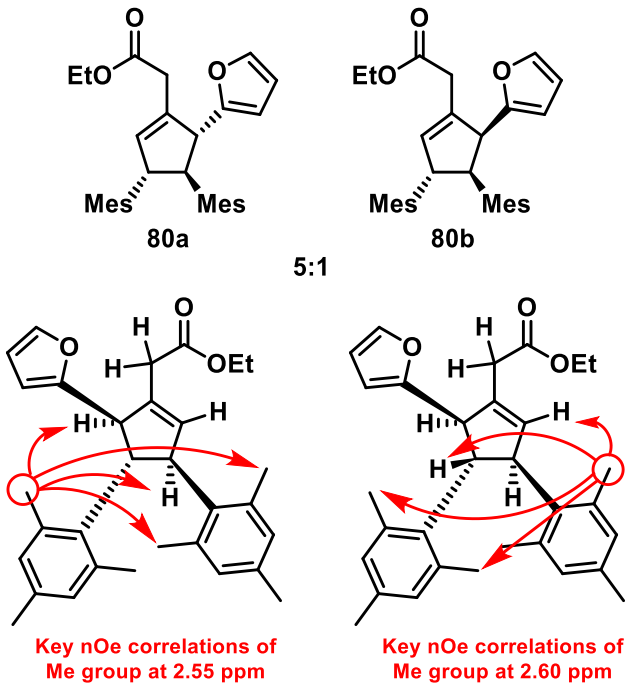

The product **80**, an inseparable mixture of **80a** and **80b**, was obtained following the general procedure **F**, method A with compound **40c**. Column chromatography (EtOAc/hexanes 1:9), gave **80** (26 mg, 38%, 5:1). To determine the structures and assign resonances ^{1}H NMR was used. The NMR data for the mixture was taken and major diastereomer **80a** peaks were subtracted to identify the resonances belonging to **80b**.

Ethyl 2-((3*R,4*S**,5*R**)-5-(furan-2-yl)-3,4-dimesitylcyclopent-1-en-1-yl)acetate (80a):** colorless oil; R_f 0.44 (EtOAc/hexanes 1:9); IR (cast film) ν_{max} 2961, 2918, 1735, 1480 cm^{-1}; ^{1}H NMR (500 MHz, $CDCl_3$) δ 7.36 (dd, *J* = 1.8, 0.8 Hz, 1H), 6.87 (s, 1H), 6.82 (s, 1H), 6.65 (s, 1H), 6.60 (s, 1H), 6.27 (dd, *J* = 3.2, 1.8 Hz, 1H), 6.04 (dd, *J* = 3.2, 0.9 Hz, 1H), 5.96 (br s, 1H), 4.79 (app d, *J* = 9.1 Hz, 1H), 4.51 (d, *J* = 9.1 Hz, 1H), 4.34 (t, *J* = 9.1 Hz, 1H), 4.18–4.11 (m, 2H), 3.22 (d, *J* = 16.1 Hz, 1H), 3.00 (d, *J* = 16.1 Hz, 1H), 2.62 (s, 3H), 2.55 (s, 3H), 2.22 (s, 6H), 1.75 (s, 3H), 1.59 (s, 3H), 1.29 (t, *J* = 7.1 Hz, 3H); ^{13}C NMR (126 MHz, $CDCl_3$) δ 171.1, 156.2, 141.6, 137.5, 137.4, 137.2, 136.3, 135.9, 135.8, 135.4, 135.2, 134.8, 134.5, 131.0, 130.7, 128.9, 128.6, 110.2, 106.9, 60.7, 52.8, 51.7, 51.2, 35.5, 21.5, 20.8, 20.8, 20.7, 20.6, 20.4, 14.3; HRMS (EI) *m/z* calcd for $C_{31}H_{36}O_3$ (M+) 456.2665, found 456.2672.

A strong nOe correlations were observed between *ortho*-methyl groups of mesityl ring, which is situated in the middle (between the other mesityl ring and furan ring), and

CHs next to the furan ring and the neighboring mesityl ring. Inequivalence of the methyl groups and aromatic protons on mesityl rings is probably due to slow rotation of the hindered mesityl groups.

Proton at 5.96 ppm appears as broad singlet and has COSY correlations with 2 cyclopentene protons at 4.51 and 4.79 ppm. I indicated that correlation in the structure under the data.

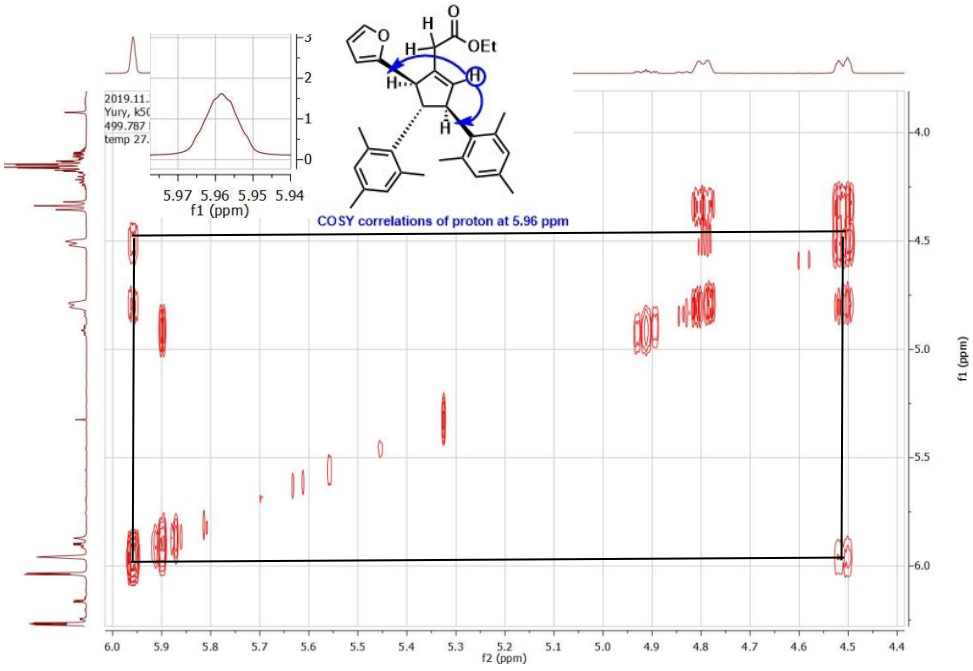

Ethyl 2-((3*R,4*S**,5*S**)-5-(furan-2-yl)-3,4-dimesitylcyclopent-1-en-1-yl)acetate (80b) (partial data)**: ^{1}H NMR (500 MHz, $CDCl_3$) δ 7.40 (dd, *J* = 1.9, 0.8 Hz, 1H), 6.99 (s, 1H), 6.77 (s, 1H), 6.74 (s, 1H), 6.32 (dd, *J* = 3.2, 1.9 Hz, 1H), 6.16 (dd, *J* = 3.2, 0.9 Hz, 1H), 5.90 (d, *J* = 2.8 Hz, 1H), 5.87 (s, 1H), 4.91 (dd, *J* = 7.5, 2.8 Hz 1H), 4.86–4.80 (m, 1H), 4.14–4.09 (m, 2H), 3.04 (d, *J* = 2.8 Hz, 2H), 2.74 (dd, 12.5, 7.5 Hz, 1H), 2.28 (s, 3H), 2.27 (s, 3H), 2.25 (s, 3H), 2.23 (s, 3H), 1.41 (s, 6H), 1.21 (t, *J* = 7.1 Hz, 3H); ^{13}C NMR (126 MHz, $CDCl_3$) δ 171.1, 169.9, 158.2, 150.1, 147.1, 145.5, 135.9, 134.3, 133.4, 130.6, 129.1, 128.9, 126.4, 110.0, 104.2, 60.4, 60.4, 50.2, 48.9, 43.9, 42.3, 34.3, 21.4, 20.9, 20.9, 20.8, 14.2.

Cyclopentene methine proton at 4.86–4.80 has partial overlap with major compound proton at 4.79 ppm. Methyl protons at 3.04 ppm neighboring C=O has allylic coupling with vinyl proton at 5.90 ppm.

Not all carbon sp^2 resonances could be detected due to overlap with the major diastereomer. The structure of minor compound **80b** was proposed in analogy to the major isomer and based on CH doublet of doublets at 4.91 ppm, and presence of two H shifts: methylene next to the C=O, and alkene CH.

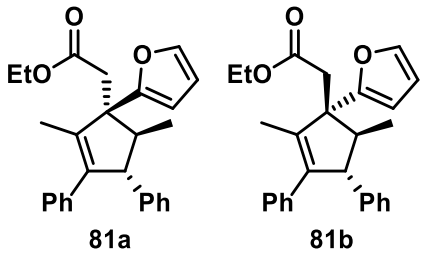

The product **81**, an inseparable mixture of **80a** and **80b**, was obtained following the general procedure **F**, method B with compound **40a**. Column chromatography (EtOAc/hexanes 1:9), gave mixture **81** (31 mg, 52%, 4.2:1). It was possible to isolate major isomer **81a** as pure substance. To determine the structures and assign resonances ^{1}H NMR was used. The NMR data for the mixture was taken and major diastereomer **81a** peaks were subtracted to identify the resonances belonging to **81b**.

Ethyl 2-((1*S,4*R**,5*S**)-1-(furan-2-yl)-2,5-dimethyl-3,4-diphenylcyclopent-2-en-1-yl)acetate (81a):** colorless oil; R_f 0.56 (EtOAc/hexanes 1:9); IR (cast film) ν_{max} 3059, 3025, 2961, 2928, 1732, 1601, 1492, 1453 cm^{-1}; ^{1}H NMR (500 MHz, $CDCl_3$) δ 7.41 (dd, *J* = 1.9, 0.8 Hz, 1H), 7.23–7.02 (m, 10H), 6.35 (dd, *J* = 3.2, 1.9 Hz, 1H), 6.06 (dd, *J* = 3.2, 0.8 Hz, 1H), 4.15 (app q, *J* = 7.1 Hz, 2H), 3.96 (dq, *J* = 9.3, 2.4 Hz, 1H), 3.09 (d, *J* = 14.6 Hz, 1H), 2.96 (d, *J* = 14.7 Hz, 1H), 2.43 (dq, *J* = 9.2, 6.8 Hz, 1H), 1.85 (d, *J* = 2.3 Hz, 3H), 1.33 (t, *J* = 7.1 Hz, 3H), 0.76 (d, *J* = 6.8 Hz, 3H); ^{13}C NMR (126 MHz, $CDCl_3$) δ 171.1, 156.4, 143.9, 141.8, 140.9, 138.8, 137.4, 128.6, 128.5, 128.0, 127.7, 126.1, 125.9, 110.0, 106.5, 60.4, 59.6, 57.6, 51.5, 38.2, 14.4, 13.2, 12.7; HRMS (EI) *m/z* calcd for $C_{27}H_{28}O_3$ (M+) 400.2039, found 400.2045.

Ethyl 2-((1*R,4*R**,5*S**)-1-(furan-2-yl)-2,5-dimethyl-3,4-diphenylcyclopent-2-en-1-yl)acetate (81b) (partial data):** ^{1}H NMR (500 MHz, $CDCl_3$) δ 7.39 (dd, *J* = 1.9, 0.8 Hz, 1H), 7.23–7.01 (m, 8H), 6.79–6.73 (m, 2H), 6.29 (dd, *J* = 3.2, 1.8 Hz, 1H), 6.01 (dd, *J* = 3.2, 0.9 Hz, 1H), 4.19–4.08 (m, 3H), 3.23 (dq, *J* = 9.1, 6.8 Hz, 1H), 2.43 (d, *J* = 6.5 Hz, 1H), 2.41 (d, *J* = 6.5 Hz, 1H), 1.47 (s, 3H), 1.27 (t, *J* = 7.1 Hz, 3H), 1.09 (d, *J* = 6.9 Hz, 3H); ^{13}C NMR (126 MHz, $CDCl_3$) δ 173.7, 157.9, 144.5, 142.9, 128.7, 128.4, 127.7, 127.5, 126.4, 126.4, 110.1, 107.2, 60.3, 55.1, 54.8, 47.7, 35.3, 23.6, 18.7, 14.2.

Not all sp^2 carbon resonances could be detected due to overlap with the major diastereomer.

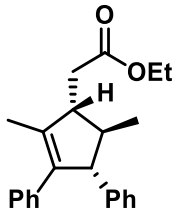

82

The product **82** was obtained following the general procedure **F**, method B with compound **40a**. Column chromatography (EtOAc/hexanes 1:9), gave compound **82** (44 mg, 87%).

Ethyl 2-((1*R,4*R**,5*R**)-2,5-dimethyl-3,4-diphenylcyclopent-2-en-1-yl)acetate (82):** colorless oil; R_f 0.41 (EtOAc/hexanes 1:9); IR (cast film) ν_{max} 3025, 2979, 2956, 2927, 1733, 1494, 1453 cm^{-1}; ^{1}H NMR (700 MHz, $CDCl_3$) δ 7.18–7.11 (m, 4H), 7.09–7.02 (m, 6H), 4.14 (app q, *J* = 7.2 Hz, 2H), 3.80 (d, *J* = 7.3 Hz, 1H), 2.76 (app q, *J* = 7.0 Hz, 1H), 2.67 (dd, *J* = 14.9, 5.8 Hz, 1H), 2.40 (dd, *J* = 14.9, 7.4 Hz, 1H), 1.85–1.81 (m, 4H), 1.26 (t, *J* = 7.2 Hz, 3H), 1.17 (d, *J* = 6.9 Hz, 3H); ^{13}C NMR (176 MHz, $CDCl_3$) δ 172.9, 144.8, 138.3, 138.1, 137.4, 128.4, 128.1, 128.1, 127.7, 126.0, 125.8, 62.1, 60.3, 53.7, 49.1, 38.7, 18.6, 14.2, 14.1; HRMS (EI) *m/z* calcd for $C_{23}H_{26}O_2$ (M+) 334.1933, found 334.1932.

3.5.4 Spectral Data for Compounds 92–100, 103

3.5.4.1 Propargylic Alcohols and Dendralenes with Intramolecular Trap

For the preparation of propargylic alcohols and dendralenes, general procedure A was used.

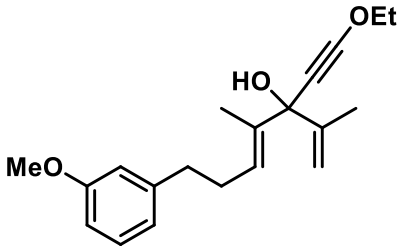

92

The product **92** was obtained following the general procedure **A**, Step 1. Column chromatography (EtOAc/hexanes 1:9), gave **92** (282 mg, 90%) as a yellow oil.

(*E*)-3-(Ethoxyethynyl)-7-(3-methoxyphenyl)-2,4-dimethylhepta-1,4-dien-3-ol (92): yellow oil; R_f 0.15 (EtOAc/hexanes 1:9); IR (cast film) ν_{max} 3484, 2982, 2941, 2922, 2262, 1601, 1584, 1488 cm^{-1}; ^1H NMR (500 MHz, $CDCl_3$) δ 7.20 (t, *J* = 7.8 Hz, 1H), 6.81 (d, *J* = 7.5 Hz, 1H), 6.78–6.71 (m, 2H), 5.97 (t, *J* = 7.2 Hz, 1H), 5.32 (s, 1H), 4.94 (s, 1H), 4.11 (q, *J* = 7.1 Hz, 2H), 3.81 (s, 3H), 2.70 (t, *J* = 7.3, 2H), 2.40 (q, *J* = 7.4 Hz, 2H), 1.95 (s, 1H), 1.65 (s, 3H), 1.55 (s, 3H), 1.38 (t, *J* = 7.1 Hz, 3H); ^{13}C NMR (126 MHz, $CDCl_3$) δ 159.6, 146.3, 143.8, 136.1, 129.2, 125.6, 120.9, 114.2, 111.5, 111.1, 95.3, 77.4 (by HMBC), 74.6, 55.1, 39.9, 35.7, 29.9, 18.3, 14.5, 11.9; HRMS (EI) *m/z* calcd for $C_{20}H_{26}O_3$ (M+) 314.1882, found 314.1886.

The peak at 77.4 ppm is overlapping with solvent peaks (although it is still visible on ^{13}C NMR) and can be additionally inferred from 2D correlations.

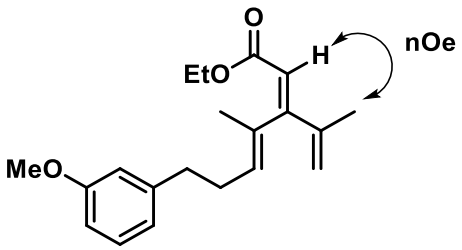

(*Z*)-93

The product **(*Z*)-93** was obtained following the general procedure **A**, Step 2. Column chromatography (EtOAc/hexanes 1:9), gave **(*Z*)-93** (25 mg, 9%) as an orange oil.

(2*Z*,4*E*)-Ethyl 7-(3-methoxyphenyl)-4-methyl-3-(prop-1-en-2-yl)hepta-2,4-dienoate ((*Z*)-93): orange oil; R_f 0.34 (EtOAc/hexanes 1:9); IR (cast film) ν_{max} 2976, 2925, 1721, 1599 cm^{-1}; ^1H NMR (500 MHz, $CDCl_3$) δ 7.20 (t, *J* = 7.8 Hz, 1H), 6.81 (d, *J* = 7.5 Hz, 1H), 6.79–6.71 (m, 2H), 5.76 (s, 1H), 5.23 (s, 1H), 5.21 (s, 1H), 5.15 (t, *J* = 6.2 Hz, 1H), 4.14 (q, *J* = 7.1 Hz, 2H), 3.81 (s, 3H), 2.70 (t, *J* = 7.8 Hz, 2H), 2.45 (q, *J* = 7.6 Hz, 2H), 1.91 (s, 3H), 1.80 (s, 3H), 1.27 (t, *J* = 7.1 Hz, 3H); ^{13}C NMR (126 MHz, $CDCl_3$) δ 166.7, 159.9, 159.6, 143.8, 141.8, 133.4, 129.2, 127.3, 121.3, 120.9, 115.1, 114.2, 111.2, 59.9, 55.1, 35.5, 29.8, 20.3, 17.1, 14.3; HRMS (EI) *m/z* calcd for $C_{20}H_{26}O_3$ (M+) 314.1882, found 314.1886.

The (*Z*) geometry of the ester-substituted alkene was confirmed by the observation of an nOe correlation between the alkenyl proton α to the ester group and the methyl group of the 1,1-disubstituted alkene. I would also indicate that correlation in the structure above the data.

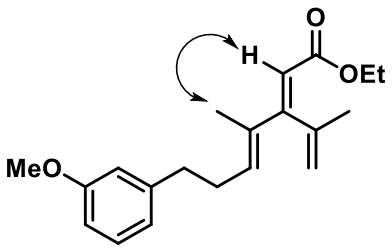

(*E*)-93

The product **(*E*)-93** was obtained following the general procedure **A**, Step 2. Column chromatography (EtOAc/hexanes 1:9), gave **(*E*)-93** (37 mg, 13%) as an orange oil.

(2*E*,4*E*)-Ethyl 7-(3-methoxyphenyl)-4-methyl-3-(prop-1-en-2-yl)hepta-2,4-dienoate ((*E*)-93): orange oil; R_f 0.27 (EtOAc/hexanes 1:9); IR (cast film) ν_{max} 2924, 1722, 1595 cm^{-1}; ^1H NMR (500 MHz, $CDCl_3$) δ 7.20 (t, *J* = 7.8 Hz, 1H), 6.80–6.71 (m, 3H), 6.03 (t, *J* = 7.1 Hz, 1H), 5.71 (s, 1H), 5.11 (s, 1H), 4.66 (s, 1H), 4.15 (q, *J* = 7.1 Hz,

2H), 3.80 (s, 3H), 2.70 (t, *J* = 7.7 Hz, 2H), 2.50 (q, *J* = 7.4 Hz, 2H), 1.91 (s, 3H), 1.76 (s, 3H), 1.28 (t, *J* = 6.8 Hz, 3H); ^{13}C NMR (126 MHz, $CDCl_3$) δ 166.6, 160.6, 159.7, 143.2, 143.2, 136.3, 133.6, 129.3, 120.9, 114.2, 114.0, 113.2, 111.3, 59.8, 55.2, 35.4, 31.0, 23.5, 14.2, 13.7; HRMS (EI) *m/z* calcd for $C_{20}H_{26}O_3$ (M+) 314.1882, found 314.1885.

The (*E*) geometry of the ester-substituted alkene was confirmed by the observation of an nOe correlation between the alkenyl proton α to the ester group and the methyl group of the alkene, which is bearing intramolecular trap.

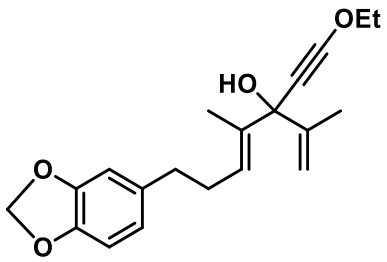

94

The product **94** was obtained following the general procedure **A**, Step 1. Column chromatography (EtOAc/hexanes 1:2), gave **94** (252 mg, 77%) as a colorless oil.

(*E*)-7-(Benzo[*d*][1,3]dioxol-5-yl)-3-(ethoxyethynyl)-2,4-dimethylhepta-1,4-dien-3-ol (94): colorless oil; R_f 0.48 (EtOAc/hexanes 1:2); IR (cast film) ν_{max} 3528, 2982, 2923, 2896, 2262, 1503, 1489, 1442 cm^{-1}; ^{1}H NMR (500 MHz, $CDCl_3$) δ 6.73 (d, *J* = 7.9 Hz, 1H), 6.70 (d, *J* = 1.7 Hz, 1H), 6.65 (dd, *J* = 7.9, 1.7 Hz, 1H), 5.94 (tq, *J* = 7.3, 1.5 Hz, 1H), 5.92 (s, 2H), 5.32 (s, 1H), 4.94 (s, 1H), 4.12 (q, *J* = 7.1 Hz, 2H), 2.64 (t, *J* = 7.7 Hz, 2H), 2.35 (q, *J* = 7.5 Hz, 2H), 1.95 (s, 1H), 1.65 (s, 3H), 1.54 (br s, 3H), 1.39 (t, *J* = 7.1 Hz, 3H); ^{13}C NMR (126 MHz, $CDCl_3$) δ 147.5, 146.3, 145.6, 136.1, 136.0, 125.5, 121.2, 111.5, 108.9, 108.1, 100.7, 95.3, 77.1 (by HMBC), 74.6, 39.9, 35.4, 30.3, 18.2, 14.5, 11.9; HRMS (EI) *m/z* calcd for $C_{20}H_{24}O_4$ (M+) 328.1675, found 328.1677.

The peak at 77.1 ppm is overlapping with solvent peaks (although it is still visible on ^{13}C NMR) and can be additionally inferred from 2D correlations.

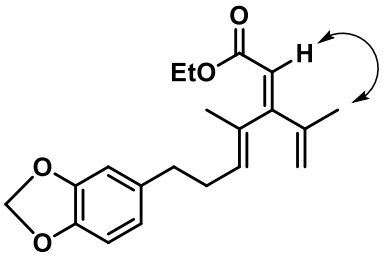

(*Z*)-95

The product **(*Z*)-95** was obtained following the general procedure **A**, Step 2. Column chromatography (EtOAc/hexanes 1:9), gave **(*Z*)-95** (13 mg, 5%) as a colorless oil.

(2*Z*,4*E*)-Ethyl 7-(benzo[*d*][1,3]dioxol-5-yl)-4-methyl-3-(prop-1-en-2-yl)hepta-2,4-dienoate ((*Z*)-95): colorless oil; R_f 0.63 (EtOAc/hexanes 1:9); ^{1}H NMR (500 MHz, $CDCl_3$) δ 6.75–6.69 (m, 2H), 6.65 (d, *J* = 7.9 Hz, 1H), 5.92 (s, 2H), 5.76 (s, 1H), 5.24 (s, 1H), 5.22 (s, 1H), 5.13 (t, *J* = 7.3 Hz, 1H), 4.14 (q, *J* = 7.1 Hz, 2H), 2.64 (t, *J* = 7.5 Hz Hz, 2H), 2.40 (q, *J* = 7.5 Hz, 2H), 1.91 (s, 3H), 1.79 (s, 3H), 1.27 (t, *J* = 7.1 Hz, 3H); ^{13}C NMR (126 MHz, $CDCl_3$) δ 166.7, 159.9, 147.5, 145.6, 141.9, 136.0, 133.4, 127.2, 121.3, 121.2, 115.1, 108.9, 108.1, 100.7, 59.9, 35.2, 30.1, 20.3, 17.1, 14.3; HRMS (EI) *m/z* calcd for $C_{20}H_{24}O_4$ (M+) 328.1675, found 328.1676.

The (*Z*) geometry of the ester-substituted alkene was confirmed by the observation of an nOe correlation between the alkenyl proton α to the ester group and the methyl group of the 1,1-disubstituted alkene. I would also indicate that correlation in the structure above the data.

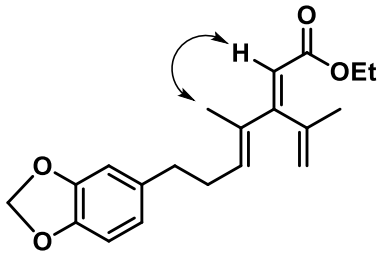

(*E*)-95

The product **(*E*)-95** was obtained following the general procedure **A**, Step 2. Column chromatography (EtOAc/hexanes 1:9), gave **(*E*)-95** (18 mg, 7%) as a colorless oil.

(2*E*,4*E*)-Ethyl 7-(benzo[*d*][1,3]dioxol-5-yl)-4-methyl-3-(prop-1-en-2-yl)hepta-2,4-dienoate ((*E*)-95): colorless oil; R_f 0.57 (EtOAc/hexanes 1:9); IR (cast film) ν_{max} 2979, 2920, 1720, 1597, 1503, 1489, 1442 cm^{-1}; ^1H NMR (500 MHz, $CDCl_3$) δ 6.72 (d, *J* = 7.9 Hz, 1H), 6.67 (d, *J* = 1.7 Hz, 1H), 6.61 (dd, *J* = 7.9, 1.7 Hz, 1H), 6.01 (t, *J* = 7.3 Hz, 1H), 5.92 (s, 2H), 5.71 (s, 1H), 5.11 (s, 1H), 4.65 (s, 1H), 4.15 (q, *J* = 7.1 Hz, 2H), 2.64 (t, *J* = 7.6 Hz, 2H), 2.46 (q, *J* = 7.5 Hz, 2H), 1.91 (s, 3H), 1.75 (s, 3H), 1.28 (t, *J* = 7.1 Hz, 3H); ^{13}C NMR (126 MHz, $CDCl_3$) δ166.7, 160.5, 147.6, 145.7, 143.2, 136.2, 135.4, 133.6, 121.2, 114.0, 113.2, 108.9, 108.1, 100.8, 59.8, 35.1, 31.3, 23.5, 14.2, 13.7; HRMS (EI) *m/z* calcd for $C_{20}H_{24}O_4$ (M+) 328.1675, found 328.1676.

The (*E*) geometry of the ester-substituted alkene was confirmed by the observation of an nOe correlation between the alkenyl proton α to the ester group and the methyl group of the alkene, which is bearing intramolecular trap. I would also indicate that correlation in the structure above the data.

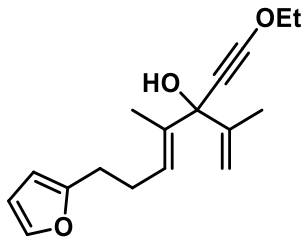

96

The product **96** was obtained following the general procedure **A**, Step 1. Column chromatography (EtOAc/hexanes 1:2), gave **96** (101 mg, 37%) as an orange oil.

(*E*)-3-(Ethoxyethynyl)-7-(furan-2-yl)-2,4-dimethylhepta-1,4-dien-3-ol (96): orange oil; R_f 0.44 (EtOAc/hexanes 1:2); IR (cast film) ν_{max} 3447, 2981, 2936 2247, 1720, 1583, 1446 cm^{-1}; ^1H NMR (700 MHz, $CDCl_3$) δ 7.28 (dd, *J* = 1.9, 0.8 Hz, 1H); 6.25 (dd, *J* = 3.1, 1.9 Hz, 1H), 5.97 (dd, *J* = 3.1, 1.0 Hz, 1H), 5.92 (t, *J* = 7.2 Hz, 1H), 5.31 (s, 1H), 4.92 (s, 1H), 4.10 (q, *J* = 7.1 Hz, 2H), 2.71 (t, *J* = 7.9 Hz, 2H), 2.40 (q, *J* = 7.5 Hz, 2H), 1.93 (s, 1H), 1.63 (s, 3H), 1.54 (s, 3H), 1.36 (t, *J* = 7.1 Hz, 3H); ^{13}C NMR (176 MHz, $CDCl_3$) δ 155.8, 146.2, 140.8, 136.4, 125.0, 111.5, 110.1, 104.9, 95.2, 76.8, 74.6, 39.8, 27.8, 26.6, 18.1, 14.4, 11.8; HRMS (EI) *m/z* calcd for $C_{17}H_{22}O_3$ (M+) 274.1569, found 274.1564.

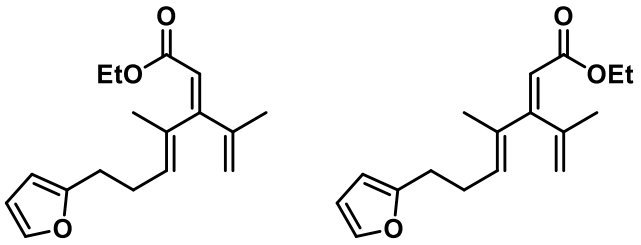

(*Z*)-97 **(*E*)-97**

1:1.4

The product **97**, an inseparable mixture of **(*Z*)-97** and **(*E*)-97**, was obtained following the general procedure **A**, Step 2. Column chromatography (EtOAc/hexanes 1:9), gave a mixture of **(*Z*)-97** (26 mg, 26% with *E*:*Z* 1.3:1) as an orange oil. To determine the structures and assign resonances ^{1}H NMR was used. To obtain ^{1}H NMR and ^{13}C NMR of the minor isomer **(*Z*)-97** the NMR data for the mixture was taken and major isomer **(*E*)-97** peaks were deducted from it.

(2*E*,4*E*)-Ethyl 7-(furan-2-yl)-4-methyl-3-(prop-1-en-2-yl)hepta-2,4-dienoate ((*E*)-97): orange oil; R_f 0.55 (EtOAc/hexanes 1:9); IR (cast film) ν_{max} 2959, 2929, 1725, 1632, 1447 cm^{-1}; ^{1}H NMR (700 MHz, $CDCl_3$) δ 7.28 (d, *J* = 1.8 Hz, 1H); 6.25 (dd, *J* = 4.8, 1.9 Hz, 1H), 5.97 (t, *J* = 7.2 Hz, 1H), 5.95 (d, *J* = 4.8 Hz, 1H), 5.70 (s, 1H), 5.09 (s, 1H), 4.63 (s, 1H), 4.13 (q, *J* = 7.1 Hz, 2H), 2.73 (t, *J* = 7.4 Hz, 2H), 2.51 (q, *J* = 7.4 Hz, 2H), 1.89 (s, 3H), 1.76 (s, 3H), 1.25 (t, *J* = 7.1 Hz, 3H); ^{13}C NMR (176 MHz, $CDCl_3$) δ 166.6, 155.2, 143.1, 141.0, 135.6, 121.3, 115.1, 114.0, 113.3, 110.1, 105.2, 59.8, 27.7, 27.5, 23.4, 14.2, 13.6; HRMS (EI) *m/z* calcd for $C_{17}H_{22}O_3$ (M+) 274.1569, found 274.1573.

(2*Z*,4*E*)-Ethyl 7-(furan-2-yl)-4-methyl-3-(prop-1-en-2-yl)hepta-2,4-dienoate ((*Z*)-97) (partial data): orange oil; ^{1}H NMR (700 MHz, $CDCl_3$) δ 7.28 (d, *J* = 1.8 Hz, 1H), 5.98 (d, *J* = 2.6 Hz, 1H), 5.95 (d, *J* = 3.1 Hz, 1H), 5.74 (s, 1H), 5.23 (s, 1H), 5.22 (s, 1H), 5.11 (t, *J* = 7.1 Hz, 1H), 4.12 (q, *J* = 7.1 Hz, 2H), 2.71 (t, *J* = 7.5 Hz, 2H), 2.45 (q, *J* = 7.4 Hz, 2H), 2.03 (s, 3H), 1.78 (s, 3H), 1.26 (t, *J* = 7.1 Hz, 3H); ^{13}C NMR (176 MHz, $CDCl_3$) δ 160.5, 155.8, 140.9, 140.8, 133.8, 126.8, 110.1, 104.9, 59.8, 27.6, 26.5, 23.4, 17.1, 14.0.

Not all sp^2 carbon resonances could be detected due to overlap with the major isomer.

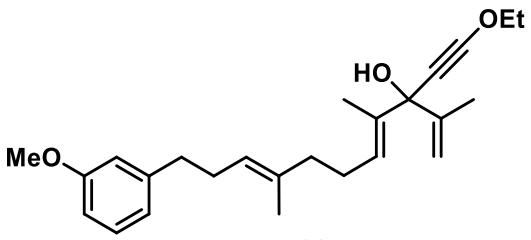

98

The product **98** was obtained following the general procedure **A**, Step 1. Column chromatography (EtOAc/hexanes 1:2), gave **98** (245 mg, 64%) as a colorless oil.

(4*E*,8*E*)-3-(Ethoxyethynyl)-10-(3-methoxyphenyl)-2,4,8-trimethyldeca-1,4,8-trien-3-ol (98): colorless oil; R_f 0.45 (EtOAc/hexanes 1:2); IR (cast film) ν_{max} 3435, 2938, 2868, 2263, 1720, 1601, 1584, 1488, 1454, 1438 cm^{-1}; ^1H NMR (700 MHz, $CDCl_3$) δ 7.18 (t, *J* = 7.8 Hz, 1H), 6.78 (d, *J* = 7.6 Hz, 1H), 6.75–6.70 (m, 2H), 5.87 (t, *J* = 7.0 Hz, 1H), 5.32 (s, 1H), 5.19 (t, *J* = 7.3 Hz, 1H), 4.93 (s, 1H), 4.10 (q, *J* = 7.1 Hz, 2H), 3.79 (s, 3H), 2.60 (t, *J* = 7.3 Hz, 2H), 2.28 (q, *J* = 7.5 Hz, 2H), 2.14 (q, *J* = 7.4 Hz, 2H), 2.05 (t, 7.1 Hz, 2H), 1.95 (s, 1H), 1.66 (s, 3H), 1.56 (s, 6H), 1.36 (t, *J* = 7.1 Hz, 3H); ^{13}C NMR (176 MHz, $CDCl_3$) 159.5, 146.3, 144.0, 135.5, 135.3, 129.1, 126.2, 123.8, 120.9, 114.3, 111.4, 110.9, 95.2, 77.1 (by HMBC), 74.5, 55.1, 40.0, 39.2, 36.1, 29.9, 26.7, 18.2, 15.9, 14.4, 11.8; HRMS (EI) *m/z* calcd for $C_{25}H_{34}O_3$ (M+) 382.2508, found 382.2506.

The peak at 77.1 ppm is overlapping with solvent peaks (although it is still visible on ^{13}C NMR) and can be additionally inferred from 2D correlations.

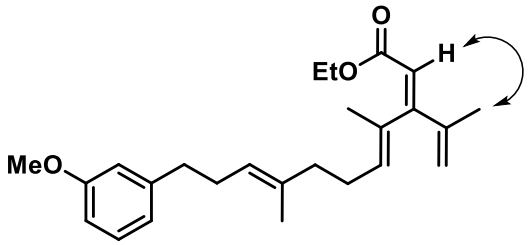

(*Z*)-99

The product **(*Z*)-99** was obtained following the general procedure **A**, Step 2. Column chromatography (EtOAc/hexanes 1:9), gave **(*Z*)-99** (20 mg, 8%) as a colorless oil.

(2*Z*,4*E*,8*E*)-Ethyl 10-(3-methoxyphenyl)-4,8-dimethyl-3-(prop-1-en-2-yl)deca-2,4,8-trienoate ((*Z*)-99): colorless oil; R_f 0.35 (EtOAc/hexanes 1:9); IR (cast film) ν_{max} 2977, 2936, 1721, 1601, 1585, 1488, 1453 cm^{-1}; ^1H NMR (700 MHz, $CDCl_3$) δ 7.18 (t, *J* = 7.8 Hz, 1H), 6.77 (d, *J* = 7.6 Hz, 1H), 6.75–6.70 (m, 2H), 5.74 (s, 1H), 5.32 (s, 1H), 5.24 (br s, 1H), 5.19 (t, *J* = 7.0 Hz, 1H), 5.06 (t, *J* = 7.1 Hz, 1H), 4.12 (q, *J* = 7.1 Hz, 2H), 3.79 (s, 3H), 2.59 (t, *J* = 7.3 Hz, 2H), 2.28 (q, *J* = 7.5 Hz, 2H), 2.20 (q, *J* = 7.4 Hz, 2H), 2.05 (t, *J* = 7.7 Hz, 2H), 1.90 (s, 3H), 1.78 (s, 3H), 1.57 (s, 3H), 1.25 (t, *J* = 7.1 Hz, 3H); ^{13}C NMR (176 MHz, $CDCl_3$) δ 166.7, 160.0, 159.5, 144.0, 142.0, 135.5, 132.6, 129.1, 128.0, 123.8, 121.1, 120.9, 115.1, 114.2, 110.9, 59.8, 55.1, 39.0, 36.1, 29.8, 26.6, 20.3, 17.1, 15.9, 14.2; HRMS (EI) *m/z* calcd for $C_{25}H_{34}O_3$ (M+) 382.2508, found 382.2506.

The (*Z*) geometry of the ester-substituted alkene was confirmed by the observation of an nOe correlation between the alkenyl proton α to the ester group and the methyl group of the 1,1-disubstituted alkene. I would also indicate that correlation in the structure above the data.

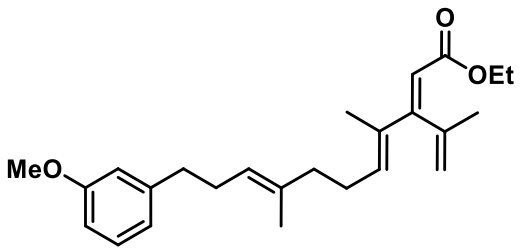

(*E*)-99

The product **(*E*)-99** was obtained following the general procedure **A**, Step 2. Column chromatography (EtOAc/hexanes 1:9), gave **(*E*)-99** (25 mg, 10%) as a colorless oil.

(2*E*,4*E*,8*E*)-Ethyl 10-(3-methoxyphenyl)-4,8-dimethyl-3-(prop-1-en-2-yl)deca-2,4,8-trienoate ((*E*)-99): colorless oil; R_f 0.30 (EtOAc/hexanes 1:9); IR (cast film) ν_{max} 2977, 2936, 1721, 1601, 1585, 1488, 1453 cm^{-1}; ^1H NMR (700 MHz, $CDCl_3$) δ 7.21–7.15 (m, 1H), 6.80–6.69 (m, 3H), 5.96 (t, *J* = 7.3 Hz, 1H), 5.70 (s, 1H), 5.18 (t, *J* = 6.9

Hz, 1H), 5.09 (s, 1H), 4.63 (s, 1H), 4.13 (q, J = 7.2 Hz, 2H), 3.79 (s, 3H), 2.59 (t, J = 7.6 Hz, 2H), 2.33–2.23 (m, 4H), 2.06 (t, J = 7.6 Hz, 2H), 1.90 (s, 3H), 1.78 (s, 3H), 1.56 (s, 3H), 1.26 (t, J = 7.2 Hz, 3H); ^{13}C NMR (176 MHz, $CDCl_3$) δ 166.7, 160.7, 159.6, 143.9, 143.3, 137.3, 134.9, 132.9, 129.2, 124.3, 120.8, 114.2, 113.8, 112.9, 110.9, 59.7, 55.1, 38.9, 36.1, 29.8, 27.7, 23.5, 15.9, 14.2, 13.7; HRMS (EI) *m/z* calcd for $C_{25}H_{34}O_3$ (M+) 382.2508, found 382.2506.

3.5.4.2 Intramolecular Interrupted Vinylogous Nazarov Cyclization Products

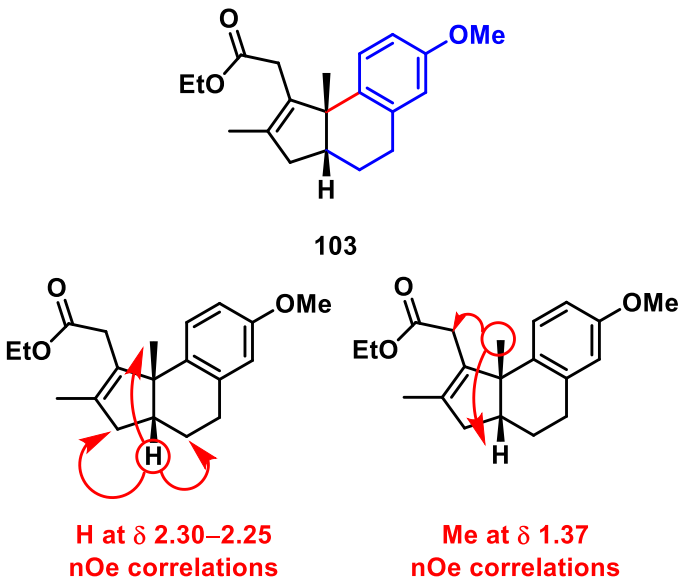

The product **103** was obtained from the substrate **93** and N,O-dimethylhydroxylamine hydrochloride following the general procedure **D** (40 mg, 80%).

Ethyl 2-((3a*R,9b*R**)-7-methoxy-2,9b-dimethyl-3a,4,5,9b-tetrahydro-3H-cyclopenta[*a*]naphthalen-1-yl)acetate (103):** colorless oil; R_f 0.30 (EtOAc/hexanes 1:9); IR (cast film) ν_{max} 2951, 2924, 2838, 1731, 1608, 1499, 1464 cm^{-1}; ^{1}H NMR (500 MHz, $CDCl_3$) δ 7.34 (d, J = 8.6 Hz, 1H), 6.75 (dd, J = 8.6, 2.9 Hz, 1H), 6.61 (d, J = 2.9 Hz, 1H), 3.93 (app q, J = 7.1 Hz, 2H), 3.78 (s, 3H), 2.98 (d, J = 15.9 Hz, 1H), 2.93 (d, J = 16.0 Hz, 1H), 2.77–2.66 (m, 2H), 2.58 (ddd, J = 15.5, 6.9, 4.3 Hz, 1H), 2.30–2.25 (m, 1H), 2.09 (dd, J = 16.1, 2.2 Hz, 1H), 1.68 (s, 3H), 1.77–1.63 (m, 2H), 1.37 (s, 3H), 1.15 (t, J = 7.1 Hz, 3H); ^{13}C NMR (126 MHz, $CDCl_3$) δ 171.8, 157.2, 140.3, 135.4, 133.9,

133.9, 128.0, 113.4, 111.3, 60.3, 55.1, 52.4, 44.0, 42.8, 31.7, 28.8, 28.3, 27.0, 14.8, 14.1; HRMS (EI) *m/z* calcd for $C_{20}H_{26}O_3$ (M+) 314.1882, found 314.1883.

A strong nOe correlation was observed between the methylene protons α to the ester carbonyl and the angular methyl group. This same angular methyl displayed an nOe correlation to the neighboring angular methine. I would also indicate that correlation in the structure above the data.

3.5.4.3 General Procedure H for preparation of Dendralenes 100, 108

Into a flame dried round bottom flask under argon atmosphere was added dry THF (10 mL), *i*-PrMgBr (1.0 M in THF, 2 equiv), and secondary amine (2 equiv).[185] The reaction vessel was cooled down to -5 °C and a solution of trienoate (1 equiv) in THF (1.0 M) was added into the flask dropwise. After 30 min the reaction was quenched by saturated aqueous solution of NH_4Cl (5 mL). The aqueous layer was extracted with Et_2O (3 x 50 mL). The combined organic layers were washed with brine (50 mL), dried over $MgSO_4$, filtered and concentrated under vacuum. The crude reaction mixture was purified using flash column chromatography.

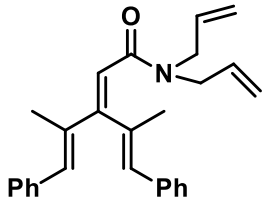

108

The reaction was performed by the general procedure **H** with compound **40a** (1 mmol) and diallylamine. Column chromatography (EtOAc/hexanes 1:4) gave **108** (326 mg, 85%) as a colorless oil.

(*E*)-N,N-Diallyl-4-methyl-5-phenyl-3-((*E*)-1-phenylprop-1-en-2-yl)penta-2,4-dienamide (108): colorless oil; R_f 0.24 (EtOAc/hexanes 1:4); IR (cast film) ν_{max} 3079, 3055, 3021, 2980, 2917, 1635, 1599, 1443, 1411 cm^{-1}; ^1H NMR (500 MHz, $CDCl_3$) δ 7.40–7.23 (m, 10H), 6.80 (s, 1H), 6.38 (s, 1H), 6.16 (s, 1H), 5.81 (ddt, *J* = 16.9, 10.3, 5.2 Hz, 1H), 5.67 (ddt, *J* = 17.2, 10.3, 5.8 Hz, 1H), 5.29–5.20 (m, 2H), 5.10 (d, *J* = 17.0, 1H),

5.03 (d, J = 10.1, 1H), 4.06–3.99 (m, 4H), 2.16 (s, 3H), 2.09 (s, 3H); ^{13}C NMR (126 MHz, $CDCl_3$) δ 168.7, 155.4, 137.7, 137.5, 136.8, 135.1, 133.2, 133.1, 133.0, 132.3, 129.3, 129.2, 129.1, 128.2, 128.1, 127.0, 126.6, 119.1, 117.2, 50.0, 46.8, 19.2, 15.7; HRMS (EI) *m/z* calcd for $C_{27}H_{29}ON$ (M+) 383.2249, found 383.2246.

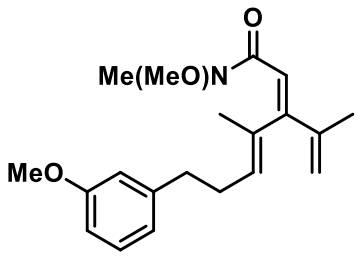

(*Z*)-100

The product **(*Z*)-100** was obtained following the general procedure **H** with N,N-dimethylhydroxyamine hydrochloride (ratio of *i*-PrMgBr loading was increased to 2.5:1) and compound **93** (0.17 mmol). Column chromatography (EtOAc/hexanes 1:9), gave **(*Z*)-100** (10 mg, 18%) as a colorless oil. *E* and *Z* assignment was based on analogy to the previously reported examples.

(2*Z*,4*E*)-N-Methoxy-7-(3-methoxyphenyl)-N,4-dimethyl-3-(prop-1-en-2-yl)hepta-2,4-dienamide ((*Z*)-100): colorless oil; R_f 0.46 (EtOAc/hexanes 1:9); IR (cast film) ν_{max} 2933, 1749, 1656, 1601, 1585, 1490, 1455 cm^{-1}; ^{1}H NMR (500 MHz, $CDCl_3$) δ 7.19 (t, J = 7.8 Hz, 1H), 6.80 (d, J = 7.7 Hz, 1H), 6.78–6.70 (m, 2H), 6.14 (br s, 1H), 5.19 (t, J = 7.4 Hz, 1H), 5.17 (s, 1H), 5.13 (s, 1H), 3.80 (s, 3H), 3.67 (s, 3H), 3.20 (s, 3H), 2.68 (t, J = 7,4 Hz, 2H), 2.44 (q, J = 7.5 Hz, 2H), 1.91 (s, 3H), 1.81 (s, 3H); ^{13}C NMR (126 MHz, $CDCl_3$) δ 168.1 (by HMBC), 159.6, 143.8, 142.1, 134.2, 129.6, 129.2, 127.5, 120.9, 119.6, 115.0, 114.2, 111.1, 61.5, 55.1, 35.5, 32.7 (by HSQC), 29.7, 20.5, 17.3; HRMS (EI) *m/z* calcd for $C_{20}H_{27}O_3N$ (M+) 329.1991, found 329.1992.

The peak at 32.7 ppm is inferred from 2D correlations (HSQC of CH_3 at 3.20). The peak at 168.1 ppm is inferred from 2D correlations (HMBC of CH_3 at 3.20). The absence in the ^{13}C NMR experiment can be a combination of lower sensitivity, slow relaxation or broadens of signals.

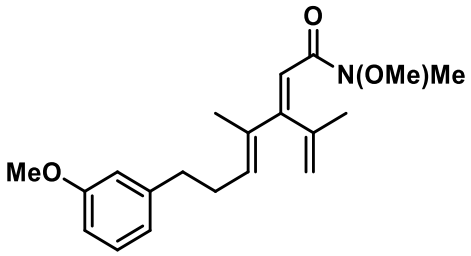

(*E*)-100

The product **(*E*)-100** was obtained following the general procedure **H** with N,N-dimethylhydroxyamine hydrochloride (ratio of *i*-PrMgBr loading was increased to 2.5:1) and compound **93** (0.17 mmol). Column chromatography (EtOAc/hexanes 1:9), gave **(*E*)-100** (16 mg, 28%) as a colorless oil. *E* and *Z* assignment was based on analogy to the previously reported examples.

(2*E*,4*E*)-N-Methoxy-7-(3-methoxyphenyl)-N,4-dimethyl-3-(prop-1-en-2-yl)hepta-2,4-dienamide ((*E*)-100): colorless oil; R_f 0.25 (EtOAc/hexanes 1:9); ^{1}H NMR (500 MHz, $CDCl_3$) δ 7.20 (dt, *J* = 5.2, 1.3 Hz, 1H), 6.79 (d, *J* = 7.3 Hz, 1H), 6.76–6.73 (m, 2H), 6.13 (br s, 1H), 5.94 (t, *J* = 7.2 Hz, 1H), 5.07 (s, 1H), 4.68 (s, 1H), 3.80 (s, 3H), 3.70 (s, 3H), 3.21 (s, 3H), 2.71 (t, *J* = 7.7 Hz, 2H), 2.50 (q, *J* = 7.5 Hz, 2H), 1.93 (s, 3H), 1.77 (s, 3H); ^{13}C NMR (126 MHz, $CDCl_3$) δ 168.1, 159.6, 144.1, 143.3, 134.4, 133.8, 129.3, 120.9, 114.3, 113.9, 113.1, 113.0, 111.2, 61.5, 55.1, 35.5, 32.5, 30.9, 23.6, 13.9; HRMS (EI) *m/z* calcd for $C_{20}H_{27}O_3N$ (M+) 329.1991, found 329.1992.

Chapter 4

Synthesis of Butenolides from Dendralenes

4.1 Butenolides

Butenolides are known class of organic compounds represented as five-membered unsaturated ring systems **1** and **2** (Figure 4.1).[186] Butenolide structural motif can be found frequently as a core structure of a bioactive compounds like **3**, **4** and **5** (Figure 4.2).[187,188,189] Search for fast and convenient methods of preparation of these structures became an impetus towards field development.[190,191]

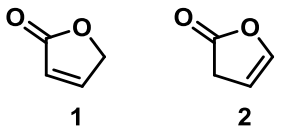

Figure 4.1. Butenolides.

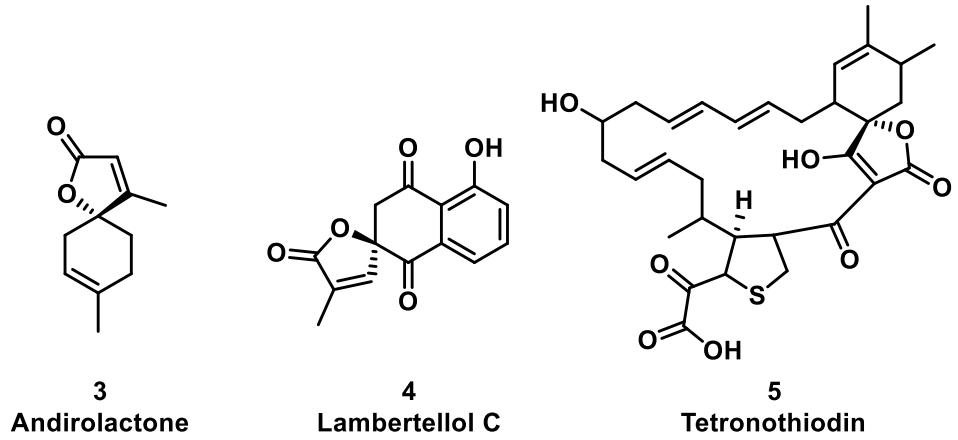

Figure 4.2. Butenolide containing natural products with biological activity.

There are three general methods developed towards formation of butenolides (Scheme 4.1). The first route (a) involves ring-closing metathesis, whereby the ring is generated from dialkenes **6** in the presence of a ruthenium catalyst.[192] The second one (b) utilizes allenic esters and acids **7** and is catalized by either copper or palladium.[193] The

last pathway (c) requires cyclization of hydroxyalkynes **8** in the presence of different metal catalyst to form the desired scaffolds.[194,]

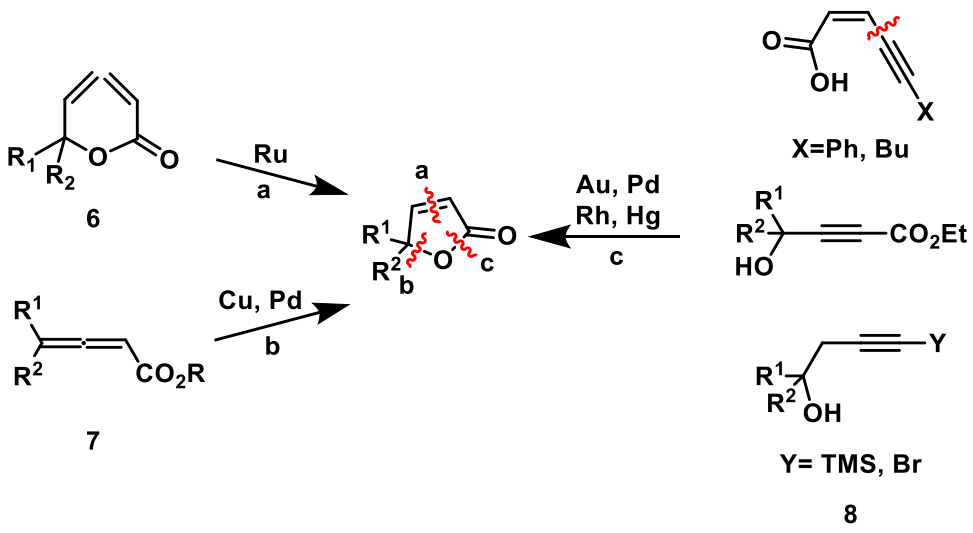

Scheme 4.1. Synthetic routes towards formation of butenolides.

The Langer group reported the preparation of butenolides by application of ring-closing metathesis (Scheme 4.2).[195] In order to prepare the starting material, they treated ketones **9** with vinylmagnesium bromide. Followed by acylation of the intermediate alcohol **10** with acryloyl chloride to obtain the desired product **11** in a high yield. Finally, the formation of butenolides **12** was achieved via ring closing methathesis, using Grubbs' 1st generation catalyst in the presence of a catalytic amount of titanium isopropoxide. Even though the protocol was limited to unsubstituted spirocycles, the reaction was shown to have high diastereoselectivity (98:2) allowing formation of the desired product in moderate to high yields (57–80%). Steric effects imposed by substituents result in drastic reductions in yield, and in some cases, no reaction at all.

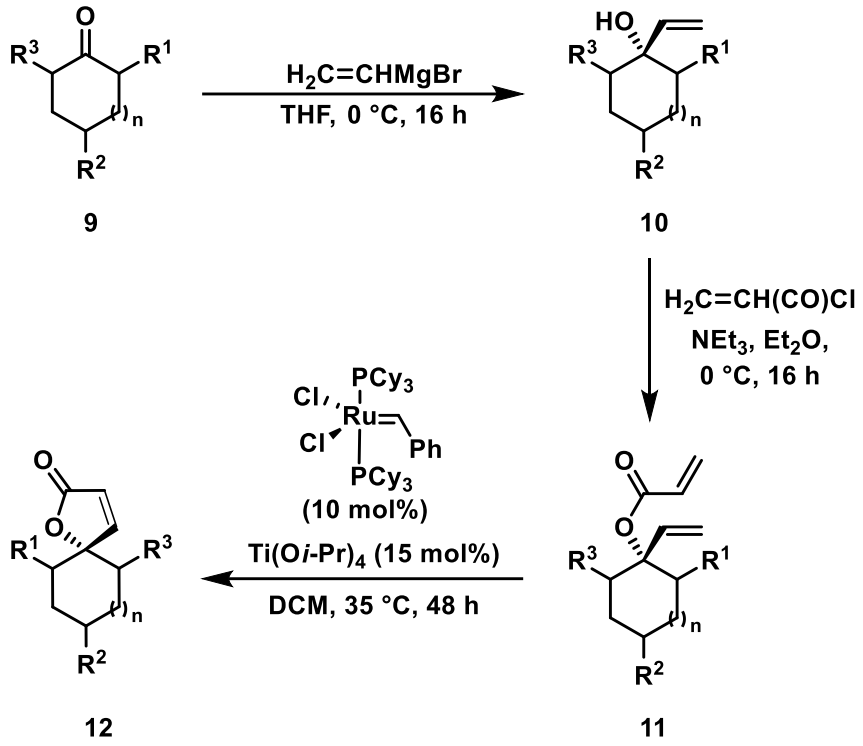

Scheme 4.2. The Langer group synthetic route.

The Yu group applied an oxidative cyclization/dimerization reaction of allenes **13** and **14** in the presence of the active palladium (II) to obtain furanyl-butenolide derivatives **15** (Scheme 4.3).[191,193] The reaction was shown to be high yielding (61–92%) with a variety of the substituents. The group is continuing to study the reaction mechanism and synthetic applications.

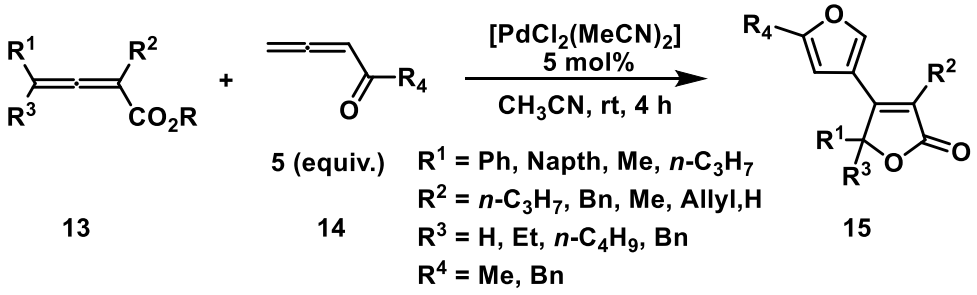

Scheme 4.3. Preparation of butenolides from allenes.

The Marinelli group reported a novel methodology of the rhodium-catalyzed addition of boron reagents to propargylic alcohols **16** followed by lactonization to yield

butenolides **17** (Scheme 4.4).[194] The reaction of the alkynoates was shown to be regioselective, yielding 39–77%, and was not affected by the bulkiness of R and R^1 groups. Since the reaction proceeds under harsh conditions, it leads to the formation of side products of multiple addition.

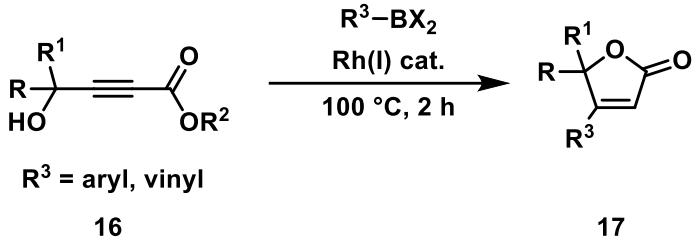

Scheme 4.4. Marinelli group lactonization route towards formation of butenolides.

During our studies on $Sc(OTf)_3$ mediated intramolecular vinylogous Nazarov cyclization the formation of some unexpected butenolides was observed (Chapter 3, Section 3.3.3.2, Scheme 3.34). Analogous reactivity to the one we discovered for dendralenes was previously observed for silyl pentadienic acids and esters under Ritter conditions, which were providing self-cyclization products with exocyclic double bond (Scheme 4.5).[196] Therefore, we set out to explore our reactivity generality as a method for the construction of the substituted butenolides.

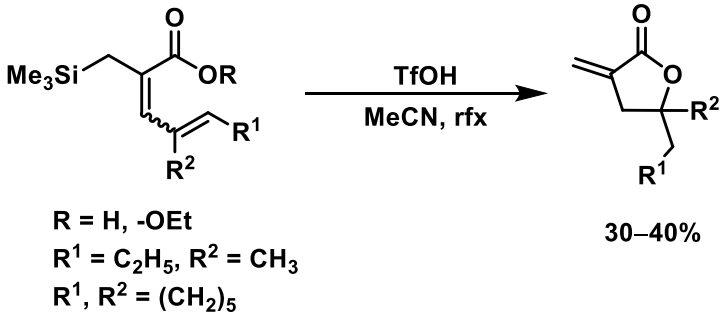

Scheme 4.5. Silyl pentadienic acids and esters self-cyclization.

4.2 Results and Discussion

Addition of 10 mol% of $Sc(OTf)_3$ to substrate **18** and heating it up to 80 °C in DCE resulted in unexpected cyclization and formation of product **19** in 58% yield (Scheme 4.6). Initially, the vinylogous iso-Nazarov cyclization was proposed, although the probability of this type of cyclization was considered to be low (Scheme 4.7).[197] To explore this new type of reactivity, we performed subsequent studies on analogous dendralene substrates that we had prepared earlier.

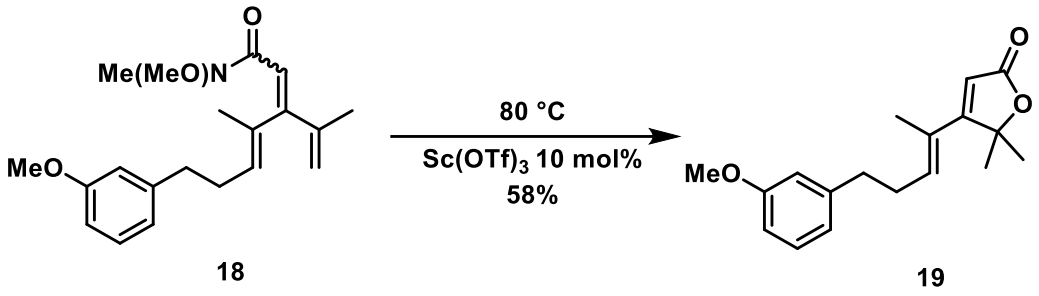

Scheme 4.6. The formation of butenolide **19**.

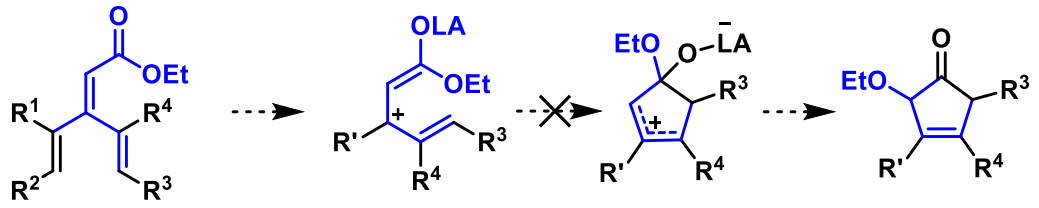

Scheme 4.7. Proposed iso-Nazarov cyclization.

In Chapter 3, substrate **20** was shown to undergo cyclization in the presence of $TiCl_4$ giving tricycle **21** as the sole product isolated from the reaction. The same product **19** was formed in 58–60% yield when $Sc(OTf)_3$ was applied as a catalyst with both amide **18** and ester **20** (Scheme 4.8). Analysis of the NMR spectral data indicated that the terminal alkene protons from the substrates **18** or **20** were not found in product **19**, and that an additional methyl group was present. Furthermore, the alkene proton α to the lactone carbonyl group displayed an nOe correlation to the allylic methyl group found on the side-chain C=C bond. (Figure 4.3). Same proton has HMBC correlations with neighboring quaternary alkene carbon and sp^3 carbon, which bears two methyl groups.

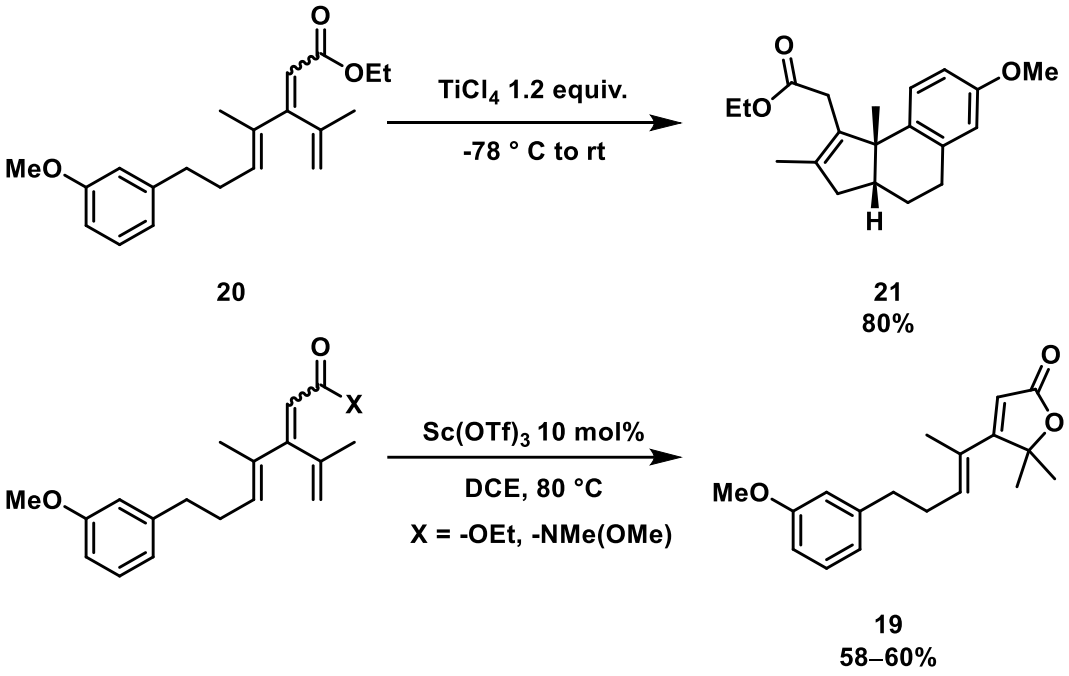

Scheme 4.8. Different reactivity of dendralene **20** based on the choice of conditions.

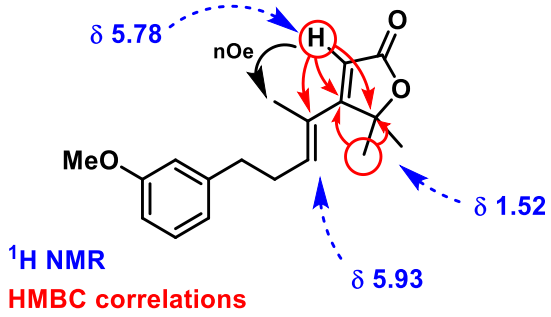

Figure 4.3. The structure elucidation of product **19**.

To explore the scope of this new reactivity and build further support for the structural assignment of **19**, we decided to perform the synthesis of the previously reported butenolide using this new methodology. The cyclization in case of the β-phenyl substituted compound **22** required the stoichiometric amount of $Sc(OTf)_3$. Low loading of Lewis acid resulted in the formation of only the trace amounts of the desired product. A subsequent study with a substoichiometric amount of triflic acid made it clear that Brønsted acid was also capable to initiate the cyclization. This experiment was performed in order to study if partial hydrolysis of scandium triflate salt because of trace amounts of water in DCE is the reason of observed reactivity.[198] It was shown that the reaction

could be catalyzed by the trace amount of TfOH (Scheme 4.9). If one terminal alkene of compound **24** was changed to the aliphatic side-chain (Figure 4.4), no butenolide formation was observed with $Sc(OTf)_3$. The reasonable explanation for this observation would be that cross-conjugated system has to be present to form butenolides. Substrates with γ-aromatic substituent (relatively to ester) underwent vinylogous Nazarov cyclization (Scheme 4.10).

The reaction mechanism was proposed to start with alkene activation by Brønsted acid, and attack of the carbocation by the C=O (Scheme 4.11).[196] During the quenching process, attack of electrophilic carbon by water molecule and loss of the leaving group results in the generation of butenolide.

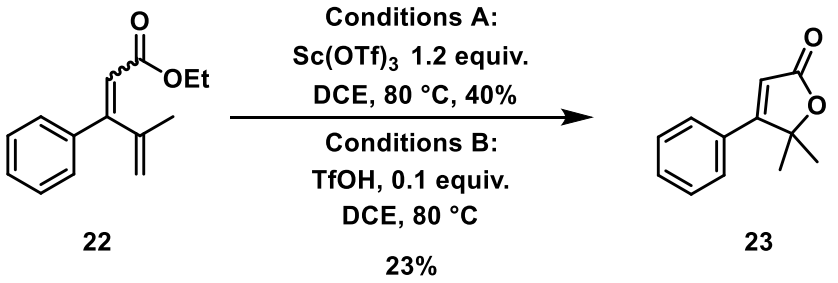

Scheme 4.9. The synthesis of previously reported compound **23**.

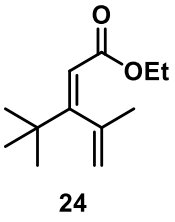

Figure 4.4. Substrate **24** with aliphatic side-chain.

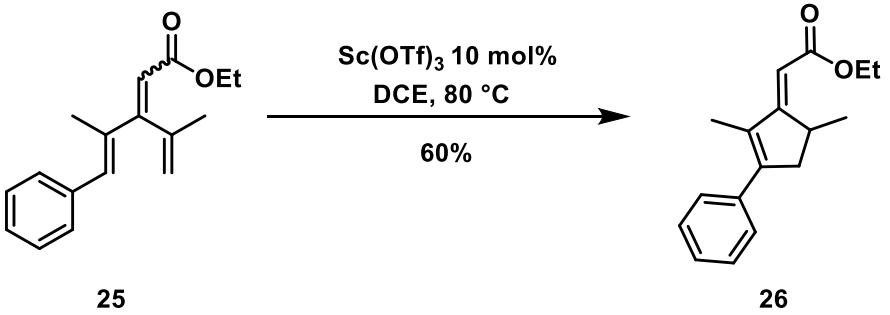

Scheme 4.10. Vinylogous Nazarov cyclization of **25**.

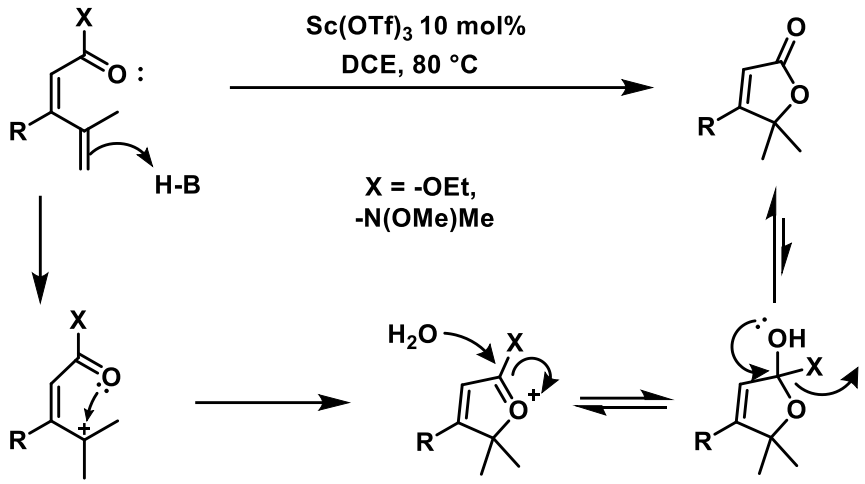

Scheme 4.11. The proposed mechanism for butenolide formation.

4.3 Conclusions

In summary, a new reactivity of the [3]denralenes was discovered. In a few cases, it was shown that dendralenes can undergo lactonization with no presence of a precious catalyst in the reaction media. The initial studies of the reaction scope showed that dendralenes are the necessary scaffolds to undergo the desired cyclization. A substrate with an aliphatic chain in place of the unsaturated branch found in dendralenes **18** and **20** and phenyl-substituted dienoate **22** proved to be inert under the standard conditions. Further exploration of more forcing conditions should be examined in the future.

4.4 Experimental

4.4.1 General Information

Reactions were carried out in flame-dried glassware under a positive argon atmosphere unless otherwise stated. Transfer of anhydrous solvents and reagents was accomplished with oven-dried syringes or cannulae. The 4 Å molecular sieves were stored in an oven and flame-dried before use. THF and DCM solvents were purified using the LC Technology Solutions Inc. solvent purification system. All solvents were purchased as ACS reagents and used without further purification. Thin-layer chromatography was performed on glass plates precoated with 0.25 mm Kieselgel 60 F254 (Merck). Flash chromatography columns were packed with 230–400 mesh silica gel (Silicycle). ^{1}H NMR and ^{13}C spectra were recorded at 400/500/700 and 100/125/175 MHz, respectively, and coupling constants (J) are reported in Hertz (Hz). NMR chemical shifts are reported relative to the residual $CHCl_3$ in $CDCl_3$ (7.26 ppm) internal standard. Standard notation is used to describe the multiplicity of signals observed in 1H NMR spectra: broad (br), apparent (app), multiplet (m), singlet (s), doublet (d), triplet (t), etc. Infrared (IR) spectra were measured with a Mattson Galaxy Series FT-IR 3000 spectrophotometer. High-resolution mass spectrometry (HRMS) data (APPI/ESI technique) were recorded using an Agilent Technologies 6220 oaTOF instrument. HRMS data (EI technique) were recorded using a Kratos MS50 instrument.

Substrate **19** was previously mentioned in Chapter 3, Section 3.3.3.2 as compound **106**.

4.4.2 Representative Procedure A for the Synthesis of Butenolides

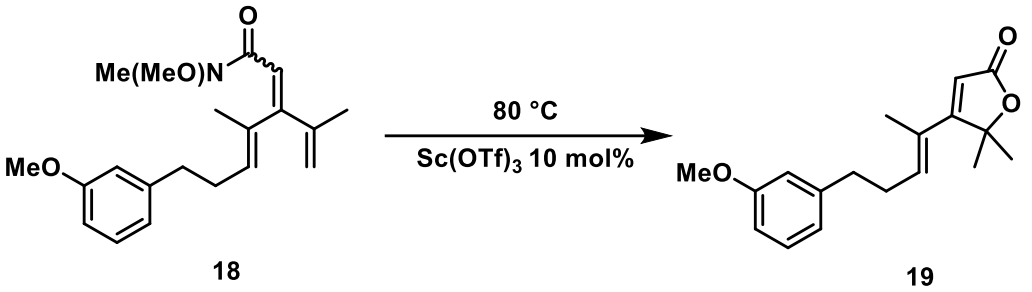

18 19

Into a 25 mL flame dried round-bottom flask equipped with condenser with a magnetic stir bar under argon atmosphere was added $Sc(OTf)_3$ (4 mg, 0.01 mmol, 10 mol%). Starting material **18** (20 mg, 0.06 mmol) was dissolved in DCE (1 mL) predried by molecular sieves. Then, the solution with starting material **18** was added into flask via cannula into the flask with $Sc(OTf)_3$. The reaction vessel was heated up to 80 °C and held at this temperature for 24 h. After cooling down the reaction mixture, the solution was filtered through a silica plug and flushed with DCM (3 x 20 mL). The crude mixture was purified by flash column chromatography (EtOAc/hexanes 1:9) to obtain **19** (10 mg, 58%).

4.4.3 Synthesis of Butenolide Products 19 and 23

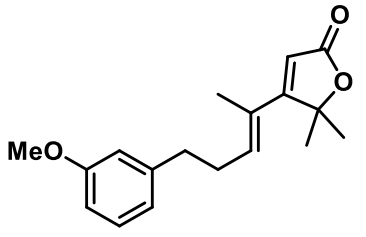

19

The compound was prepared by the representative procedure **A** with starting materials **18** or **20**. Column chromatography (EtOAc/hexanes 1:9) gave **19** (10 mg, 58%).

(*E*)-4-(5-(3-methoxyphenyl)pent-2-en-2-yl)-5,5-dimethylfuran-2(5H)-one (19): colorless oil; R_f 0.19 (EtOAc/hexanes 1:9); IR (cast film) ν_{max} 2921, 2850, 1746, 1585 cm^{-1}; ^1H NMR (700 MHz, $CDCl_3$) δ 7.20 (t, *J* = 7.8 Hz, 1H), 6.77–6.73 (m, 2H), 6.72–

6.70 (m, 1H), 5.88 (t, J = 7.3, 1H), 5.77 (s, 1H), 3.78 (s, 3H), 2.75 (t, J = 7.5 Hz, 2H), 2.57 (q, J = 7.4 Hz, 2H), 1.83 (s, 3H), 1.52 (s, 6H); ^{13}C NMR (176 MHz, $CDCl_3$) δ 172.5, 171.7, 159.8, 142.4, 137.0, 129.5, 127.7, 120.8, 114.4, 113.8, 111.3, 86.9, 55.2, 35.1, 30.5, 27.0, 15.0; HRMS (EI) *m/z* calcd for $C_{18}H_{22}O_2$ (M+) 286.1569, found 286.1568.

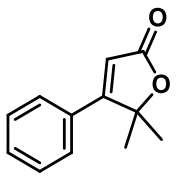

23

The compound was prepared by the representative procedure **A** with starting material **22** (0.1 mmol). Column chromatography (EtOAc/hexanes 1:9) gave **23** (8 mg, 40%). Obtained ^{1}H NMR and ^{13}C NMR are analogous to the one reported in literature.[199]

5,5-dimethyl-4-phenylfuran-2(5H)-one (23): colorless liquid; R_f = 0.30 (EtOAc/hexanes 1:9); IR (neat) ν_{max} 3020, 1744, 1613, 1216 cm^{-1}; ^{1}H NMR (400 MHz, $CDCl_3$) δ 7.52–7.49 (m, 3H), 6.97–6.94 (m, 2H), 6.23 (s, 1H), 1.68 (s, 6H); ^{13}C NMR (100 MHz, $CDCl_3$) δ 171.8, 171.4, 130.8, 130.3, 129.1, 127.6, 114.7, 87.3, 26.5.

4.4.4 Preparation of Substrates 22 and 24

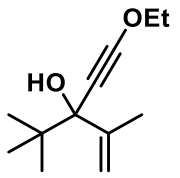

The compound was prepared by the standard procedure **A** reported in Chapter 3, Section 3.5.2.1, Step 1. Column chromatography (EtOAc/hexanes 1:4) gave **25** (88 mg, 45%) as a colorless oil.

3-(tert-butyl)-5-ethoxy-2-methylpent-1-en-4-yn-3-ol: colorless oil; R_f 0.46 (EtOAc/hexanes 1:4); IR (cast film) ν_{max} 3477, 2979, 2960, 2262 cm^{-1}; ^{1}H NMR (700 MHz, $CDCl_3$) δ 5.17 (s, 1H), 5.04 (s, 1H), 4.08 (q, J = 7.1 Hz, 2H), 1.91 (s, 3H), 1.80 (s, 1H), 1.37 (t, J = 7.1 Hz, 3H), 1.02 (s, 9H); ^{13}C NMR (176 MHz, $CDCl_3$) δ 147.4, 114.1,

94.1, 79.2, 74.3, 40.9, 39.5, 25.9, 22.2, 14.5; HRMS (ESI) *m/z* calcd for $C_{12}H_{20}O_2$ (M+) 196.1463, found 196.1464.

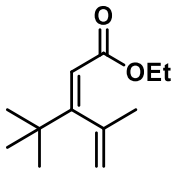

24

The compound was prepared by the standard procedure **A** reported in Chapter 3, Section 3.5.2.1, Step 2. Column chromatography (EtOAc/hexanes 1:9) gave **24** (40 mg, 45%) as a colorless oil.

(*E*)-ethyl 3-(tert-butyl)-4-methylpenta-2,4-dienoate (24): colorless oil; R_f 0.69 (EtOAc/hexanes 1:9); IR (cast film) ν_{max} 2956, 2923, 2852, 1462 cm^{-1}; ^1H NMR (700 MHz, $CDCl_3$) δ 5.63 (s, 1H), 4.85 (s, 1H), 4.68 (s, 1H), 4.19 (q, *J* = 7.2 Hz, 2H), 1.91 (s, 3H), 1.32 (t, *J* = 7.1 Hz, 3H), 1.28 (s, 9H); ^{13}C NMR (126 MHz, $CDCl_3$) δ 167.5, 166.6, 148.6, 117.4, 112.4, 60.2, 35.6, 29.7, 24.8, 14.2; HRMS (EI) *m/z* calcd for $C_{12}H_{20}O_2$ (M+) 196.1463, found 196.1462.

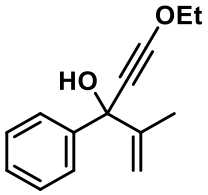

The compound was prepared by the standard procedure **A** reported in Chapter 3, Section 3.5.2.1, Step 1. Column chromatography (EtOAc/hexanes 1:9) gave **26** (136 mg, 63%) as a colorless oil.

5-ethoxy-2-methyl-3-phenylpent-1-en-4-yn-3-ol: colorless oil; R_f 0.26 (EtOAc/hexanes 1:9); IR (cast film) ν_{max} 3451, 3059, 2981, 2957, 2264, 1448 cm^{-1}; ^1H NMR (700 MHz, $CDCl_3$) δ 7.62–7.58 (m, 2H), 7.34–7.30 (m, 2H), 7.27–7.25 (m, 1H), 5.43 (br s Hz, 1H), 4.93 (br s, 1H), 4.15 (q, *J* = 7.1 Hz, 2H), 2.30 (s, 1H), 1.66 (s, 3H), 1.40 (t, *J* = 7.1 Hz, 3H); ^{13}C NMR (176 MHz, $CDCl_3$) δ 148.2, 143.7, 127.9, 127.5, 126.0,

110.7, 95.5, 75.4, 74.7, 40.6, 18.6, 14.5; HRMS (EI) *m/z* calcd for $C_{14}H_{16}O_2$ (M+) 216.1150, found 216.1148.

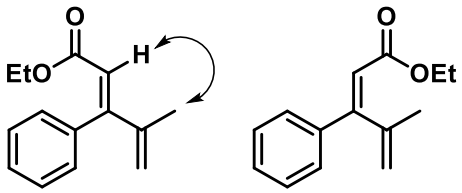

22a **22b**

2.6:1

The compound was prepared by the standard procedure reported in Chapter 3, Section 3.5.2.1. Column chromatography (EtOAc/hexanes 1:9) gave **22**, an inseparable mixture of **22a** and **22b**, (53 mg, 39%) as a colorless oil with *E*:*Z* ratio 2.6:1. To determine the structures and assign resonances ^{1}H NMR was used. The NMR data for the mixture was taken and major diastereomer **22a** peaks were subtracted to identify the resonances belonging to **22b**.

(*Z*)-ethyl 4-methyl-3-phenylpenta-2,4-dienoate (22a): colorless oil; R_f 0.48 (EtOAc/hexanes 1:9); IR (cast film) ν_{max} 2980, 2935, 1724, 1446 cm^{-1}; ^{1}H NMR (700 MHz, $CDCl_3$) δ 7.53–7.48 (m, 2H), 7.38–7.26 (m, 3H), 6.05 (s, 1H), 5.32 (s, 1H), 4.84 (s, 1H), 3.96 (q, *J* = 7.1 Hz, 2H), 2.03 (s, 3H), 1.03 (t, *J* = 7.1 Hz, 3H); ^{13}C NMR (176 MHz, $CDCl_3$) δ 166.4, 156.3, 143.9, 138.4, 128.5, 127.6, 127.3, 123.5, 117.1, 59.9, 20.5, 13.9; HRMS (EI) *m/z* calcd for $C_{14}H_{16}O_2$ (M+) 216.1150, found 216.1147.

The (Z) geometry of the ester-substituted alkene was confirmed by the observation of an nOe correlation between the alkenyl proton α to the ester group and the methyl group of the 1,1-disubstituted alkene. I would also indicate that correlation in the structure above the data.

(*E*)-ethyl 4-methyl-3-phenylpenta-2,4-dienoate (22b) (partial data): ^{1}H NMR (700 MHz, $CDCl_3$) δ 7.38–7.26 (m, 3H), 7.13–7.07 (m, 2H), 6.11 (s, 1H), 5.23 (s, 1H), 4.90 (s, 1H), 4.19 (q, *J* = 7.1 Hz, 2H), 1.94 (s, 3H), 1.29 (t, *J* = 7.2 Hz, 3H); ^{13}C NMR (176 MHz, $CDCl_3$) δ 166.2, 158.3, 143.4, 138.0, 129.4, 116.1, 115.1, 60.0, 22.6, 14.1. Not all sp^2 carbon resonances could be detected due to overlap with the major isomer.

Chapter 5

Conclusions and Future Directions

5.1 The Double Interrupted Nazarov Cyclization

As previously shown, a new one-pot, multi-component reaction was reported to synthesize α-halocyclopentanones via the organoaluminum mediated double interrupted Nazarov cyclization. The use of organoaluminum reagent had the following purposes: it serves as a Lewis acid and traps oxyallyl cation via migration of one of the alkyl substituents from aluminum to the oxyallyl cation. The new method provided desired products in 54–96% yield with diastereoselectivities varying from 3:1 to 49:1 while forming up to four new stereogenic centers and two new carbon bonds (Scheme 5.1). The deeper understanding of the organoaluminum mediated double interrupted Nazarov cyclization can help in the development of double interrupted Nazarov cyclization processes initiated by other nucleophiles (like Et_3SiH). The first stereogenic centers will be set during the nucleophile attack on oxyallyl cation. Newly formed enolate can be used to trap electrophiles.

A good example of the interrupted Nazarov reaction (described in Chapter 1) is the reductive Nazarov cyclization (Scheme 5.2),[18,70] where a nucleophilic attack of Et_3SiH on the oxyallyl cation happened in a highly stereoselective fashion. However, the subsequent trapping event of the resulting enolate with an electrophile was not studied. Control of enolate trapping process can provide stereoselective formation of reaction products containing four stereogenic centers (Scheme 5.3).

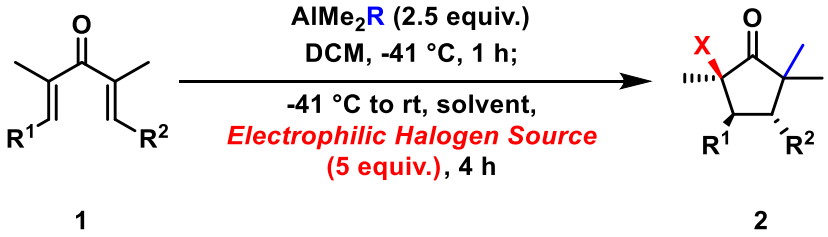

Scheme 5.1. Organoaluminum double interrupted Nazarov reaction.

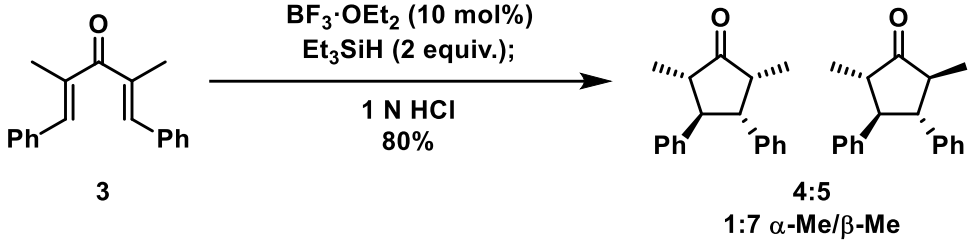

Scheme 5.2. The reductive Nazarov cyclization.

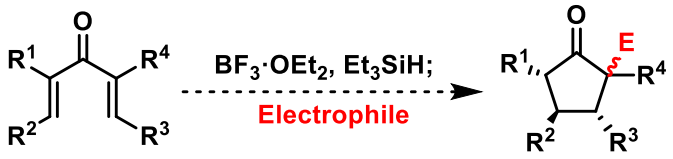

Scheme 5.3. Study of possible electrophiles for the double interrupted Nazarov cyclization.

5.2 The Vinylogous Nazarov Cyclization

5.2.1 Intermolecular Interrupted Vinylogous Nazarov Cyclization

The dendralenes undergo the desired intermolecular interrupted vinylogous Nazarov cyclization in the presence of a trimethylaluminum reagent, furan, and Et_3SiH. The utilization of other than the reported traps can result in the preparation of other complex cyclopentanones (Scheme 5.4). And could be considered as a direction to gain deeper understanding on the reaction mechanism and expand the scope of the vinylogous Nazarov cyclization simultaneously. The effect of EDG and EWG on the process, as well as presence of extended aromatic system and non-aromatic substituents should be studied. It is also required to understand, which electrophiles can be utilized as traps for the newly formed zwitterionic intermediate **11** after allyl cation trapping. To understand this, a separate study on the scope of electrophiles will be required.

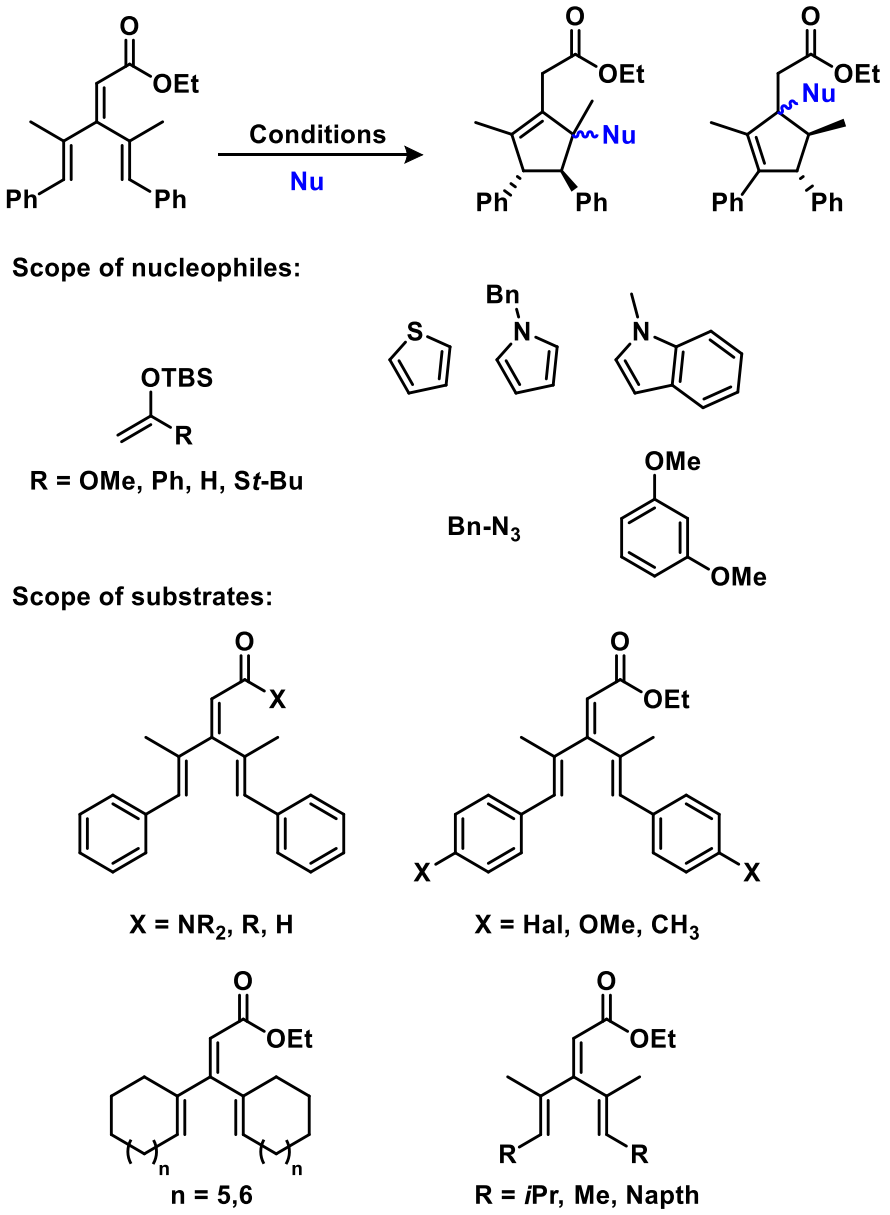

Scheme 5.4. Proposed scope of nucleophiles and substrates for intermolecular vinylogous Nazarov cyclization.

The dendralenes can undergo intramolecular vinylogous Nazarov cyclization, as well; however, scope of it is limited. It results in the stereoselective formation of the polycyclic system. The possibility of forming an endocyclic alkene and two new stereogenic centers in a single step in a stereoselective fashion is intriguing. To learn if it is possible to deliver a potential trap via the carbonyl moiety further studies are required (Scheme 5.5). It is also necessary to study the possibility to cyclize substrate **6** in presence

of $TiCl_4$ and heating as soon as we are aware that substrate **6** can tolerate elevated temperatures and does not undergo decomposition (Scheme 5.6). This experiment was not performed due to the lack of starting material and its complex preparation.

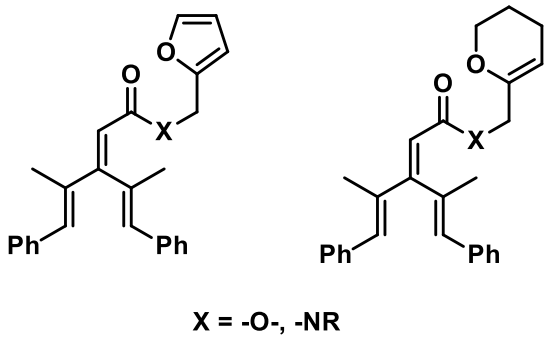

Scheme 5.5. Proposed substrates scope for delivery of a potential trap via the carbonyl moiety.

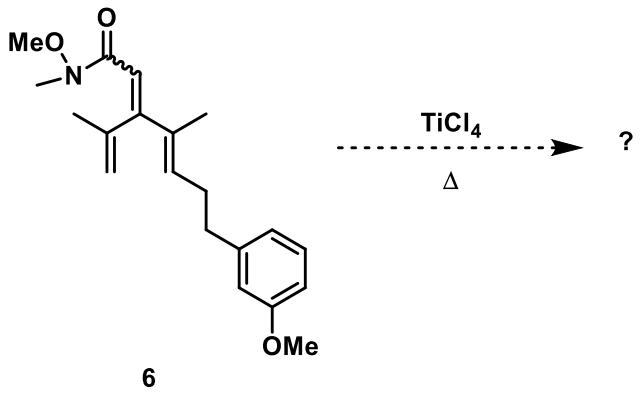

Scheme 5.6. Intramolecular interrupter vinylogous Nazarov cyclization initiated with $TiCl_4$ with heating.

Double interrupted concept should be applied for interrupted vinylogous Nazarov reaction. Based on precedent reported by the Sudhakar group (Scheme 5.7)[179] one can imagine that after trapping of oxyallyl cation with a nucleohile the formed intermediate can undergo subsequent addition of an electrophile to form a compound with higher level of complexity (Scheme 5.8). It is questionable now, which position of the enolate **11** will undergo trapping: the methylene in alpha position to the ester or the conventional Nazarov cyclization position on the γ sp^2 carbon relative to the ester, or both. To test the hypothesis, the nucleophilic trapping has to be performed in a tandem fashion to form the desired compound **11** selectively.

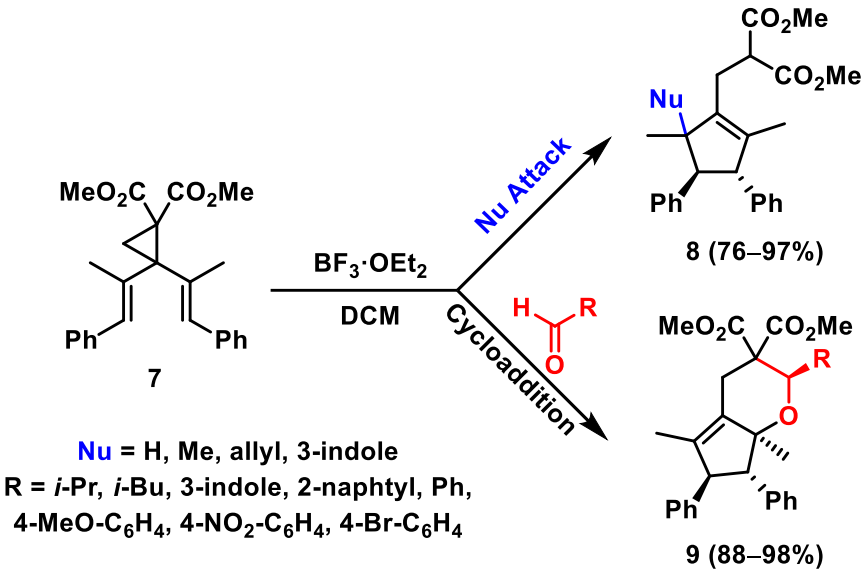

Scheme 5.7. The Sudhakar group precedent.

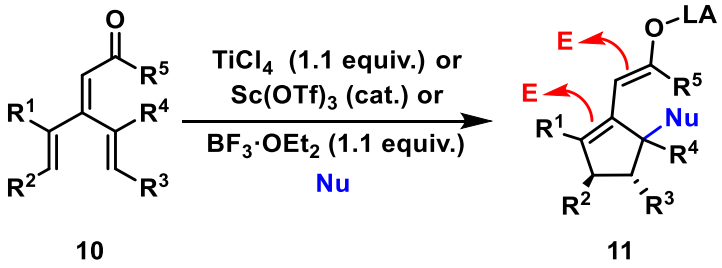

Scheme 5.8. Proposed double interrupted vinylogous Nazarov cyclization.

5.2.2 The Meyer–Schuster/Nazarov Reaction

During optimization studies to furnish dendralenoates from propargylic alcohols, the starting material **12** was submitted to treatment with $TiCl_4$, which was found to effect a 2-step conversion to cyclized products **13** and **14** via sequential Meyer-Schuster rearrangement and vinylogous Nazarov cyclization (Scheme 5.9). Use of 1.2 equiv. of $TiCl_4$ provided the mixture of regioisomers **13** (50%) and **14** (16%). The previous group member, Dr. C. Reider observed an analogous transformation of the non-aromatic [3]dendralene substrate **15** during his reaction optimization studies, as well.[168]

Further examination of this preliminary result was carried out by undergraduate research Seifeddine Khalifa, who explored a variety of conditions with an ultimate goal of determining the reaction scope using a library of substrates. An additional goal was to

improve the reaction selectivity towards the formation of a single cyclization product. The idea of modifying the existing process into a cascade reaction was considered beneficial for further investigation of the interrupted vinylogous Nazarov cyclization. Optimization studies showed that several Lewis acids such as $Sc(OTf)_3$, $BF_3 \cdot OEt_2$ were not able to initiate the desired cyclization. Hydrochloric acid was shown to form the mixture of desired regioisomers in 59% yield, although with different selectivity (Scheme 5.10).

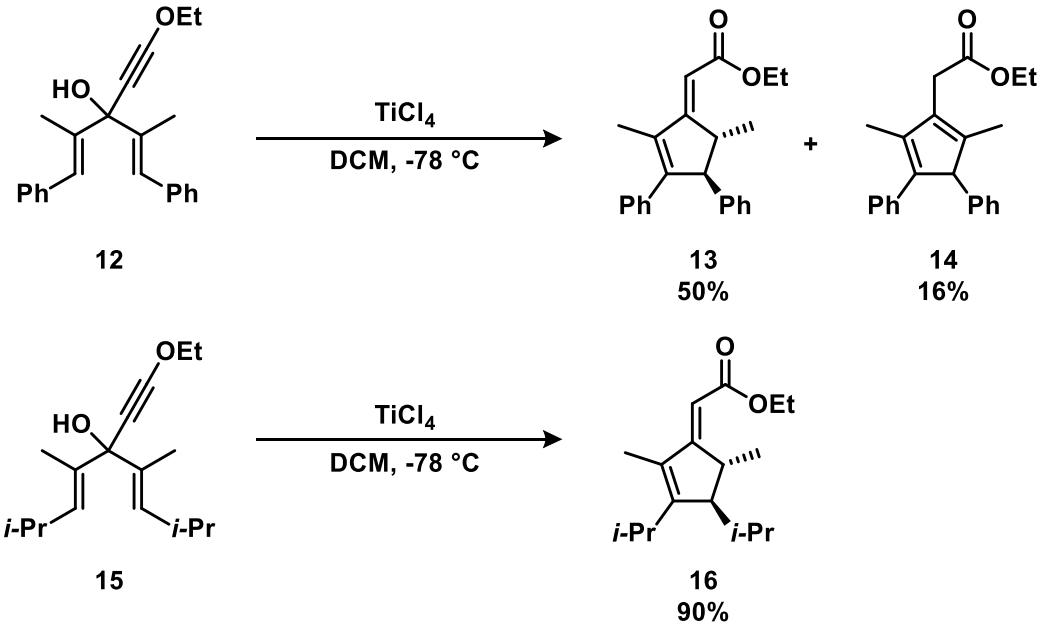

Scheme 5.9. Initially observed Meyer–Schuster–Nazarov cyclization.

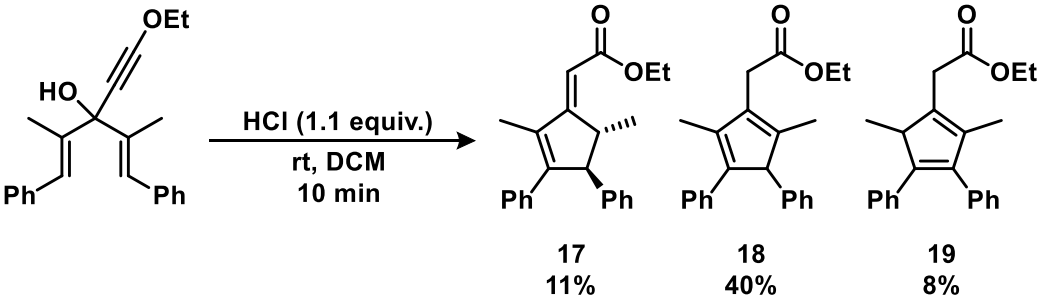

Scheme 5.10. The Meyer–Schuster/Nazarov cyclization initiated by HCl.

Both previously reported successful examples of domino intra- and intermolecular vinylogous Nazarov cyclization **20** and **21** were shown to be unsuccessful in Meyer-Schuster/Nazarov cyclization reaction (Scheme 5.11). For this sequence, it was shown that the presence of the trap resulted in the decomposition of the starting materials. Although, trap addition after cyclization was not tested in the case of the intermolecular interrupted vinylogous Nazarov cyclization. It was planned to test the scope of the reaction on a variety of previously prepared propargylic alcohols such as substrates bearing aromatic β-substituents, non-aromatic substrates, and ones with no α-methyl groups (Figure 5.1). This work is still ongoing.

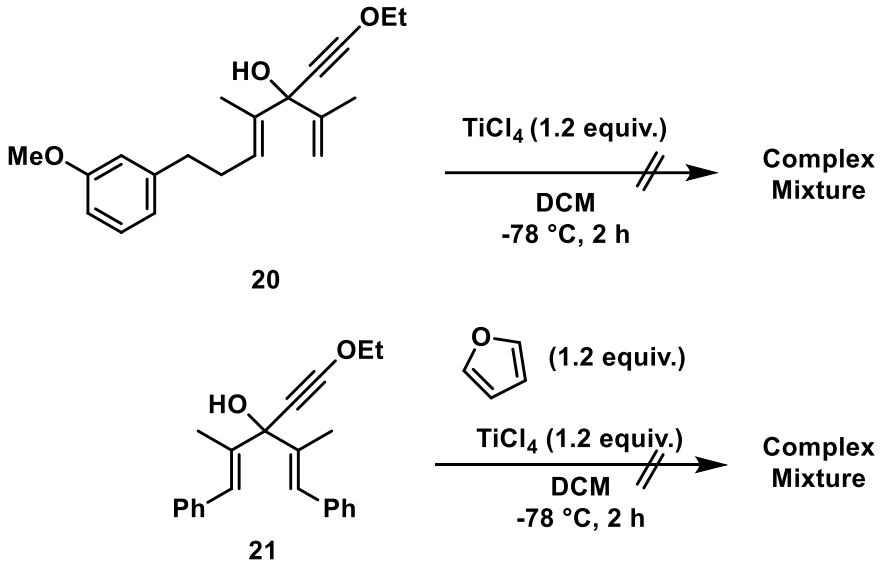

Scheme 5.11. The Meyer–Schuster–Nazarov cyclization in the presence of nucleophilic traps.

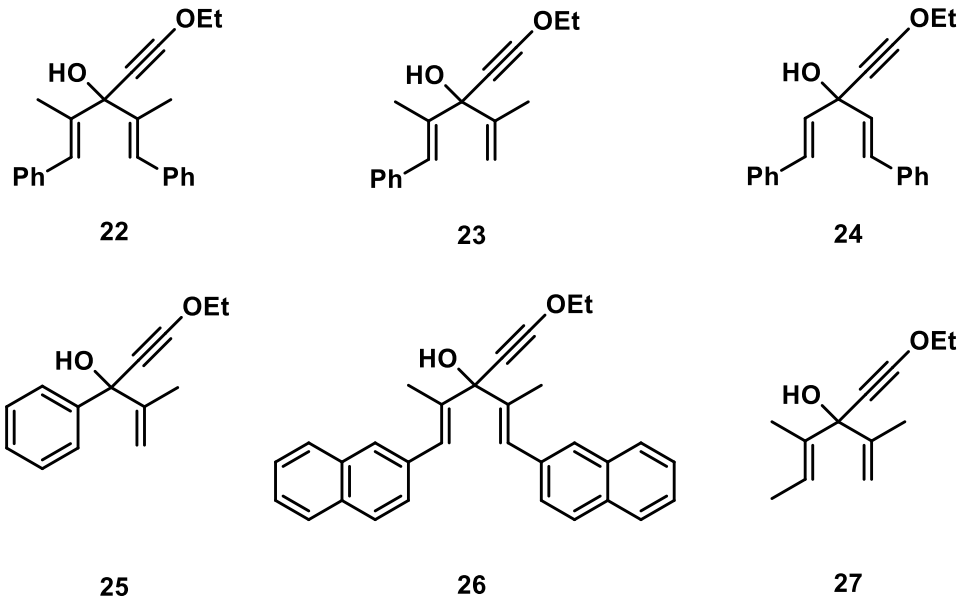

Figure 5.1. Planned substrates scope.

5.2.3 Butenolides Formation

Further investigation of butenolide scope is required. Our studies with dialkenes showed that it is necessary to have a cross-conjugated system present in the substrate to allow butenolide formation (Scheme 5.12). This indicates that substrates lacking the extra conjugation seem to be unreactive to the conditions explored so far, and further examination of more forcing conditions is planned. It is also important to understand how the substitution can affect the reaction.

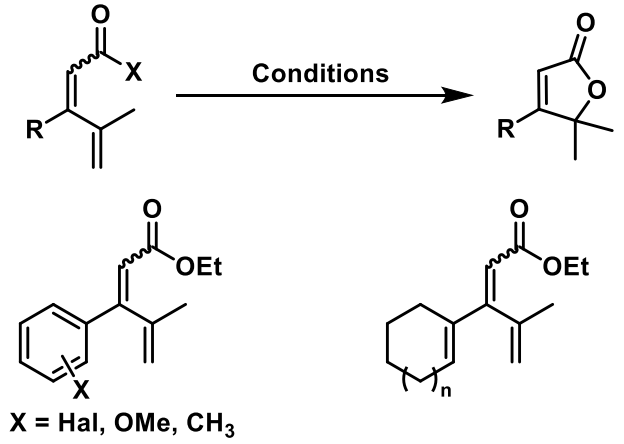

Scheme 5.12. Planned substrate scope for the butenolides formation.

References

[1] L. Birladeanu, *J. Chem. Educ.* **2000**, *77*, 7, 858–864.

[2] Book chapter: A. Laurent, *Methode de Chimie*; English translation by Odling, W.; Cavendish Society: London, 1855; quoted from Brook, W. H. History of Chemistry; Norton: New York, **1993**; p 210.

[3] Rocke, Alan J. *The Quiet Revolution: Hermann Kolbe and the Science of Organic Chemistry.* Berkeley: University of California Press, 1993.

[4] R. Fittig, Liebigs *Ann. Chem.* **1860**, *114*, 54–63.

[5] E. Linnemann, *Liebigs Ann. Chem.* **1865**, *3*, 378–382.

[6] A. M. Butlerov, *Liebigs Ann. Chem.* **1874**, *174*, 125–128.

[7] I. Fleming, *Pericyclic Reactions*. Oxford: Oxford University Press, 1999.

[8] F. A. Carey, R. J. Sundberg, Structure and Mechanisms, in *Advanced Organic Chemistry*, Part A, 5th edition, Springer: New York, **2007**, pp. 833–951.

[9] O. Diels, K. Alder, *Justus Liebigs Annalen der Chemie,* **1928**, *460,* 98–122.

[10] Woodward described work towards vitamin B_{12} preparation in *Chem. Soc. Special Publications (Aromaticity)*, **1967**, *21*, 217.

[11] R. B. Woodward, R. Hoffmann, *Angew. Chem. Int. Ed.* **1969**, *8*, 781-853; *Angew. Chem.* **1969**, *81*, 797–869.

[12] R. B. Woodward, R. Hoffmann, *The Conservation of Orbital Symmetry*; Verlag Chemie: Weinheim, **1970**.

[13] a) K. C. Nicolaou, N. A. Petasis, R. E. Zipkin and J. Uenishi, *J. Am. Chem. Soc.* **1982**, *104*, 5555–5556; b) K. C. Nicolaou, N. A. Petasis, J. Uenishi and R. E. Zipkin, *J. Am. Chem. Soc.* **1982**, *104*, 5557; c) K. C. Nicolaou, R. E. Zipkin and N. A. Petasis, *J. Am. Chem. Soc.* **1982**, *104*, 5558–5559; d) K. C. Nicolaou, N. A. Petasis and R. E. Zipkin, *J. Am. Chem. Soc.* **1982**, *104*, 5560; S. L. Drew, A. L. Lawrence and M. S. Sherburn, *Chem. Sci.* **2015**, *6*, 3886–3890.

[14] a) S. F. Brady, S. M. Bondi, J. Clardy, *J. Am. Chem. Soc.* **2001**, *123*, 9900–9901; b) S. F. Brady, M. P. Singh, J. E. Janso, J. Clardy, *J. Am. Chem. Soc.* **2000**, *122*, 2116–2117;

M. P. Singh, J. E. Janso, S. W. Luckman, S. F. Brady, J. Clardy, M. Greenstein, W. M. Maiese, *J. Antibiot.* **2000**, *53*, 256–261.

[15] M. Bing, L. Li, H. Ding, *Synthesis,* **2017**, *49*, 4383–4413.

[16] C. Souris, A. Misale, Y. Chen, M. Luparia, N. Maulide, *Org. Lett.* **2015**, *17*, 4486–4489.

[17] C. C. Fu, Y. B. Zhang, J. Xuan, C. L. Zhu, B. N. Wang, H. F. Ding, *Org. Lett.* **2014**, *16*, 3376–3379.

[18] A. Shvartsbart, A. B. Smith, *J. Am. Chem. Soc.* **2015**, *137*, 3510–3519; A. Shvartsbart, A. B. Smith, *J. Am. Chem. Soc.* **2014**, *136,* 870–873.

[19] a) Book Chapter: F. G. West, O. Scadeng, Y.-K. Wu, R. J. Fradette and S. Joy, in *Comprehensive Organic Synthesis, 2nd Edition*, *Vol. 5* (Eds.: G. A. Molander, P. Knochel), Elsevier: Oxford, **2014**, pp. 827–866. Recent reviews: b) M. A. Tius, *Chem. Soc. Rev*. **2014**, *43*, 2979–3002; c) W. T. Spencer, T. Vaidya and A. J. Frontier, *Eur. J. Org. Chem*. **2013**, 3621–3633; d) N. Shimada, C. Stewart and M. A. Tius, *Tetrahedron,* **2011**, *67*, 5851–5870; e) W. Nakanishi and F. G. West, *Curr. Opin. Drug Discov.* **2009**, *12*, 732–751.

[20] Recent examples: a) T. Takeda, S. Harada and A. Nishida, *Org. Lett.* **2015**, *17*, 5184–5187; b) K. Kitamura, N. Shimada, C. Stewart, A. C. Atesin, T. A. Ateşin and M. A. Tius, *Angew. Chem. Int. Ed.* **2015**, *54*, 6288–6291; c) A. Jolit, P. M. Walleser, G. P. A. Yap and M. A. Tius, *Angew. Chem. Int. Ed*. **2014**, *53*, 6180–6183; d) G. E. Hutson, Y. E. Türkmen and V. H. Rawal, *J. Am. Chem. Soc.* **2013**, *135*, 4988–4991.

[21] P. L. Pauson, I. U. Khand, *Ann. N. Y. Acad. Sci.* **1977**, *295*, 2–14.

[22] a) Electronic Theories in Organic Chemistry. (n.d.) *The Great Soviet Encyclopedia, 3rd Edition*. (1970-1979). Retrieved April 1, 2020 from: https://encyclopedia2.thefreedictionary.com/Electronic+Theories+in+Organic+Chemistry; b) J. B. Stothers and C. T. Tan, *J. Chem. Soc., Chem. Commun.*, **1974**, 738–739.

[23] a)I. N. Nazarov, *Uspehi Himii* **1951**, *20*, 71–103; b) I. N. Nazarov, I. I. Zaretskaya, *Bull. Acad. Sci. USSR, Div. chem. Sci.* **1944**, 65.

[24] a) H. Pellissier, *Tetrahedron,* **2005**, *61*, 6479–6517; b) A. J. Frontier, C. Collison, *Tetrahedron,* **2005**, *61*, 7577–7606; c) M. A. Tius, *Eur. J. Org. Chem.* **2005**, 2193–2206; d) K. L. Habermas, S. E. Denmark, T. K. Jones, *Org. React.* **1994**, *45*, 1–158.

[25] D. Vorländer; G. Schroedter, *Ber. Dtsch. Chem. Ges.* **1903**, *36*, 1490–1497.

[26] C. F. H. Allen, J. A. VanAllan, J. F. Tinker, *J. Org. Chem.* **1955**, *20*, 1387–1391.

[27] E. A. Braude, J. A. Coles, *J. Chem. Soc.* **1952**, 1430–1433.

[28] J. L. Vicario, D. Badia, *ChemCatChem.* **2010**, *2*, 375–378.

[29] T. N. Grant, C. J. Rieder and F. G. West, *Chem. Commun.* **2009**, 5676–5688.

[30] D. K. Mandal, *Pericyclic Chemistry : Orbital Mechanisms and Stereochemistry*; Amsterdam, Netherlands: Elsevier, 2018.

[31] a) C. W. Shoppee and R. E. Lack, *J. Chem. Soc. C*, **1969**, 1346–1349; C. W. Shoppes and B. J. A. Cooke *J. Chem. Soc., Perkin Trans. 1*, **1972**, 2271–2276.

[32] a) K. E. Harding and K. S. Clement *J. Org. Chem.* **1984**, *49*, 20, 3870–3871; b) A. Yoshitsugu, T. Kunio, M. Katsutada, K. Toru, *Chem Lett*. **1985**, *14*, 10, 1531–1534; c) P. E. Harrington, M. A. Tius, *Org. Lett.* **1999**, *1*, 4, 649–652; d) V. B. Birman and S. J. Danishefsky, *J. Am. Chem. Soc.* **2002**, *124*, 10, 2080–2081.

[33] C. Santelli-Rouvier, M. Santelli, *Synthesis,* **1983**, 429–442; C. Morel-Fourrier, J. P. Dulcere, M. Santelli, *J. Am. Chem. Soc.* **1991**, *113*, 21, 8062–8069.

[34] a) J. P. Marino, Lindermann, *J. Org. Chem.* **1981**, *46*, 3696–3702; b) J. F. P. Andrews, A. C. Regan, *Tetrahedron Lett.* **1991**, *32*, 7731–7734; d) M. A. Tius, *Acc. Chem. Res.* **2003**, *36*, 284–290.

[35] a) S. H. Kim, J. K. Cha, *Synthesis,* **2000**, 2113–2116; b) M. Janka, W. He, A. J. Frontier, R. Eisenberg, *J. Am. Chem. Soc.* **2004**, *126*, 6864–6865; c) M. Janka, W. He, A. J. Frontier, C. Flaschemreim, R. Eisenberg, *Tetrahedron,* **2005**, *61*, 6193–6206.

[36] S. E. Denmark, In B. M. Trost, I. Fleming, Eds.; Comprehensive Organic Synthesis; Pergamon: Oxford, **1991**; Vol. 5, p 751.

[37] S. E. Denmark, K. L. Habermas, G. A. Hite, *Helv. Chim. Acta* **1988**, *71*, 168–194.

[38] S. Casson, P. Kocienski, *J. Chem. Soc.*, *Perkin Trans. 1* **1994**, 1187–1191.

[39] G. Liang, S. N. Gradl, and D. Trauner, *Org. Lett.* **2003**, *5*, *26*, 4931–4934.

[40] V. K. Aggarwal and A. J. Belfield, *Org. Lett.* **2003**, *26*, 5075–5078.

[41] W.He, I. R. Herrick, T. A. Atesin, P. A. Caruana, C. A. Kellenberger and A. J. Frontier, *J. Am. Chem. Soc.* **2008**, *130*, 3, 1003–1011; M. Harmata, *Chemtracts: Org. Chem.* **2004**, *17*, 416–435.

[42] S. Qian, Z. Xie, J. Liu, M. Li, S. Wang, N. Luo, C. Wang. *J. Org. Chem.* **2018**, *83*, 14768–14776; M. L. King, C. C. Chiang, H. C. Ling, *J.Chem. Soc.* **1982**, *20*,1150–1151.

[43] M. Y. Zhang, L. R. Malins, J. S. Ward, R. A. Barrow. *Org. Lett.* **2018**, *20,* 22, 7304–7307.

[44] W. L. Ashley, E. L. Timpy, and T. C. Coombs. *J. Org. Chem.* **2018**, *83,* 5, 2516–2529.

[45] J. A. Malona, K. Cariou, W. T. Spencer, A. J. Frontier, *J. Org. Chem.* **2012**, *77*, 4, 1891–1908.

[46] E. G. Occhiato, C. Prandi, A. Ferrali, A. Guarna, P. J. Venturello, *Org. Chem.* **2003**, *68*, 9728–9741.

[47] a) M. Janka, W. He, I. E. Haedicke, F. R. Fronczek, A. J. Frontier and R. Eisenberg, *J. Am. Chem. Soc.* **2006**, *128*, 5312–5313; b) I. Walz and A. Togni, *Chem. Commun.* **2008**, 4315–4317; c) M. Fujiwara, M. Kawatsura, S. Hayase, M. Nanjo and T. Itoh, *Adv. Synth. Catal.* **2009**, *351*, 123–128; d) R. M. Roberts, R. G. Landolt, R. N. Greene and E. W. Heyer, *J. Am. Chem. Soc.* **1967**, *89*, 1404–1411; e) K. C. W. Chong and J. R. Scheffer, *J. Am. Chem. Soc.* **2003**, *125*, 4040–4041; f) H. J. Lee, F. D. Toste, *Angew. Chem. Int. Ed.* **2007**, *46*, 912–914.

[48] J. A. Bender, A. E. Blize, C. C. Browder, S. Giese, F. G. West, *J. Org. Chem.* **1998**, *63*, 2430–2431.

[49] C. C. Browder and F. G. West, *Synlett,* **1999**, 1363–1366.

[50] S. Giese, R. D. Mazzola, Jr., C. M. Amann, A. M. Arif and F. G. West, *Angew. Chem., Int. Ed.* **2005**, *44*, 6546–6549.

[51] J. A. Bender, A. M. Arif and F. G. West, *J. Am. Chem. Soc.* **1999**, *121*, 7443–7444.

[52] F. G. West and D. W. Willoughby, *J. Org. Chem.*, **1993**, *58*, 3796–3797; C. C. Browder, F. P. Marmsäter and F. G. West, *Org. Lett.*, **2001**, *3*, 3033–3035; C. C. Browder, F. P. Marmsäter and F. G. West, *Can. J. Chem.*, **2004**, *82*, 375–385.

[53] R. Volpe, R. J. Lepage, J. M. White, E. H. Krenske and B. L. Flynn, *Chem. Sci.*, **2018**, *9*, 4644-4649.

[54] Y. Wang, A. M. Arif, and F. G. West, *J. Am. Chem. Soc.* **1999**, *121*, 4, 876–877.

[55] V. Nair, S. Bindu, V. Sreekumar and A. Chiaroni, *Org. Lett.*, **2002**, *4*, 2821–2823.

[56] A. Rostami, Y. Wang, A. M. Arif, R. McDonald and F. G. West, *Org. Lett.,* **2007**, *9*, 703–706.

[57] G. Wagner, *J. Russ. Phys. Chem. Soc.* **1899**, *31*: 690; b) H. Meerwein, *Eur. J. Org. Chem.* **1914**, *405*, 129–175.

[58] L. Birladeanu, *J. Chem. Educ.* **2000**, *77*, 858–864.

[59] D. R. Wenz, J. R. de Alaniz, *Eur. J. Org. Chem.* **2015**, 23–37.

[60] For a review of Wagner–Meerwein shifts see: J. R. Hanson, in: *Comprehensive Organic Synthesis* vol. 3 (Eds.: B. M. Trost, I.Fleming), Pergamon, Oxford, UK, **1991**, p. 705–719; For historical examples of Wagner–Meerwein shifts in Nazarov reactions, see: a) G. Ohloff, K. H. Schulte-Elte, E. Demole, *Helv. Chim. Acta,* **1971**, *54*, 2913–2915; b) L. A. Paquette, W. E. Fristad, D. S. Dime, T. R. Bailey, *J. Org. Chem.* **1980**, *45*, 3017–3028; c) J. Motoyoshiya, T. Yazaki, S. Hayashi, *J. Org. Chem.* **1991**, *56*, 735–740.

[61] C. Kuroda, H. Koshio, A. Koito, H. Sumiya, A. Murase, Y. Hirono, *Tetrahedron,* **2000**, *56*, 6441–6455.

[62] J. Huang, A. J. Frontier, *J. Am. Chem. Soc.* **2007**, *129*, 8060–8061.

[63] J. Huang, D. Leboeuf, A. J. Frontier, *J. Am. Chem. Soc.* **2011**, *133*, 6307–6317.

[64] D. Leboeuf, V. Gandon, J. Ciesielski, A. J. Frontier, *J. Am. Chem. Soc.* **2012**, *134*, 6296–6308.

[65] D. Leboeuf, J. Huang, V. Gandon, A. J. Frontier, *Angew. Chem. Int. Ed.* **2011**, *50*, 10981–10985; *Angew. Chem.* **2011**, *123*, 11173–11176; D. Leboeuf, C. M. Wright, A. J. Frontier, *Chem. Eur. J.* **2013**, *19*, 4835–4841.

[66] P. Chiu, S. Li, *Org. Lett.* **2004**, *6*, 613–616.

[67] Y.-K. Wu, C. R. Dunbar, R. McDonald, M. J. Ferguson, F. G. West, *J. Am. Chem. Soc.* **2014**, *136*, 14903–14911.

[68] J. Nie, H.-W. Zhu, H.-F. Cui, M.-Q. Hua, J.-A. Ma, *Org. Lett.* **2007**, *9*, 3053–3056.

[69] For [4+3]-cycloadditions reviews: a) M. Harmata, *Adv. Synth. Catal.*, **2006**, *348*, 2297–2306; b) M. Harmata and P. Rashatasakhon, *Tetrahedron*, **2003**, *59*, 2371–2395; c) M. Lautens, W. Klute and W. Tam, *Chem. Rev.*, **1996**, *96*, 49–92; d) H. M. R. Hoffmann, *Angew. Chem., Int. Ed. Engl.*, **1984**, *23*, 1–19.

[70] S. Giese and F. G. West, *Tetrahedron Lett.*, **1998**, *39*, 8393–8396.

[71] T. E. Jones and S. E. Denmark, *Helv. Chim. Acta*, **1983**, *66*, 2377–2396.

[72] For more examples on catalytic Nazarov cyclization: a) M. Janka, W. He, A. J. Frontier, C. Flaschenriem and R. Eisenberg, *Tetrahedron*, **2005**, *61*, 6193–6206; b) W. He, J.

Juang, X. Sun and A. J. Frontier, *J. Am. Chem. Soc.* **2007**, *129*, 498–499; c) J. A. Malona, J. M. Colbourne and A. J. Frontier, *Org. Lett.* **2006**, *8*, 5661–5664; d) P. Larini, A. Guarna and E. G. Occhiato, *Org. Lett.* **2006**, *8*, 781–784;

e) M. Rueping, W. Ieawsuwan, A. P. Antonchick and B. J. Nachtsheim, *Angew. Chem. Int. Ed.* **2007**, *46*, 2097–2100.

[73] a) M. F. Gotta and H. Mayr, *J. Org. Chem.* **1998**, *63*, 9769–9775; b) H. Mayr and M. Patz, *Angew. Chem., Int. Ed.* **1994**, *33*, 938–957.

[74] S. Giese, L. Kastrup, D. Stiends and F. G. West, *Angew. Chem. Int. Ed.* **2000**, *39*, 1970–1973.

[75] a) A. Hosomi and H. Sakurai, *J. Am. Chem. Soc.* **1977**, *99*, 1673–1675; b) H. Sakurai, A. Hosomi and J. Hayashi, *Org. Synth.* **1984**, *62*, 86–90.

[76] R. Noyori, F. Shimizu, K. Fukuta, H. Takaya and Y. Hayakawa, *J. Am. Chem. Soc.* **1977**, *99*, 5196–5198.

[77] B. Mahmoud and F. G. West, *Tetrahedron Lett.* **2007**, *48*, 5091–5094.

[78] Y.-K. Wu, R. McDonald, F. G. West, *Org. Lett.*, **2011**, *13*, 3584–3587.

[79] a) Y.-K. Wu, F. G. West, *Org. Lett.* **2014**, *16*, 2534–2537; b) B. M. Trost, H. Gholami, *J. Am. Chem. Soc.* **2018**, *140*, 11623–11626.

[80] R. William, S. Wang, A. Malick, X.-W. Liu, *Org. Lett.* **2016**, *18*, 4458–4461.

[81] Y.-K. Wu, R. Lin, F. G. West, *Synlett*, **2017**, *28*, 1486–1490.

[82] Y. Wang, B. D. Schill, A. M. Arif and F. G. West, *Org. Lett.* **2003**, *5*, 2747–2750.

[83] A. Yungai and F. G. West, *Tetrahedron Lett.* **2004**, *45*, 5445–5448.

[84] C. J. Rieder, R. J. Fradette, F. G. West, *Heterocycles*, **2010**, *80*, 1413–1427.

[85] C. R. Rieder, R. J. Fradette and F. G. West, *Chem. Commun.* **2008**, 1572–1574.

[86] R. L. Davis, D. J. Tantillo, *Curr. Org. Chem.*, **2010**, *14*, 1561–1577; B. L. Flynn, N. Manchala, E. H. Krenske, *J. Am. Chem. Soc.* **2013**, *135*, 9156–9163.

[87] N. Shimada, C. Stewart, M. A. Tius, *Tetrahedron*, **2010**, *67*, 5851–5870; D. J. Kerr, M. Miletic, J. H. Chaplin, J. M. White, B. L. Flynn, *Org. Lett.* **2012**, *14*, 1732–1735.

[88] F. Dhoro and M. A. Tius, *J. Am. Chem. Soc.* **2005**, *127*, 12472–12473.

[89] F. Dhoro, T. E. Kristensen, V. Stockmann, G. P. A. Yap and M. A. Tius, *J. Am. Chem. Soc.* **2007**, *129*, 7256–7257.

[90] D. Song, A. Rostami and F. G. West, *J. Am. Chem. Soc.* **2007**, *129*, 12019–12023.

[91] O. Scadeng, M. J. Ferguson, F. G. West, *Org. Lett.* **2011**, *13*, 114–117; Song, D.; Rostami, A.; West, F. G. *J. Am. Chem. Soc.* **2007**, *129*, 12019–12022.

[92] V. M. Marx, D. J. Burnell, *Org. Lett.* **2009**, *11*, 1229–1231.

[93] M. Shindo, K. Yaji, T. Kita, K. Shishido, *Synlett,* **2007**, 1096–1100.

[94] Y. Kwon, D. J. Schatz, F. G. West, *Angew. Chen. Int. Ed.* **2015**, *54*, 9940–9943.

[95] M. Janka, W. He, I. E. Haedicke, F. R. Fronczek, A. J. Frontier, R. Eisenberg, *J. Am. Chem. Soc.* **2006**, *128*, 5312–5313.

[96] Y. Naganawa, K. Maruoka, *Topics in Organometallic Chemistry*, Vol. 41 (Eds: S. Woodward, S. Dagorne), Springer-Verlag Berlin Heidelberg, **2013**, pp. 187–214.

[97] G. A. Papoian, R. Hoffmann, *Angew. Chem. Int. Ed.,* **2000**, *39*, 2408–2448.

[98] J. C. Huffman, W. E. J. Streib, *J. Chem. Soc.,* **1971**, 911–912.

[99] G. Muller, J. Lachmann, A. Rufinska, *Organometallics*, **1992**, *11*, 2970–2972.

[100] M. L. Munzarova, R. Hoffman, *J. Am. Chem. Soc.,* **2002**, *124*, 4787–4795.

[101] a) K. Ziegler, *Adv. Organomet. Chem*., **1968**, *6*, 1; K. Ziegler, E. Holzkamp, H. Breil and H. Martin, *Angew. Chem.,* **1955**, *67*, 541–547; K. Ziegler, *Angew. Chem.,* **1964**, *76*, 545–553.

[102] A. G. Davies and B. P. Roberts, *J. Chem. Soc.,* **1968**, 1074–1078; H. M. T. Nguyen, H. Y. Tang, W. F. Huang, M. C. Lin, *Comput. Theor. Chem.,* **2014**, *1035*, 39–43.

[103] J. F. Allan, W. Clegg, M. R. J. Elsegood, K. W. Henderson, A. E. McKeown, P. H. Moran, I. M. Rakov, *J. Organomet. Chem.,* **2000**, *602*, 15–23.

[104] A. J. Lundeen, A. C. Oehlschlager, *J. Organomet. Chem*., **1970**, *25*, 337–344.

[105] E. C. Ashby, S. Yu, *Chem. Commun*., **1971**, *7*, 351–352.

[106] E. C. Ashby, J. T. Laemmle, H. M. Neumann, *J. Amer. Chem. Soc*., **1968**, *90*, 5179–5188.

[107] a) B. B. Snider, R. Cordova, R. T. Price, *J. Org. Chem.,* **1982**, *47*, 3643–3646; b) B. B. Snider, D. J. Rodini, M. Karras, T. C. Kirk, E. A. Deutach, R. Cordova, R. T. Price, *Tetrahedron*, **1981**, 3927–3934.

[108] B. B. Snider, G. B. Phillips, *J. Org. Chem*., **1983**, *48*, 2789–2792.

[109] M. Ramaiah, *Synthesis* **1984**, 529–570; b) S. E. Denmark, in *Comprehensive Organic Synthesis, Vol. 5* (Eds.: B. M. Trost, I. Fleming), Pergamon, Oxford, **1991**, pp. 751–784; c) B. M. Trost, *Chem. Soc. Rev.* **1982**, *11*, 141–170.

[110] Y. Kwon, R. McDonald, F. G. West, *Angew. Chem. Int. Ed.*, **2013**, *52*, 8616–8619.

[111] Y. Kwon, O. Scadeng, R. McDonald, F. G. West, *Chem. Commun.*, **2014**, *50*, 5558–5560.

[112] F. A. Davis, S. Chattopadhyay, J. C. Towson, S. Lal, T. Reddy, *J. Org. Chem.*, **1988**, *53*, 2087–2089.

[113] S. Gelozia, Y. Kwon, R. McDonald, F. G. West, *Chem. Eur. J.*, **2018**, *24*, 6052–6056.

[114] Gelozia, S. *Lewis Acid Mediated Approaches for the Generation of 4- and 5-Membered Ring System.* Ph.D. Dissertation, University of Alberta, **2018**

[115] G. Suss-Fink, S. Stanislas, G. B. Shul'pin, G. V. Nizova, H. Stoeckli-Evans, A. Neels, C. Bobillier S. J. Claude, *J. Chem. Soc. Dalton Trans.,* **1999**, 3169–3175; b) R. Hiatt, R. J. Smythe, C. McColeman, *Can. J. Chem.,* **1971**, *49*, 1707–1711.

[116] a) F. De Simone, T. Saget, F. Benfatti, S. Almeida, J. Waser, *Chem. Eur. J.,* **2011**, *17*, 14527–14538; b) M. D. Martin, R. Shenje, S. France, *Isr. J. Chem.,* **2016**, *56*, 499–511; c) S. Takada, N. Takaki, K. Yamada, Y. Nishii, *Org. Biomol. Chem.,* **2017**, *16*, 2443–2449.

[117] Kwon Y. *Organoaluminum Mediated Interrupted Nazarov Reaction.* Ph.D. Dissertation, University of Alberta, **2015**

[118] S. Giese and F. G. West, *Tetrahedron,* **2000**, *56*, 10221–10228.

[119] T. D. White and F. G. West, *Tetrahedron Lett.,* **2005**, *46*, 5629–5632; P. Hofmann, A. Sieber, E. Beck, Schubert V. Z. *Naturforsch,* **1983**, *38*, 1192–1198.

[120] For more information on Prins type cyclizations check: a) C. E. Davis and R. M. Coates, *Angew. Chem., Int. Ed.*, **2002**, *41*, 491–493; b) N. D. Willmore, R. Goodman, H. H. Lee and R. M. Kennedy, *J. Org. Chem.*, **1992**, *57*, 1216–1219; c) H. J. Liu and D. Sun, *Tetrahedron Lett.*, **1997**, *38*, 6159–6162.

[121] a) M. Harmata, S. Elomari and C. L. Barnes, *J. Am. Chem. Soc.*, **1996**, *118*, 2860–2871;b) S. E. Denmark and R. C. Klix, *Tetrahedron*, **1988**, *44*, 4043–4060; c) V. Fiandanese, G. Marchese, A. Punzi and G. Ruggieri, *Tetrahedron Lett.*, **1996**, *37*, 8455–8458.

[122] V. M. Marx, F. M. LeFort, D. J. Burnell, *Adv. Synth. Catal.,* **2011**, *353*, 64–68.

[123] V. M. Marx, D. J. Burnell, *J. Am. Chem. Soc.*, **2010**, *132*, 1685–1689.

[124] V. M. Marx, T. S. Cameron, D. J. Burnell, *Tetrahedron Lett.*, **2009**, *50*, 7213–7216.

[125] J. Nie, H.-W. Zhu, H.-F. Cui, M.-Q. Hua, J.-A. Ma, *Org. Lett*., **2007**, *9*, 3053–3056; H.-F. Cui, K.-Y. Dong, G.-W. Zhang, L. Wang, J.-A. Ma, *Chem. Commun.* **2007**, 2284–2286.

[126] M. Rueping, W. Ieawsuwan, *Chem. Commun*., **2011**, *47*, 11450–11452.

[127] H. Zhang, B. Cheng, Z. Lu, *Org. Lett.,* **2018**, *20*, 4028–4031.

[128] D. J. Schatz, Y. Kwon, T. W. Scully, F. G. West, *J. Org. Chem.,* **2016**, *81*, 12494–12498.

[129] Hu, D. X.; Seidl, F. J.; Bucher, C.; Burns, N. Z. *J. Am. Chem. Soc.,* **2015***, 137*, 3795–3798.

[130] A. Novak, L. D. Humphreys, M. D. Walker, S. Woodward, *Tetrahedron Lett.*, **2006**, *47*, 5767–5769.

[131] A. Arnold, M. Markert, R. Mahrwald, *Synthesis,* **2006**, *7*, 1099–1102.

[132] O. Scadeng, M. J. Ferguson, F. G. West, *Org. Lett*. **2011**, *13*, 114–117.

[133] C. J. Rieder, K. J. Winberg, F. G. West, *J. Org. Chem.* **2011**, *76*, 50–56.

[134] Y. Wang, B. D. Schill, A. M. Arif, F. G. West, *Org. Lett*. **2003**, *5*, 2747–2750.

[135] Acetonitrile with dry ice was used to obtain a stable bath temperature of –41 ºC. See: R. E. Rondeau, Slush baths. *J. Chem. Eng. Data*, **1966**, *11*, 124.

[136] V. Aureggi, G. Sedelmeier, *Angew, Chem. Int. Ed.* **2007**, *46*, 8440–8444.

[137] N-Chlorosuccinimide. *e-EROS Encyclopedia of Reagents for Organic Synthesis* [Online]; Wiley & Sons, Posted April 15, 2006. http://onlinelibrary.wiley.com/doi/10.1002/ 047084289X.rc145.pub2/pdf (accessed July 20, 2017); N-Bromosuccinimide. *e-EROS Encyclopedia of Reagents for Organic Synthesis* [Online]; Wiley & Sons, Posted September 15, 2006. http://onlinelibrary.wiley.com/doi/10.1002/ 047084289X.rb318.pub2/pdf (accessed July 20, 2017)

[138] Z. Daneshfar, A. Rostami, *RSC Adv*. **2015**, *5*, 104695–104707.

[139] H. Hopf in *Classics in Hydrocarbon Chemistry*, Wiley-VCH, Weinheim, **2000**, pp. 218–227.

[140] A. P. Scott, I. Agranat, P. U. Biedermann, N. V. Riggs, L. Radom, *J. Org. Chem.* **1997**, *62*, 2026–2038.

[141] H. Hopf and M. S. Sherburn, *Angew. Chem. Int. Ed.* **2012**, *51*, 2298–2338.

[142] R. R. Tykwinski, M. Gholami, S. Eisler, Y. Zhao, F. Melin, L. Echegoyen, *Pure Appl. Chem.* **2008**, *80*, 621–637; H. Hopf, G. Maas in *The Chemistry of Dienes and Polyenes*, Vol. 1 (Ed.: Z. Rappoport), Wiley, Chichester, **1997**; H. Hopf, G. Maas, *Angew. Chem.* **1992**, *104*, 953–977; *Angew. Chem. Int. Ed. Engl.* **1992**, *31*, 931–954.

[143] A. Arnone, R. Cardillo, V. Dimodugno, G. Nasini, *J. Chem. Soc. Perkin Trans.* **1989**, *1*, 1995–2000.

[144] D. H. E. Tattje, R. Bos, A. P. Bruins, *Planta Med.* **1980**, *38*, 79–85.

[145] J. Wang, Z. Hu, J. Feng, Z. Su, X. Zhang, *Xibei Zhiwu Xuebao* **2008**, *28*, 1239–1245; L.-L. Xu, T. Han, J.-Z. Wu, Q.-Y. Zhang, H. Zhang, B.-K. Huang, K. Rahman, L.-P. Qin, *Phytomedicine*, **2009**, *16*, 609–616.

[146] G. R. Flematti, E. L. Ghisalberti, K.W. Dixon, R. D. Trengove, *Science*, **2004**, *305*, 977–978; N. Dennis, A. R. Katritzky, G. J. Sabounji, *Tetrahedron Lett.* **1976**, *17*, 2959–2960.

[147] T. Maccurin, J. Reilly, *Nature*, **1940**, *146*, 335.

[148] H. Hopf, *Angew. Chem.* **1984**, *96*, 947–958; *Angew. Chem. Int. Ed. Engl.* **1984**, *23*, 948–960.

[149] H. Hopf, *Nature*, **2009**, *460*, 183–184; H. Hopf, *Angew. Chem.* **2001**, *113*, 727–729; *Angew. Chem. Int. Ed.* **2001**, *40*, 705–707.

[150] H. Hopf in *Organic Synthesis Highlights V* (Eds.: H.-G. Schmalz, T.Wirth), Wiley-VCH, Weinheim, **2003**, pp. 419–427.

[151] A. D. Payne, G. Bojase, M. N. Paddon-Row, M. S. Sherburn, *Angew. Chem. Int. Ed.* **2009**, *48*, 4836–4839.

[152] M. F. Saglam, T. Fallon, M. N. Paddon-Row, M. S. Sherburn *J. Am. Chem. Soc.* **2016**, *138*, 1022−1032.

[153] A. D. Payne, G. Bojase, M. N. Paddon-Row, M. S. Sherburn, *Angew. Chem.* **2009**, *121*, 4930–4933; *Angew. Chem. Int. Ed.*, **2009**, *48*, 4836–4839.

[154] U. Norinder, *THEOCHEM*, **1987**, *150*, 85–91; B. Pullman, *Rev. Sci.* **1947**, *85*, 860–861; D. S. Bomse, T. H. Morton, *Tetrahedron Lett.* **1974**, *15*, 3491–3494; P. T. Brain, B. A. Smart, H. E. Robertson, M. J. Davis, D. W. H. Rankin, W. J. Henry, I. Gosney, *J. Org. Chem.* **1997**, *62*, 2767–2773.

[155] M. Gholami, R. R. Tykwinski, *Chem. Rev.* **2006**, *106*, 4997–5027; M. Coenen, O. Riester, J. Liebigs *Ann. Chem.,* **1960**, *633*, 110–118; V. Kral, L. Jelinek, D. Saman, *Collect. Czech. Chem. Commun.* **1989**, *54*, 2721–2730; Z. Arnold, V. Kral, G. V. Kryshtal, L. A. Yanovskaya, *Russ. Chem. Bull.* **1984**, *33*, 421–423; Z. Arnold, V. Kral, G. V. Kryshtal, L. A. Yanovskaya, *Izv. Akad. Nauk SSSR Ser. Khim.* **1984**, 457–459; F. Pochat, *Bull. Soc. Chim. Fr.* **1974**, *7*, 1373–1377; R. Vianello, B. Kovacevic, Z. B. Maksic, *New J. Chem.* **2002**, *26*, 1324–1328.

[156] A. W. V. Hofmann and J. Clark, *Phil. Trans. R. Soc.* **1997**, *141*, 357–398.

[157] V. M. Vdovin, E. S. Finkelshtein, A. V. Shelkov, M. S. Yatsenko, *Russ. Chem. Bull.* **1986**, *35*, 2364–2366; V. M. Vdovin, E. S. Finkelshtein, A. V. Shelkov, M. S. Yatsenko, *Izv. Akad. Nauk SSSR Ser. Khim.* **1986**, *35*, 2578–2580; S.-H. Dai, W. R. Dolbier, Jr., *J. Org. Chem.* **1972**, *37*, 950–955.

[158] H. Priebe, H. Hopf, *Angew. Chem.* **1982**, *94*, 299–300; *Angew. Chem. Int. Ed. Engl.* **1982**, *21*, 286–287; E. J. Corey, M. D. Alarcao, *Tetrahedron Lett.* **1986**, *27*, 3589–3590.

[159] J. I. G. Cadogan, S. Cradock, S. Gillam, I. Gosney, *J. Chem. Soc. Chem. Commun.* **1991**, 114–115.

[160] G. Bojase, A. D. Payne, A. C. Willis, M. S. Sherburn, *Angew. Chem.* **2008**, *120*, 924–926; *Angew. Chem. Int. Ed.* **2008**, *47*, 910–912. T. A. Bradford, A. D. Payne, A. C. Willis, M. N. Paddon-Row, M. S. Sherburn, *Org. Lett.* **2007**, *9*, 4861–4864; A. D. Payne, A. C. Willis, M. S. Sherburn, *J. Am. Chem. Soc.* **2005**, *127*, 12188–12189.

[161] S. Fielder, D. D. Rowan, M. S. Sherburn, *Angew. Chem.* **2000**, *112*, 4501–4503; *Angew. Chem. Int. Ed.* **2000**, *39*, 4331–4333.

[162] S. P. Bew, J. B. Sweeney, *Synlett*, **1997**, 1273–1274; S. P. Bew, J. B. Sweeney, *Synthesis*, **1994**, 698–699.

[163] A. D. Payne, G. Bojase, M. N. Paddon-Row, M. S. Sherburn, *Angew. Chem.* **2009**, *121*, 4930–4933; *Angew. Chem. Int. Ed.* **2009**, *48*, 4836–4839.

[164] T. A. Bradford, A. D. Payne, A. C. Willis, M. N. Paddon-Row, M. S. Sherburn, *J. Org. Chem.* **2010**, *75*, 491–494.

[165] R. Paul, S. Tchelitcheff, C. R. Hebd. *Seances Acad. Sci.* **1951**, *232*, 1939–1941.

[166] M. M. Selim, H. Gault, J. Delahaye, C. R. *Hebd. Seances Acad. Sci.* **1963**, *257*, 4191–4192.

[167] P. Miginiac, L. Miginiac, C. R. *Hebd. Seances Acad. Sci.* **1964**, *258*, 236–237; C. W. Spangler, *Tetrahedron*, **1976**, *32*, 2681–2684.

[168] C. J. Rieder, K. J. Winberg, F. G. West, *J. Org. Chem.* **2011**, *76*, 50–56.

[169] For additional information on the Meyer-Schuster rearrangement see: a) S. S. Lopez, D. A. Engel, G. B. Dudley, *Synlett* **2007**, 949–953; b) N. Marion, P. Carlqvist, R. Gealageas, P. de Frémont, F. Maseras, S. P. Nolan, *Chem., Eur. J.* **2007**, *13*, 6437–6451; c) S. I. Lee, J. Y. Baek, S. H. Sim, *Synthesis* **2007**, 2107–2114; d) D. A. Engel, S. S. Lopez, G. B. Dudley, *Tetrahedron,* **2008**, *64*, 6988–6996; e) B. M. Trost, R. C. Livingston, *J. Am. Chem. Soc.* **2008**, *130*, 11970–11978; f) D. A. Engel, G. B. Dudley, *Org. Biomol. Chem.* **2009**, *7*, 4149–4158; g) V. Cadierno, J. Frandos, J. Gimeno, *Tetrahedron Lett.* **2009**, *50*, 4773–4776.

[170] C. J. Rieder, K. J.Winberg, F. G.West, *J. Am. Chem. Soc.* **2009**, *131*, 7504–7505.

[171] P. A. Wender, V. A. Verma, T. J. Paxton, T. H. Pillow, *Acc. Chem. Res.* **2007**, *41*, 40–49; L. F. Tietze, *Chem. Rev.* **1996**, *96*, 115–136; L. F. Tietze, U. Beifuss, *Angew. Chem.* **1993**, *105*, 137–170; *Angew. Chem. Int. Ed. Engl.* **1993**, *32*, 131–163.

[172] O. Tsuge, E. Wada, S. Kanemasa, H. Sakoh, *Bull. Chem. Soc. Jpn.* **1984**, *57*, 3221–3233; O. Tsuge, S. Kanemasa, H. Sakoh, E. Wada, *Chem. Lett.* **1984**, 273–276; O. Tsuge, E. Wada, S. Kanemasa, *Chem. Lett.* **1983**, 239–242; S. Kanemasa, H. Sakoh, E. Wada, O. Tsuge, *Bull. Chem. Soc. Jpn.* **1986**, *59*, 1869–1876; O. Tsuge, T. Hatta, T. Fujiwara, T. Yokohari, A. Tsuge, T. Moriguchi, *Heterocycles,* **1999**, *50*, 661–666; O. Tsuge, T. Hatta, K. Yakata, H. Maeda, *Chem. Lett.* **1994**, 1833–1836; O. Tsuge, T. Hatta, H. Yoshitomi, K. Kurosaka, T. Fujiwara, H. Maeda, A. Kakehi, *Heterocycles*, **1995**, *41*, 225–228; E. Wada, S. Kanemasa, O. Tsuge, *Bull. Chem. Soc. Jpn.* **1989**, *62*, 1198–1204; O. Tsuge, S. Kanemasa, H. Sakoh, E. Wada, *Bull. Chem. Soc. Jpn.* **1984**, *57*, 3234–3241; O. Tsuge, S. Kanemasa, H. Sakoh, E. Wada, *Chem. Lett.* **1984**, 277–278; O. Tsuge, E. Wada, S. Kanemasa, *Chem. Lett.* **1983**, 1525–1528; S. Kanemasa, H. Sakoh, E. Wada, O. Tsuge, *Bull. Chem. Soc. Jpn.* **1985**, *58*, 3312–3319.

[173] R. R. Kostikov, A. P. Molchanov, *Zh. Org. Khim.* **1975**, *11*, 449–450; R. R. Kostikov, A. P. Molchanov, *Zh. Org. Khim.* **1975**, *11*, 438–439.

[174] E. G. Ter-Gabrielyan, Z. N. Parnes, N. P. Gambaryan, L. A. Simonyan, *Russ. Chem. Bull.* **1983**, *32*, 1504–1506; E. G. Ter-Gabrielyan, Z. N. Parnes, N. P. Gambaryan, L. A.

Simonyan, *Izv. Akad. Nauk SSSR Ser. Khim.* **1983**, *33*, 1656–1658; M. Y. Antipin, Y. T. Struchkov, E. G. Ter-Gabrielyan, N. P. Gambaryan, *Russ. Chem. Bull.* **1981**, *30*, 431–437; M. Y. Antipin, Y. T. Struchkov, E. G. Ter-Gabrielyan, N. P. Gambaryan, *Izv. Akad. Nauk SSSR Ser. Khim.* **1981**, *30*, 588–592; I. L. Knunyants, E. G. Ter-Gabrielyan, Y. V. Zeifman, Z. V. Safronova, N. P. Gambaryan, E. I. Mysov, A. I. Lutsenko, P. V. Petrovskii, *Dokl. Akad. Nauk SSSR*, **1976**, *228*, 438–440; I. L. Knunyants, E. G. Ter-Gabrielyan, Y. V. Zeifman, Z. V. Safronova, N. P. Gambaryan, E. I. Mysov, A. I. Lutsenko, P. V. Petrovskii, *Dokl. Akad. Nauk SSSR,* **1976**, *228*, 1344–1346.

[175] E. G. Ter-Gabrielyan, N. P. Gambaryan, E. P. Lure, P. V. Petrovskii, *Russ. Chem. Bull.* **1979**, *28*, 992–994; E. G. Ter-Gabrielyan, N. P. Gambaryan, E. P. Lure, P. V. Petrovskii, *Izv. Akad. Nauk SSSR Ser. Khim.* **1979**, 1061–1064.

[176] E. G. Ter-Gabrielyan, N. P. Gambaryan, *Russ. Chem. Bull.* **1986**, *35*, 1217–1219; E. G. Ter-Gabrielyan, N. P. Gambaryan, *Izv. Akad. Nauk SSSR Ser. Khim.* **1986**, 1341–1344; V. G. Ter-Gabrielyan, N. P. Gambaryan, E. P. Lure, I. L. Knunyants, *Dokl. Akad. Nauk SSSR,* **1980**, *228*, 459–462; V. G. Ter-Gabrielyan, N. P. Gambaryan, E. P. Lure, I. L. Knunyants, *Dokl. Akad. Nauk SSSR*, **1980**, *254*, 898–902.

[177] a) N. Boccara, P. Maitte, *Bull. Soc. Chim. Fr.* **1972**, 3810–3814; b) W. Li, M. Shi, Y. Li, *Chem. Eur. J.* **2009**, *15*, 8852–8860.

[178] H. Pellissier, *Tetrahedron*, **2005**, *61*, 6479–6517; A. J. Frontier, C. Collison, *Tetrahedron,* **2005**, *61*, 7577–7606; M. A. Tius, Eur. *J. Org. Chem.* **2005**, 2193–2206.

[179] G. Sudhakar, S. K. Mahesh, S. P. B. Vemulapalli, J. B. Nanubolu, *Org. Lett.,* **2017**, *19*, 4500–4503.

[180] K. R. Bharucha, B. C. L. Weedon, *J. Chem. Soc.*, **1953**, 1571–1577.

[181] a) S. Matsubara, T. Okazoe, K. Oshima, K. Takai, H. Nozaki, *Bull. Chem. Soc. Jpn.* **1985**, *58*, 844–849; b) S. Bellemin–Laponnaz, J.–P. Le Ny, *C. R. Chimie,* **2002**, *5*, 217–224; c) S. Akai, K. Tanimoto, Y. Kanao, M. Egi, T. Yamamoto, Y. Kita, *Angew. Chem.* **2006**, *118*, 2653–2657.

[182] R. J.Fradette, M. Kang, F. G. West, *Angew. Chem. Int. Ed.* **2017**, *56*, 6335–6338.

[183] G. Schröder in *Ullmann's Encyclopedia of Industrial Chemistry.* Wiley-VCH, Weinheim, **2000,** vol 28, pp. 481–485.

[184] a) B. A. Hess and J.E. Baldwin, *J. Org. Chem.* **2002**, *67*, 17, 6025–6033; b) B. S. Jursic, *THEOCHEM*, **1998**, *423*, 189–194; c) N. J. Saettel, O. Wiest, *J. Org. Chem.* **2000**, *65*, 2331–2336.

[185] T. Yasunori, H. Yoshitaka, S. Mikiko, *Org Lett.* **2006**, *8*, 4851–4854.

[186] a) R. A. Pilli, G. B. Rosso and M. C. F. de Oliveira, *Nat. Prod. Rep.*, **2010**, *27*, 1908–1937; b) R. R. Parvatkar, C. D. Souza, A. Tripathi and C. G. Naik, *Phytochemistry*, **2009**, *70*, 128–132; c) Y. Aoyagi, A. Yamazaki, C. Nakatsugawa, H. Fukaya, K. Takeya, S. Kawauchi and H. Izumi, *Org. Lett.*, **2008**, *10*, 4429–4432; d) T. Murakami, Y. Morikawa, M. Hashimoto, T. Okuno and Y. Harada, *Org. Lett.*, **2004**, *6*, 157–160; e) G. R. Flematti, E. L. Ghisalberti, K. W. Dixon and R. D. Trengove, *Science*, **2004**, *305*, 977.

[187] Reviews: a) T. M. Ugurchieva, V. V. Veselovsky, *Russ. Chem. Rev.* **2009**, *78*, 337–373; b) N. B. Carter, A. E. Nadany, J. B. Sweeney, *J. Chem. Soc.,* **2002**, *1*, 2324–2342.

[188] a) T. Murakami, A. Sasaki, E. Fukushi, J. Kawabata, M. Hashimoto, T. Okuno, *Bioorg. Med. Chem. Lett*. **2005**, *15*, 2591–2595; b) T. Kuwahara, T. Kudoh, H. Nagase, M. Takamiya, A. Nakano, T. Ohtsuka, H. Yoshizaki and M. Arisawa, *Eur. J. Pharmacol.*, **1992**, *221*, 99–105.

[189] Y. Li, T. Zhang, Y.-L. Li, *Tetrahedron Lett.*, **2007**, *48*, 1503–1505.

[190] For more information on lactam's synthesis: a) K. Kim and S. H. Hong, *J. Org. Chem.*, **2015**, *80*, 41524–41527; b) A. S. Touchy, S. M. A. H. Siddiki, K. Kon and K.-I. Shimizu, *ACS Catal.*, **2014**, *4*, 3045–3050; c) R.-Q. Ran, J. He, S.-D. Xiu, K.-B. Wang and C.-Y. Li, *Org. Lett.*, **2014**, *16*, 3704–3707; d) Y. Hoshimoto, T. Ohata, Y. Sasaoka, M. Ohashi and S. Ogoshi, *J. Am. Chem. Soc.*, **2014**, *136*, 15877–15880; e) M. K. Ghorai and D. P. Tiwari, *J. Org. Chem.*, **2010**, *75*, 6173–6181.

[191] Unsaturated lactones synthesis: a) S. Li, B. Miao, W. Yuan and S. Ma, *Org. Lett.*, **2013**, *15*, 977–979; b) M. Egi, Y. Ota, Y. Nishimura, K. Shimizu, K. Azechi and S. Akai, *Org. Lett.*, **2013**, *15*, 4150–4153; c) D. M. Browne, O. Niyomura and T. Wirth, *Org. Lett.*, **2007**, *9*, 3169–3171; d) M. Alfonsi, A. Arcadi, M. Chiarini and F. Marinelli, *J. Org. Chem.*, **2007**, *72*, 9510–9157; e) Y. Liu, F. Song and S. Guo, *J. Am. Chem. Soc.*, **2006**, *128*, 11332–11333; f) C. Fu and S. Ma, *Eur. J. Org. Chem.*, **2005**, 3942–3943.

[192] a) A. D'Annibale, L. Ciaralli, M. Bassetti, C. Pasquini, *J. Org. Chem.* **2007**, *72*, 6067–6074; b) J. A. Marco, M. Carda, S. Rodrıguez, E. Castillo, M. N. Kneeteman, *Tetrahedron*, **2003**, *59*, 4085–4101.

[193] a) S. Ma, Z. Yu, *Angew. Chem., Int. Ed.* **2002**, *41*, 1775–1778; b) R. Lin, L. Cao and F. G. West, *Org Lett.* **2017**, *19*, 3, 552–555.

[194] M. Alfonsi, A. Arcadi, M. Chiarini, F. Marinelli, *J. Org. Chem.* **2007**, *72*, 9510–9517; b) C. H. Oh, S. J. Park, J. H. Ryu, A. K. Gupta, *Tetrahedron Lett.* **2004**, *45*, 7039–7042.

[195] U. Albrecht, P. Langer, *Tetrahedron*, **2007**, *63*, 4648–4654.

[196] C. Kuroda, N. Mitsumata and C. Y. Tang, *Bull. Chem. Soc. Jpn.*, **1996**, *69*, 1409–1416.

[197] M. J. Riveira, L. A. Marsili and M. P. Mischme, *Org. Biomol. Chem.*, **2017**, *15*, 9255–9274.

[198] S. A. Bonderoff, T. N. Grant, F. G. West, and M. Tremblay, *Org. Lett.* **2013**, *15*, 11, 2888–2891.

[199] Y. K. Kumar, G. R. Kumar and M. S. Reddy, *Org. Biomol. Chem.*, **2016**, ***14***, 1252–1260.

Appendix I: Selected Organoaluminum Initiated Nazarov Cyclization NMR Spectra (Chapter 2)

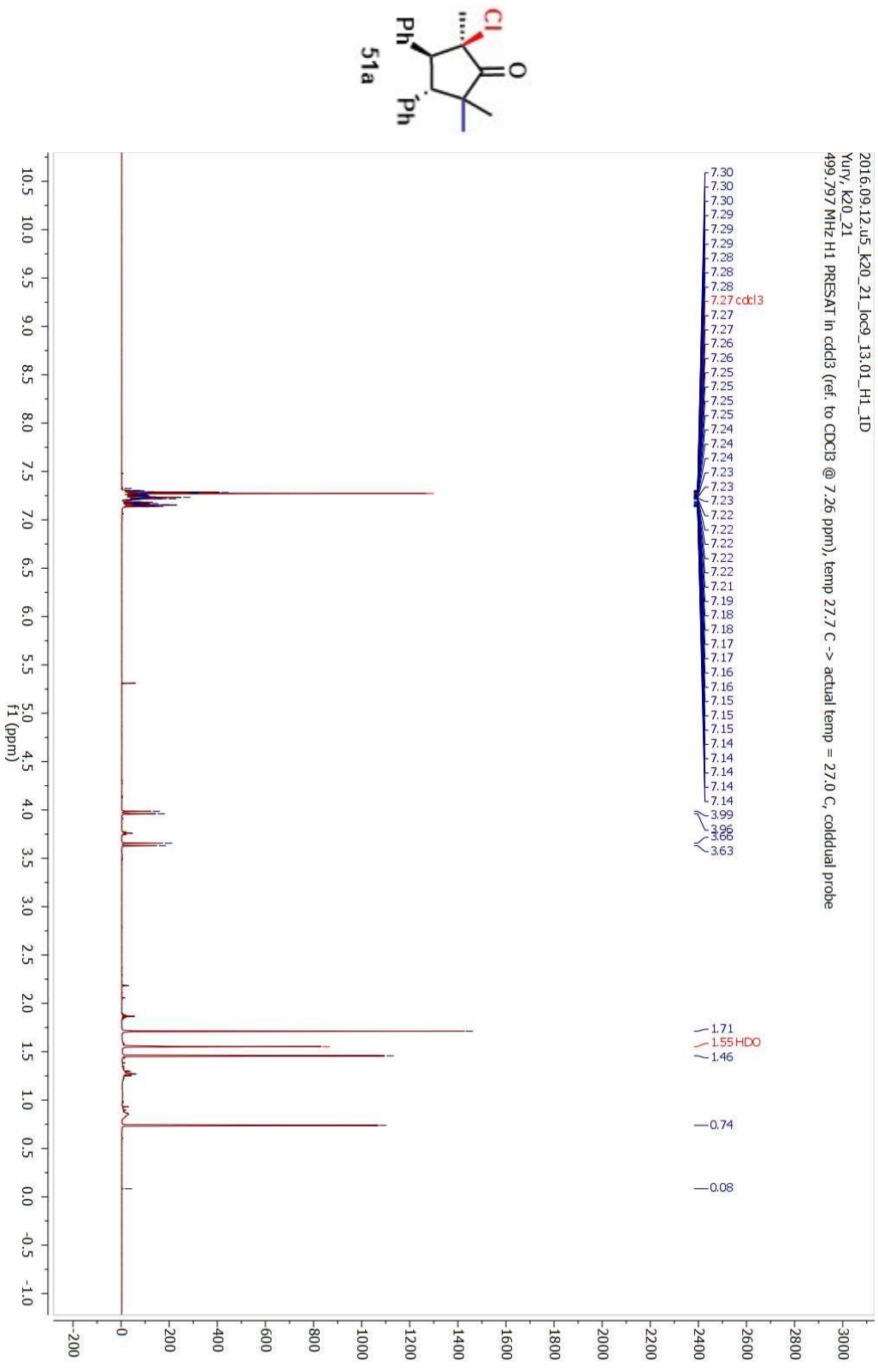
51a
Cl
O
Ph
Ph
2016.09.12.u5_k20_21_loc9_13.01_H1_1D
Yury, k20_21
499.797 MHz H1 PRESAT in cdcl3 (ref. to CDCl3 @ 7.26 ppm), temp 27.7 C -> actual temp = 27.0 C, colddual probe
7.27 cdcl3
1.71
1.55 HDO
1.46
0.74
0.08
f1 (ppm)

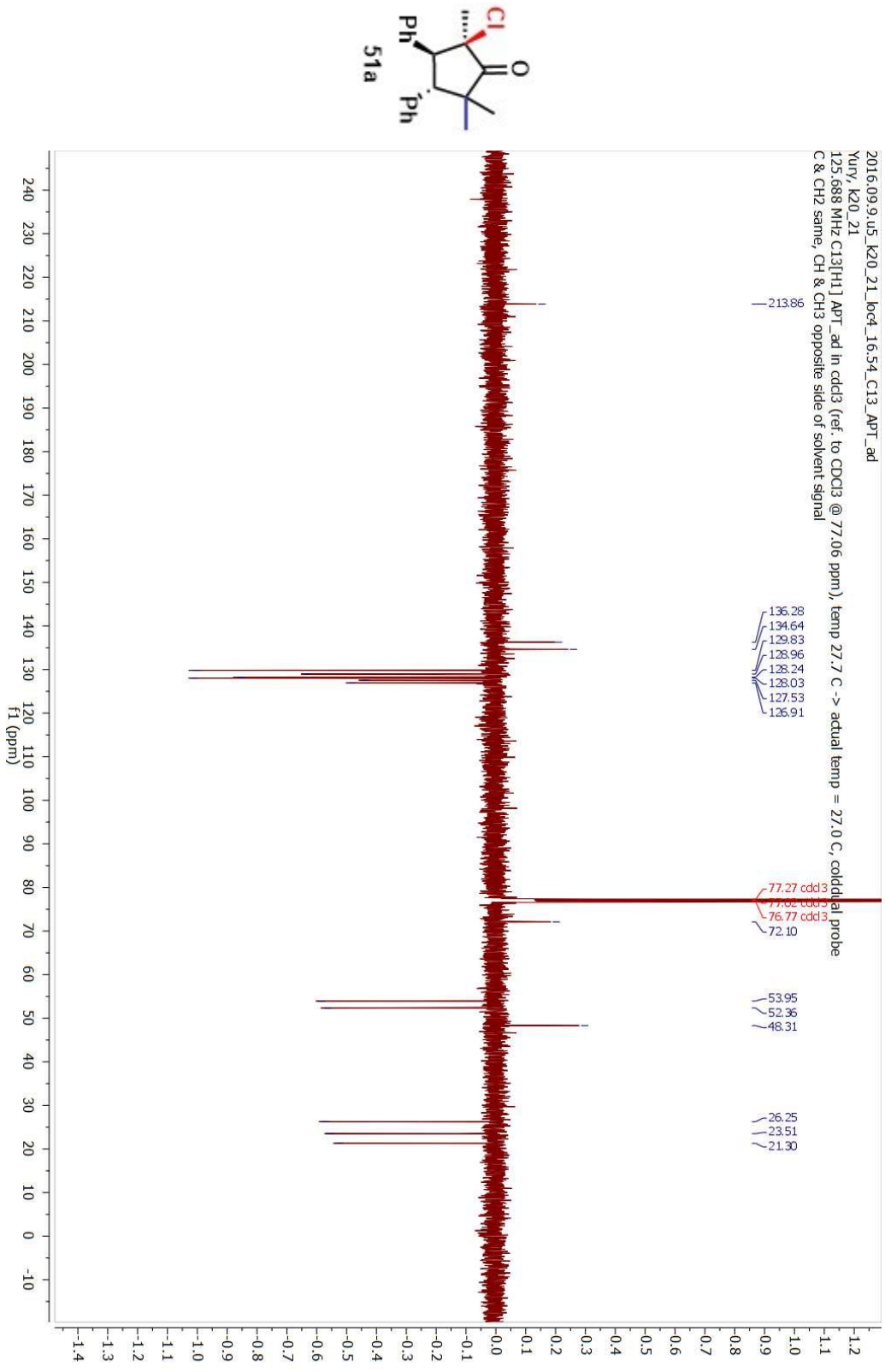
51a
Cl
O
Ph
Ph
2016.09.9.u5_K20_21_loc4_16.54_C13_APT_ad
Yury, k20_21
125.688 MHz C13[H1] APT_ad in cdcl3 (ref. to CDCl3 @ 77.06 ppm), temp 27.7 C -> actual temp = 27.0 C, colddual probe
C & CH2 same, CH & CH3 opposite side of solvent signal
213.86
136.28
134.64
129.83
128.96
128.24
128.03
127.53
126.91
77.27 cdcl3
76.77 cdcl3
72.10
53.95
52.36
48.31
26.25
23.51
21.30
f1 (ppm)

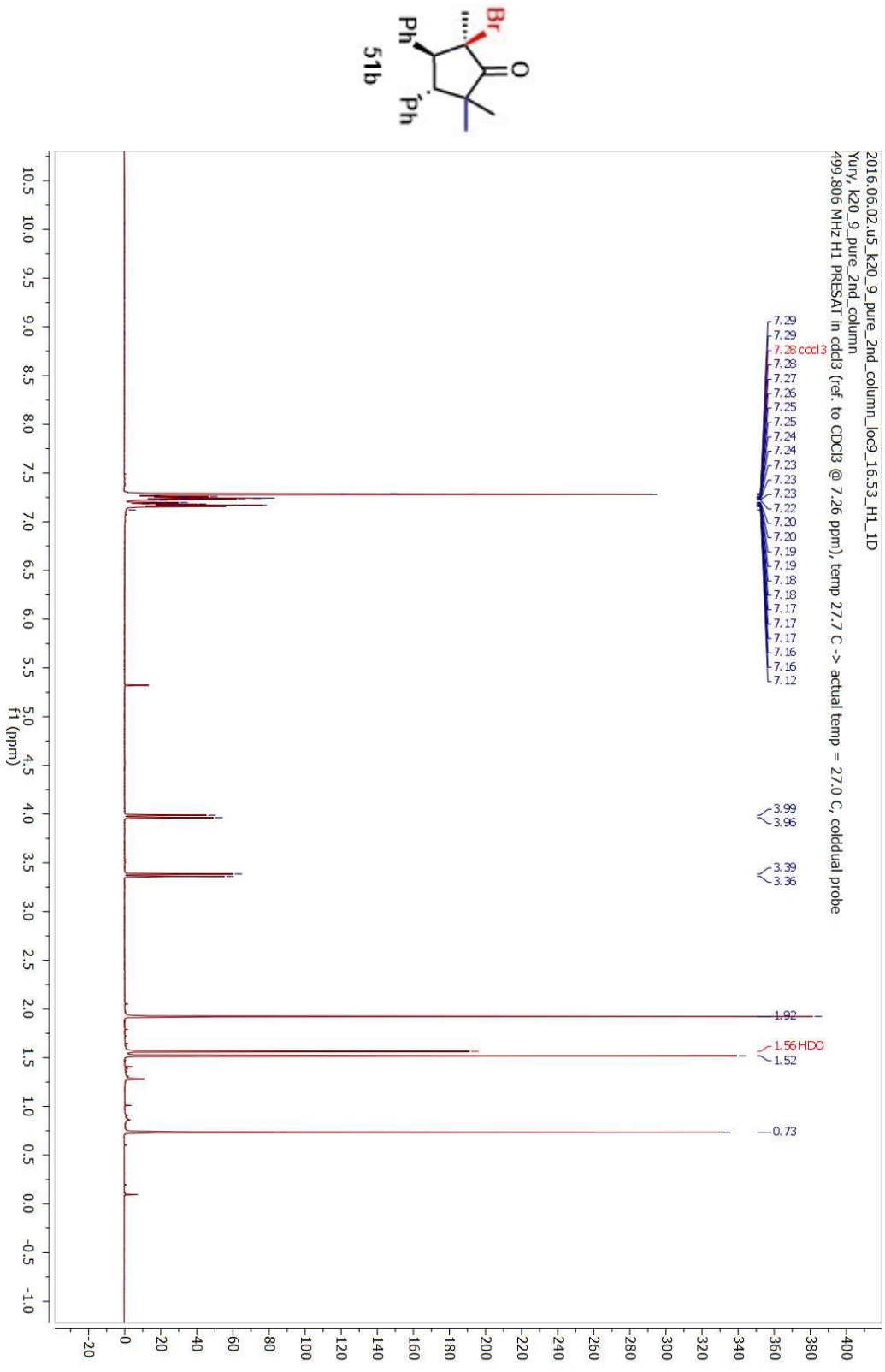
Br
O
Ph
Ph
51b
2016.06.02.u5_k20_9_pure_2nd_column_loc9_16.53_H1_1D
Yury, k20_9_pure_2nd_column
499.806 MHz H1 PRESAT in cdcl3 (ref. to CDCl3 @ 7.26 ppm), temp 27.7 C -> actual temp = 27.0 C, colddual probe
7.29
7.29
7.28 cdcl3
7.28
7.27
7.26
7.25
7.25
7.24
7.24
7.23
7.23
7.23
7.22
7.20
7.20
7.19
7.19
7.18
7.18
7.17
7.17
7.17
7.16
7.16
7.12
3.99
3.96
3.39
3.36
1.92
1.56 HDO
1.52
0.73
f1 (ppm)

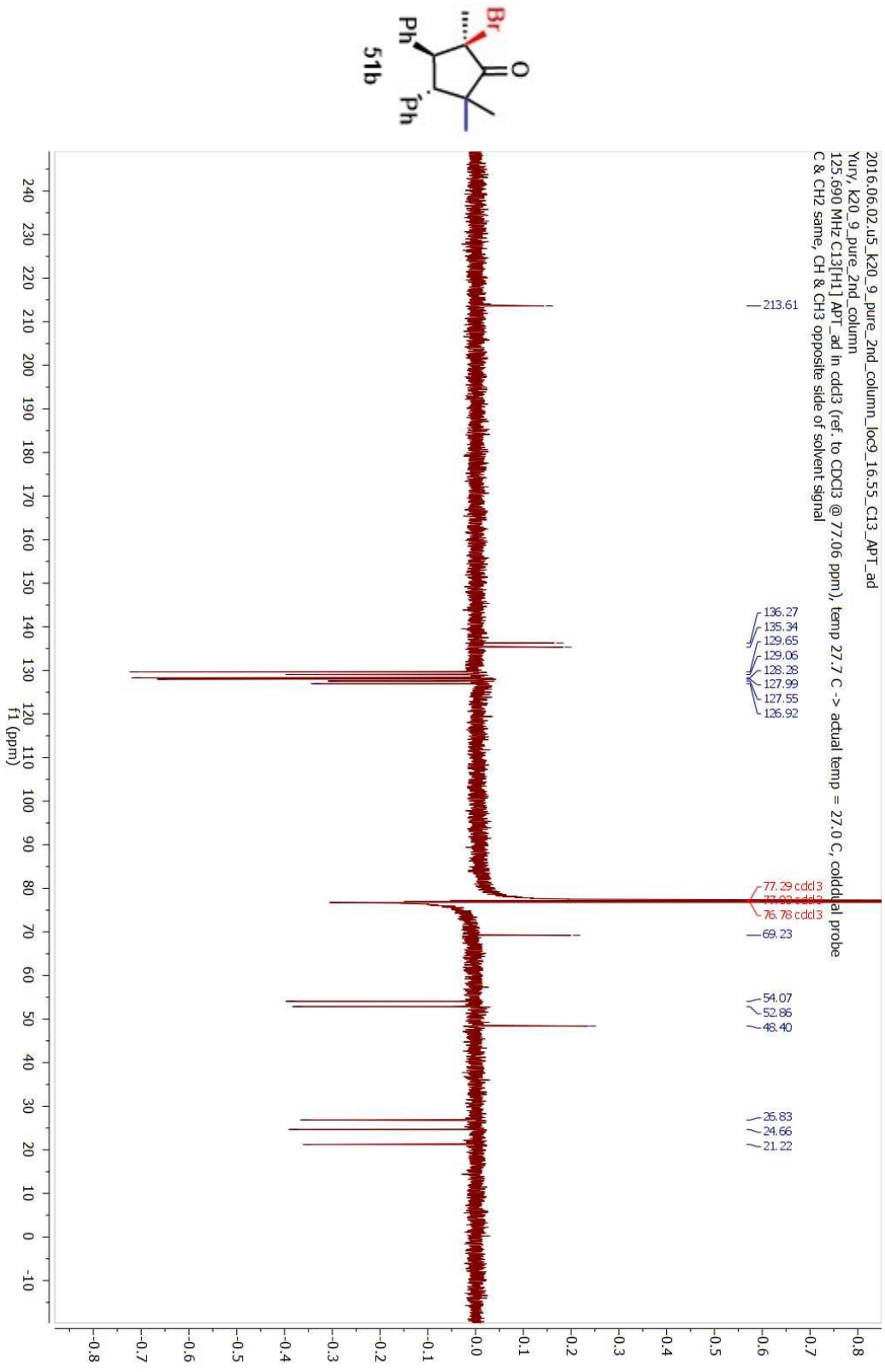
Br
O
Ph
Ph
51b
2016.06.02.u5_k20_9_pure_2nd_column_loc9_16:55_C13_APT_ad
Yury, k20_9_pure_2nd_column
125.690 MHz C13[H1] APT_ad in cdcl3 (ref. to CDCl3 @ 77.06 ppm), temp 27.7 C -> actual temp = 27.0 C, colddual probe
C & CH2 same, CH & CH3 opposite side of solvent signal
213.61
136.27
135.34
129.65
129.06
128.28
127.99
127.55
126.92
77.29 cdcl3
76.78 cdcl3
69.23
54.07
52.86
48.40
26.83
24.66
21.22
f1 (ppm)

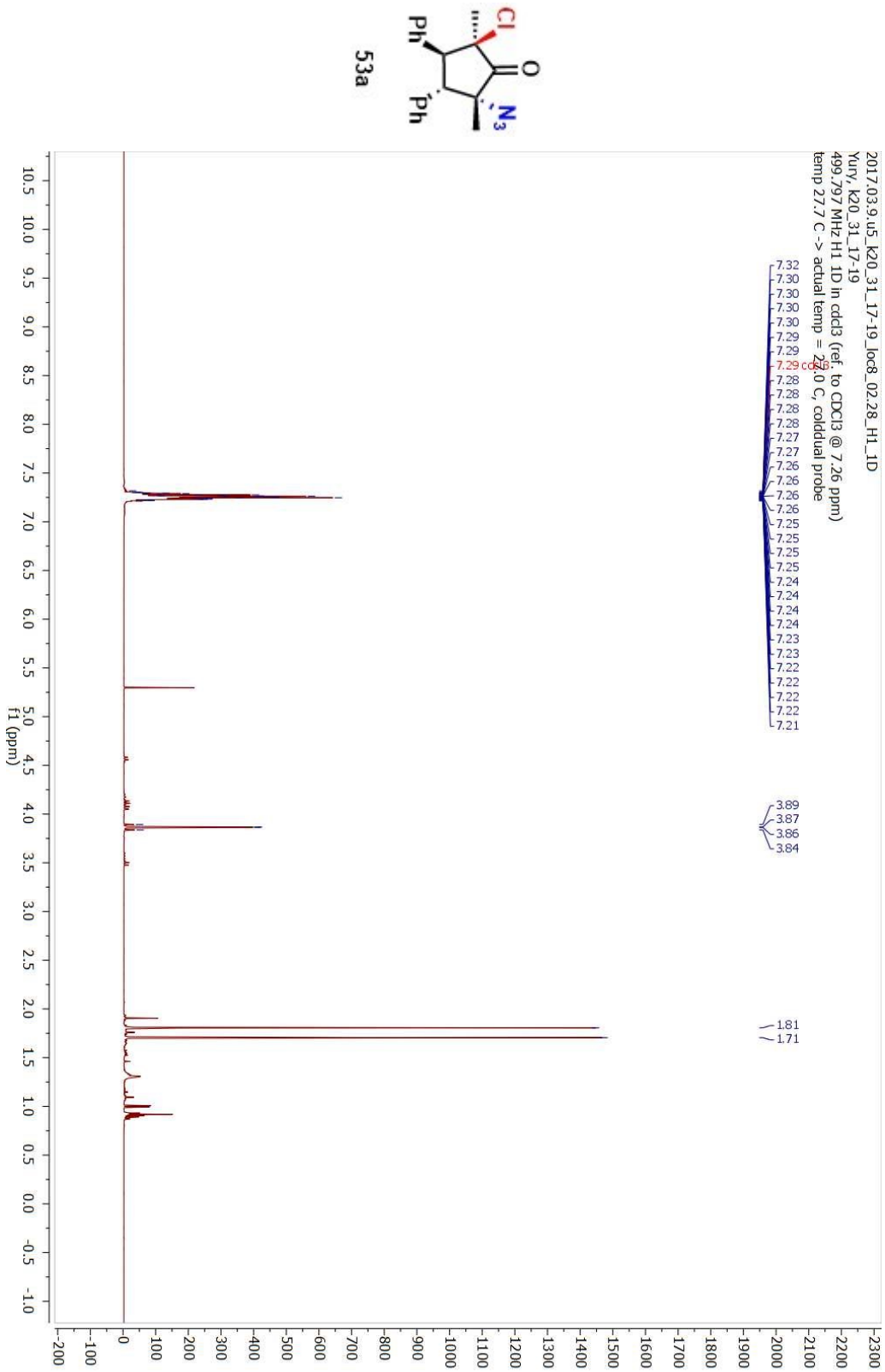
53a
Cl
O
N3
Ph
Ph
2017.03.9.u5_k20_31_17-19_loc8_02.28_H1_1D
Yury, k20_31_17-19
499.797 MHz H1 1D in cdcl3 (ref. to CDCl3 @ 7.26 ppm)
temp 27.7 C -> actual temp = 21.0 C, colddual probe
7.32
7.30
7.30
7.30
7.30
7.29
7.29
7.29 CDCl3
7.28
7.28
7.28
7.28
7.27
7.27
7.26
7.26
7.26
7.26
7.25
7.25
7.25
7.25
7.24
7.24
7.24
7.24
7.23
7.23
7.22
7.22
7.22
7.22
7.21
3.89
3.87
3.86
3.84
1.81
1.71
f1 (ppm)

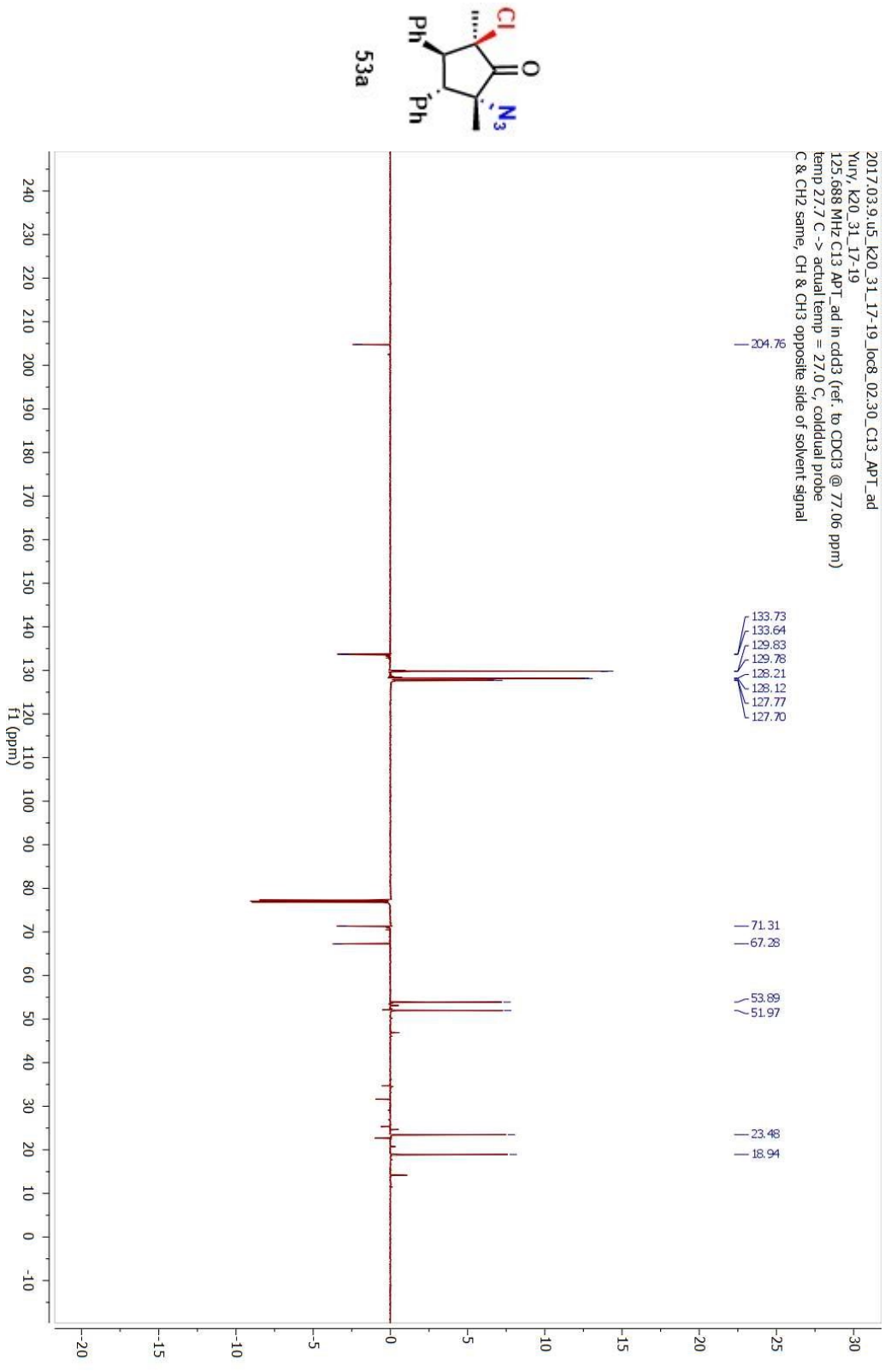
2017.03.9.u5_k20_31_17-19_loc8_02.30_C13_APT_ad
Yury, k20_31_17-19
125.688 MHz C13 APT_ad in cdcl3 (ref. to CDCl3 @ 77.06 ppm)
temp 27.7 C -> actual temp = 27.0 C, colddual probe
C & CH2 same, CH & CH3 opposite side of solvent signal
53a
Cl
O
N3
Ph
Ph
204.76
133.73
133.64
129.83
129.78
128.21
128.12
127.77
127.70
71.31
67.28
53.89
51.97
23.48
18.94
f1 (ppm)

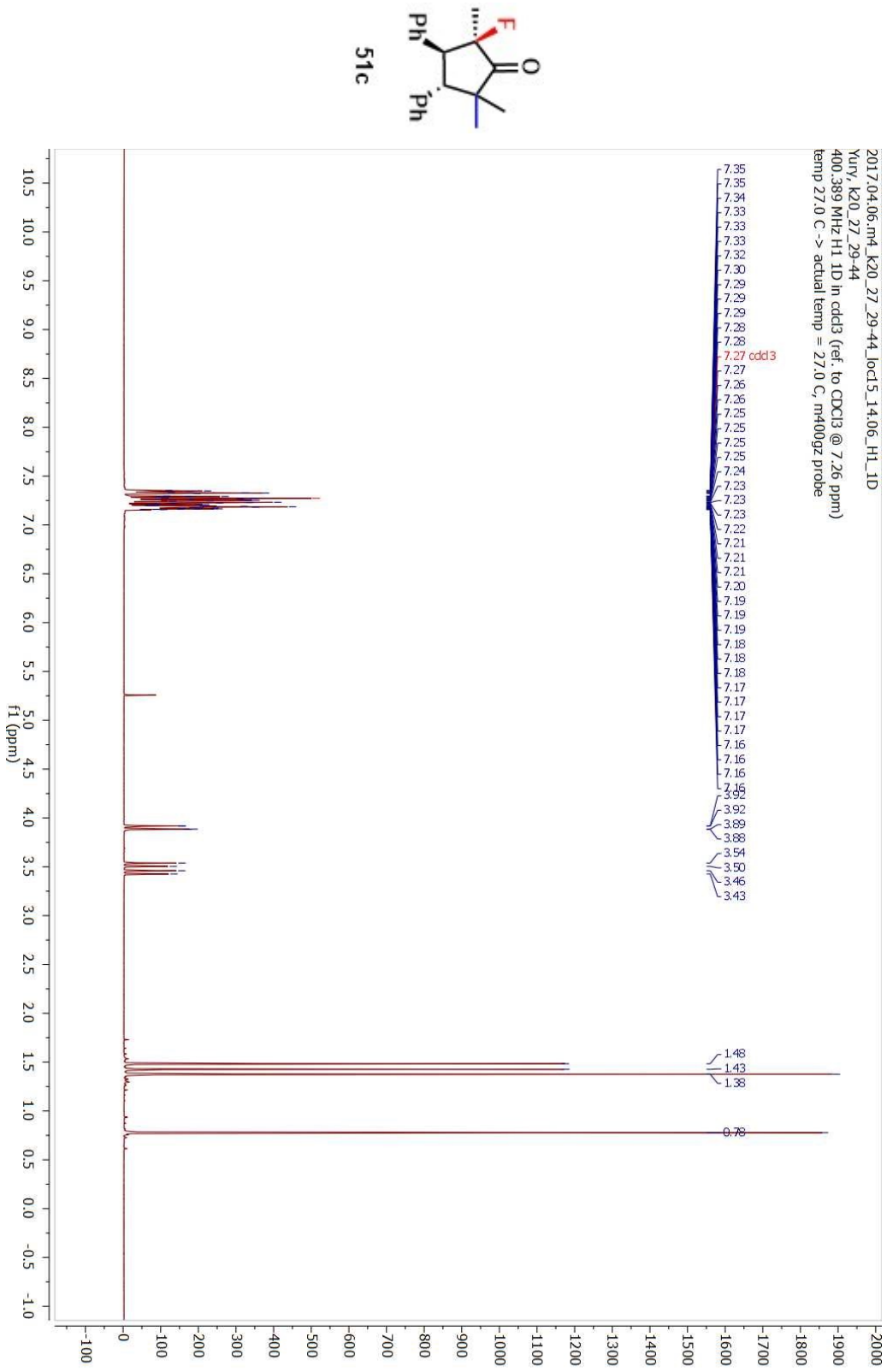
51c
Ph
Ph
F
O
2017.04.06.m4_k20_27_29-44_loc15_14.06_H1_1D
Yury, k20_27_29-44
400.389 MHz H1 1D in cdcl3 (ref. to CDCl3 @ 7.26 ppm)
temp 27.0 C -> actual temp = 27.0 C, m400gz probe
7.27 cddl3
1.48
1.43
1.38
0.78
f1 (ppm)

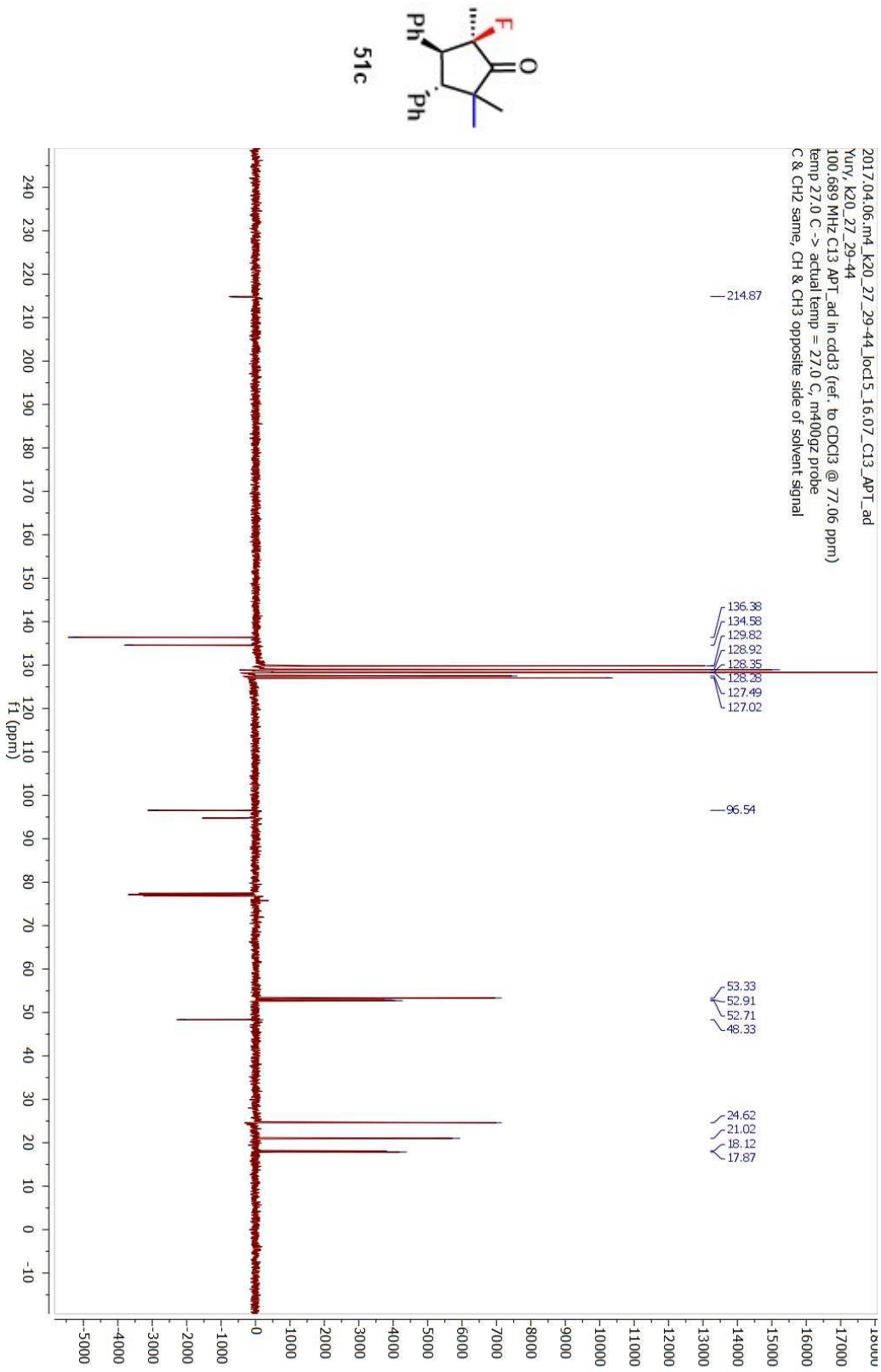
51c
F
O
Ph
Ph
2017.04.06.m4_k20_27_29-44_loct5_16.07_C13_APT_ad
Yury, k20_27_29-44
100.689 MHz C13 APT_ad in cdd3 (ref. to CDCl3 @ 77.06 ppm)
temp 27.0 C -> actual temp = 27.0 C, m400gz probe
C & CH2 same, CH & CH3 opposite side of solvent signal
214.87
136.38
134.58
129.82
128.92
128.35
128.28
127.49
127.02
96.54
53.33
52.91
52.71
48.33
24.62
21.02
18.12
17.87
f1 (ppm)


O
F
Ph
Ph

51c

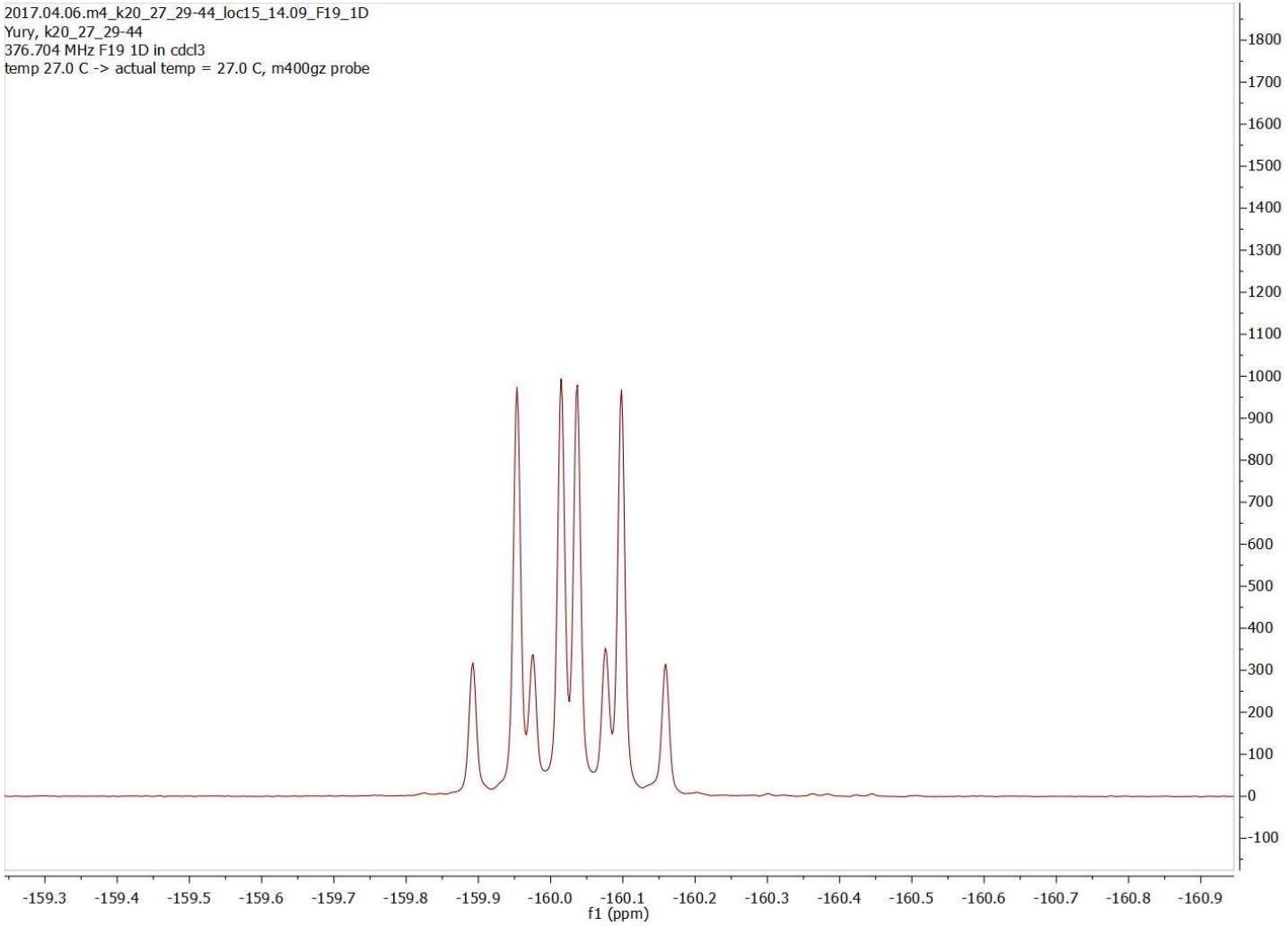
2017.04.06.m4_k20_27_29-44_loc15_14.09_F19_1D
Yury, k20_27_29-44
376.704 MHz F19 1D in cdcl3
temp 27.0 C -> actual temp = 27.0 C, m400gz probe
1800
1700
1600
1500
1400
1300
1200
1100
1000
900
800
700
600
500
400
300
200
100
0
-100
-159.3
-159.4
-159.5
-159.6
-159.7
-159.8
-159.9
-160.0
-160.1
-160.2
-160.3
-160.4
-160.5
-160.6
-160.7
-160.8
-160.9
f1 (ppm)

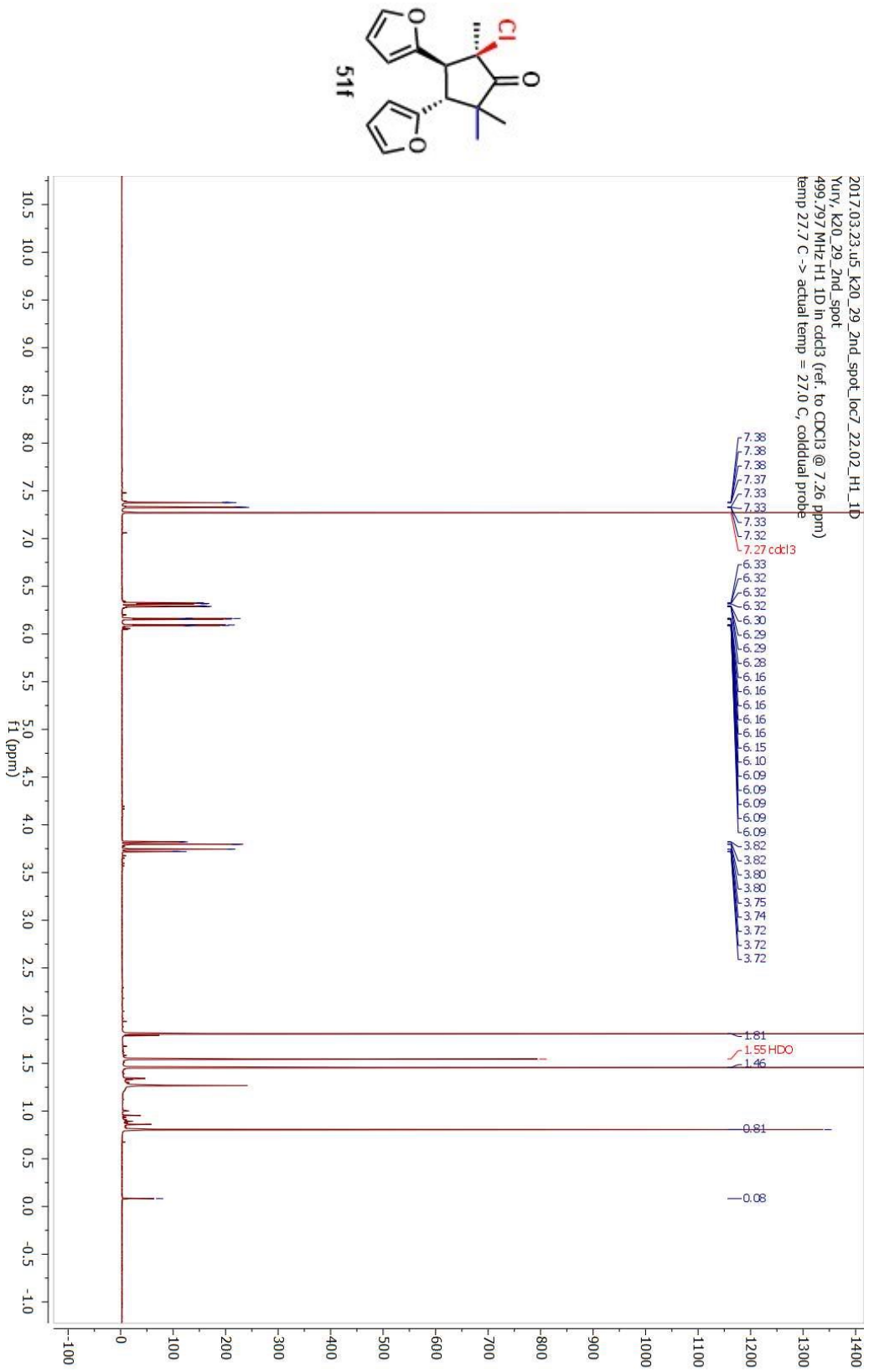
51f
Cl
O
O
O
2017.03.23.u5_k20_29_2nd_spot_loc7_22.02_H1_1D
Yury, k20_29_2nd_spot
499.797 MHz H1 1D in cdcl3 (ref. to CDCl3 @ 7.26 ppm)
temp 27.7 C -> actual temp = 27.0 C, colddual probe
7.38
7.38
7.38
7.37
7.33
7.33
7.33
7.32
7.27 cdcl3
6.33
6.32
6.32
6.32
6.30
6.29
6.29
6.28
6.16
6.16
6.16
6.16
6.16
6.15
6.10
6.09
6.09
6.09
6.09
6.09
3.82
3.82
3.80
3.80
3.75
3.74
3.72
3.72
3.72
1.81
1.55 HDO
1.46
0.81
0.08
f1 (ppm)

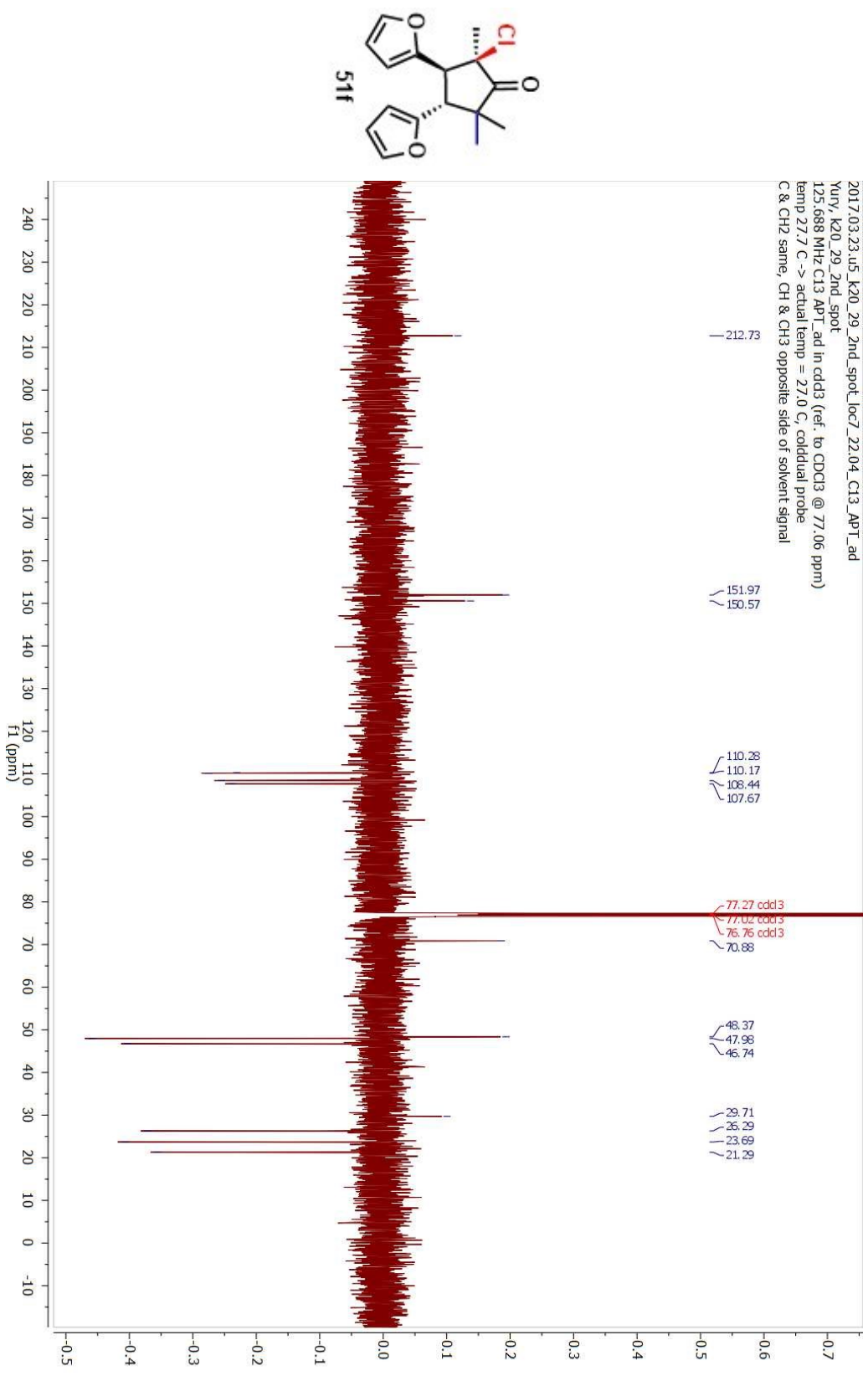
51f
Cl
O
O
O
2017.03.23.u5_k20_29_2nd_spot_loc7_22.04_C13_APT_ad
Yury, k20_29_2nd_spot
125.688 MHz C13 APT_ad in cdcl3 (ref. to CDCl3 @ 77.06 ppm)
temp 27.7 C -> actual temp = 27.0 C, colddual probe
C & CH2 same, CH & CH3 opposite side of solvent signal
212.73
151.97
150.57
110.28
110.17
108.44
107.67
77.27 cdcl3
77.02 cdcl3
76.76 cdcl3
70.88
48.37
47.98
46.74
29.71
26.29
23.69
21.29
f1 (ppm)

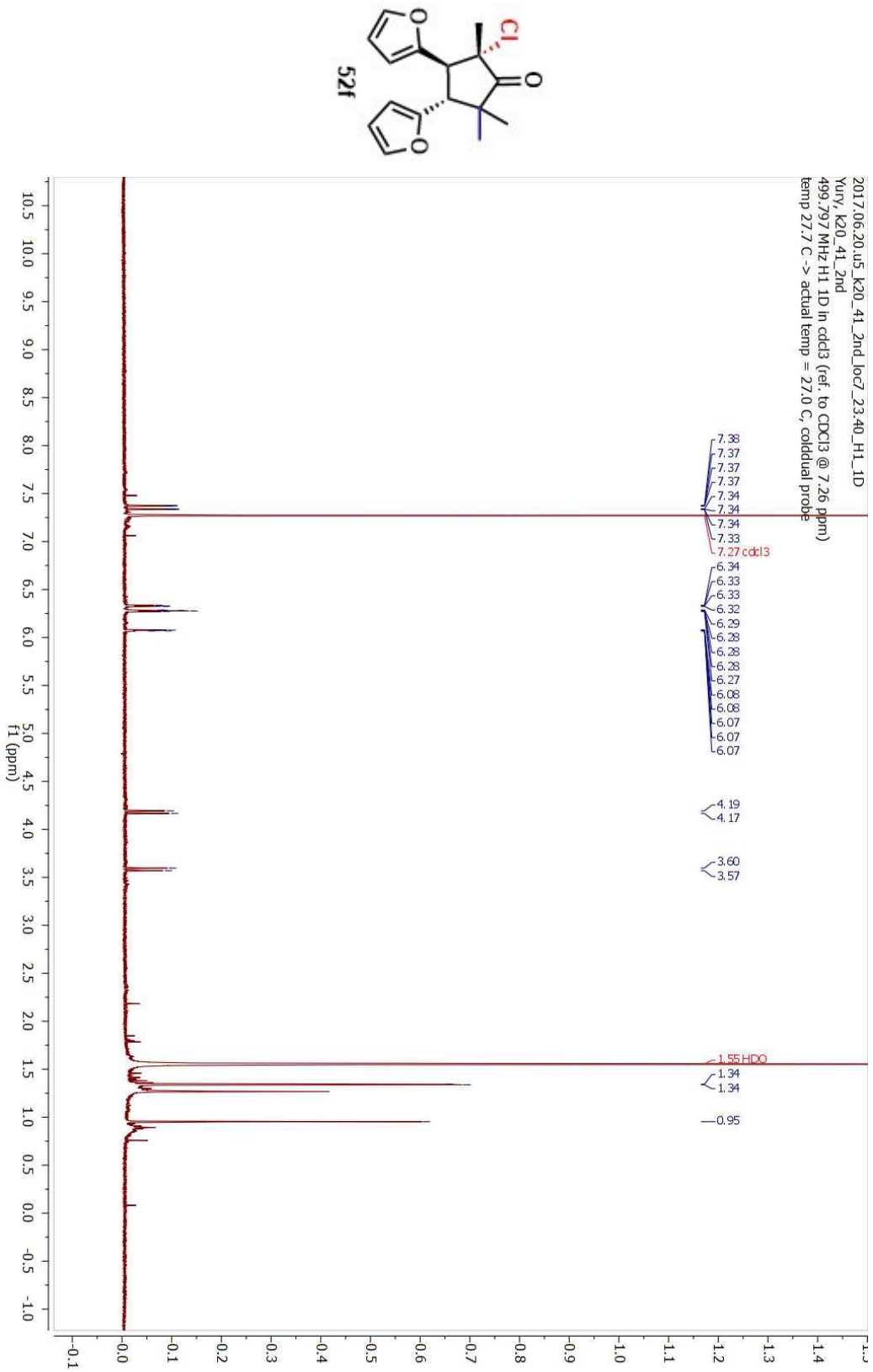
52f
Cl
O
O
O
2017.06.20.u5_k20_41_2nd_loc7_23.40_H1_1D
Yury, k20_41_2nd
499.797 MHz H1 1D in cdcl3 (ref. to CDCl3 @ 7.26 ppm)
temp 27.7 C -> actual temp = 27.0 C, colddual probe
7.38
7.37
7.37
7.37
7.34
7.34
7.34
7.33
7.27 cdcl3
6.34
6.33
6.33
6.32
6.29
6.28
6.28
6.28
6.27
6.08
6.08
6.07
6.07
6.07
4.19
4.17
3.60
3.57
1.55 HDO
1.34
1.34
0.95
f1 (ppm)

Appendix II: Selected Intramolecular Interrupted Nazarov Cyclization NMR Spectra (Chapter 3)

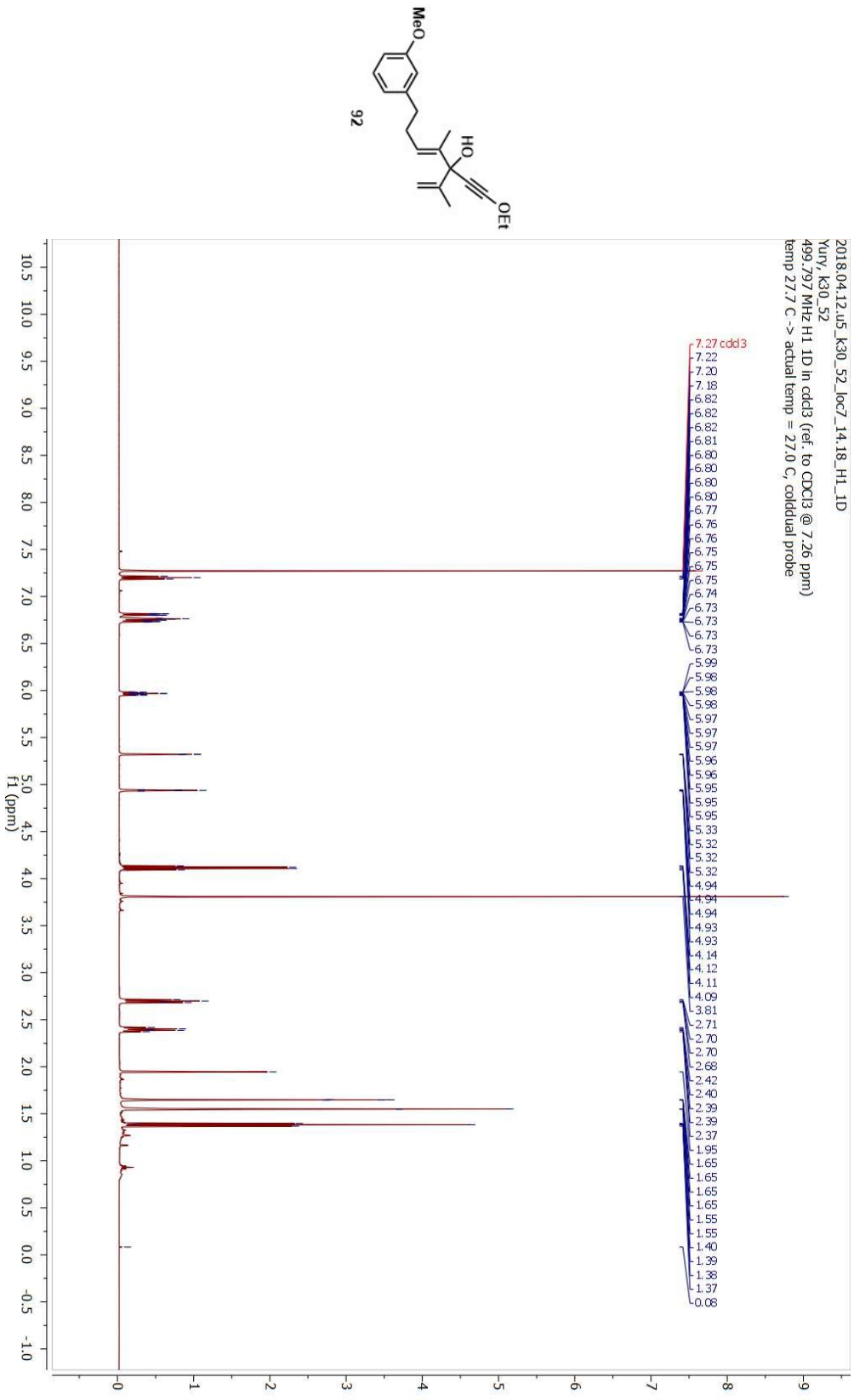
MeO
HO
OEt
92
2018.04.12.u5_k30_52_loc7_14.18_H1_1D
Yury, k30_52
499.797 MHz H1 1D in cdcl3 (ref. to CDCl3 @ 7.26 ppm)
temp 27.7 C -> actual temp = 27.0 C, colddual probe
7.27 cdcl3
f1 (ppm)

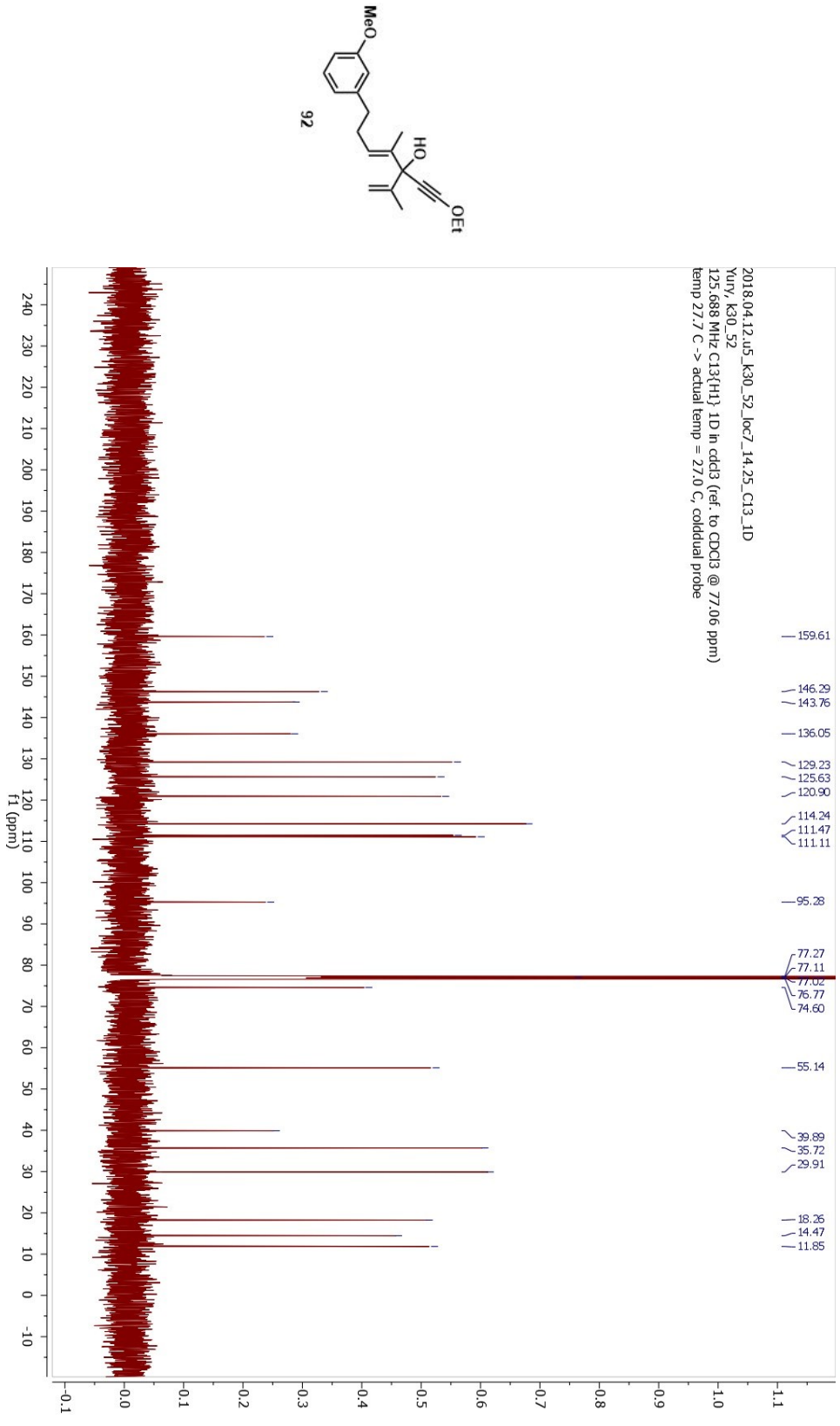
MeO
HO
OEt
92
2018.04.12.u5_k30_52_loc7_14.25_C13_1D
Yury, k30_52
125.688 MHz C13{H1} 1D in cdcl3 (ref. to CDCl3 @ 77.06 ppm)
temp 27.7 C -> actual temp = 27.0 C, colddual probe
159.61
146.29
143.76
136.05
129.23
125.63
120.90
114.24
111.47
111.11
95.28
77.27
77.11
77.02
76.77
74.60
55.14
39.89
35.72
29.91
18.26
14.47
11.85
f1 (ppm)

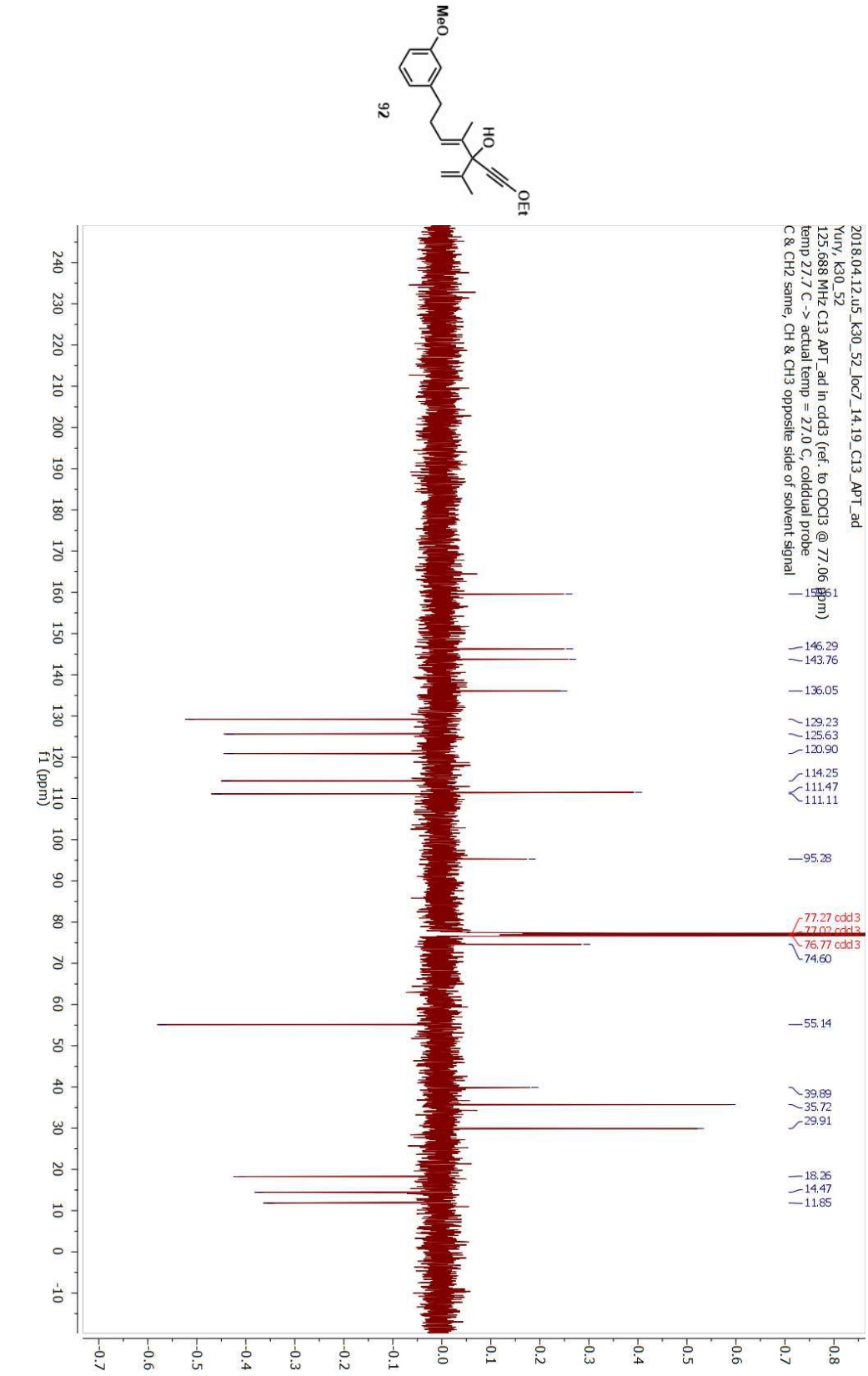
MeO
HO
OEt
92
2018.04.12.u5_k30_52_loc7_14.19_C13_APT_ad
Yury, k30_52
125.688 MHz C13 APT_ad in cdcl3 (ref. to CDCl3 @ 77.06 ppm)
temp 27.7 C -> actual temp = 27.0 C, colddual probe
C & CH2 same, CH & CH3 opposite side of solvent signal
151.61
146.29
143.76
136.05
129.23
125.63
120.90
114.25
111.47
111.11
95.28
77.27 cdcl3
77.02 cdcl3
76.77 cdcl3
74.60
55.14
39.89
35.72
29.91
18.26
14.47
11.85
f1 (ppm)

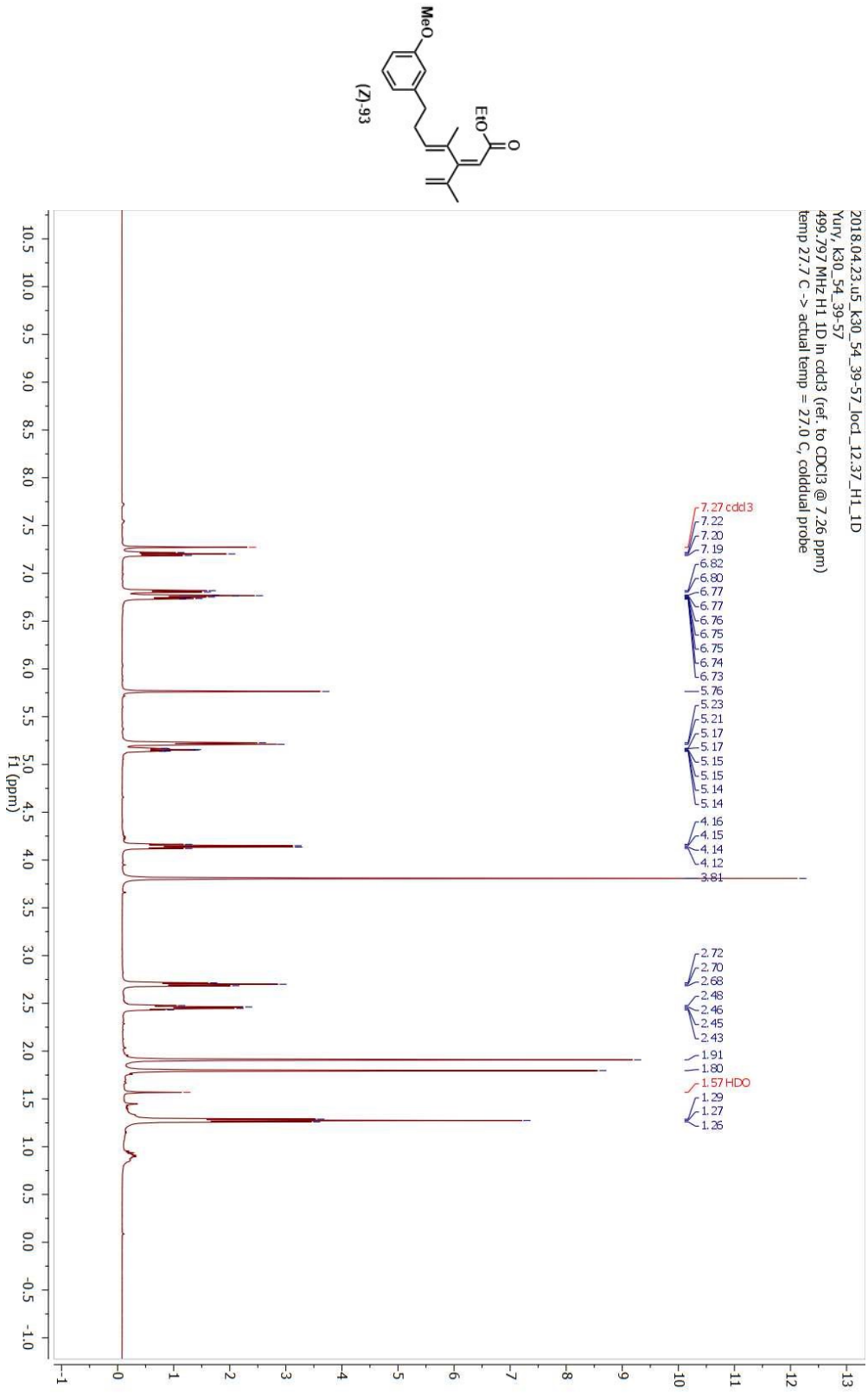
MeO
EtO
O
(Z)-93
2018.04.23.u5_k30_54_39-57_loc1_12.37_H1_1D
Yury, k30_54_39-57
499.797 MHz H1 1D in cdcl3 (ref. to CDCl3 @ 7.26 ppm)
temp 27.7 C -> actual temp = 27.0 C, colddual probe
7.27 cdcl3
7.22
7.20
7.19
6.82
6.80
6.77
6.77
6.76
6.75
6.75
6.74
6.73
5.76
5.23
5.21
5.17
5.17
5.15
5.15
5.14
5.14
4.16
4.15
4.14
4.12
3.81
2.72
2.70
2.68
2.48
2.46
2.45
2.43
1.91
1.80
1.57 HDO
1.29
1.27
1.26
f1 (ppm)

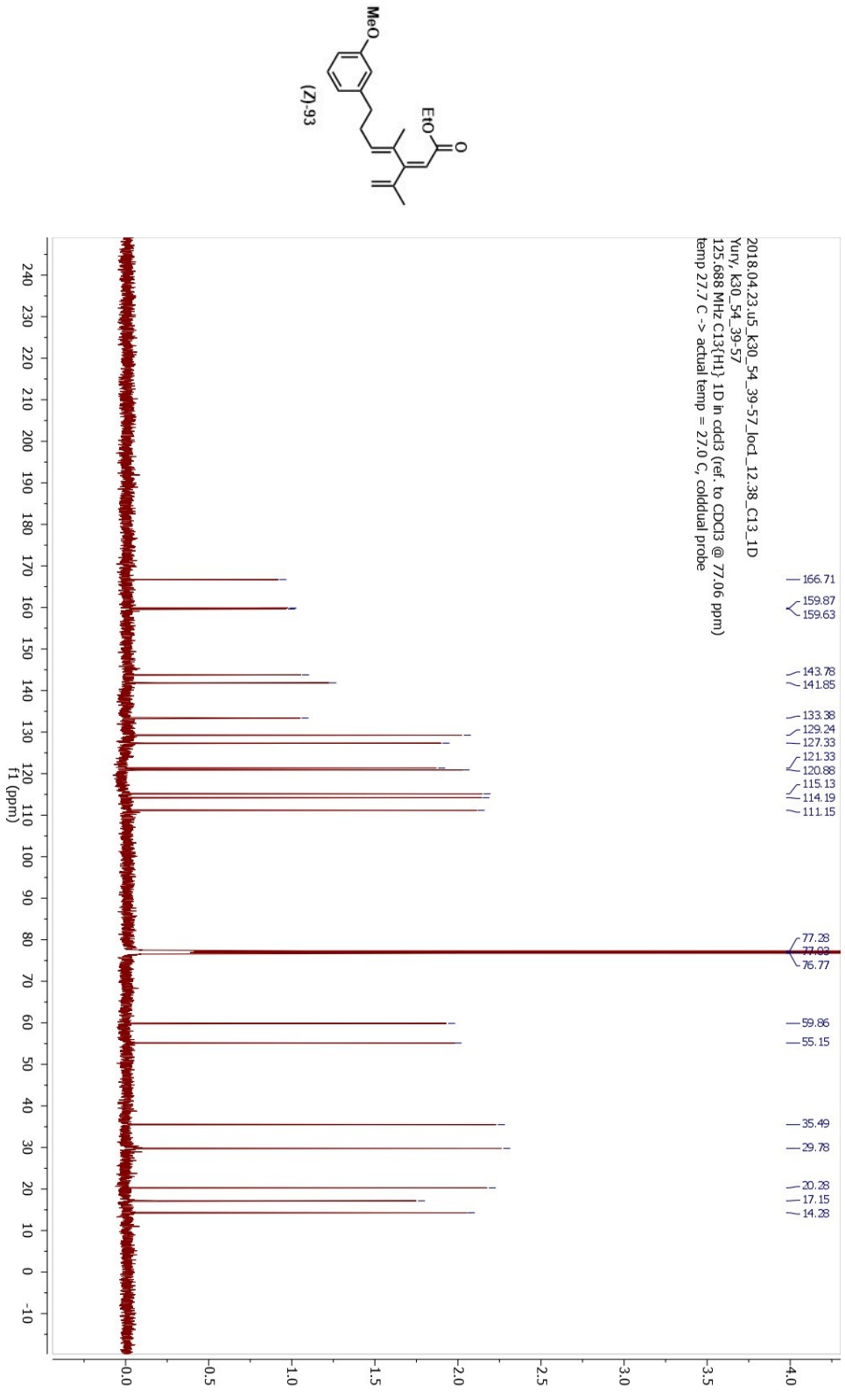
MeO
EtO
O
(Z)-93
2018.04.23.u5_k30_54_39-57_loc1_12.38_C13_1D
Yury, k30_54_39-57
125.688 MHz C13{H1} 1D in cdcl3 (ref. to CDCl3 @ 77.06 ppm)
temp 27.7 C -> actual temp = 27.0 C, colddual probe
166.71
159.87
159.63
143.78
141.85
133.38
129.24
127.33
121.33
120.88
115.13
114.19
111.15
77.28
77.03
76.77
59.86
55.15
35.49
29.78
20.28
17.15
14.28
f1 (ppm)

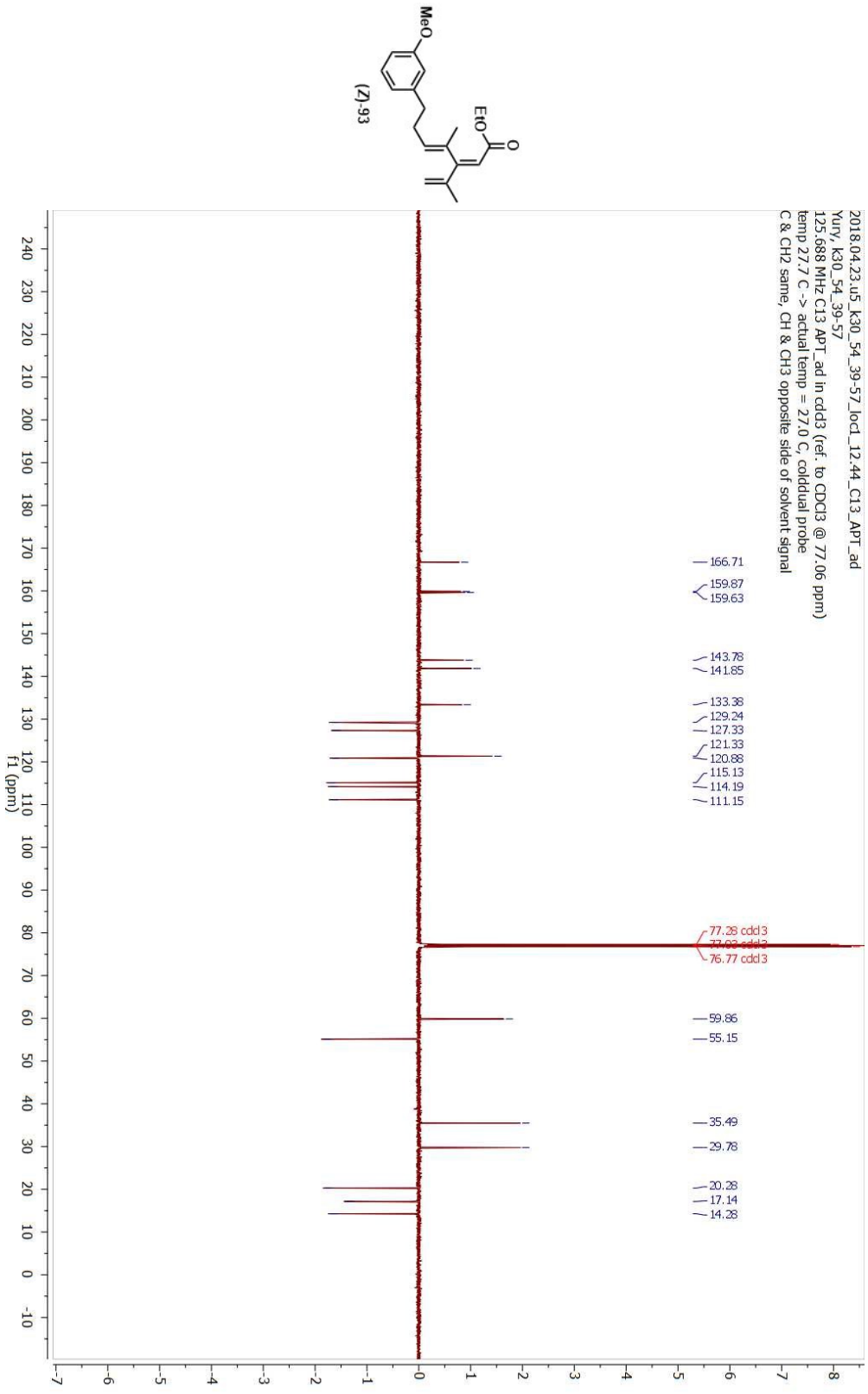
2018.04.23.u5_k30_54_39-57_loc1_12.44_C13_APT_ad
Yury, k30_54_39-57
125.688 MHz C13 APT_ad in cdd3 (ref. to CDCl3 @ 77.06 ppm)
temp 27.7 C -> actual temp = 27.0 C, colddual probe
C & CH2 same, CH & CH3 opposite side of solvent signal
MeO
EtO
O
(Z)-93
166.71
159.87
159.63
143.78
141.85
133.38
129.24
127.33
121.33
120.88
115.13
114.19
111.15
77.28 cdcl3
76.77 cdcl3
59.86
55.15
35.49
29.78
20.28
17.14
14.28
f1 (ppm)

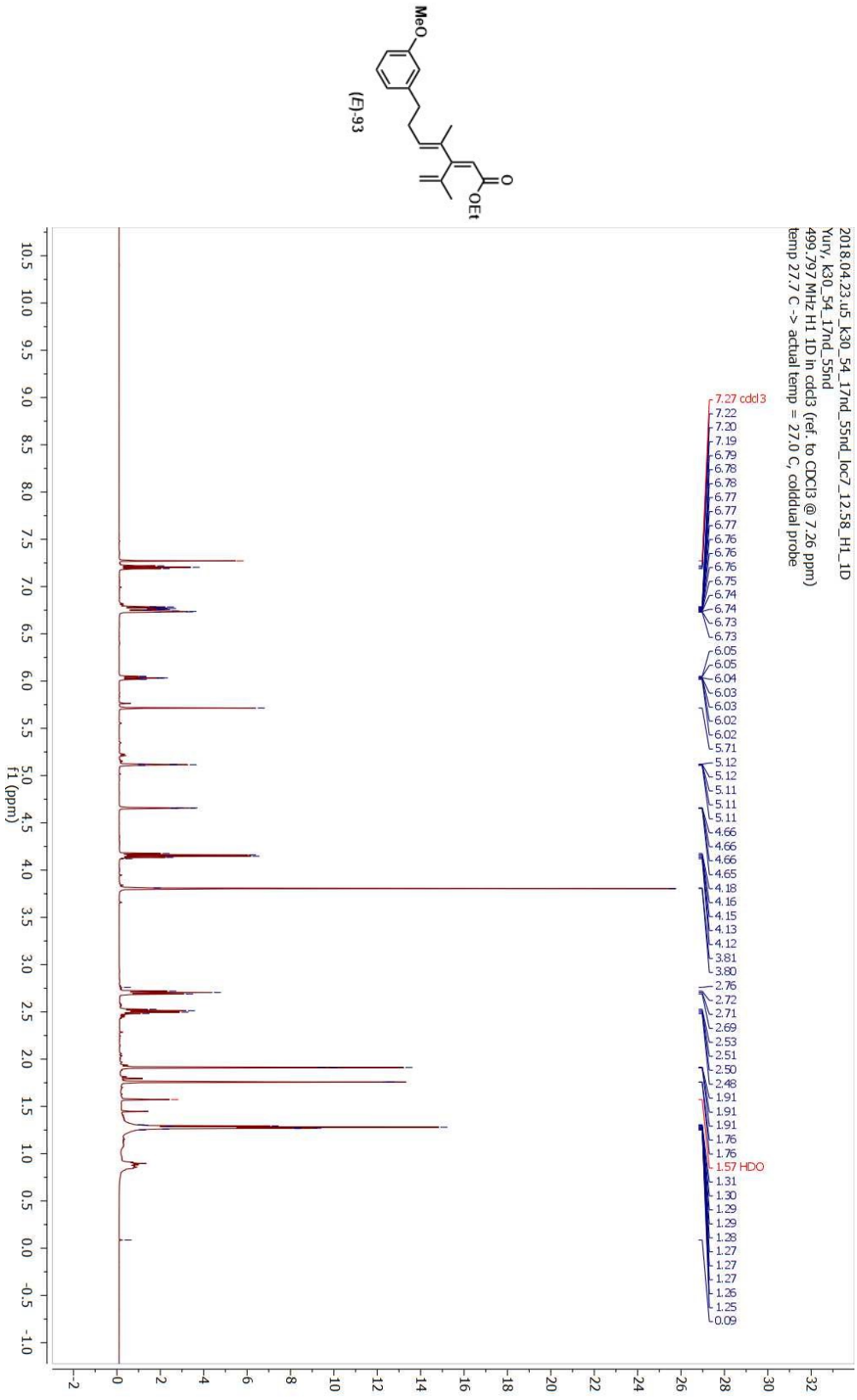
(E)-93
MeO
OEt
O
2018.04.23.u5_k30_54_17nd_55nd_loc7_12.58_H1_1D
Yury, k30_54_17nd_55nd
499.797 MHz H1 1D in cdcl3 (ref. to CDCl3 @ 7.26 ppm)
temp 27.7 C -> actual temp = 27.0 C, colddual probe
7.27 cdcl3
1.57 HDO
f1 (ppm)

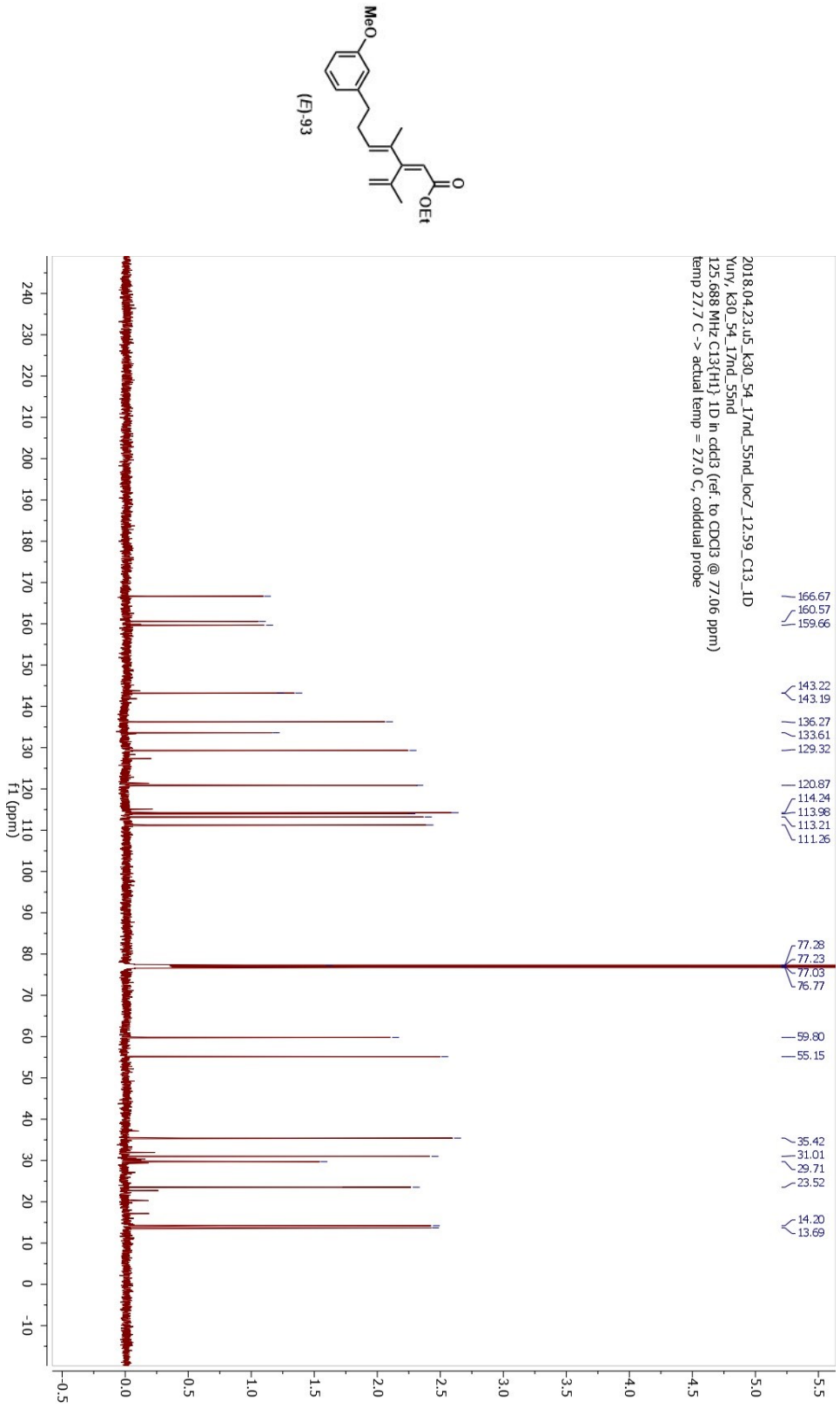
MeO
O
OEt
(E)-93
2018.04.23.u5_k30_54_17nd_55nd_loc7_12.59_C13_1D
Yury, k30_54_17nd_55nd
125.688 MHz C13{H1} 1D in cdcl3 (ref. to CDCl3 @ 77.06 ppm)
temp 27.7 C -> actual temp = 27.0 C, coldDual probe
166.67
160.57
159.66
143.22
143.19
136.27
133.61
129.32
120.87
114.24
113.98
113.21
111.26
77.28
77.23
77.03
76.77
59.80
55.15
35.42
31.01
29.71
23.52
14.20
13.69
f1 (ppm)

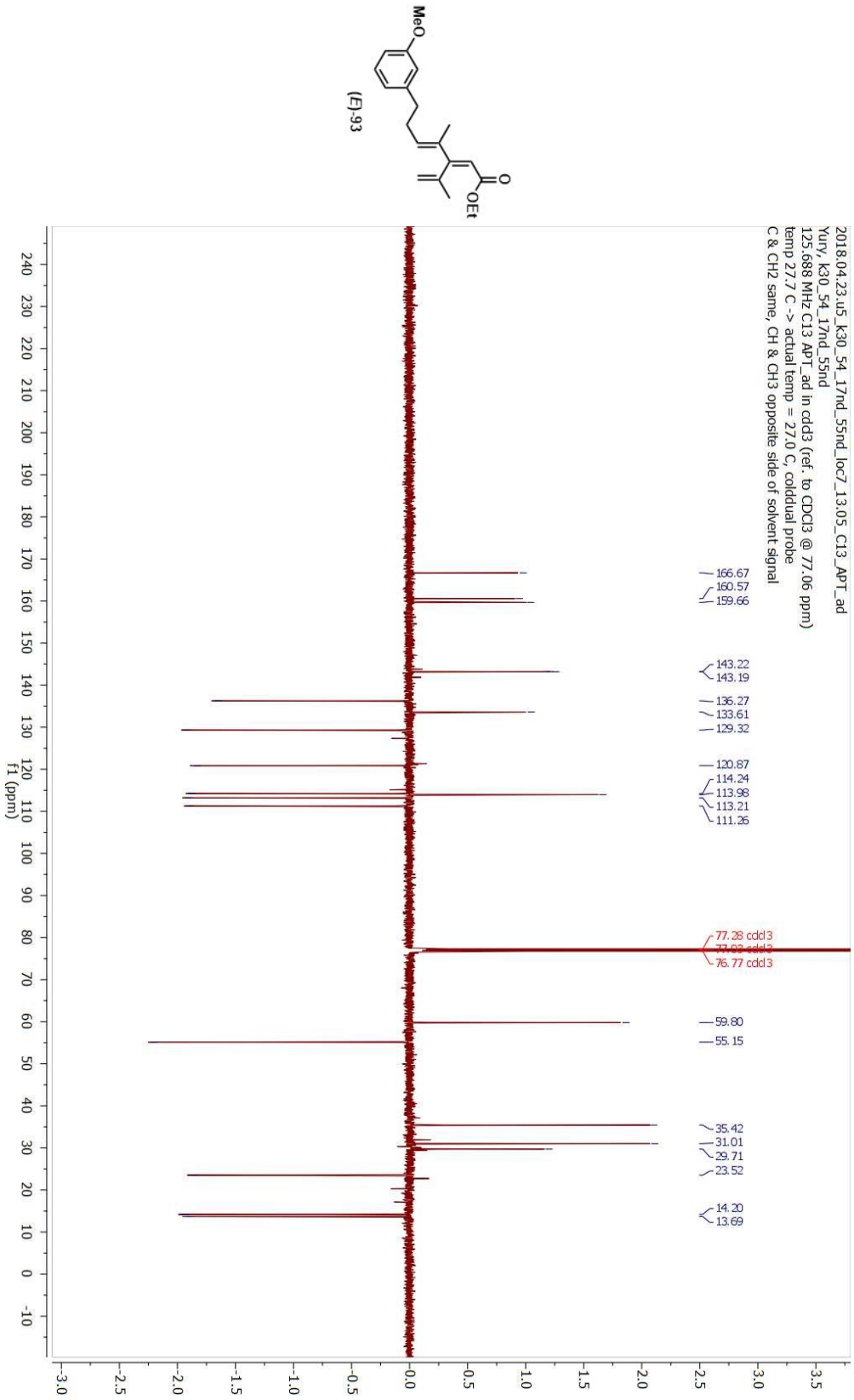
2018.04.23.u5_k30_54_17nd_55nd_loc7_13.05_C13_APT_ad
Yury, k30_54_17nd_55nd
125.688 MHz C13 APT_ad in cdcl3 (ref. to CDCl3 @ 77.06 ppm)
temp 27.7 C -> actual temp = 27.0 C, colddual probe
C & CH2 same, CH & CH3 opposite side of solvent signal
MeO
OEt
O
(E)-93
166.67
160.57
159.66
143.22
143.19
136.27
133.61
129.32
120.87
114.24
113.98
113.21
111.26
77.28 cdcl3
76.77 cdcl3
59.80
55.15
35.42
31.01
29.71
23.52
14.20
13.69
f1 (ppm)

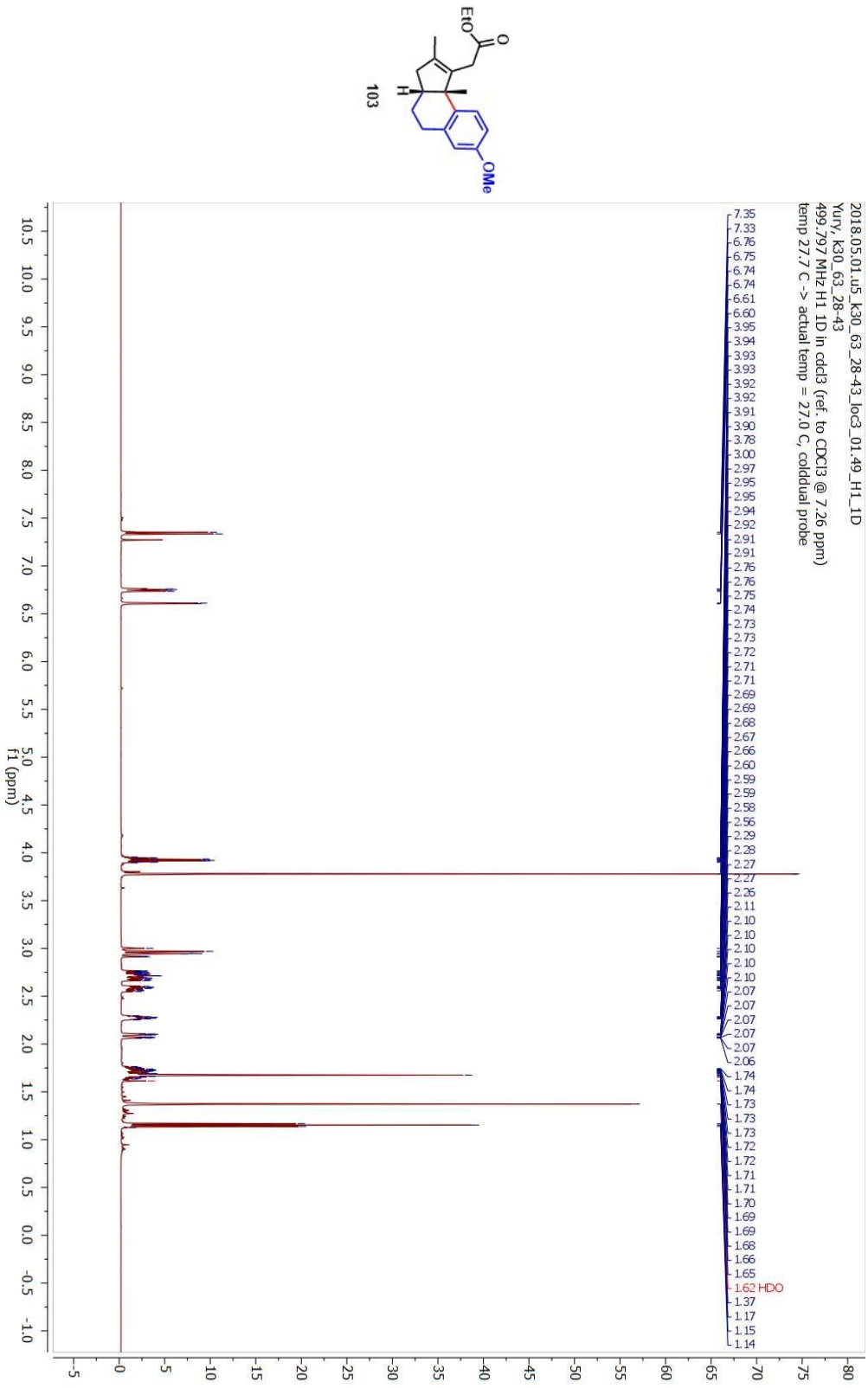
EtO
O
H
OMe
103
2018.05.01.u5_k30_63_28-43_loc3_01.49_H1_1D
Yury, K30_63_28-43
499.797 MHz H1 1D in cdcl3 (ref. to CDCl3 @ 7.26 ppm)
temp 27.7 C -> actual temp = 27.0 C, colddual probe
1.62 HDO
f1 (ppm)

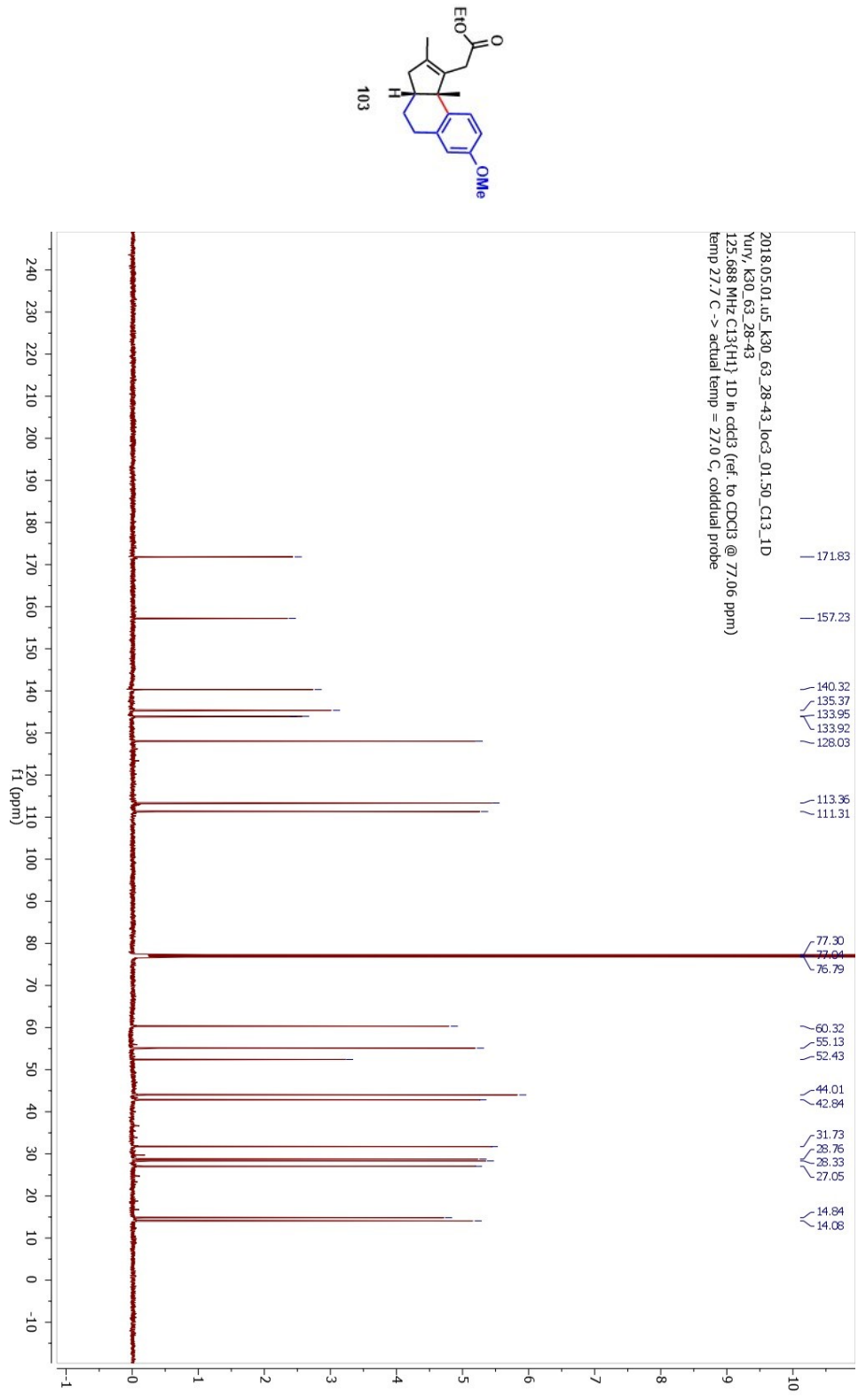
EtO
O
H
OMe
103
2018.05.01.u5_k30_63_28-43_loc3_01.50_C13_1D
Yury, k30_63_28-43
125.688 MHz C13{H1} 1D in cdcl3 (ref. to CDCl3 @ 77.06 ppm)
temp 27.7 C -> actual temp = 27.0 C, colddual probe
171.83
157.23
140.32
135.37
133.95
133.92
128.03
113.36
111.31
77.30
77.04
76.79
60.32
55.13
52.43
44.01
42.84
31.73
28.76
28.33
27.05
14.84
14.08
f1 (ppm)

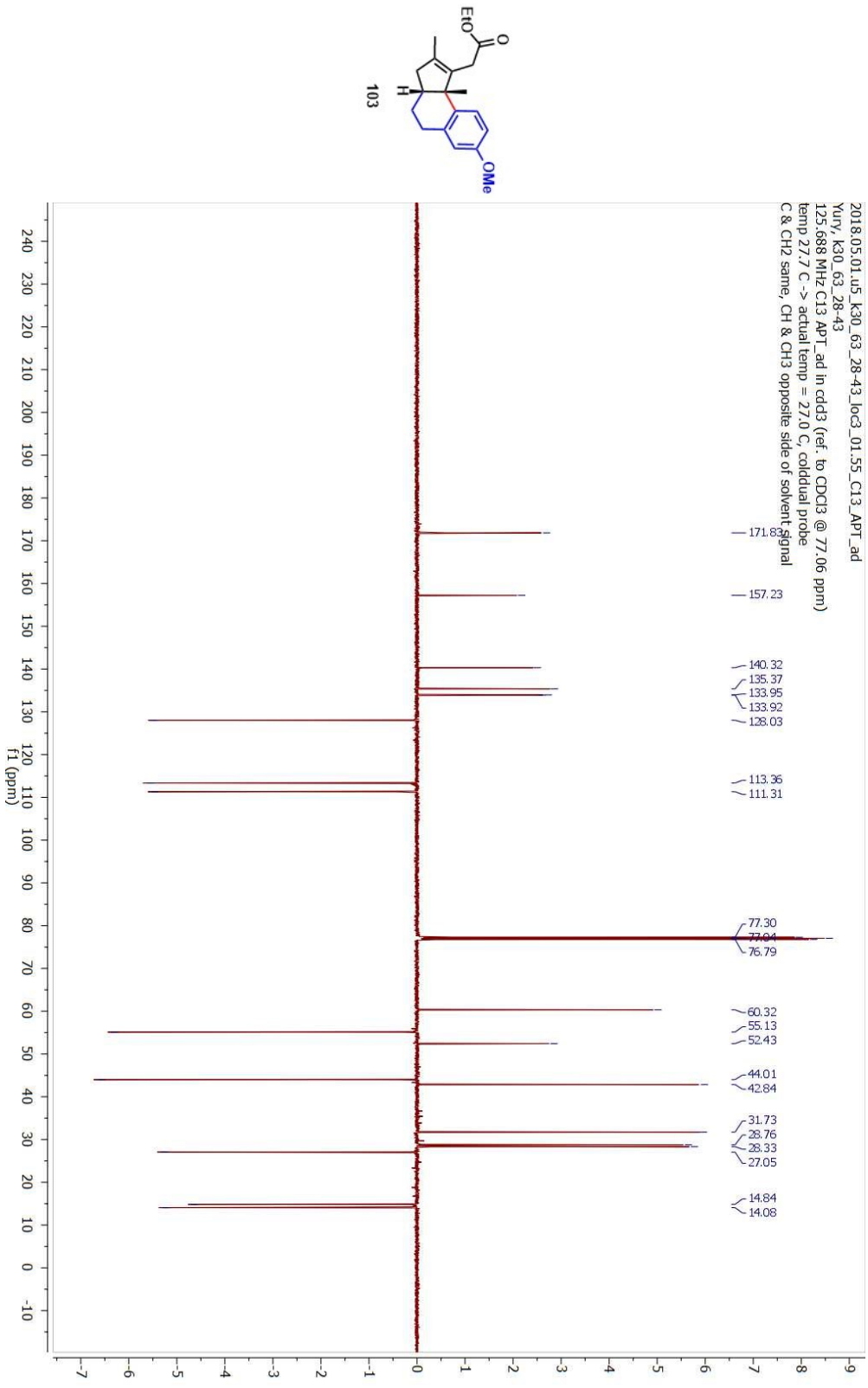
EtO
O
H
OMe
103
2018.05.01.u5_k30_63_28-43_loc3_01.55_C13_APT_ad
Yury, k30_63_28-43
125.688 MHz C13 APT_ad in cdd3 (ref. to CDCl3 @ 77.06 ppm)
temp 27.7 C -> actual temp = 27.0 C, colddual probe
C & CH2 same, CH & CH3 opposite side of solvent signal
171.83
157.23
140.32
135.37
133.95
133.92
128.03
113.36
111.31
77.30
77.04
76.79
60.32
55.13
52.43
44.01
42.84
31.73
28.76
28.33
27.05
14.84
14.08
f1 (ppm)

Appendix III: Selected Intermolecular Interrupted Nazarov Cyclization NMR Spectra (Chapter 3)

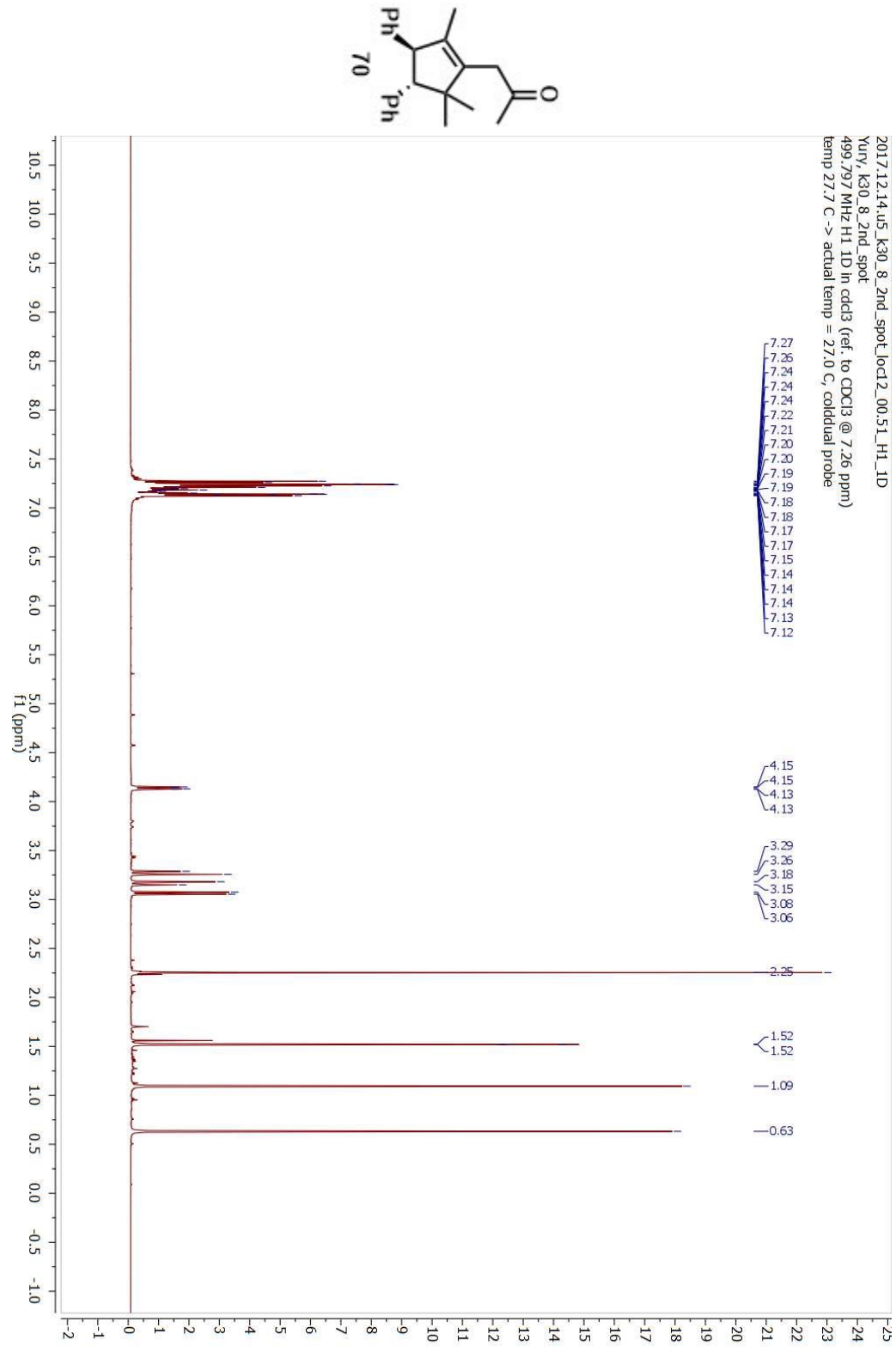
Ph
Ph
O
70
2017.12.14.u5_k30_8_2nd_spot_loc12_00.51_H1_1D
Yury, k30_8_2nd_spot
499.797 MHz H1 1D in cdcl3 (ref. to CDCl3 @ 7.26 ppm)
temp 27.7 C -> actual temp = 27.0 C, colddual probe
7.27
7.26
7.24
7.24
7.24
7.22
7.21
7.20
7.20
7.19
7.19
7.18
7.18
7.17
7.17
7.15
7.14
7.14
7.14
7.13
7.12
4.15
4.15
4.13
4.13
3.29
3.26
3.18
3.15
3.08
3.06
2.25
1.52
1.52
1.09
0.63
f1 (ppm)

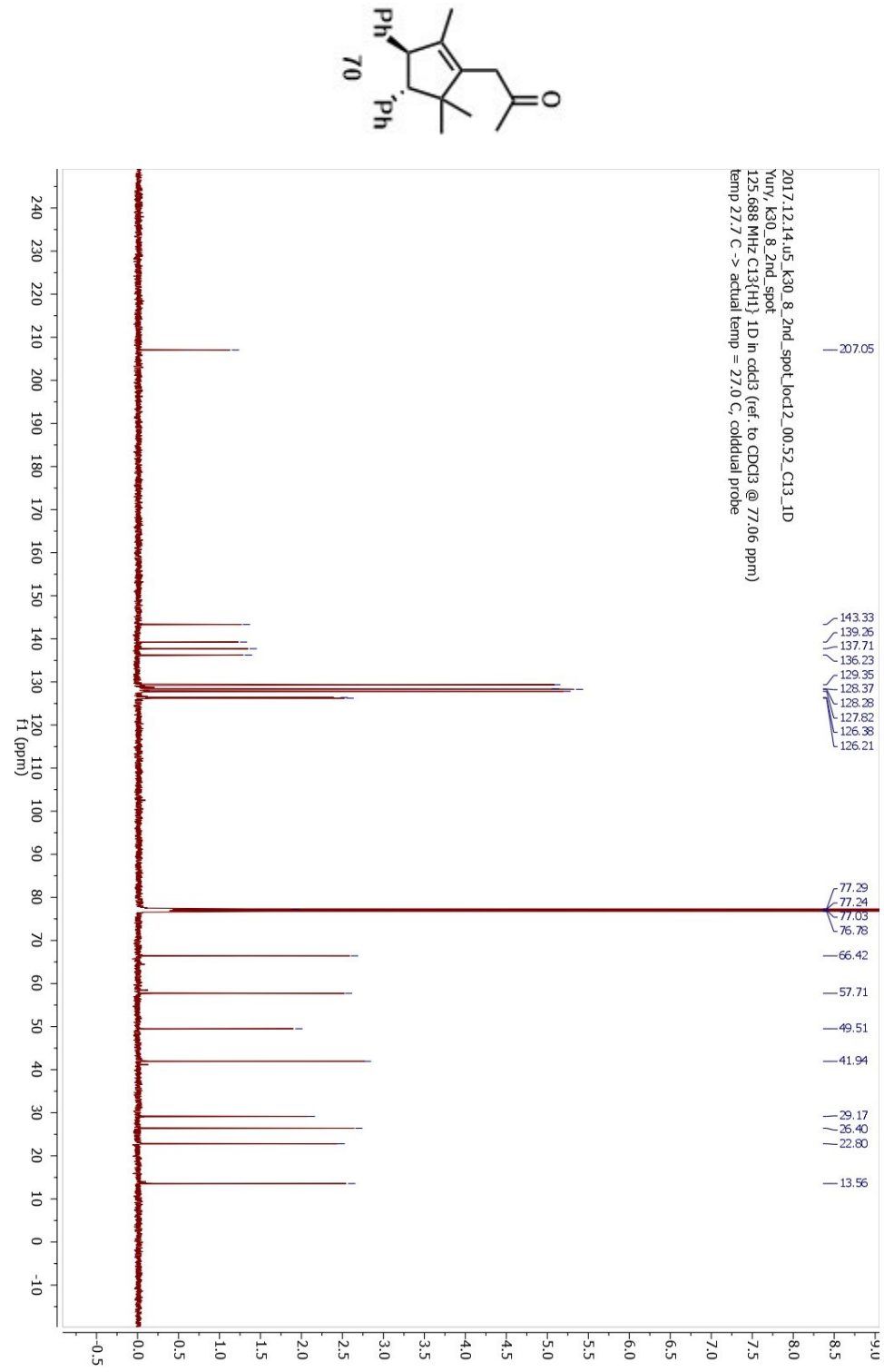
70
Ph
Ph
O
2017.12.14.u5_k30_8_2nd_spot_loct2_00.52_C13_1D
Yury, k30_8_2nd_spot
125.688 MHz C13{H1} 1D in cdcl3 (ref. to CDCl3 @ 77.06 ppm)
temp 27.7 C -> actual temp = 27.0 C, colddual probe
207.05
143.33
139.26
137.71
136.23
129.35
128.37
128.28
127.82
126.38
126.21
77.29
77.24
77.03
76.78
66.42
57.71
49.51
41.94
29.17
26.40
22.80
13.56
f1 (ppm)

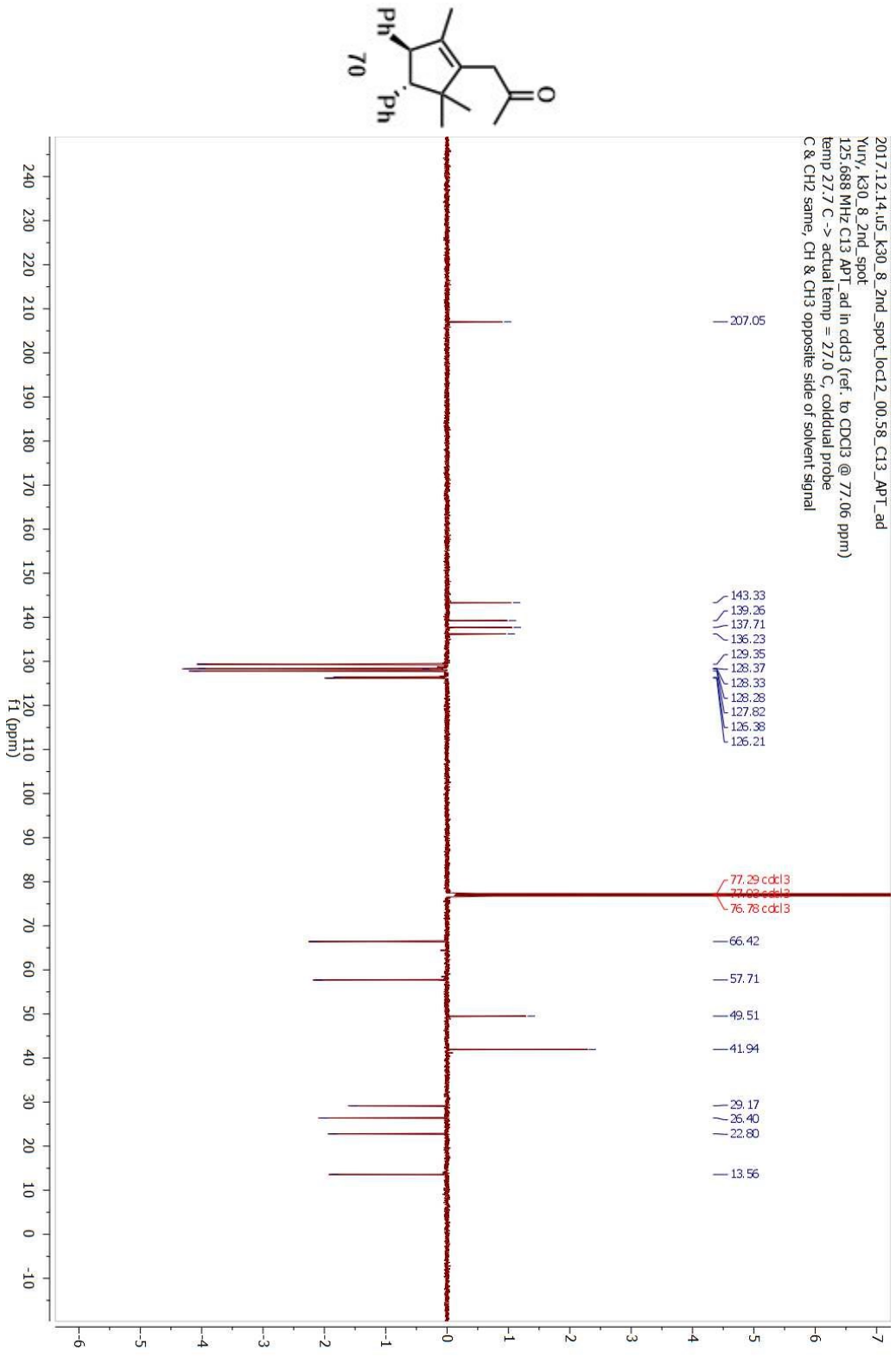
70
Ph
Ph
O
2017.12.14.u5_k30_8_2nd_spot_loc12_00.58_C13_APT_ad
Yury, k30_8_2nd_spot
125.688 MHz C13 APT_ad in cdcl3 (ref. to CDCl3 @ 77.06 ppm)
temp 27.7 C -> actual temp = 27.0 C, colddual probe
C & CH2 same, CH & CH3 opposite side of solvent signal
207.05
143.33
139.26
137.71
136.23
129.35
128.37
128.33
128.28
127.82
126.38
126.21
77.29 cdcl3
77.03 cdcl3
76.78 cdcl3
66.42
57.71
49.51
41.94
29.17
26.40
22.80
13.56
f1 (ppm)

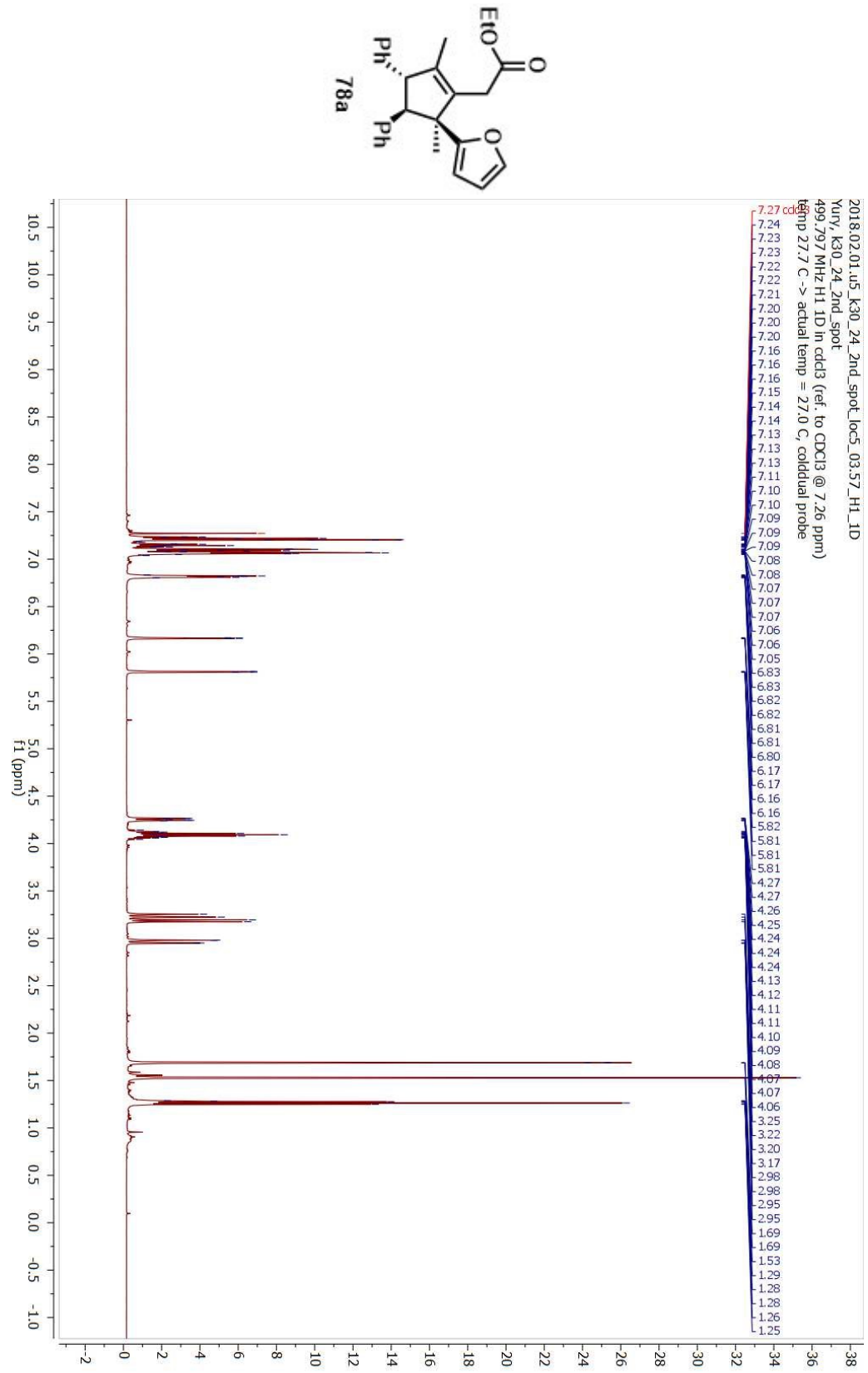
EtO
O
Ph
Ph
O
78a
2018.02.01.u5_k30_24_2nd_spot_loc5_03.57_H1_1D
Yury, k30_24_2nd_spot
499.797 MHz H1 1D in cdcl3 (ref. to CDCl3 @ 7.26 ppm)
temp 27.7 C -> actual temp = 27.0 C, colddual probe
7.27 cdcl3
f1 (ppm)

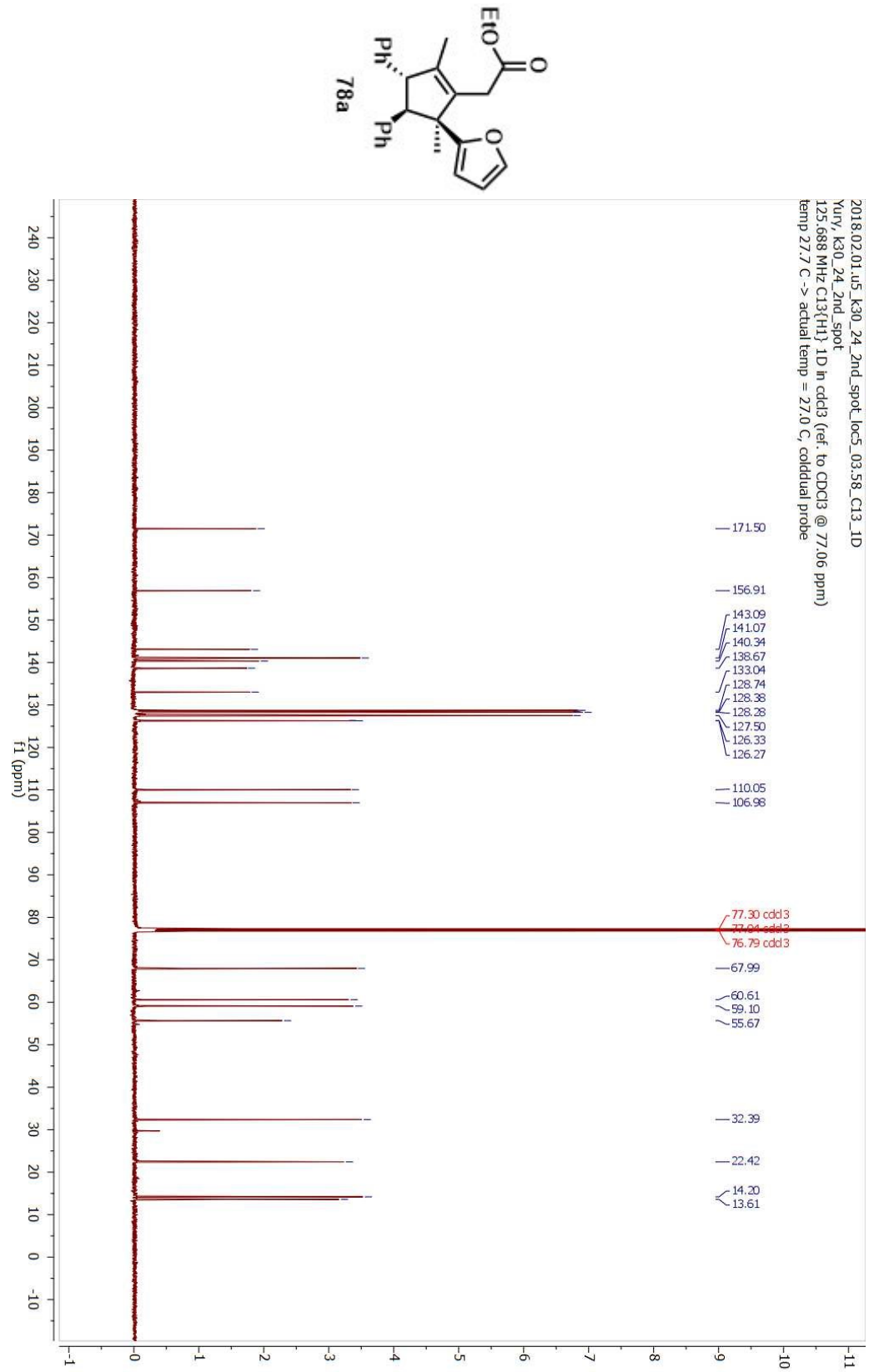
78a
Ph
Ph
EtO
O
O
2018.02.01.u5_k30_24_2nd_spot_loc5_03.58_C13_1D
Yury, k30_24_2nd_spot
125.688 MHz C13{H1} 1D in cdcl3 (ref. to CDCl3 @ 77.06 ppm)
temp 27.7 C -> actual temp = 27.0 C, colddual probe
171.50
156.91
143.09
141.07
140.34
138.67
133.04
128.74
128.38
128.28
127.50
126.33
126.27
110.05
106.98
77.30 cdcl3
77.04 cdcl3
76.79 cdcl3
67.99
60.61
59.10
55.67
32.39
22.42
14.20
13.61
f1 (ppm)

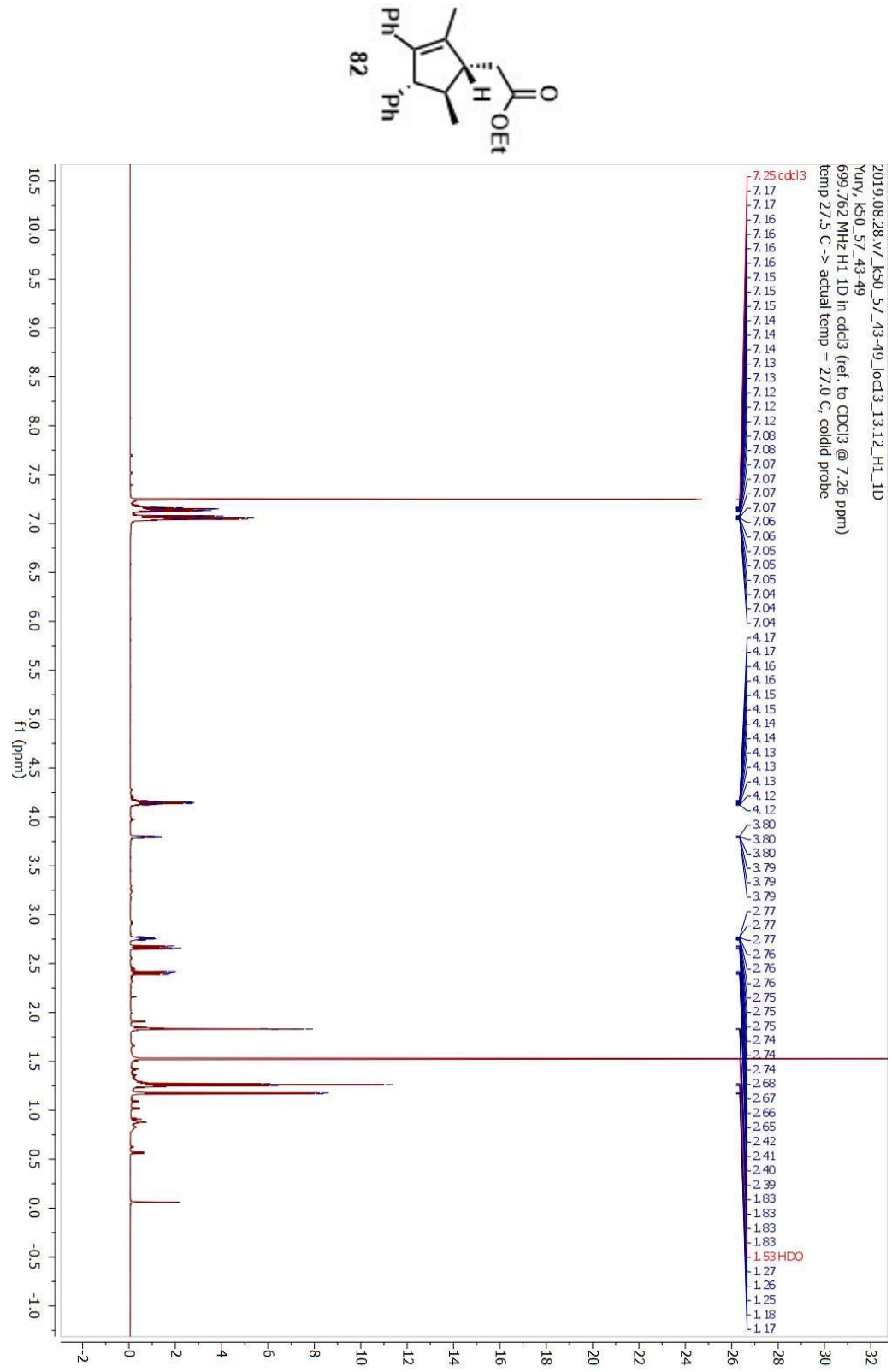
82
Ph
Ph
H
O
OEt
2019.08.28.v7_k50_57_43-49_locl3_13.12_H1_1D
Yury, k50_57_43-49
699.762 MHz H1 1D in cdcl3 (ref. to CDCl3 @ 7.26 ppm)
temp 27.5 C -> actual temp = 27.0 C, coldid probe
7.25 cdcl3
1.53 HDO
f1 (ppm)

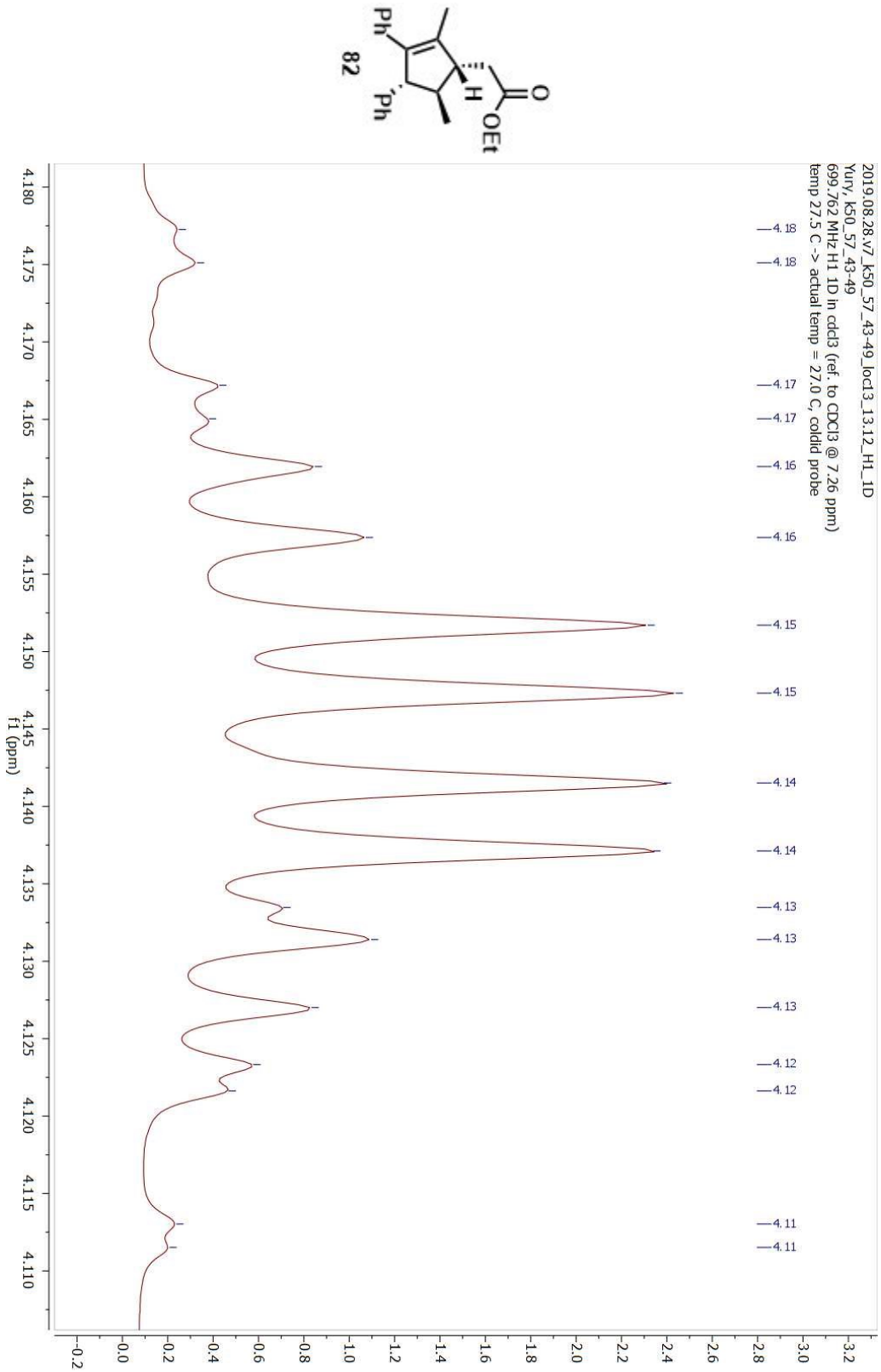
2019.08.28.v7_k50_57_43-49_locl3_13.12_H1_1D
Yury, k50_57_43-49
699.762 MHz H1 1D in cdcl3 (ref. to CDCl3 @ 7.26 ppm)
temp 27.5 C -> actual temp = 27.0 C, coldid probe
Ph
Ph
H
O
OEt
82
f1 (ppm)

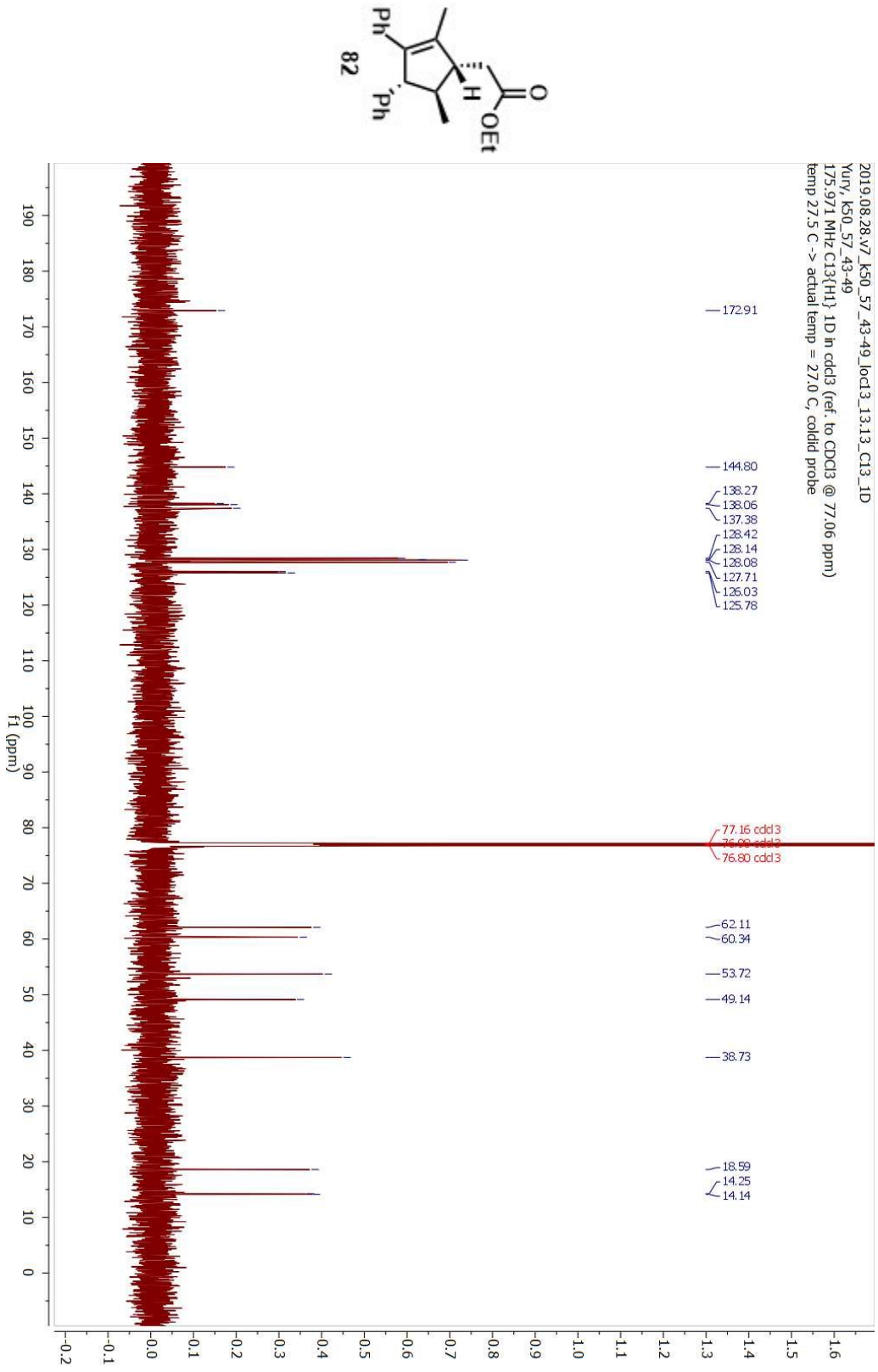
82
Ph
Ph
H
O
OEt
2019.08.28.v7_k50_57_43-49_locl3_13.13_C13_1D
Yury, K50_57_43-49
175.971 MHz C13{H1} 1D in cdcl3 (ref. to CDCl3 @ 77.06 ppm)
temp 27.5 C -> actual temp = 27.0 C, coldid probe
172.91
144.80
138.27
138.06
137.38
128.42
128.14
128.08
127.71
126.03
125.78
77.16 cdcl3
76.80 cdcl3
62.11
60.34
53.72
49.14
38.73
18.59
14.25
14.14
f1 (ppm)

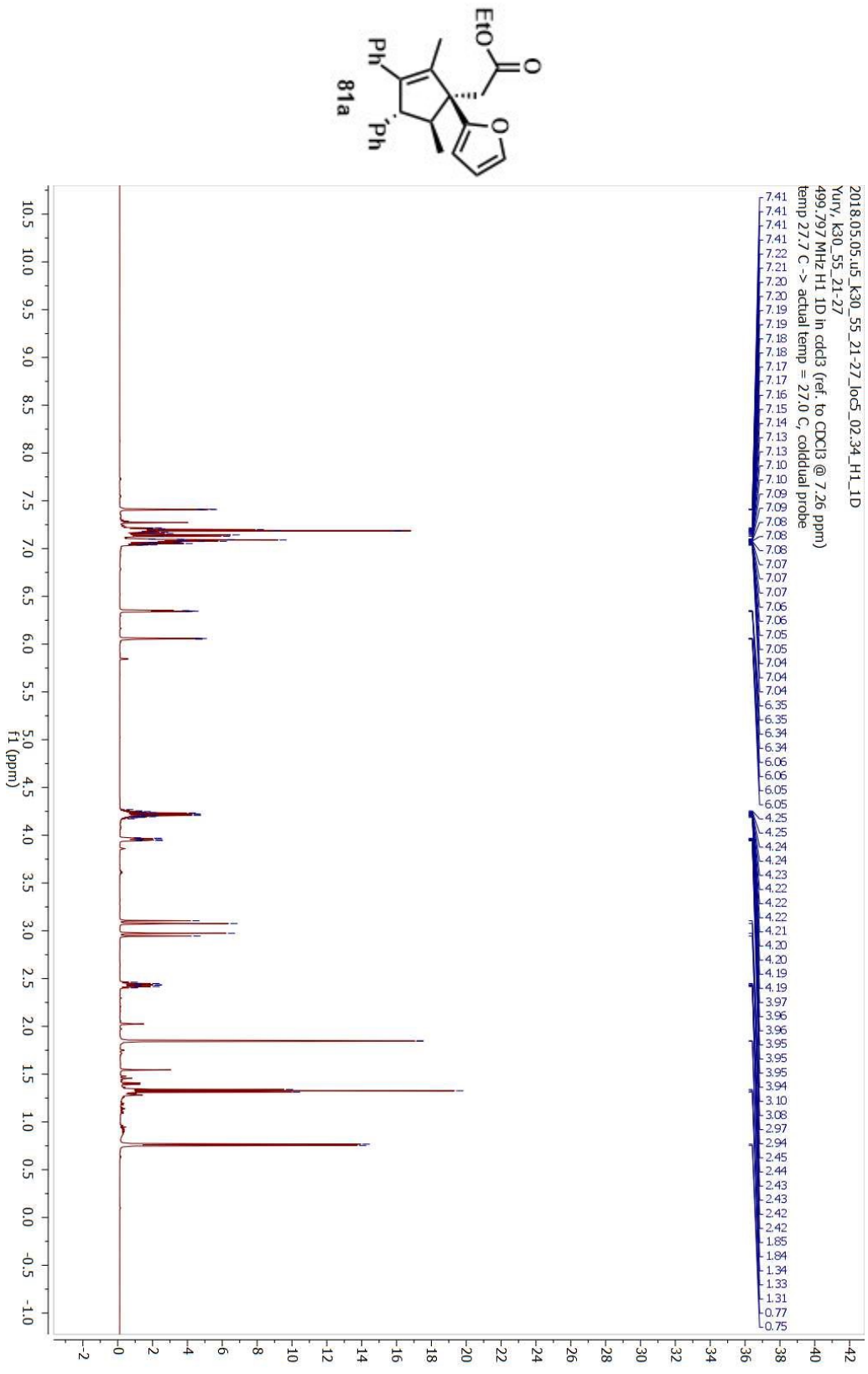
EtO
O
Ph
Ph
O
81a
2018.05.05.u5_k30_55_21-27_loc5_02.34_H1_1D
Yury, k30_55_21-27
499.797 MHz H1 1D in cdcl3 (ref. to CDCl3 @ 7.26 ppm)
temp 27.7 C -> actual temp = 27.0 C, colddual probe
f1 (ppm)

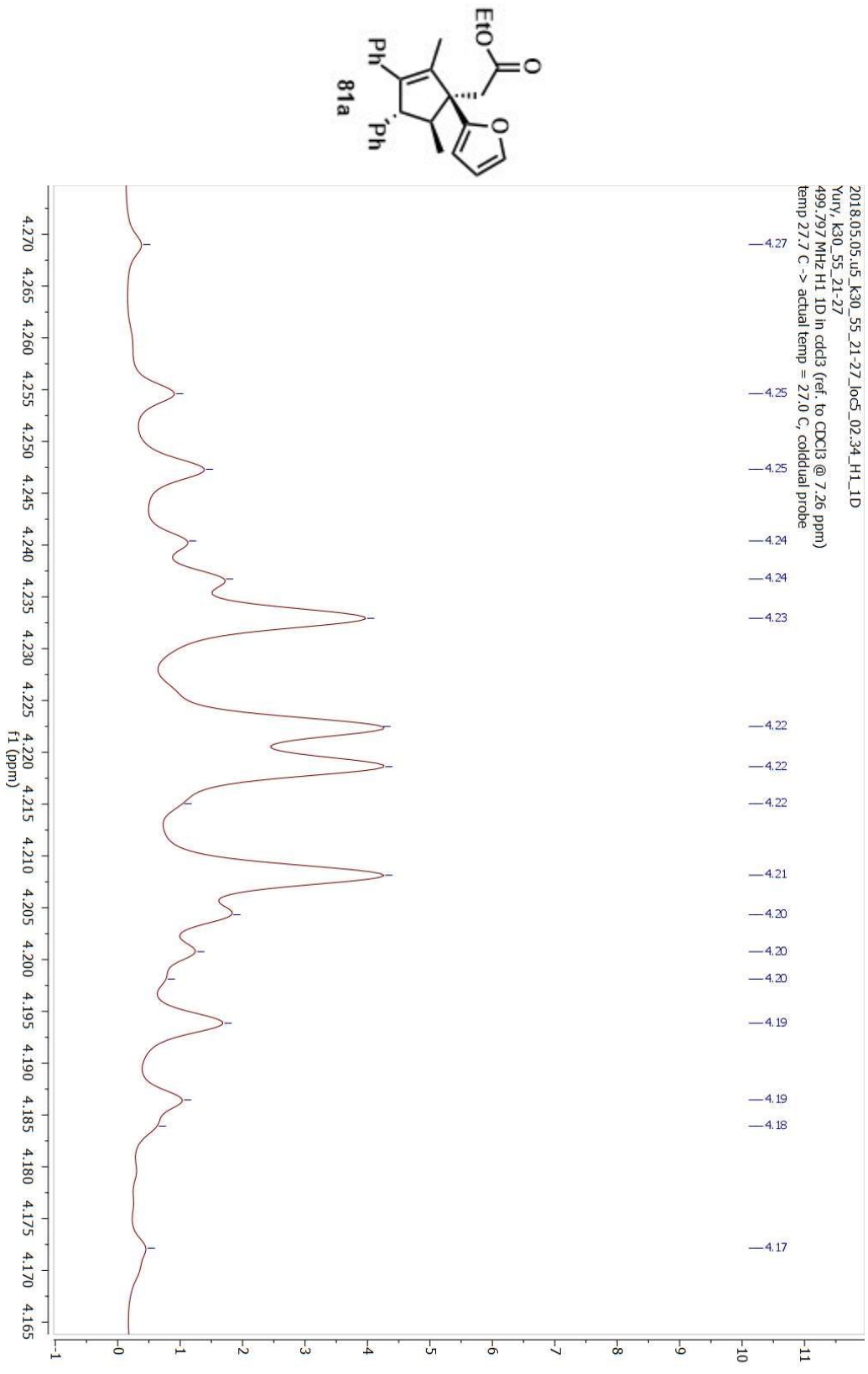
2018.05.05.u5_k30_55_21-27_loc5_02.34_H1_1D
Yury, k30_55_21-27
499.797 MHz H1 1D in cdcl3 (ref. to CDCl3 @ 7.26 ppm)
temp 27.7 C -> actual temp = 27.0 C, colddual probe
EtO
O
Ph
Ph
O
81a
4.27
4.25
4.25
4.24
4.24
4.23
4.22
4.22
4.22
4.21
4.20
4.20
4.20
4.19
4.19
4.18
4.17
f1 (ppm)

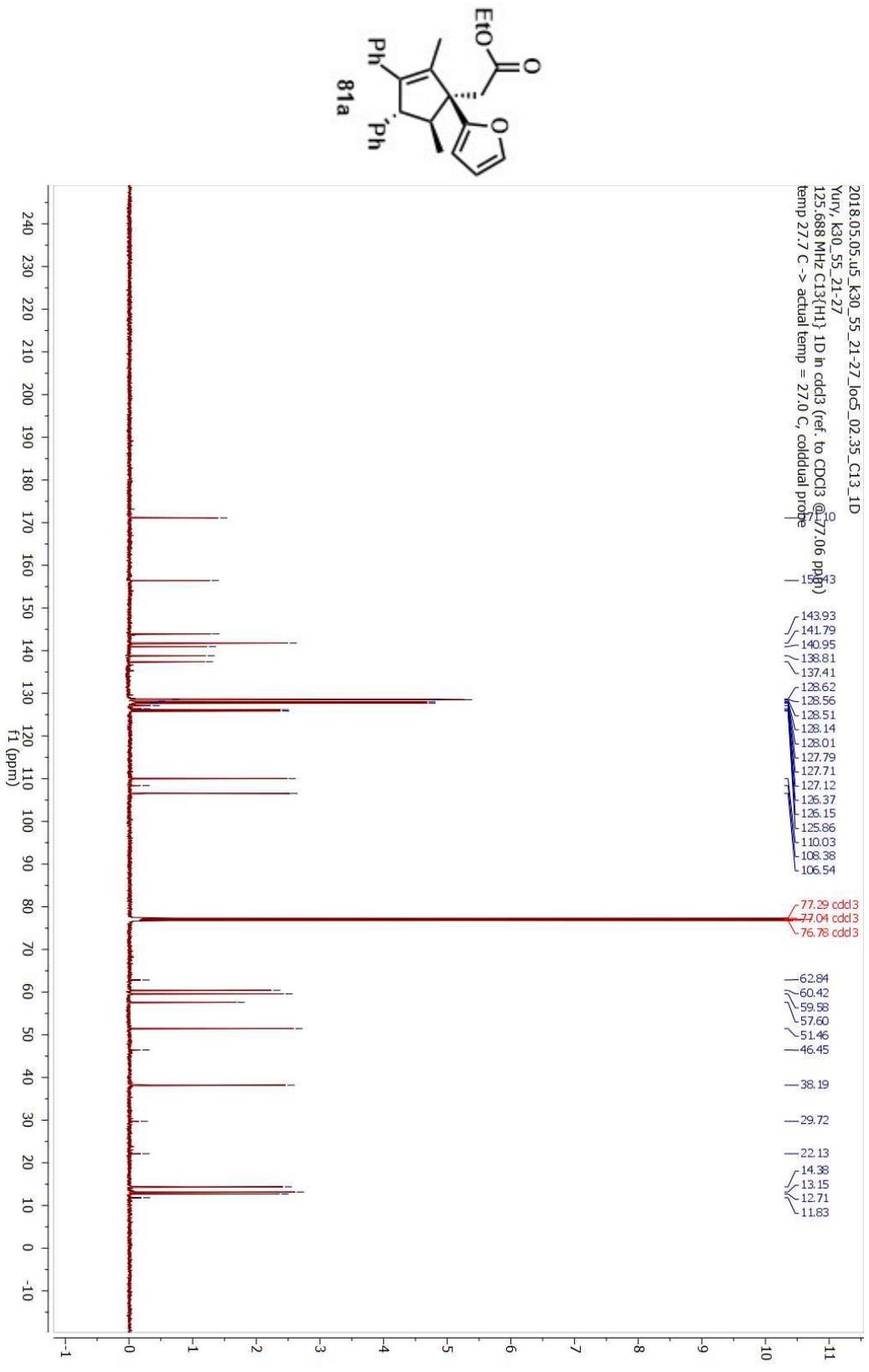
EtO
O
Ph
Ph
O
81a
2018.05.05.u5_k30_55_21-27_loc5_02.35_C13_1D
Yury, k30_55_21-27
125.688 MHz C13{H1} 1D in cdcl3 (ref. to CDCl3 @ 77.06 ppm)
temp 27.7 C -> actual temp = 27.0 C, colddual probe
157.10
155.43
143.93
141.79
140.95
138.81
137.41
128.62
128.56
128.51
128.14
128.01
127.79
127.71
127.12
126.37
126.15
125.86
110.03
108.38
106.54
77.29 cdcl3
77.04 cdcl3
76.78 cdcl3
62.84
60.42
59.58
57.60
51.46
46.45
38.19
29.72
22.13
14.38
13.15
12.71
11.83
f1 (ppm)

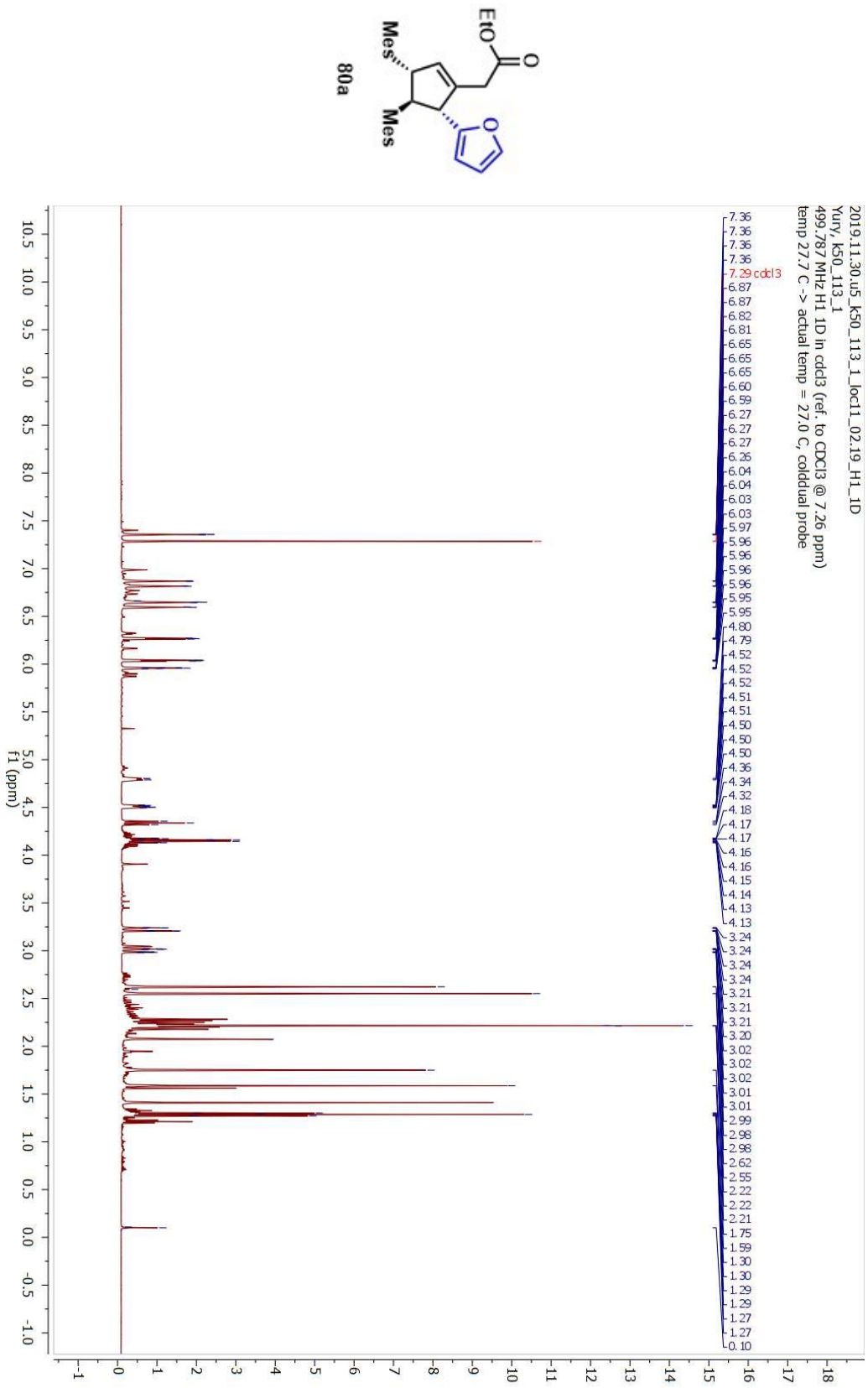
EtO
O
Mes
Mes
O
80a
2019.11.30.u5_k50_113_1_loc11_02.19_H1_1D
Yury, K50_113_1
499.787 MHz H1 1D in cdcl3 (ref. to CDCl3 @ 7.26 ppm)
temp 27.7 C -> actual temp = 27.0 C, colddual probe
7.29 cdcl3
f1 (ppm)

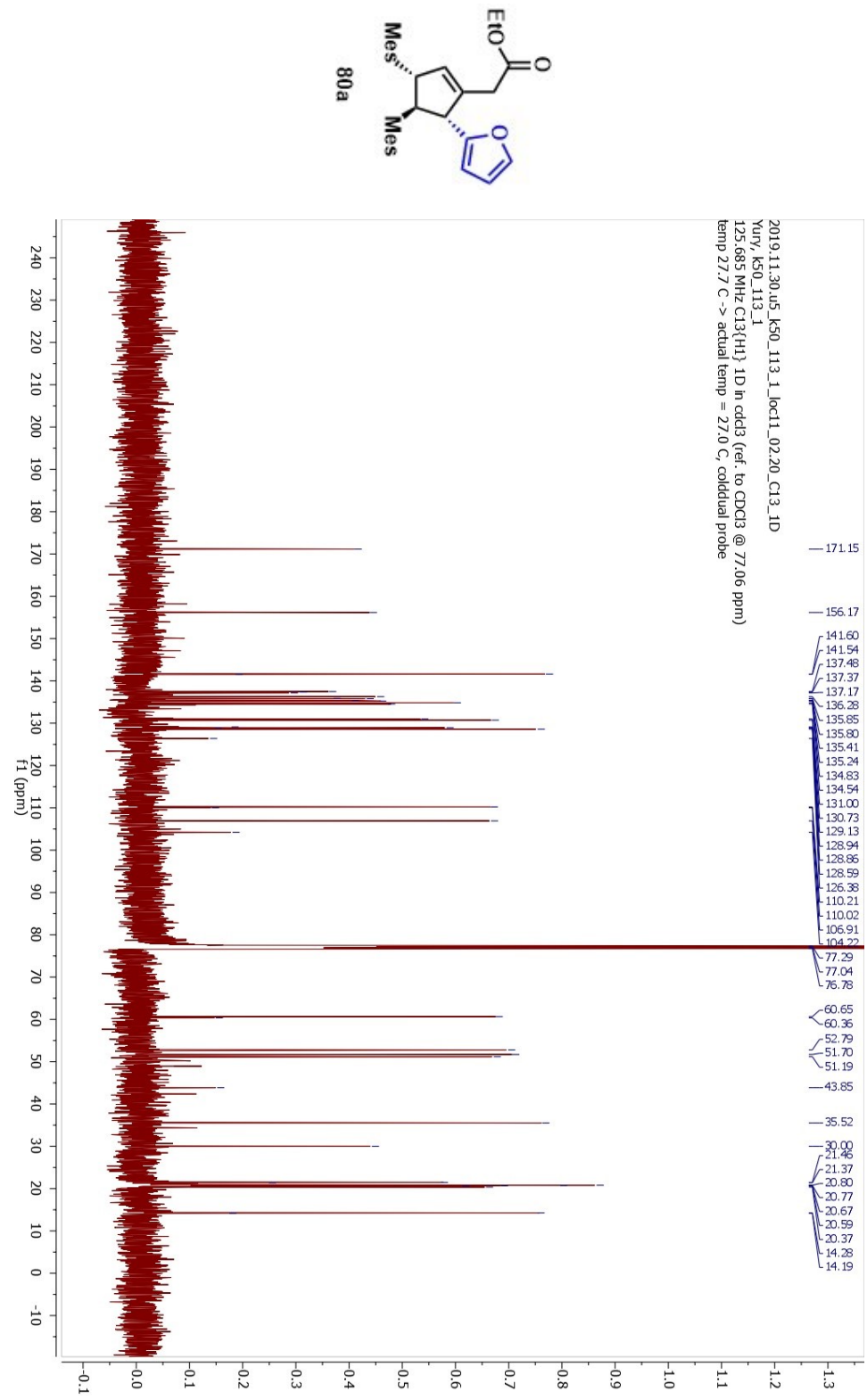
EtO
O
Mes
Mes
O
80a
2019.11.30.u5_k50_113_1_loc11_02.20_C13_1D
Yury, k50_113_1
125.685 MHz C13{H1} 1D in cdcl3 (ref. to CDCl3 @ 77.06 ppm)
temp 27.7 C -> actual temp = 27.0 C, colddual probe
171.15
156.17
141.60
141.54
137.48
137.37
137.17
136.28
135.85
135.80
135.41
135.24
134.83
134.54
131.00
130.73
129.13
128.94
128.86
128.59
126.38
110.21
110.02
106.91
104.22
77.29
77.04
76.78
60.65
60.36
52.79
51.70
51.19
43.85
35.52
30.00
21.46
21.37
20.80
20.77
20.67
20.59
20.37
14.28
14.19
f1 (ppm)

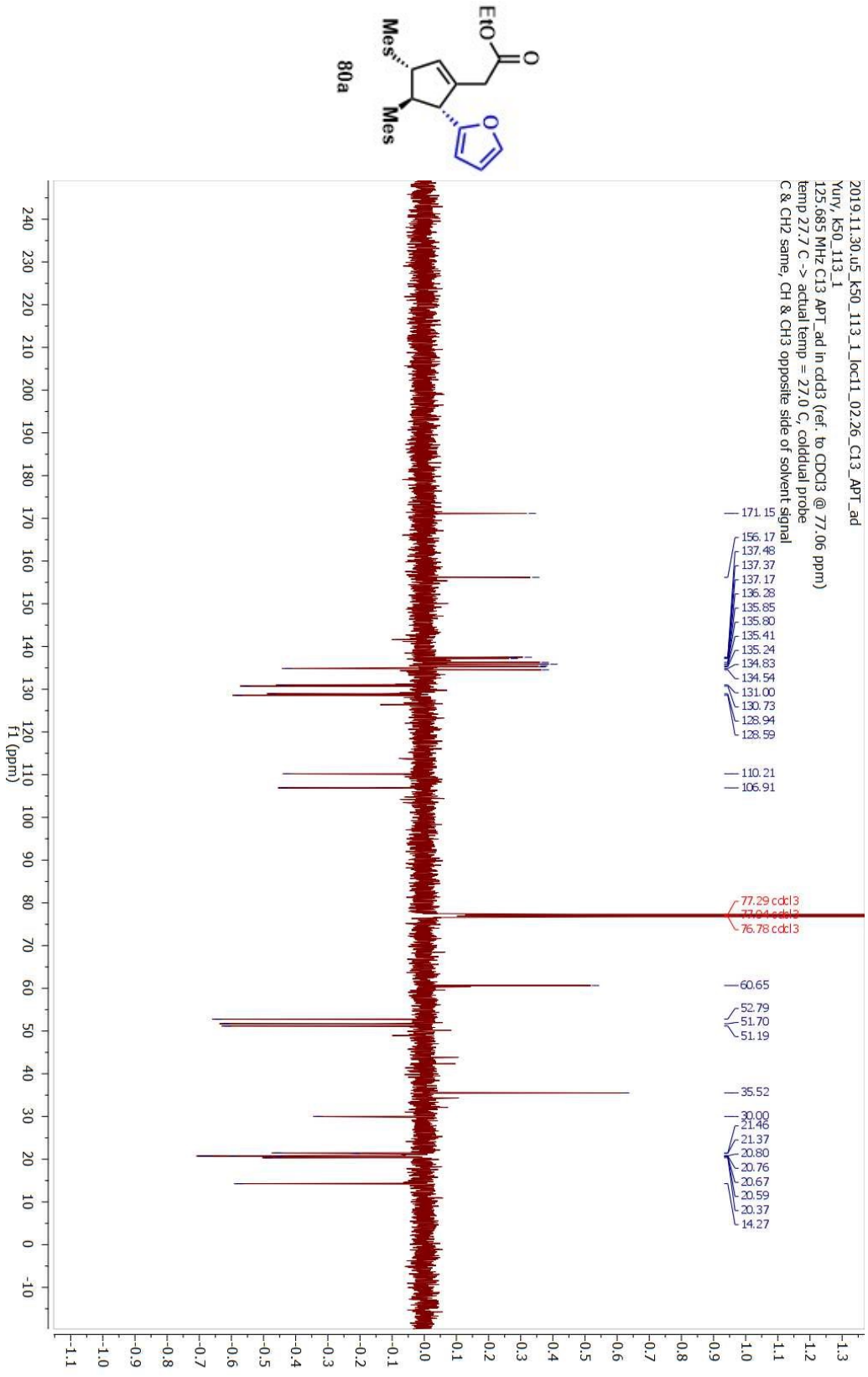
80a
Mes
Mes
EtO
O
2019.11.30.u5_k50_113_1_loc11_02.26_C13_APT_ad
Yury, k50_113_1
125.685 MHz C13 APT_ad in cdd3 (ref. to CDCl3 @ 77.06 ppm)
temp 27.7 C -> actual temp = 27.0 C, colddual probe
C & CH2 same, CH & CH3 opposite side of solvent signal
171.15
156.17
137.48
137.37
137.17
136.28
135.85
135.80
135.41
135.24
134.83
134.54
131.00
130.73
128.94
128.59
110.21
106.91
77.29 cdcl3
77.04 cdcl3
76.78 cdcl3
60.65
52.79
51.70
51.19
35.52
30.00
21.46
21.37
20.80
20.76
20.67
20.59
20.37
14.27
f1 (ppm)

Appendix IV: Selected NMR Spectra (Chapter 4)

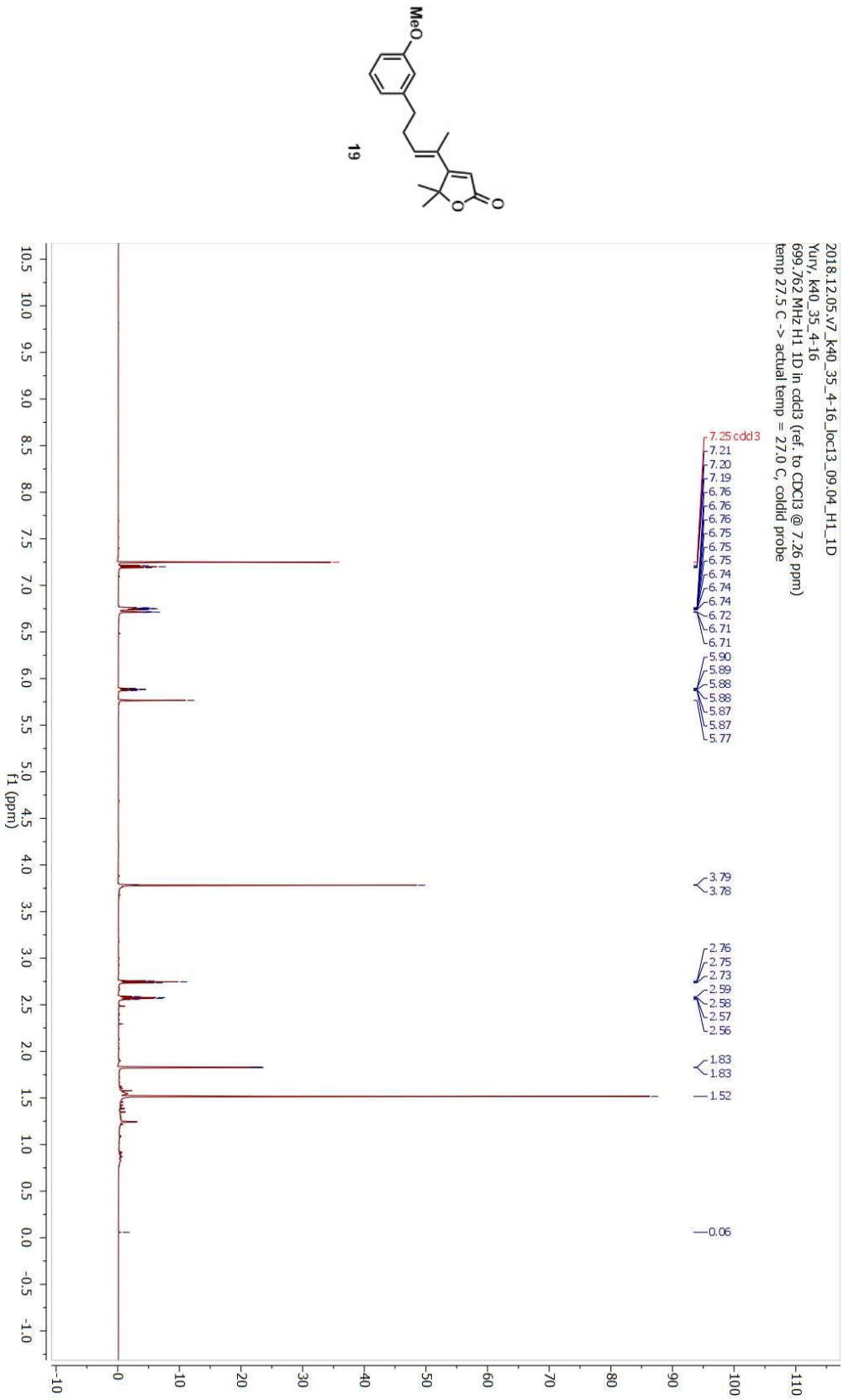
MeO
O
O
19
2018.12.05.v7_k40_35_4-16_loc13_09.04_H1_1D
Yury, k40_35_4-16
699.762 MHz H1 1D in cdcl3 (ref. to CDCl3 @ 7.26 ppm)
temp 27.5 C -> actual temp = 27.0 C, colddl probe
7.25 cddl3
7.21
7.20
7.19
6.76
6.76
6.76
6.75
6.75
6.75
6.74
6.74
6.74
6.72
6.71
6.71
5.90
5.89
5.88
5.88
5.87
5.87
5.77
3.79
3.78
2.76
2.75
2.73
2.59
2.58
2.57
2.56
1.83
1.83
1.52
0.06
f1 (ppm)

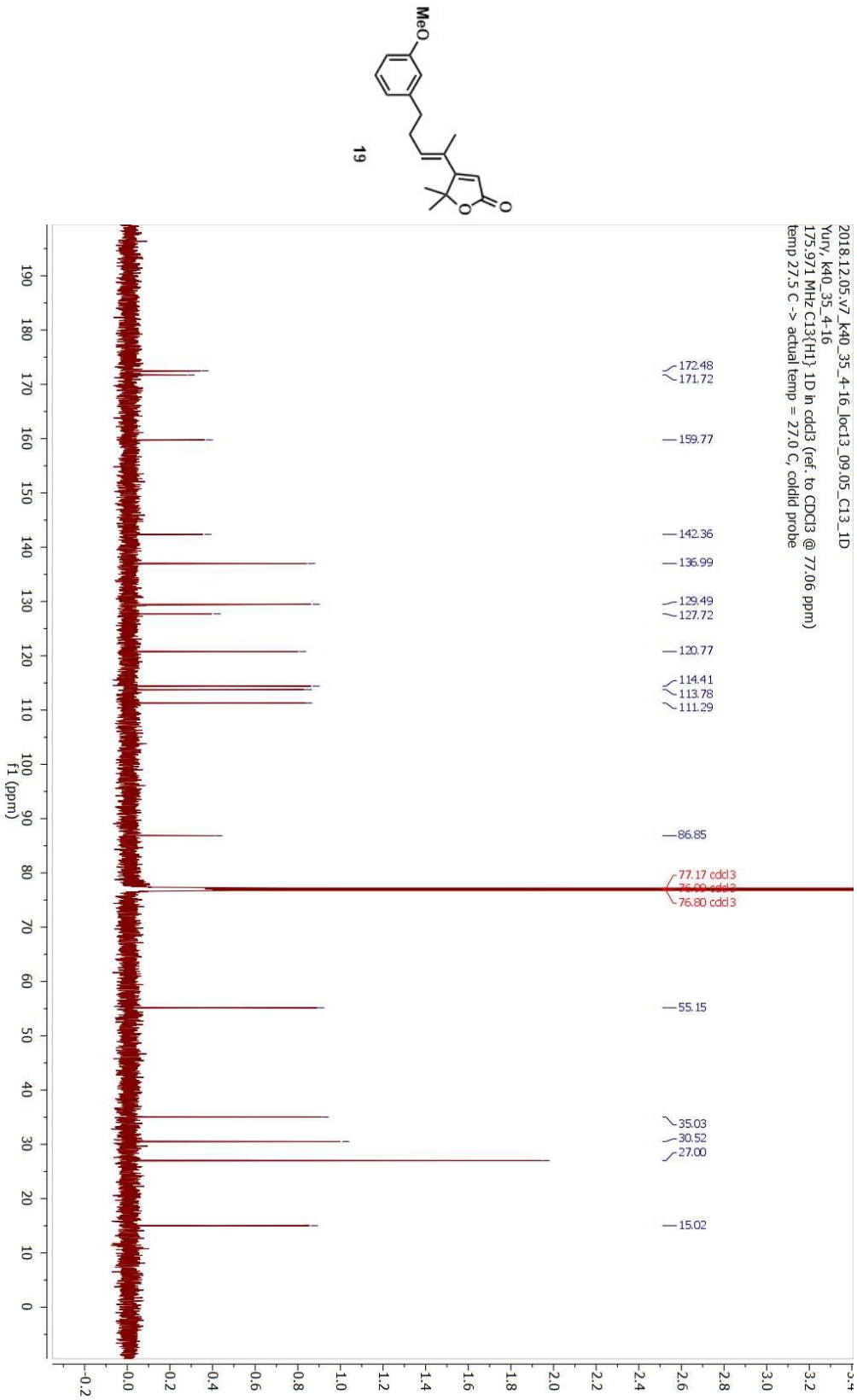
MeO
O
O
19
2018.12.05.v7_k40_35_4-16_loct3_09.05_C13_1D
Yury, k40_35_4-16
175.971 MHz C13{H1} 1D in cdcl3 (ref. to CDCl3 @ 77.06 ppm)
temp 27.5 C -> actual temp = 27.0 C, coldid probe
172.48
171.72
159.77
142.36
136.99
129.49
127.72
120.77
114.41
113.78
111.29
86.85
77.17 cdcl3
76.80 cdcl3
55.15
35.03
30.52
27.00
15.02
f1 (ppm)

Appendix V: X-ray Crystallographic Data for Compound 54a (Chapter 2)

STRUCTURE REPORT

XCL Code: FGW1703 **Date:** 7 April 2017

Compound: 2-Azido-5-chloro-2,5-dimethyl-3,4-diphenylcyclopentanone
Formula: $C_{19}H_{18}ClN_3O$

Supervisor: F. G. West **Crystallographer:** R. McDonald

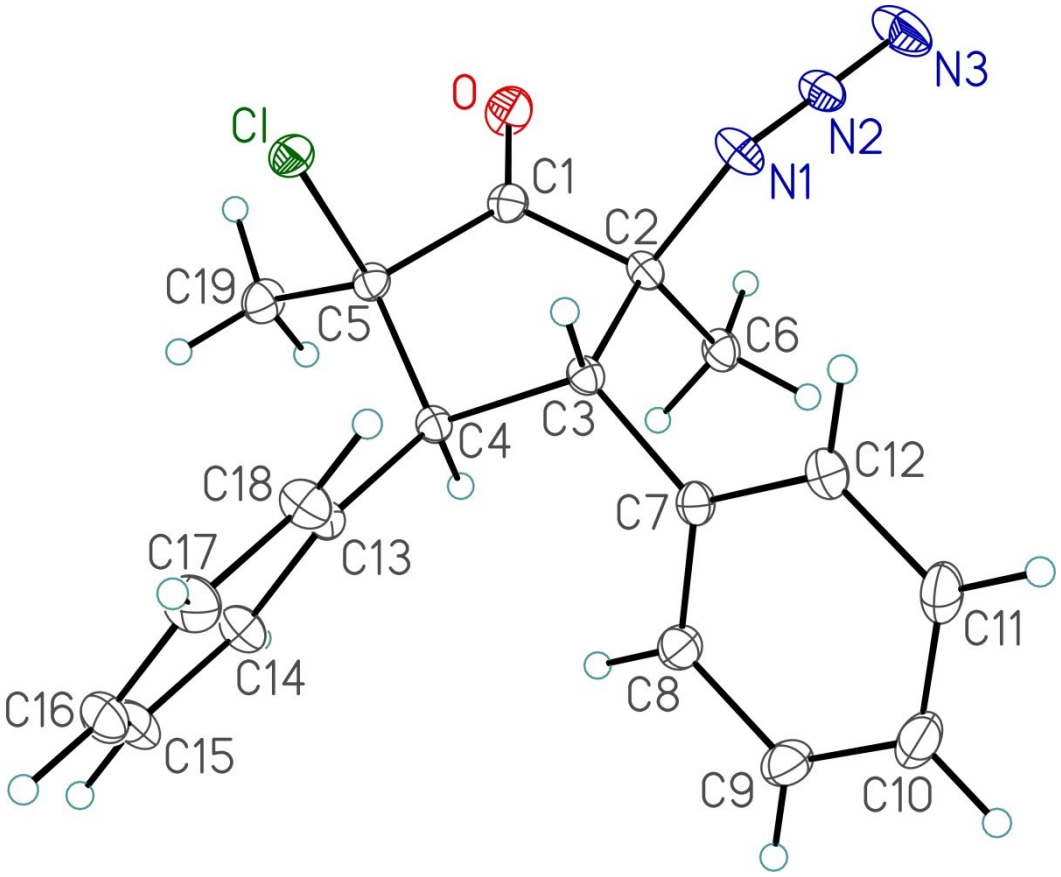

Figure Legends

Figure 1. Perspective view of the 2-azido-5-chloro-2,5-dimethyl-3,4-diphenyl-cyclopentanone molecule showing the atom labelling scheme. Non-hydrogen atoms are represented by Gaussian ellipsoids at the 30% probability level. Hydrogen atoms are shown with arbitrarily small thermal parameters.

Figure 2. Alternate view of the molecule.

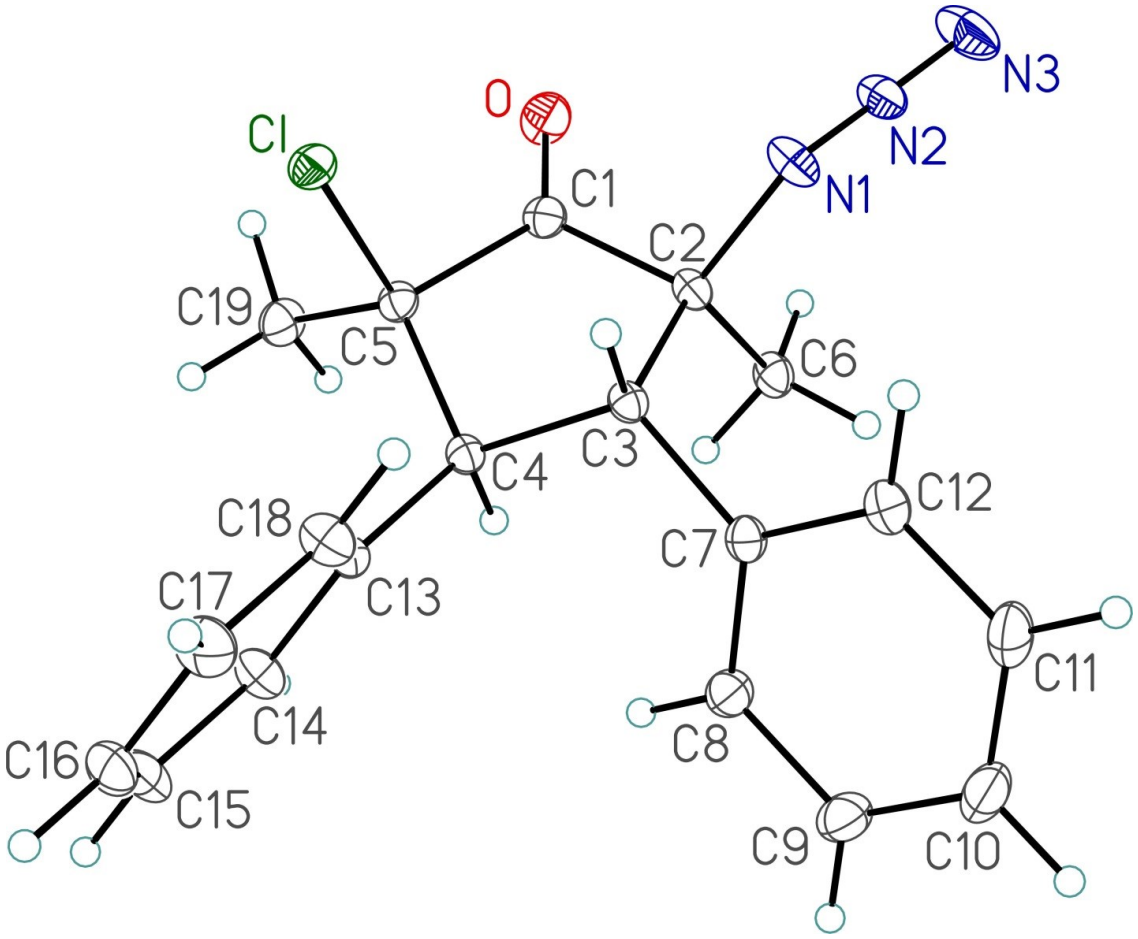
N3
N2
N1
O
Cl
C1
C2
C19
C5
C6
C3
C4
C12
C18
C7
C17
C13
C11
C14
C8
C16
C15
C9
C10

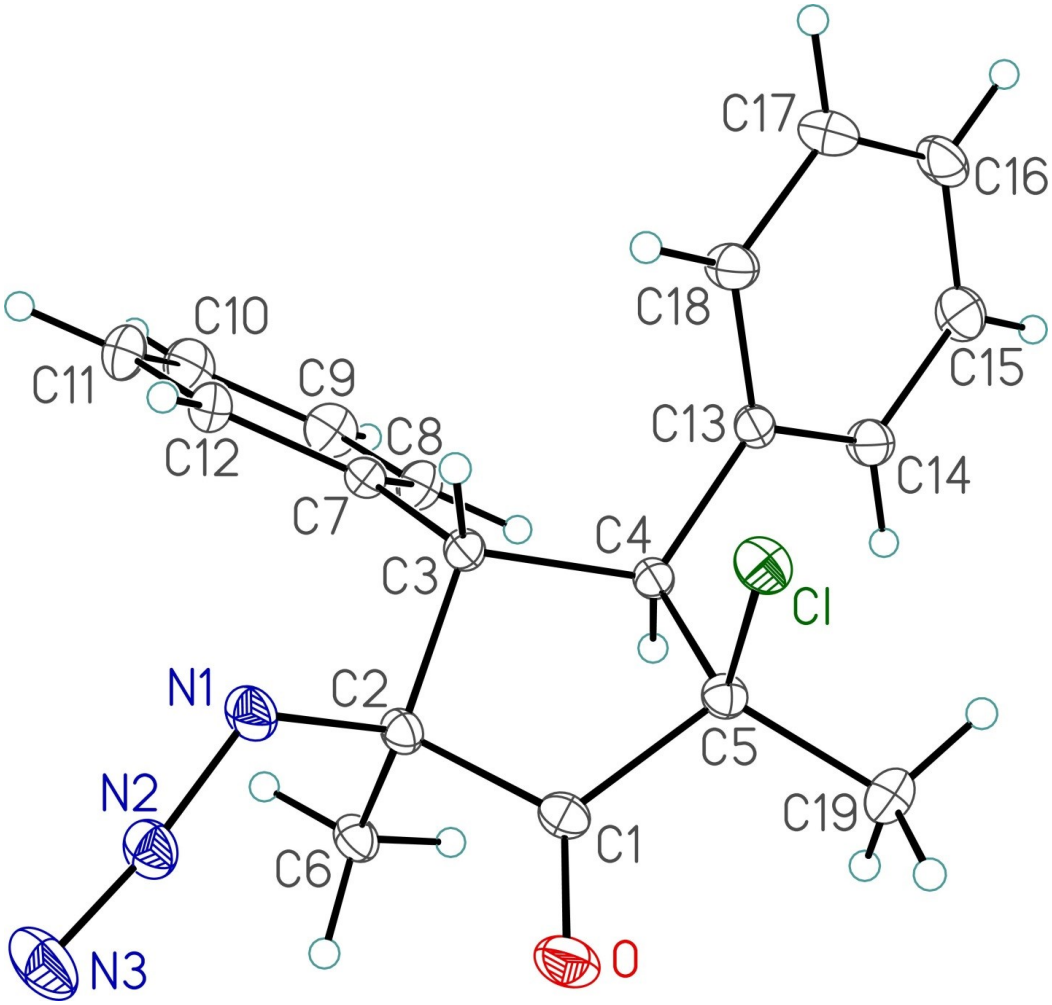
C17
C16
C18
C15
C10
C11
C9
C13
C8
C12
C14
C7
C4
C3
Cl
N1
C2
C5
N2
C19
C1
C6
O
N3

List of Tables

Table 1. Crystallographic Experimental Details

A. Crystal Data	
formula	$C_{19}H_{18}ClN_3O$
formula weight	339.81
crystal dimensions (mm)	0.70 × 0.47 × 0.22
crystal system	triclinic
space group	$P\bar{1}$ (No. 2)
unit cell parameters[a]	
	a (Å) 5.9522 (3)
	b (Å) 11.0896 (6)
	c (Å) 13.0054 (7)
	α (deg) 87.0074 (7)
	β (deg) 82.3735 (6)
	γ (deg) 82.0682 (6)
	V (Å^3) 842.22 (8)
	Z 2
ρ_{calcd} (g cm^{-3})	1.340
μ (mm^{-1})	0.237
B. Data Collection and Refinement Conditions	
diffractometer	Bruker D8/APEX II CCD[b]
radiation (λ [Å])	graphite-monochromated Mo Kα (0.71073)
temperature (°C)	–100
scan type	ω scans (0.4°) (15 s exposures)
data collection 2θ limit (deg)	56.49
total data collected	7950 (-7 ≤ h ≤ 7, -14 ≤ k ≤ 14, -17 ≤ l ≤ 17)
independent reflections	4057 (R_{int} = 0.0093)
number of observed reflections (*NO*)	3733 [$F_o^2 \geq 2\sigma(F_o^2)$]
structure solution method	direct methods/dual space (*SHELXD*[c])
refinement method	full-matrix least-squares on F^2 (*SHELXL–2014*[d])
absorption correction method	Gaussian integration (face-indexed)
range of transmission factors	0.9820–0.8955
data/restraints/parameters	4057 / 0 / 217
goodness-of-fit (*S*)[e] [all data]	1.081
final *R* indices[f]	
	R_1 [$F_o^2 \geq 2\sigma(F_o^2)$] 0.0315
	wR_2 [all data] 0.0845
largest difference peak and hole	0.346 and –0.190 e Å^{-3}

[a]Obtained from least-squares refinement of 8765 reflections with 4.80° < 2θ < 56.38°.

Table 1. Crystallographic Experimental Details (continued)

[b]Programs for diffractometer operation, data collection, data reduction and absorption correction were those supplied by Bruker.

[c]Schneider, T. R.; Sheldrick, G. M. *Acta Crystallogr.* **2002**, *D58*, 1772-1779.

[d]Sheldrick, G. M. *Acta Crystallogr.* **2015**, *C71*, 3–8.

[e]$S = [\Sigma w(F_o^2 - F_c^2)^2/(n - p)]^{1/2}$ (n = number of data; p = number of parameters varied; $w = [\sigma^2(F_o^2) + (0.0400P)^2 + 0.2585P]^{-1}$ where $P = [\mathrm{Max}(F_o^2, 0) + 2F_c^2]/3$).

[f]$R_1 = \Sigma||F_o| - |F_c||/\Sigma|F_o|$; $wR_2 = [\Sigma w(F_o^2 - F_c^2)^2/\Sigma w(F_o^4)]^{1/2}$.

Table 2. Atomic Coordinates and Equivalent Isotropic Displacement Parameters

Atom	*x*	*y*	*z*	U_{eq}, Å^2
Cl	-0.15231(4)	0.06910(2)	0.32333(2)	0.02649(8)*
O	0.23010(17)	-0.04449(8)	0.13693(7)	0.0359(2)*
N1	0.09436(17)	0.20169(10)	0.04612(7)	0.0299(2)*
N2	0.17341(18)	0.16075(9)	-0.04015(8)	0.0297(2)*
N3	0.2258(2)	0.13134(13)	-0.12283(9)	0.0469(3)*
C1	0.21126(18)	0.04942(10)	0.18119(8)	0.0229(2)*
C2	0.24707(18)	0.17397(10)	0.12828(8)	0.0209(2)*
C3	0.16396(17)	0.26509(9)	0.21623(8)	0.01919(19)*
C4	0.22564(17)	0.18990(9)	0.31434(7)	0.01849(19)*
C5	0.15740(17)	0.06342(9)	0.29927(8)	0.0202(2)*
C6	0.50030(18)	0.17136(10)	0.08653(8)	0.0250(2)*
C7	0.25791(18)	0.38542(9)	0.19770(8)	0.0214(2)*
C8	0.4422(2)	0.41207(10)	0.24410(9)	0.0277(2)*
C9	0.5293(2)	0.52206(12)	0.22208(10)	0.0346(3)*
C10	0.4330(2)	0.60665(12)	0.15324(11)	0.0381(3)*
C11	0.2497(2)	0.58149(11)	0.10617(10)	0.0359(3)*
C12	0.1623(2)	0.47208(10)	0.12851(9)	0.0275(2)*
C13	0.14092(18)	0.24683(9)	0.41793(8)	0.0202(2)*
C14	0.2761(2)	0.22525(11)	0.49810(9)	0.0285(2)*
C15	0.2031(2)	0.27464(12)	0.59480(9)	0.0349(3)*
C16	-0.0051(2)	0.34749(11)	0.61242(9)	0.0339(3)*
C17	-0.1406(2)	0.37055(12)	0.53315(10)	0.0343(3)*
C18	-0.0685(2)	0.32082(11)	0.43657(9)	0.0281(2)*
C19	0.2646(2)	-0.04221(10)	0.36231(9)	0.0289(2)*

Anisotropically-refined atoms are marked with an asterisk (*). The form of the anisotropic displacement parameter is: $\exp[-2\pi^2(h^2a^{*2}U_{11} + k^2b^{*2}U_{22} + l^2c^{*2}U_{33} + 2klb^*c^*U_{23} + 2hla^*c^*U_{13} + 2hka^*b^*U_{12})]$.

Table 3. Selected Interatomic Distances (Å)

Atom1	Atom2	Distance
Cl	C5	1.8213(10)
O	C1	1.2008(14)
N1	N2	1.2411(14)
N1	C2	1.4862(13)
N2	N3	1.1310(15)
C1	C2	1.5394(15)
C1	C5	1.5380(14)
C2	C3	1.5513(14)
C2	C6	1.5297(14)
C3	C4	1.5449(13)
C3	C7	1.5127(14)
C4	C5	1.5420(14)
C4	C13	1.5128(13)
C5	C19	1.5111(14)
C7	C8	1.3921(15)
C7	C12	1.3970(15)
C8	C9	1.3919(16)
C9	C10	1.3821(19)
C10	C11	1.386(2)
C11	C12	1.3870(17)
C13	C14	1.3910(15)
C13	C18	1.3945(15)
C14	C15	1.3897(16)
C15	C16	1.3816(19)
C16	C17	1.3837(19)
C17	C18	1.3892(16)

Table 4. Selected Interatomic Angles (deg)

Atom1	Atom2	Atom3	Angle
N2	N1	C2	115.17(9)
N1	N2	N3	172.40(13)
O	C1	C2	124.93(10)
O	C1	C5	125.56(10)
C2	C1	C5	109.47(8)
N1	C2	C1	109.58(9)
N1	C2	C3	108.08(8)
N1	C2	C6	112.95(9)
C1	C2	C3	103.62(8)
C1	C2	C6	108.58(8)
C3	C2	C6	113.59(8)
C2	C3	C4	102.85(8)
C2	C3	C7	113.90(8)
C4	C3	C7	116.13(8)
C3	C4	C5	104.16(8)
C3	C4	C13	117.00(8)
C5	C4	C13	116.67(8)
Cl	C5	C1	103.58(7)
Cl	C5	C4	109.99(7)
Cl	C5	C19	108.65(7)
C1	C5	C4	102.75(8)
C1	C5	C19	114.02(9)
C4	C5	C19	116.97(9)
C3	C7	C8	122.62(9)
C3	C7	C12	119.09(10)
C8	C7	C12	118.26(10)
C7	C8	C9	120.93(11)
C8	C9	C10	120.04(12)
C9	C10	C11	119.79(12)
C10	C11	C12	120.13(11)
C7	C12	C11	120.86(11)
C4	C13	C14	119.19(9)
C4	C13	C18	122.53(9)
C14	C13	C18	118.28(10)
C13	C14	C15	120.95(11)
C14	C15	C16	120.22(11)
C15	C16	C17	119.48(11)
C16	C17	C18	120.41(11)
C13	C18	C17	120.65(11)

Table 5. Torsional Angles (deg)

Atom1	Atom2	Atom3	Atom4	Angle
N2	N1	C2	C1	-86.83(12)
N2	N1	C2	C3	160.90(10)
N2	N1	C2	C6	34.36(14)
O	C1	C2	N1	55.88(14)
O	C1	C2	C3	171.04(11)
O	C1	C2	C6	-67.91(14)
C5	C1	C2	N1	-126.34(9)
C5	C1	C2	C3	-11.19(10)
C5	C1	C2	C6	109.87(9)
O	C1	C5	Cl	-82.07(12)
O	C1	C5	C4	163.40(11)
O	C1	C5	C19	35.82(15)
C2	C1	C5	Cl	100.17(8)
C2	C1	C5	C4	-14.36(10)
C2	C1	C5	C19	-141.94(9)
N1	C2	C3	C4	148.46(8)
N1	C2	C3	C7	-85.01(10)
C1	C2	C3	C4	32.25(10)
C1	C2	C3	C7	158.77(8)
C6	C2	C3	C4	-85.37(10)
C6	C2	C3	C7	41.16(12)
C2	C3	C4	C5	-42.23(9)
C2	C3	C4	C13	-172.63(8)
C7	C3	C4	C5	-167.31(8)
C7	C3	C4	C13	62.29(12)
C2	C3	C7	C8	-99.83(12)
C2	C3	C7	C12	77.80(12)
C4	C3	C7	C8	19.40(14)
C4	C3	C7	C12	-162.97(9)
C3	C4	C5	Cl	-75.17(8)
C3	C4	C5	C1	34.61(9)
C3	C4	C5	C19	160.30(9)
C13	C4	C5	Cl	55.43(10)
C13	C4	C5	C1	165.21(8)
C13	C4	C5	C19	-69.10(12)
C3	C4	C13	C14	-145.07(10)
C3	C4	C13	C18	34.83(14)
C5	C4	C13	C14	90.65(12)
C5	C4	C13	C18	-89.45(12)
C3	C7	C8	C9	177.55(10)

C12	C7	C8	C9	-0.10(17)
C3	C7	C12	C11	-177.35(10)
C8	C7	C12	C11	0.38(17)
C7	C8	C9	C10	-0.05(19)
C8	C9	C10	C11	-0.1(2)
C9	C10	C11	C12	0.4(2)
C10	C11	C12	C7	-0.52(19)
C4	C13	C14	C15	-179.20(11)
C18	C13	C14	C15	0.90(18)
C4	C13	C18	C17	179.50(11)
C14	C13	C18	C17	-0.60(18)
C13	C14	C15	C16	-0.7(2)
C14	C15	C16	C17	0.2(2)
C15	C16	C17	C18	0.1(2)
C16	C17	C18	C13	0.11(19)

Table 6. Anisotropic Displacement Parameters (U_{ij}, Å^2)

Atom	U_{11}	U_{22}	U_{33}	U_{23}	U_{13}	U_{12}
Cl	0.01911(13)	0.03316(15)	0.02759(14)	-0.00197(10)	-0.00084(10)	-0.00657(10)
O	0.0452(5)	0.0295(4)	0.0321(4)	-0.0105(3)	0.0072(4)	-0.0090(4)
N1	0.0298(5)	0.0391(5)	0.0207(4)	-0.0047(4)	-0.0088(4)	0.0026(4)
N2	0.0310(5)	0.0354(5)	0.0245(5)	-0.0034(4)	-0.0089(4)	-0.0051(4)
N3	0.0464(7)	0.0694(9)	0.0268(6)	-0.0145(5)	-0.0092(5)	-0.0054(6)
C1	0.0186(5)	0.0264(5)	0.0231(5)	-0.0036(4)	0.0004(4)	-0.0029(4)
C2	0.0205(5)	0.0254(5)	0.0167(4)	-0.0012(4)	-0.0035(4)	-0.0013(4)
C3	0.0172(4)	0.0219(5)	0.0180(4)	-0.0002(4)	-0.0029(3)	-0.0008(4)
C4	0.0166(4)	0.0210(5)	0.0176(4)	-0.0003(4)	-0.0024(3)	-0.0015(3)
C5	0.0167(4)	0.0224(5)	0.0210(5)	-0.0005(4)	-0.0009(4)	-0.0026(4)
C6	0.0221(5)	0.0314(5)	0.0202(5)	-0.0009(4)	0.0010(4)	-0.0025(4)
C7	0.0215(5)	0.0221(5)	0.0193(5)	-0.0004(4)	0.0003(4)	-0.0009(4)
C8	0.0269(5)	0.0271(5)	0.0298(6)	0.0020(4)	-0.0061(4)	-0.0048(4)
C9	0.0322(6)	0.0347(6)	0.0389(7)	-0.0019(5)	-0.0028(5)	-0.0129(5)
C10	0.0467(8)	0.0286(6)	0.0382(7)	0.0036(5)	0.0044(6)	-0.0136(5)
C11	0.0463(7)	0.0281(6)	0.0309(6)	0.0085(5)	-0.0022(5)	-0.0031(5)
C12	0.0295(6)	0.0283(5)	0.0237(5)	0.0025(4)	-0.0046(4)	-0.0008(4)
C13	0.0222(5)	0.0204(5)	0.0182(4)	-0.0008(4)	-0.0014(4)	-0.0042(4)
C14	0.0304(6)	0.0312(6)	0.0234(5)	-0.0026(4)	-0.0069(4)	0.0017(4)
C15	0.0457(7)	0.0383(6)	0.0219(5)	-0.0044(5)	-0.0102(5)	-

0.0029(5)						
C16	0.0454(7)	0.0331(6)	0.0226(5)	-0.0091(5)	0.0034(5)	-0.0073(5)
C17	0.0316(6)	0.0354(6)	0.0335(6)	-0.0100(5)	0.0022(5)	0.0013(5)
C18	0.0254(5)	0.0318(6)	0.0264(5)	-0.0052(4)	-0.0043(4)	0.0016(4)
C19	0.0293(6)	0.0242(5)	0.0333(6)	0.0049(4)	-0.0073(5)	-0.0026(4)

The form of the anisotropic displacement parameter is:
$\exp[-2\pi^2(h^2a^{*2}U_{11} + k^2b^{*2}U_{22} + l^2c^{*2}U_{33} + 2klb^*c^*U_{23} + 2hla^*c^*U_{13} + 2hka^*b^*U_{12})]$

Table 7. Derived Atomic Coordinates and Displacement Parameters for Hydrogen Atoms

Atom	*x*	*y*	*z*	U_{eq}, Å^2
H3	-0.0065	0.2822	0.2216	0.023
H4	0.3964	0.1784	0.3088	0.022
H6A	0.5927	0.1528	0.1438	0.030
H6B	0.5439	0.1086	0.0346	0.030
H6C	0.5265	0.2510	0.0545	0.030
H8	0.5094	0.3544	0.2915	0.033
H9	0.6550	0.5390	0.2544	0.042
H10	0.4922	0.6818	0.1382	0.046
H11	0.1837	0.6393	0.0585	0.043
H12	0.0359	0.4559	0.0963	0.033
H14	0.4203	0.1760	0.4866	0.034
H15	0.2967	0.2583	0.6490	0.042
H16	-0.0549	0.3815	0.6784	0.041
H17	-0.2838	0.4207	0.5449	0.041
H18	-0.1629	0.3374	0.3827	0.034
H19A	0.2231	-0.0271	0.4364	0.035
H19B	0.2088	-0.1172	0.3461	0.035
H19C	0.4313	-0.0508	0.3453	0.035